

## **Waves of change**

Immunomodulation of the innate immune response  
by low frequency electromagnetic field exposure

**Lieke A. Golbach**

## **Thesis committee**

### **Promotor**

Prof. Dr H.F.J. Savelkoul  
Professor of the Cell Biology and Immunology  
Wageningen University

### **Co-promotor**

Dr. B.M.L. Verburg-Van Kemenade  
Assistant professor, Cell Biology and Immunology Group  
Wageningen University

### **Other members**

Prof. Dr. M.E. Janson, Wageningen University  
Dr. J.F.B. Bolte, RIVM Utrecht  
Prof. Dr. M. Simkó, Austrian Institute of Technology Vienna  
Prof. Dr. L. Koendermans, UMC Utrecht

This research was conducted under the auspices of the Graduate School  
Wageningen Institute of Animal Sciences

# **Waves of change**

Immunomodulation of the innate immune response  
by low frequency electromagnetic field exposure

**Lieke A. Golbach**

## **Thesis**

submitted in fulfilment of the requirements for the degree of doctor  
at Wageningen University  
by the authority of the Rector Magnificus  
Prof. Dr A.P.J. Mol,  
in the presence of the  
Thesis Committee appointed by the Academic Board  
to be defended in public  
on Friday 18 September 2015  
at 1:30 p.m. in the Aula.

Lieke A. Golbach

Waves of change: Immunomodulation of the innate immune response by low frequency electromagnetic field exposure  
182 pages.

PhD thesis, Wageningen University, Wageningen, NL (2015)  
With references, with summaries in Dutch and English

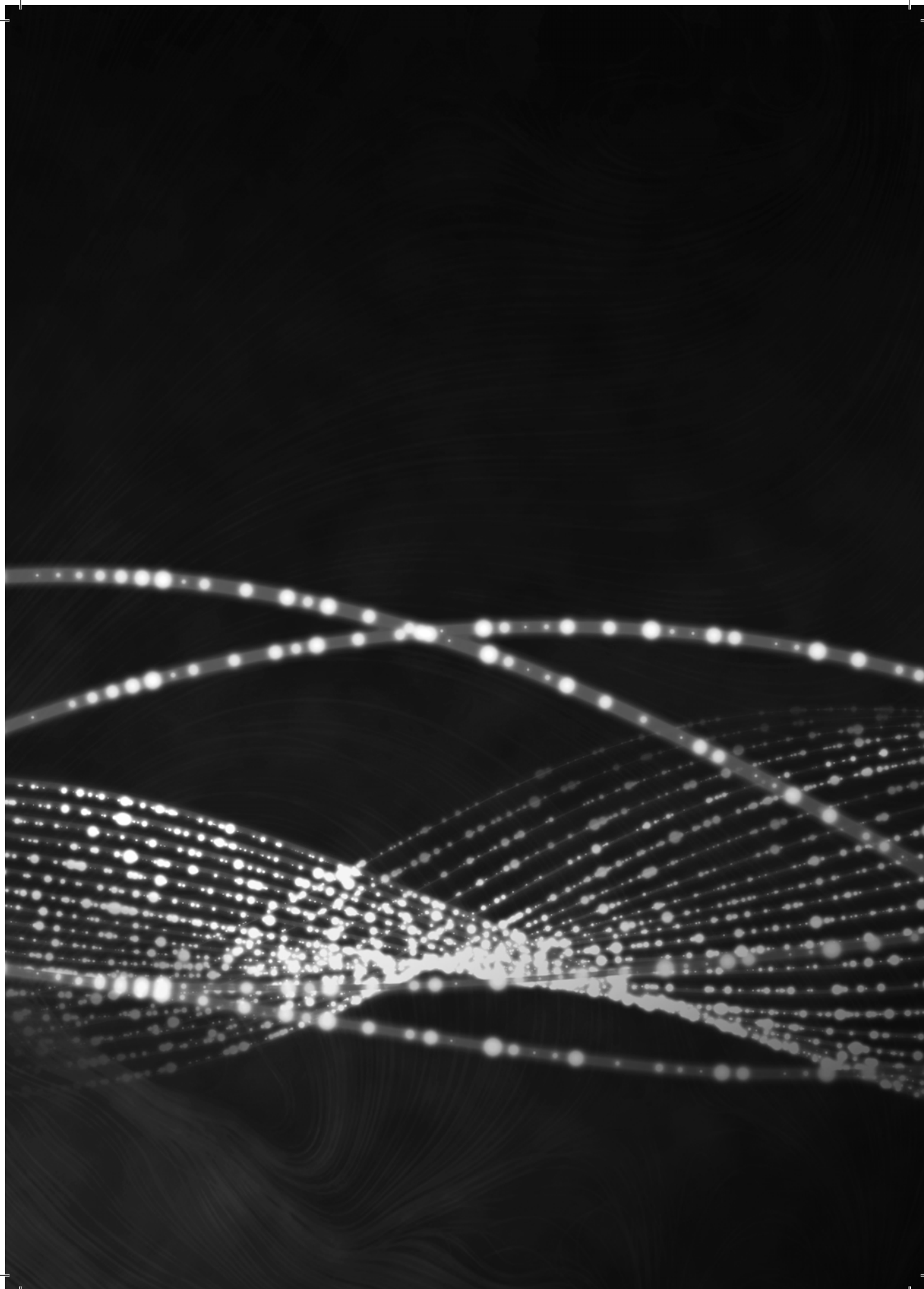
ISBN 978-94-6257-409-0

**Voor pap en mam**



## CONTENTS

Chapter 1	<i>General Introduction</i>	.....1
Chapter 2	<i>Calcium signalling in human neutrophil cell lines is not affected by low-frequency electromagnetic fields</i>	.....17
Chapter 3	<i>Calcium homeostasis and low-frequency magnetic and electric field exposure: A systematic review and meta-analysis of in vitro studies</i>	.....37
Chapter 4	<i>A novel method to investigate filopodia dynamics during low frequency electromagnetic field exposure</i>	.....63
Chapter 5	<i>Effects of 50 Hz electromagnetic field exposure on epithelial cell migration during wound healing</i>	.....77
Chapter 6	<i>Low-Frequency Electromagnetic Field Exposure Enhances Extracellular Trap Formation by Human Neutrophils through the NADPH Pathway</i>	.....89
Chapter 7	<i>EHop-016, a small molecule inhibitor for Rac1-3, induces extracellular trap formation in human neutrophils via PAD4 activation</i>	.....101
Chapter 8	<i>General Discussion</i>	.....115
Appendix		
	<i>References</i>	.....135
	<i>Samenvatting</i>	.....157
	<i>Acknowledgements/Dankwoord</i>	.....163
About the author		
	<i>List of Publications</i>	.....170
	<i>Training Activities</i>	.....171
	<i>Curriculum Vitae</i>	.....172



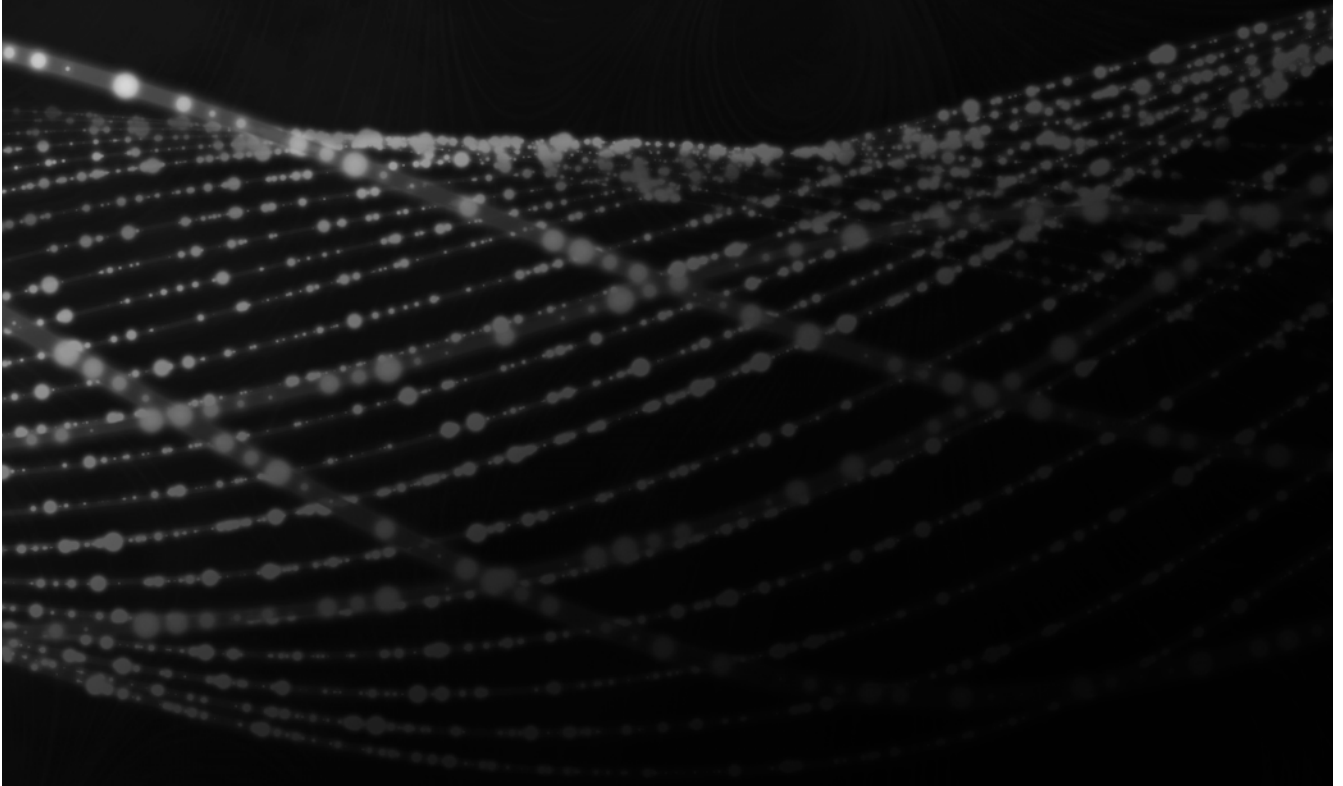


# Chapter 1

---

**General Introduction**

Lieke A. Golbach



## Electromagnetic fields

Electromagnetic radiation, fields, or waves have been around since the birth of the universe, with daylight as the most familiar one. We are exposed, mostly without even noticing them. EMF emitting wireless communication technologies and household appliances are used on daily basis and made our lives easier. However, this continuous exposure also leads to increased public concerns regarding the potential harmful effects. The waves can pass through our bodies or damage our skin, depending on the characteristics of the waves. Symptoms attributed to continuous EMF exposure in epidemiological studies range from non-specific physical symptoms, such as fatigue <sup>1</sup>, headaches <sup>2</sup>, and redness of the skin to increased prevalence of childhood leukaemia <sup>3</sup>. However, direct experimental evidence that could support an association between exposure and health status appears to be insufficient and inconsistent <sup>4,5</sup>. The large variety of health effects has led to different attempts to define a possible mechanism of interaction between EMF and cells. Most of these mechanistic studies are conducted with *in vitro* model systems of cell lines or primary cell cultures, but to date no clear mechanism of action has been elucidated. In this thesis, we investigated the potential relation between low frequency electromagnetic waves and our innate immune system.

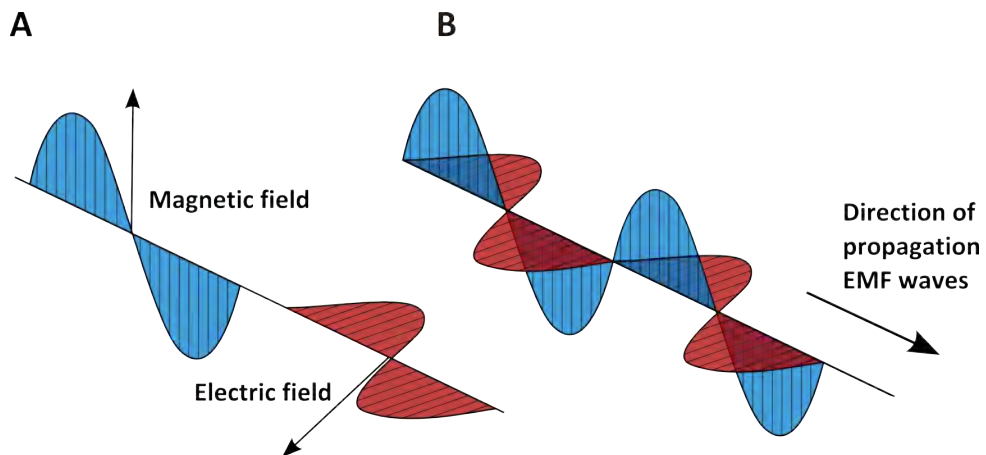


**Figure 1.** a) An electric and magnetic field oscillate in time and b) together they are the fundament of an electromagnetic field which propagates perpendicular to both fields.

### ***An Electric field plus a magnetic field yields an electromagnetic field***

Electromagnetic waves consist of an electric field combined with a magnetic field. In electric fields, positively electrically charged protons attract negatively electrically charged electrons, which are together the main building blocks of the nucleus of atoms. This combination leaves most elements in nature with a net zero electric field, since every electron is matched by a proton. When a charge separation occurs, an electric field is induced. The larger the voltage difference, the larger the electrical field that is induced. An electrical field is measured in V/m, since it depends on the voltage difference and the distance between two charges. The magnetic field components arise due to the movement of this net charge. These fields are proportional to the electrical current flowing through for instance a cable and are

inversely proportional to the distance (Figure 1). The electrical and magnetic component of electromagnetic waves are perpendicular to each other and perpendicular to the direction of energy and wave propagation (Figure 1). The magnetic flux density of electromagnetic waves is expressed with the unit Tesla (T).

### **Electromagnetic spectrum**

The electromagnetic spectrum (Figure 2) categorises all electromagnetic waves based on their frequency (wavelength), being its most important component. All electromagnetic waves are solutions of Maxwell's equations, a set of mathematical equations that together with Lorentz force law describe how electric and magnetic fields are generated and interact. However, electromagnetic waves differ in the way they interact with matter, which depends on the frequency of the waves. The spectrum is roughly divided in two main groups, ionising and non-ionising waves. Frequencies of  $10^{16}$  Hz and up are categorised as ionising, since they are able to break chemical bounds by separating electrons from atoms. X-rays or gamma rays are two well-known examples of high frequency electromagnetic radiation with detrimental effects for human health<sup>6,7</sup>. Further down the spectrum, after UV, visible light and infrared are radio-frequencies (RF), which are used for broadcasting and telecommunication. The RF spectrum is defined as the frequency range between 100 kHz and 300 GHz and is all around us since wireless communications are so closely integrated into our daily lives. Although these waves are not able to ionise atoms, *in vitro* and *in vivo* studies have linked biological effects to exposure<sup>8</sup>. However, the potential consequences for us humans are still heavily debated, since environmental exposure occurs at low level field strengths<sup>9</sup>. The waves will penetrate no more than 1 to 2 millimetres of our skin and result in no thermal effects because of the low level field strength<sup>10</sup>. At the end of the electromagnetic spectrum are the low frequencies (LF), which can be subdivided in extremely low frequencies (ELF), from 3 - 300 Hz, and very low frequencies (VLF), from 300 Hz - 100 kHz. Since LFs are not able to induce a thermal interaction or ionise ions, we speak of LF electromagnetic fields (EMFs).

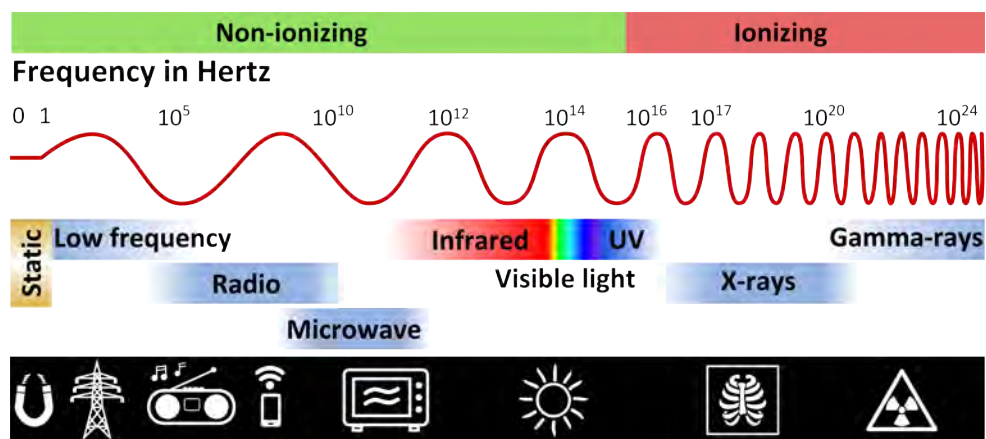


Figure 2. Electromagnetic spectrum

Electromagnetic waves can be shielded, based on the frequency or wavelength of the waves. Electric fields can be easily shielded by common materials, such as wood and plastic, but for ionising radiation, material with a heavy nucleus like lead or uranium is needed. The longer the wavelength, the higher the penetration depth. For a microwave oven or RF waves with wavelengths ranging from 12 cm to one kilometre (Table 1), a metal cage, also referred to as a Faraday cage, is able to block electric charges or radiation<sup>11</sup>. Low frequency fields are not shielded by common materials, but require highly magnetically permeable metals like  $\mu$ -metal. So low frequency fields can penetrate through walls of buildings, cars or our bodies, but like all EMF fields also diminish exponentially with distance.

Name	Frequency	Wavelength
<i>Low frequency</i>	$1 - 1 \cdot 10^5$ Hz	> 1 km
<i>Radio</i>	$1 \cdot 10^5 - 3 \cdot 10^8$ Hz	1 km – 1 m
<i>Microwave</i>	$3 \cdot 10^8 - 3 \cdot 10^{11}$ Hz	1 m – 1 mm
<i>Infrared</i>	$3 \cdot 10^{11} - 4 \cdot 10^{14}$ Hz	1 mm – 750 nm
<i>Visible light</i>	$4 \cdot 10^{14} - 8 \cdot 10^{14}$ Hz	750 nm – 390 nm
<i>Ultraviolet</i>	$8 \cdot 10^{14} - 3 \cdot 10^{16}$ Hz	400 nm – 10 nm
<i>X-ray</i>	$3 \cdot 10^{16} - 3 \cdot 10^{19}$ Hz	10 nm – 0,01 mm
<i>Gamma ray</i>	$10^{19} - 10^{24}$ Hz	< 0,02 nm

**Table 1.** Frequency and wavelength of electromagnetic waves

### ***Static and time-varying electromagnetic fields***

Time-varying electromagnetic fields occur when currents reverse their direction at a regular interval. There is an extreme variety of different time-varying fields produced by appliances using alternating current (AC): communication devices such as cellular telephone antennas, or microwave ovens. Static electromagnetic fields do not vary with time and have a frequency of 0 Hz. The earth magnetic field for instance, is a naturally occurring static field. The magnetic flux density of the Earth's static field is constant in time, however varies over the earth's surface between about 35 to 70  $\mu$ T. It is perceived by certain animals for their navigation during migration to feeding and breeding places<sup>12</sup>. Man-made static magnetic fields are generated whenever direct currents (DC) are generated, such as for electric trains or medical applications like MRI. These fields can range from 0.1 T up to 10 T and exert forces on moving charges in the blood, like ions, that generate electrical fields and currents around the heart and major blood vessels<sup>13,14</sup>.

### ***Low frequency electromagnetic fields exposure***

In a residential setting there are three major sources that generate low frequency EMFs: (household) appliances, indoor wiring, and the outdoor electrical distribution systems, consisting of above and below ground power lines. The outdoor and indoor wires are the most common sources of low frequency EMF and function at a frequency of 60 Hz in North America or 50 Hz elsewhere in the world. However, in homes the low frequency EMFs tend to be most intense close to domestic appliances that contain motors, transformers and heaters, such as an

electrical razor, induction cooker or vacuum cleaner<sup>15</sup>. They can reach up to a few mT, however these high fields are very localised and limited to a very short distance from the surface of the equipment<sup>16</sup>. Moreover, several studies measured daily exposure levels well below the exposure limit of 0.2  $\mu\text{T}$ <sup>17-19</sup>, and pooled analysis of 14 studies estimated that 98.5% of our European population is exposed to low frequency EMFs with a flux density of less than 0.2  $\mu\text{T}$ <sup>20</sup>.

Exposure to EMFs is not a new phenomenon, but for a long time frequencies below the microwave band were assumed to be safe, since the waves do not contain enough energy to heat-up or ionise tissues and induce adverse health effects. This changed in the 80's when exposure to man-made EMFs steadily increased with electricity demand. Moreover, advanced technologies and changes in our social behaviour led to an ever increasing exposure both at home and at work. In 1979 a study by Wertheimer and Leeper for the first time reported a correlation between high-voltage power lines and childhood leukaemia in the area around Denver, Colorado<sup>21</sup>. This study was repeated by numerous research groups all over the world<sup>3,22</sup>, which all tried to identify if the association is true or a coincidence introduced by confounding factors<sup>23</sup>. As they were not all conclusive, a heated discussion without consensus evolved about the capability of RF waves to affect human health.

Frequency range	E-field strength E ( $\text{kV m}^{-1}$ )	Magnetic field strength H ( $\text{A m}^{-1}$ )	Magnetic flux density B (T)
1 Hz – 8 Hz	5	$3.2 \times 10^4/f^2$	$4 \times 10^{-2}/f^2$
8 Hz – 25 Hz	5	$4 \times 10^3/f$	$5 \times 10^{-3}/f$
25 Hz – 50 Hz	5	$1.6 \times 10^2$	$2 \times 10^{-4}$
50 Hz – 400 Hz	$2.5 \times 10^2/f$	$1.6 \times 10^2$	$2 \times 10^{-4}$
400 Hz – 3 kHz	$2.5 \times 10^2/f$	$6.4 \times 10^4/f$	$8 \times 10^{-2}/f^2$
3 kHz – 10 MHz	$8.3 \times 10^{-2}$	21	$2.7 \times 10^{-5}$

**Table 2.** Reference levels for general public exposure to time-varying electric and magnetic fields (unperturbed rms values), f in Hz [24].

In 1992, an independent interdisciplinary committee, the International Non-Ionizing Radiation Committee (INIRC), was assigned to develop and disseminate science-based advice on limiting exposure to non-ionising radiation. They published the first guidelines for non-ionising radiation in 1998<sup>25</sup>, which are revised every couple of years. At this moment, exposure guidelines for low frequency electromagnetic fields from 1 to 400 Hz are established at 200  $\mu\text{T}$  for general public exposure and 1 mT for occupational exposure (Table 2)<sup>24</sup>. Nevertheless, in everyday life people are exposed to high level low frequency EMFs for short periods of time when blow drying their hair or standing next to a stove<sup>16</sup>. Modulations of human health induced by exposure might therefore not be the result of low level chronic exposure, but short high level exposures.

In search of justification, next to the epidemiological papers, also a large range of *in vivo* and *in vitro* studies arose. Whereas epidemiological studies analyse years after the actual exposure, *in vitro* and *in vivo* studies are able to examine effects on cellular and organismal functioning quickly after or even during exposure. Moreover, *in vitro* research permits simplification of the system or disease under study and this advantage allows the investigator to focus on specific cellular components. Still, to date no consensus could be reached, leaving literature scattered with different molecular mechanism that might explain a potential effect of low frequency fields on our body.

### ***Potential biological mechanisms for cellular interaction of EMF exposure***

In order to induce harmful health effects like cancer or cognitive problems, EMFs need to interact with cells or tissues in the body. This raises the question which cellular mechanism is able to convert this low field energy of LF EMF into a physiological response that requires much higher energies. Numerous hypotheses have been put forward, although none of them could explain all experimental data. Theoretical approaches and experimental studies indicate that it is highly unlikely that LF EMFs directly induce DNA damage and subsequent carcinogenetic effects, like ionising radiation is capable of. For this reason, many studies focus on other decisive fundamental biological processes and signal transduction pathways. Within the current scientific literature two common molecular interactions or pathways prevail: Calcium mobilization and free radical production. In addition, induced electric fields generated in the culture medium are suggested to provide a basic mechanism of interaction.

### ***Calcium***

Modulation of the calcium homeostasis was one of the first biological mechanisms proposed in 1980 by Adey and Bawin<sup>26</sup>. They observed alterations of calcium ion binding by weak fields, which is hypothesised to lead to a widespread conformational change within the membrane of neurons. These findings were later supported by multiple studies that report increased cytoplasmic calcium mobilization upon LF EMF exposure in T-cells<sup>27-29</sup>, neutrophils<sup>30,31</sup> and osteoblasts<sup>32-34</sup>. A rise in cytoplasmic calcium could alter cellular behaviour dramatically, as cytoskeletal changes<sup>35,36</sup>, expression of adhesion molecules<sup>37</sup> and cell migration are all regulated by calcium. However, the involved proteins or molecular interaction with LF EMF remains a matter of debate.

The complexity of the issue has led some research groups to use “simple” membrane models to explain the potential mechanisms of cellular EMF actions. They suggested that EMF exposure directly alters the lipid membrane surface of a cell, which then becomes more permeable for calcium<sup>38-40</sup>. A similar result with a direct effect of EMF exposure on calcium homeostasis was published in 2013. Interaction with calcium pumps and channels was suggested in an extensive literature review by Pall<sup>41</sup>. After examining twenty-four studies he advocated that voltage-gated channel modifications provide a biophysically plausible mechanism for EMF biological effects. The anticipated energy demand of such modifications however prohibited consensus in literature.<sup>42</sup> Adey and Bawin hypothesised already in the 80’s that an interaction proceeds by a mechanism other than thermal energy transfer. Gartzke and Lange proposed a theoretical interaction mechanism that focuses on calcium ion conduction along actin filaments in microvilli which would circumvent this energy threshold<sup>43</sup>. Microvilli

are small membrane protrusions with a structural core of dense bundles of cross-linked actin filaments. The theory focuses on the notion that the thermal energy evoked by LF EMF is not enough to influence ions like calcium by itself, but that the actin-filament core of microvilli functions as a cable-like structure to allow calcium propagation into the cytoplasm.

Arthur Pilla on the other hand, advocated that EMF might affect ion binding to intracellular signalling proteins and thereby alter the related cascade of biological processes<sup>44</sup>. In cell-free enzyme assays, it was shown that that EMF modulates the calmodulin-dependent enzyme binding to free calcium<sup>45</sup>. When calcium binds to the negatively charged binding pocket of calmodulin, the protein domains change, which triggers their ability to relieve protein inhibition, induce phosphorylation or protein dimerisation. According to Pilla, specific pulsed EMFs increase the binding affinity of calmodulin, leading to activation of the nitric oxide signalling pathway and eventually induce tissue repair after injury.

### *Reactive oxygen species*

Reactive oxygen species (ROS) and reactive nitrogen species (RNS) are the most important free radical mediators in the signalling processes of a cell. At moderate concentrations, ROS regulate proliferation and differentiation (reviewed in 46 and 47). Moreover, harmful microbes are eradicated by phagocytic cells of our immune system through controlled production of large amounts of ROS. However, during environmental stress, intracellular ROS levels increase dramatically to unfavourable levels and damage all major cellular structures, which is hazardous for living organisms (reviewed in 48,49). This oxidative stress occurs when, after a short increase, a cell is unable to re-establish its redox balance, which can be the result of impaired mitochondrial or cellular damage.

Exposure to high frequency ionising EMFs has been shown to induce oxidative stress<sup>50</sup>, but also numerous papers dispute that low frequency fields may have the same detrimental effects<sup>51-55</sup>. The effect is hypothesised to be mediated through the NADPH oxidase complex or the free radicals themselves. A first theory proposes enhanced ROS production after exposure, induced by elevated expression levels of the NADPH oxidase complex or its subunits. A transient increase of gp91phox protein expression<sup>56</sup>, one of the subunits of the NADPH oxidase complex was reported after 50 Hz EMF exposure. The other hypothesised target for the non-thermal effect of LF EMF is an enhanced free-radical lifetime<sup>57</sup>. Experiments performed with either static magnetic fields or low frequency fields showed increased stabilization of free radicals, which could contribute to an increased activity and intracellular concentration of the radicals<sup>57,58</sup>. These theories contradict with studies that find no altered ROS production after EMF exposure<sup>59-61</sup>, which could partly be explained by a cell type or frequency dependent interaction<sup>55</sup>.

### *Induced electric fields*

In 1985, William Parkinson proposed an interaction of cells with induced electric fields to explain the large diversity of effects reported for *in vitro* experiments<sup>62</sup>. A study by Liburdy et al. in 1992 substantiated this hypothesis when they observed an equal response in rat thymocytes during induced electric fields and actual AC fields<sup>63</sup>. A strong LF EMF easily passes through conducting biological media, such as a suspension or a monolayer of cultured cells in a liquid culture medium. The strong uniform magnetic component of an EM field then induces a non-uniform electrical current in the culture medium, the induced electric

field. The magnitude and spatial distribution of the induced electric field are highly dependent on the sample geometry and its relative orientation with respect to the magnetic field<sup>64</sup>. During the past decades, this phenomenon was an underestimated factor, which nevertheless might influence the cells. Many researches therefore do not report important details of the exposure system, and culture methods that are necessary to calculate the induced fields. However recently, this interaction has become more significant, and induced electric field values of the experiments are required in the material and methods section of a paper.

### ***Potential impact of electromagnetic field exposure***

With our growing demand of electricity for advancing technologies, people are increasingly exposed to man-made sources of electromagnetic fields. This electronic revolution has positively changed our lives, however recently people claim to suffer from adverse health effects induced by chronic exposure to electromagnetic fields. They are generated by our mobile phones, wireless routers, tablets, laptops, high voltage power lines and mobile phone base-stations. Since the first scientific publication about the safety of electromagnetic fields in 1979<sup>21</sup>, numerous studies have emerged that either support or reject the hypothesis that low frequency electromagnetic fields can influence the human body. Moreover, Wi-Fi and telecommunications are grouped as 2B carcinogens in 2002 by the International Agency for Research on Cancer (IARC), which implies that electromagnetic fields are possibly carcinogenic to humans. However, the associated report stated that there is inadequate evidence to confirm the impact of these fields on human health. There are large gaps in our scientific knowledge, since no experimental data could explain an unambiguous association and put forward a mechanism.

This uncertainty in combination with media hyping has led to a growing public concern that electromagnetic fields in daily life constitute a health hazard<sup>65</sup>. To deal with these societal risks, the Dutch government, through the Dutch organization for health research and development ZonMw, funds research projects that help clarify the average and peak exposures as well as positive and negative health effects of electromagnetic fields. They aim to enhance the knowledge infrastructure in the field of electromagnetic fields and health, with high-quality interdisciplinary research. In line with these objectives, we designed a series of biological experiments to elucidate if and how electromagnetic fields can modulate cells in an *in vitro* model system.

## **Neutrophils**

The two main intracellular pathways that according to literature might be influenced by LF EMF exposure are calcium mobilization and ROS generation. Although the precise theory varies from complex receptor mediated interactions to straightforward chemical redox reactions, they could all take place in polymorphonuclear leukocytes (PMN), or neutrophils in short. These sensitive immune cells are indispensable for our health and without an adequate cellular neutrophil response we would not survive (reviewed in 58).

### ***Neutrophils in infection***

When a microbe crosses the epithelial barrier and enters our body, residing tissue macrophages immediately recognise the intruder. They are the first to encounter pathogens



and quickly recruit large numbers of neutrophils to migrate to the site of infection. Neutrophils possess three main toxic effector strategies to combat invading micro-organisms: degranulation, phagocytosis and neutrophil extracellular trap (NET) formation (Figure 3). A neutrophil is packed with intracellular granules that contain a large arsenal of antimicrobial peptides ( $\alpha$ -defensins and cathelicidins), myeloperoxidase (MPO), hydrolytic enzymes (lysozyme, sialidase, and collagenase), proteases (cathepsin G, azurocidin, and elastase), cationic phospholipase, and metal chelators (lactoferrin). During degranulation, these toxic components are released upon contact with the microbes and employ extracellular killing. Intracellular killing requires phagocytosis of the microbes and subsequent generation of large amounts of ROS by the NADPH oxidase complex in the phagosomes. The third strategy, NET formation, is recently discovered by Brinkmann et al. in 2004<sup>66</sup>. The classical pathway for formation of NETs requires both ROS production and major cellular changes. In a process of two to three hours, nuclear DNA decondensates, the nuclear envelope collapses and the untangled DNA is mixed with antimicrobial peptides from the granules<sup>66</sup>. Eventually the cell membrane ruptures and the NETs, DNA fibres coated with the peptides, are released into the extracellular milieu of a cell.

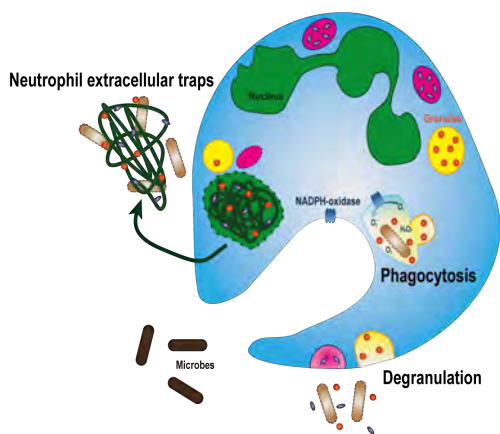


**Figure 3. The three antimicrobial strategies neutrophils use to kill microbes.** A neutrophil has a multi-lobular nucleus and the cytoplasm is packed with granules. These granules contain different anti-microbial peptides. If a neutrophil encounters a bacteria, it can release the content of the granules in the extracellular environment during *degranulation*. The microbes can also be taken up by the cell, and killed intracellularly by *phagocytosis* through release of the content of the granules and large amounts of ROS produced by NADPH oxidase. The third strategy is *neutrophil extracellular trap* formation. A process in which the neutrophil unwraps its DNA and combines it with the antimicrobial peptides. This “NET” is then released while capturing and killing the microbes, but also the neutrophil itself.

The release of NETs can be measured in two different ways. First, extracellular DNA can be stained with cell-impermeable DNA binding dyes, like Sytox. The use of these dyes is effortless and does not require medium changes, which could disturb the fragile NET-structures. Dye-binding can be quantified with a fluorescence plate reader that gives the investigator a raw fluorescent unit. A more detailed quantification is possible with microscopy and image analysis. This second method provides more information on how the NETs look and reveals a-specific staining of cells that have a compromised cell membrane. Both methods have their pros and cons, and are used extensively to investigate NET release by bacteria<sup>67,68</sup> or chemical components<sup>69,70</sup> and the influence of small-molecule-inhibitors<sup>71</sup>.

The mechanism for formation of NETs is not completely known, only the primary pathways are elucidated (Figure 4). Neutrophils engage in NET formation upon activation by interleukin 8 (IL-8)<sup>72</sup>, different types of bacteria<sup>73-75</sup>, parasites<sup>68</sup>, fungi<sup>76</sup>, or activated platelets<sup>77</sup>. Moreover, NETs can be induced with the chemical component phorbol 12-myristate

13-acetate (PMA), which mimics receptor activation through upregulation of diacyl-glycerol (DAG). The second step after activation is generation of large amounts of superoxide ( $O_2^-$ ) that are rapidly dismutated to hydrogen peroxide ( $H_2O_2$ ). Fuchs et al. showed that  $O_2^-$  production by the NADPH oxidase complex is crucial for NET formation and can be blocked with a pharmacological inhibitor of NADPH, diphenyleneiodonium (DPI) <sup>78</sup>. In addition, chronic granulomatous patients, who do not have functional NADPH oxidases, fail to form NETs or maintain phagocytosis <sup>79</sup>. ROS production might lead to the release of elastase and subsequently myeloperoxidase (MPO) from the granules. Alternatively, it is proposed that ROS serve to inactivate caspases, thereby inhibiting apoptosis and instead induce autophagy <sup>80</sup>. Cellular autophagy is initiated shortly after ROS production, probably to facilitate degradation of the granular membranes and nuclear envelop. After about one hour, nuclear chromatin is decondensated by peptidylarginine deiminase 4 (PAD4) <sup>81</sup>. In neutrophils, PAD4 catalyses the conversion of histone H3 peptides by citrullination, which is the conversion of positively charged arginine side chains of a peptide into uncharged citrulline side changes. The difference in charge loosens the tight bound between histone and the DNA wrapped around it, thereby preparing it for the next step. PAD4 operates together with elastase, which is released from granules and subsequently partially degrades specific histones to decondensate the DNA <sup>82</sup>. If the DNA is unwrapped, the nuclear membrane disintegrates to mix the DNA with the antimicrobial peptides. Shortly thereafter the cell membrane ruptures and the DNA fibres, with antimicrobial peptides, are spread over the microbes to immobilise and kill the microbes. The different pathways involved in NET formation were elucidated with specific small-molecule inhibitors. Administration of different inhibitors of distinct pathways reveal if a specific pathway is essential for the generation and release of NETs.

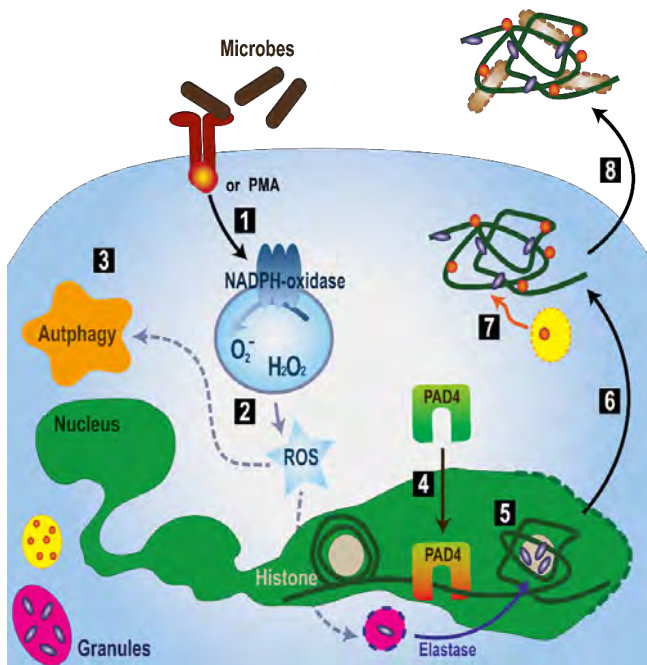


**Figure 4. The classical pathway of neutrophil extracellular trap formation.** NET formation is initiated by binding of microbial components to extracellular receptors or the addition of PMA. This activates the NADPH oxidase, which starts to produce large amounts of superoxide ( $O_2^-$ ) (1). Simultaneously, the autophagy pathway is triggered (2), to facilitate degradation of the granular membranes and nuclear envelop at a later stage. The  $O_2^-$  dismutates to  $H_2O_2$  (ROS) and enables the release of elastase. PAD4 is activated (4) and translocates into the nucleus to citrullinate histones. Together with elastase (5), the DNA is decondensated and released into the cytoplasm of the cell (6). The unwrapped DNA mixes with antimicrobial peptides (7) and is released in the external environment to capture and kill microbes.

### ***Neutrophil migration***

Neutrophils are produced in the bone marrow from stem cells that proliferate and differentiate to mature neutrophils fully equipped with an armoury of granules. When fully differentiated, these mature neutrophils leave the bone marrow and enter the blood circulation. In case of infection, circulating neutrophils are recruited to the site of infection by chemokines in a process called chemotaxis, which is the direct cell movement of a cell up a chemical gradient. Following the chemokines, such as interleukin-8 (IL-8) and complement factor C5a, the neutrophils bind to the endothelial cells of a blood vessel and subsequently transmigrate through the endothelial gap towards the infected tissue (reviewed in 83).

### ***Calcium mobilization and homeostasis***

Chemotaxis plays a central role in the accumulation of neutrophils at sites of infection or inflammation. To activate cell deformation like pseudopod formation, coordinated crawling, and later phagocytosis, a transient increase of cytoplasmic calcium is required. In neutrophils, the whole process is initiated after the exposure of a cell to chemokines<sup>84</sup> or adhesion-receptor crosslinking during phagocytosis<sup>85</sup>. A chemokine or components of bacteria bind to a G-protein coupled receptor, which then changes conformation and activates the connected intracellular G-protein. Activated G-proteins on their turn activate the cytoplasmic phospholipase C (PLC) enzyme. Phosphatidylinositol 4,5-bisphosphate (PIP<sub>2</sub>) is the next protein in the signalling cascade leading to calcium mobilization. Membrane-bound PIP<sub>2</sub> is hydrolysed by PLC to form inositol 1,4,5-trisphosphate (IP<sub>3</sub>) and diacylglycerol (DAG). DAG stays bound to the cellular membrane where it activates the protein kinase C (PKC) enzyme, while IP<sub>3</sub> diffuses towards the endoplasmic reticulum, which is the main calcium store in a cell. Massive amounts of calcium are stored in the endoplasmic reticulum (ER), to keep cytoplasmic levels low in resting cells, but also to be prepared if a calcium rise is needed. When IP<sub>3</sub> is generated and moves through the cytoplasm, it will bind to its receptor (IP<sub>3</sub> receptor) on the outer membrane of the ER. The IP<sub>3</sub> receptor is a calcium channel that releases calcium from the ER after activation, thereby generating the first intracellular calcium wave during store-operated calcium entry (SOCE). Subsequently, the actin cytoskeleton redirects the ER towards the membrane of the cell where plasma membrane channels (Orai) communicate with stromal interaction molecules (STIM) on the calcium-store membranes. This interaction releases more intracellular stored calcium as well as induces an influx of extracellular calcium<sup>86</sup>. Furthermore, the membrane-bound DAG proteins activate a second mechanism, receptor-operated calcium entry (ROCE), which induces a calcium influx directly via non-selective transient receptor potential cation (TRPC) channels in the plasma membrane<sup>87,88</sup>. The receptor-mediated calcium influx is the second calcium wave, which perfectly follows the store-mediated entry<sup>88</sup>.

An orchestrated calcium influx is vital to activate many cellular pathways, because calcium is the most important second messenger molecule in a cell. The relatively low concentration of calcium ions inside the cell (~100 nM) is maintained constant when a cell like a neutrophil is not active. Na<sup>+</sup>/Ca<sup>2+</sup> exchangers (NCX) work together with plasma-membrane Ca<sup>2+</sup>-ATPases (PMCA) to extrude calcium to the extracellular environment. Furthermore, sarco(endo)plasmic reticulum Ca<sup>2+</sup> ATPase (SERCA) pumps on the ER actively transport calcium back into the ER stores<sup>89</sup>. These pumps and channels are not only active to maintain a calcium homeostasis, but are also activated after a

calcium influx to restore the cellular concentration back to baseline level.

Reliable measurements of intracellular calcium concentrations in a cell can be performed with the stable artificial radioisotope  $^{45}\text{Ca}$ , to measure the entry of calcium from the external medium of cells. With this method, only the entry of radioactive calcium measured after a certain time, so the radioactive signal represents the accumulated calcium ions inside a cell. A second option is the use of chemical fluorescent probes, which facilitates analysis of the potential functions and regulatory mechanism, such as channels and pumps, of  $\text{Ca}^{2+}$  in a cell. The calcium dye is taken up by the cell and activated in the cytoplasm through hydrolysis. Calcium ions bind to the dye after for instance the opening of the calcium store-channels, leading to a 10 to 1000 times increase in fluorescence in the cell. Moreover, these calcium dyes are very sensitive and every small perturbation of calcium is detected with a fluorescent microscope in a real-time image acquisition setting<sup>90</sup>.

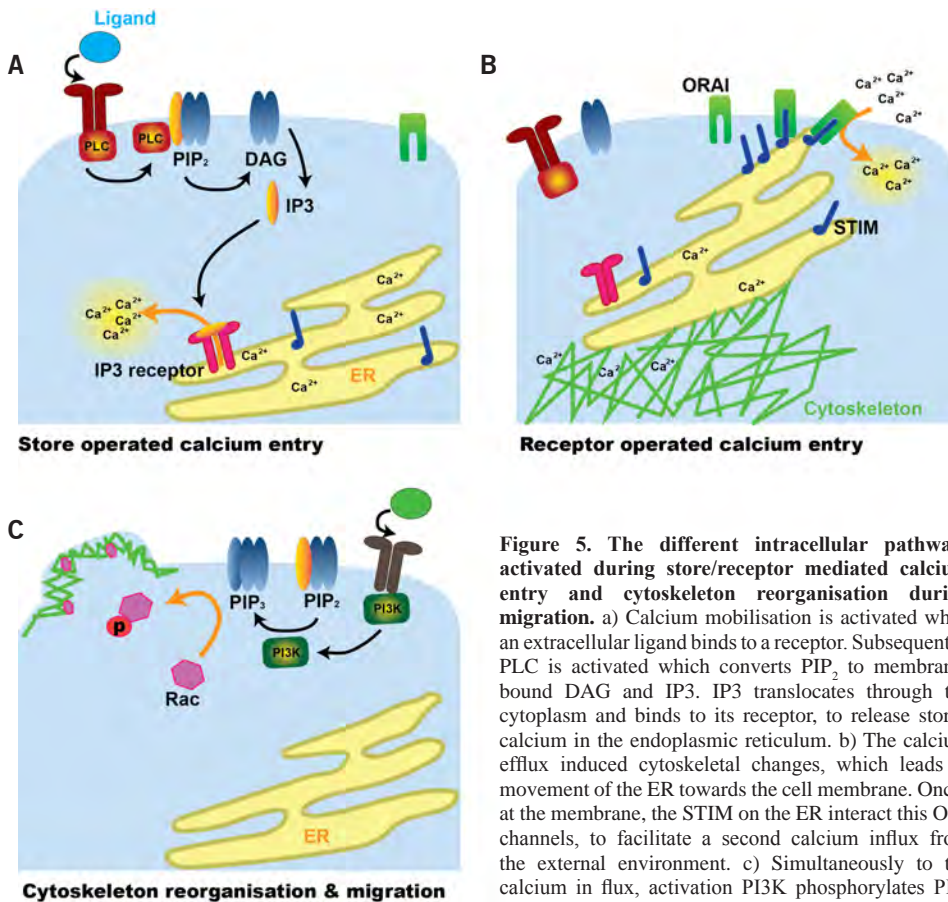


**Figure 5. The different intracellular pathways activated during store/receptor mediated calcium entry and cytoskeleton reorganisation during migration.** a) Calcium mobilisation is activated when an extracellular ligand binds to a receptor. Subsequently, PLC is activated which converts  $\text{PIP}_2$  to membrane-bound DAG and IP3. IP3 translocates through the cytoplasm and binds to its receptor, to release stored calcium in the endoplasmic reticulum. b) The calcium efflux induced cytoskeletal changes, which leads to movement of the ER towards the cell membrane. Once at the membrane, the STIM on the ER interact this Orai channels, to facilitate a second calcium influx from the external environment. c) Simultaneously to the calcium in flux, activation PI3K phosphorylates  $\text{PIP}_2$  to  $\text{PIP}_3$ .  $\text{PIP}_3$  phosphorylates many proteins involved in cytoskeleton reorganisation. Eventually, the actin filaments underneath the cell cortex rearrange and push the leading edge of the cell forward.

### ***The actin cytoskeleton during migration***

Calcium is a prominent regulator of the actin cytoskeleton, it can exert multiple effects on the structure and dynamics of the cytoskeleton. Precise spatial and temporal control of the assembly, disassembly and contractility of the actin cytoskeleton is crucial for direct cell migration<sup>36,91</sup>. Neutrophil and macrophage migration, for example, slows and stops when calcium is depleted from the extracellular medium or is chelated from the medium with EGTA<sup>92</sup>. Furthermore, cancer cells with reduced levels of Orai1 or STIM1 also show impaired migration<sup>93</sup>.

For neutrophils to migrate towards an infection, first the actin cytoskeleton needs to reorganise and become polarised, which implies that the molecular processes at the front and the back of a moving cell are different. The front, or leading edge, is the location where the actin filaments rapidly need to polymerise to push the cell forward. Leading edge formation requires the activation of two parallel localised second messenger signals: calcium and phosphatidylinositol 3,4,5-trisphosphate (PIP<sub>3</sub>) (reviewed in 36 and 94). Consequently, after binding of a microbe or chemokine to the G-protein coupled receptor not only PLC, but also phosphoinositide 3 kinase (PI3K) is activated. PI3K phosphorylates the membrane-bound PIP<sub>2</sub> into PIP<sub>3</sub>, which results in the formation of a leading edge that arises upon the localised activation of PI3K. This is followed by the accumulation of proteins containing PIP<sub>3</sub>-binding domains, such as protein kinases<sup>95</sup>, guanine nucleotide exchange factors (GEFs)<sup>96,97</sup>, and structural proteins like Rac<sup>98</sup>. Together all these signalling proteins translocate to the plasma membrane and form a complex, dynamic, signalling network that initiates actin polymerization, branching and eventually membrane protrusion and adhesion. At the same time, enzymes that mediate the breakdown of PIP<sub>3</sub> will be active at the back of the cell to release the adhesion of its “tail” from the substrate and retract. So to migrate, a cell first extends protrusions such as lamellipodia and filopodia, forms adhesions, and finally retracts its tail. A tightly orchestrated process, in which the actin filament networks rearrange to different patterns depending on the type of protrusion. Leading edge lamellipodia for instance, are a complex mesh of branching filaments, whereas filopodia and microvilli are organised into long parallel bundles (reviewed in 99).

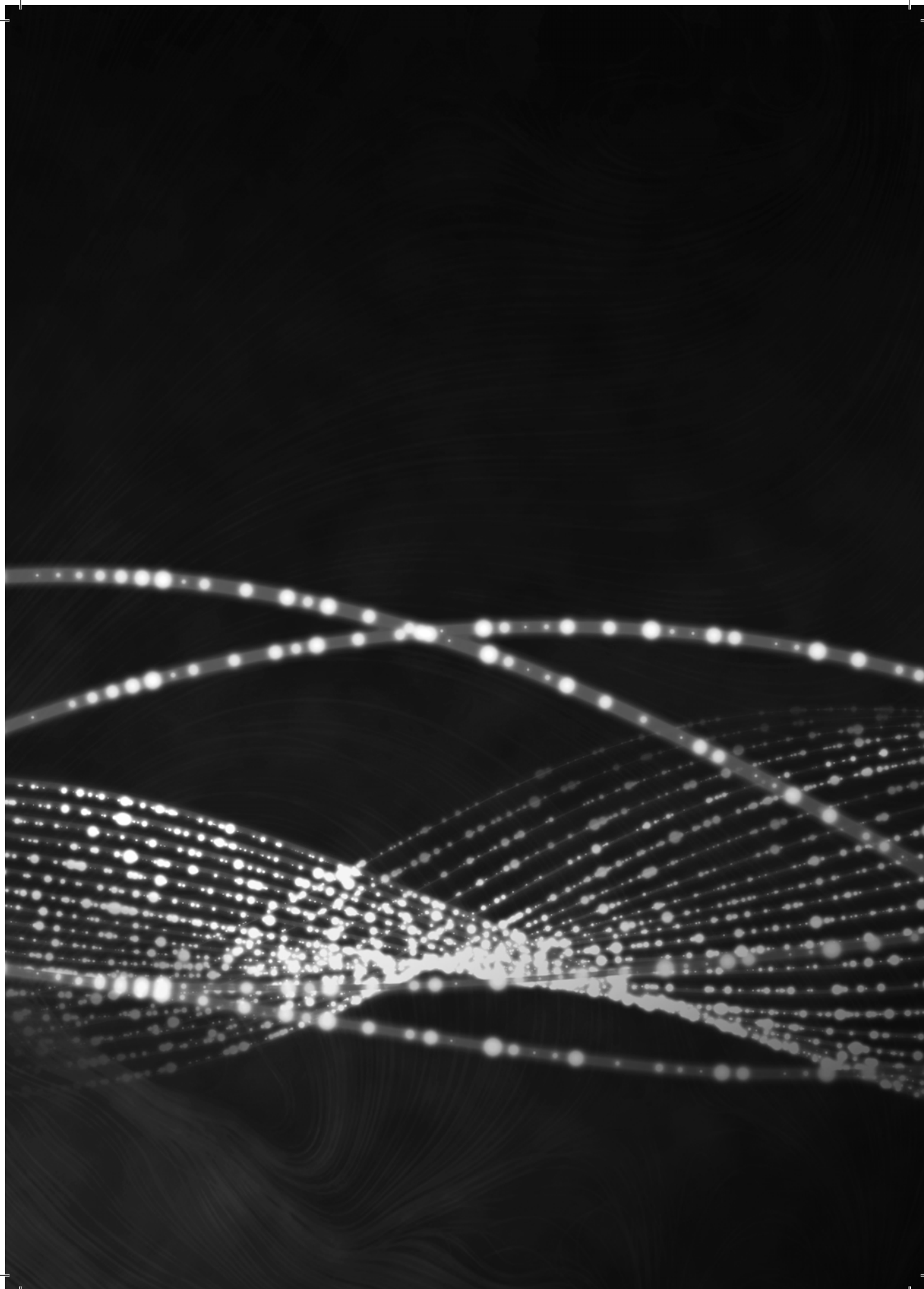
Many cells have shown to be migratory from nature or by modulation of actin-related proteins. Just like immune cell recruitment, endothelial migration during wound healing is pivotal for our health. Endothelial migration is an important process in the formation of blood vessels and the repair of damaged tissue. Moreover, endothelial migration is, like immune cell crawling, a complex and dynamic process that is regulated by the actin cytoskeleton. Migration is initiated if a layer of cells or tissue is damaged, and the wound triggers mechanical signals as well as the secretion of chemotactic molecules that attract the cells into the wound. Failure or impaired migration of endothelial and immune cells leads to severe consequences like immunosuppression<sup>100,101</sup> and wound healing defects<sup>102</sup>. A scratch wound healing assay has been widely adapted and modified to study the migration of endothelial cells. In a typical scratch wound healing assay, cells are grown in a monolayer *in vitro*. Then a part of the monolayer is scratched away to create a “wound gap”. The cells migrate towards the centre of the gap, which is referred to as “healing”. The cell migration is monitored by microscopy and can be automated in a high-throughput assay to compare numerous experimental conditions at the same time.

## Outline of this thesis

In a neutrophil, both orchestrated calcium mobilization and tightly-controlled ROS generation are indispensable for the cells function. Nevertheless, neutrophils appear to be an overlooked immune cell type in literature about the effect of EMF. Probably since they are short-lived and undergo spontaneous apoptosis within 24 hours in the absence of any extracellular stimuli. In contrast, macrophages survive longer in the body, up to a maximum of several months. Yet, neutrophils are not only important during inflammation and immune responses, but also in the pathogenesis of several inflammatory disorders including chronic infection, autoimmunity, and cancer. They shape the inflammatory/immune responses through the production of cytokines, the release of preformed pro-inflammatory mediators, such as proteases and alarmins<sup>103</sup> and through the cross-talk with other cells of the immune system<sup>104</sup>. Therefore, neutrophils are highly versatile and sophisticated cells, their functions reaching far beyond the elimination of microorganisms. A finely tuned balance of antimicrobial defence versus host damage is essential. Hence, what about EMF and these overlooked neutrophils? We expect the influence of EMFs on cells to be small and subtle, if they are influenced at all. It might be that the influences are too subtle to be picked-up with conventional methods. Also newly discovered cellular targets or pathways might be affected by EMF. While our knowledge of the different molecular pathways inside a cell become more extensive and our techniques more sensitive, an interesting starting point is created. A starting point to investigate possible molecular mechanisms underlying the potential health effects of LF EMF exposure.

In **chapter 1** we provide a framework for this thesis by describing background information on the different electromagnetic fields and the potential mechanism present in literature on how EMFs could influence cells. Furthermore, we explain the function of neutrophils and their signalling pathways that are important during an infection. To date, many research groups have attempted to associate EMF exposure with cell biological pathways and to elucidate a potential mechanism of interaction. In **chapter 2** we study if exposure to a 50 Hz sine wave EMF or an irregular waveform could influence calcium mobilization in neutrophil-like cells. We investigated the calcium influx induced with a biological stimulus, and we combined this conventional approach with gene expression patterns and detailed cell morphology analysis. With a systematic review of current literature and subsequent meta-analyses of the results, we investigate in **chapter 3** the evidence already present in current literature regarding a modulation of the cellular calcium homeostasis by LF EMF exposure. Unlike most systematic reviews examining *in vivo* studies and clinical trial data, we evaluate studies that used *ex vivo* or *in vitro* cell cultures. Furthermore, we analyse if there is an EMF sensitive cell type present and investigate the existence of specific frequency or magnetic flux density related effects of EMF, because this theory is heavily debated. Calcium homeostasis and the cytoskeleton are linked, therefore in **chapter 4** we describe a novel method to examine the effect of acute LF EMF exposure on the cytoskeleton and cell protrusions. Unlike common methods, we established a very sensitive protocol to detect subtle changes. In a time-resolved image analysis, we measure and calculate the movement of filopodia. In **chapter 5** we study the effects of LF EMF exposure on cell migration during wound healing. We apply an innovative high-throughput method and design an easy-to-use image analysis to evaluate the influence of exposure. In **chapter 6** we study a recently discovered cellular mechanism called neutrophil extracellular trap formation. ROS generation is very

important in this signalling pathway and the release of NETs have never been associated with EMF exposure. We quantify NET formation after exposure and also investigate the potential biological mechanisms. NET formation is a sensitive process with detrimental effects and in **chapter 7** we describe the discovery of an unexpected mechanism of EHop-016, a small molecule inhibitor designed to interfere with migration of cancer cells. We investigate the unexpected interaction between EHop-016 and NET formation in an *ex vivo* experimental set-up and determine. An interaction of EHop-016 with the immune system could have detrimental consequences for future drug therapies. To conclude, I place the findings of this thesis within the framework of current knowledge in **chapter 8**. I discuss the limitations, challenges and future prospective of different cellular pathway and cell functions that might be influenced by low frequency EMF exposure. Furthermore, I discuss the fundamental role of sample sizes and the importance of biological relevance versus statistical difference.





# Chapter 2

---

## **Calcium signalling in human neutrophil cell lines is not affected by low-frequency electromagnetic fields**

Lieke A. Golbach, John G.M. Philippi, Jan J.M. Cuppen, Huub F.J. Savelkoul, B.M. Lidy Verburg-van Kemenade

*Published in Journal of Bioelectromagnetics  
2015, Volume 36 (6), pages 430-443*

## Abstract

We are increasingly exposed to low-frequency electromagnetic fields (LF EMFs) by electrical devices and power lines, but if and how these fields interact with living cells remains a matter of debate. This study aimed to investigate the potential effect of LF EMF exposure on calcium signalling in neutrophils. In neutrophilic granulocytes, activation of G-protein coupled receptors leads to efflux of calcium from calcium stores and influx of extracellular calcium via specialised calcium channels. The cytoplasmic rise of calcium induces cytoskeleton rearrangements, modified gene expression patterns and cell migration. If LF EMF modulates intracellular calcium signalling, this will influence cellular behaviour and may eventually lead to health problems. We found that the calcium mobilization upon chemotactic stimulation was not altered after a short 30-minutes or long-term LF EMF exposure in human neutrophil-like cell lines HL-60 or PLB-985. None of the two investigated wave forms (Immune and 50 Hz sine wave) at three magnetic flux densities (5  $\mu$ T, 300  $\mu$ T and 500  $\mu$ T) altered the calcium signalling *in vitro*. Gene-expression patterns of calcium-signalling related genes also did not show any significant changes after exposure. Furthermore, analysis of the phenotypical appearance of microvilli by scanning electron microscopy revealed no alterations induced by LF EMF exposure. The above findings indicate that exposure to 50 Hz sinusoidal or Immune LF EMF will not affect calcium signalling in neutrophils *in vitro*.

## Introduction

The societal concern about potential adverse human health effects of chronic exposure to low-frequency electromagnetic fields (LF EMFs) is rising. Low-frequency fields ranging from 0 to 300 kHz are non-ionising and therefore unable to induce thermal effects. However, these fields are capable of penetrating deep into tissues of the human body. We are increasingly exposed to LF EMFs produced by electrical devices and power lines, but if these fields can interact with living cells remains a matter of debate. Although disputed by others, several research groups showed that various LF EMF wave forms influence calcium homeostasis in different cell types, but the molecular mechanisms are largely unknown<sup>41,105-109</sup>.

Calcium plays an important role as a receptor-mediated intracellular second messenger. The relatively low concentration of calcium ions inside a resting cell (~100 nM) is maintained constant by inducible calcium pumps and channels in the plasma membrane and in membranes of the calcium stores inside the cell. Cellular activation via G-protein coupled receptors leads to activation of phospholipase C (PLC) which stimulates the production of inositol 1,4,5-trisphosphate (IP3) and diacylglycerol (DAG). In store-operated calcium entry (SOCE), cytosolic IP3 triggers release of calcium from intracellular stores through IP3 receptors. Subsequently, stromal interaction molecules (STIM) on the calcium-store membranes communicate with plasma membrane channels (Orai) to release more intracellular stored calcium and regulate an influx of extracellular calcium<sup>86</sup>. Furthermore, the DAG proteins activate a second mechanism, receptor-operated calcium entry (ROCE), which induces a calcium influx directly via non-selective transient receptor potential cation (TRPC) channels in the plasma membrane<sup>87,88</sup>.

Neutrophils are key players in the early immune response against invading microbial pathogens. Upon infection, chemokines recruit circulating neutrophils and initiate migration to the site of injury or infection. Once in the infected tissue, phagocytosis or extracellular killing via degranulation or neutrophil extracellular trap formation eliminates pathogens. Most neutrophilic functions are vastly controlled by transient increases in cytoplasmic calcium. A rise in the cytoplasmic calcium concentration induces cytoskeletal changes<sup>35,36</sup>, degranulation<sup>110</sup>, expression of adhesion molecules<sup>37</sup> and facilitates direct migration towards the site of infection. Impaired or altered calcium mobilization in immune cells is therefore associated with major trauma<sup>111</sup> and diseases like allergy<sup>112</sup>.

In 2002, Gartzke and Lange linked the calcium signalling pathway to LF EMF when they proposed a theoretical interaction mechanism that focuses on calcium ion conduction along actin filaments in microvilli<sup>43</sup>. Microvilli are small membrane protrusions with a structural core of dense bundles of cross-linked actin filaments. The theory focuses on the notion that the thermal energy evoked by LF EMF is not enough to influence ions like calcium by itself, but that the actin-filament core of microvilli functions as a cable-like structure to allow calcium propagation into the cytoplasm. Therefore, this theory proposes microvilli to be a cellular interaction site for LF EMF. The abundant presence of microvilli on the cell surface and the importance of calcium signalling for cellular functions make neutrophils interesting prospective target cells for LF EMF interaction.

This study aimed to investigate the potential effect of LF EMF exposure on calcium mobilization in neutrophils, as these cells contain microvilli and are indispensable for the innate immune system. Since the EMF characteristics may be crucial to determine a biological

response (Pilla 2006), we focused on two LF EMF signals: a 50 Hz sine wave, which resembles the household alternating current electrical power supply in a large part of the world and a signal named Immument which represents an irregular combination of multiple frequencies. LF EMF Immument exposure has previously been reported to improve growth and resistance in goldfish and chickens <sup>113</sup>, but was unable to influence cytokine gene expression in immune cells <sup>114,115</sup>. The irregular combination of frequencies from the Immument signal shows resemblance to dirty power or dirty electricity. The term dirty electricity refers to high frequency components that are flowing along a conductor and deviate from a pure 50/60 Hz sine wave. Dirty electricity is advocated as an important biological active component of standard electromagnetic pollution. This makes it an interesting LF EMF wave forms to investigate next to the 50 Hz sine wave. We examined the effect of an environmental relevant 5  $\mu\text{T}$  magnetic flux density as well as a 300  $\mu\text{T}$  for Immument and 500  $\mu\text{T}$  for 50 Hz sine wave magnetic flux density.

To be able to reveal subtle modulatory effects of LF EMF, we set up a comprehensive study in which we measured calcium influx and examined the mRNA expression of calcium channel proteins, calcium receptors and binding proteins after exposure. In addition, we assessed the surface morphology of neutrophils by scanning electron microscopy to identify potential phenotypic changes of the microvilli upon LF EMF exposure.

## Material and Methods

### *Cell culture*

The human promyelocytic cell line HL-60 <sup>116</sup> and PLB-985 <sup>117</sup> were purchased from ATCC. Both cell lines were grown in RPMI-1640 medium without HEPES and supplemented with 10% heat-inactivated fetal bovine serum, L-glutamine (2 mM), streptomycin (100  $\mu\text{g/ml}$ ) and penicillin (100 U/ml). The cells were cultured at  $37\pm 0.2^\circ\text{C}$  in a humidified atmosphere containing 5%  $\text{CO}_2$  and passaged every three to four days. Differentiation of HL-60 and PLB-985 cells towards neutrophil-like cells, indicated by dHL-60 or dPLB-985, was induced by the addition of dimethylsulfoxide (DMSO) at a final concentration of 1.25% (v/v) to  $0.5 \times 10^6$  cells/ml <sup>116</sup>. The cells were left to differentiate in 25  $\text{cm}^2$  tissue culture flasks for four or five days at  $37\pm 0.2^\circ\text{C}$  in a humidified atmosphere containing 5%  $\text{CO}_2$ .

### *Exposure system*

Cell pre-exposure was done in the middle of a specialised custom-made exposure system by Immument BV <sup>114,115</sup>. The coil fits inside a standard cell culture incubator to ensure optimal cell culture conditions with  $37\pm 0.2^\circ\text{C}$  and 5%  $\text{CO}_2$ . The cell culture flasks were placed in the central region of the coils, perpendicular to the vertical magnetic field lines. The copper wire coil is wound on a double co-axial cylinder with an inner (65 turns;  $\text{Ø}$  184 mm) and outer cylinder (2 times 8 turns;  $\text{Ø}$  400 mm) of polymethyl methacrylate (PMMA). All positional parameters are optimised together to achieve a high homogeneity in the exposure area of  $<0.4\%$ . The system is connected to a signal generator with pre-programmed signals. The two wave-forms used are 50 Hz sine wave and the Immument signal, which is a combination of four block waves at frequencies of 320, 730, 880 and 2600 Hz <sup>114</sup>. The resulting magnetic signal  $B(t)$  is measured using a Gauss/Tesla meter with sensitive probe (Model 5180, F.W. Bell). Magnetic flux densities of 5  $\mu\text{T}$ , 300  $\mu\text{T}$  and 500  $\mu\text{T}$  were used. The maximum induced electrical field (E) for the 50 Hz sine wave was  $E < 1.57$  mV/m and  $E < 0.3$  V/m for the Immument Signal.

Two identical cell culture incubators with an identical exposure coil inside each were used and randomly assigned to be active or sham for each experiment, to eliminate any effects induced by the internal environment of one of the incubators. Background AC levels at the place of exposure and sham-exposure were less than  $0.2 \mu\text{T}$  and ambient DC fields were  $10 \mu\text{T}$ .

Real-time exposure during flow cytometry was done with a second custom-made exposure system. This system fits around a flow cytometer tube inside the flow cytometer. The circular coil consisted of  $0.5 \text{ mm}$  tightly wound copper wire around a polyether ether ketone (PEEK) body with an inner diameter of  $38 \text{ mm}$  (100 turns;  $R=1.10 \Omega$ ). The sinusoidal field  $B(t)$  was generated by a custom build power current source driven by function generator (HAMEG, HM8030-2). The resulting magnetic signal  $B(t)$  was calibrated by using a LakeShore 475 DSP Gaussmeter. The signal used in this paper is a  $50 \text{ Hz}$  sine wave at a magnetic flux density of  $2.5 \text{ mT}$ . The coil system was connected to a computer with custom-made software, to control exposure time, coil temperature and magnetic field. The sham-exposure was done with an unenergised coil. Background AC levels at the place of exposure and sham-exposure were less than  $0.3 \mu\text{T}$  and ambient DC fields were  $47 \mu\text{T}$ . The direction of the generated LF EMF was parallel to the height of the flow cytometer tube containing the cell suspension.

#### *Cell exposure*

Long-term LF EMF or sham exposure of several days during differentiation was performed simultaneously in two identical cell culture incubators at  $37 \pm 0.2^\circ\text{C}$  in a humidified atmosphere containing  $5\% \text{ CO}_2$ . Before exposure, differentiation was induced by DMSO and HL-60 or PLB-985 cells were split into two groups, sham and exposed. For both groups, culture conditions were kept identical. For the short-term LF EMF exposure of 30 minutes or flow cytometry exposure, HL-60 or PLB-985 cells were first differentiated into neutrophil-like cells for four or five days and subsequently split into two groups.

#### *Calcium assay*

Intracellular calcium mobilization was analysed with the fluorescent membrane-permeable calcium indicator Fluo-4 NW (Molecular Probes). Cell viability and density was verified before each experiment using trypan blue exclusion. Sham and exposed cells were loaded with Fluo-4 NW ( $5 \mu\text{g/ml}$ ) according to the manufacturer's protocol and incubated for 30 minutes at  $37 \pm 0.2^\circ\text{C}$ , followed by a 30-minute de-esterification at  $22 \pm 0.5^\circ\text{C}$ . For spectrofluometric analysis, small  $50 \mu\text{l}$  aliquots of both cell suspensions were transferred to a black/clear 96-well plate (Corning) to analyse calcium mobilization in a spectrofluometer (Spectramax M5, Molecular Devices) with a  $495 \text{ nm}$  excitation and  $504 \text{ nm}$  emission filter. Recording times were optimised to an initial baseline measurement for 30 seconds, after which calcium mobilization upon a chemical stimulus was measured for 150 seconds. Platelet activating factor (PAF) was used to induce a calcium influx in the differentiated neutrophil cell lines. During the assay, the temperature was controlled at room temperature ( $22 \pm 0.2^\circ\text{C}$ ). The baseline and calcium influx of three sham and three exposure samples were measured simultaneously with a minimum of three repetitions per experiment.

Since Fluo-4 is a non-ratiometric calcium indicator, the following equation was used to calculate relative fluorescent intensities of all the samples.

$$\text{Relative fluorescence} = \frac{F}{(F_b)} \quad (1)$$

$F$  is the fluorescence intensity of Fluo-4 during the induced calcium mobilization.  $F_b$  is the average baseline calcium content in the sample before stimulation and is measured for at least 30 seconds in every sample. To exclude any differences in calcium influx induced by the use of two separate incubators, sham-sham experiments were performed (Supplementary data). In these experiment, the same experimental setup as with LF EMF exposure was applied, with the difference that not one but both coils were unenergised during the sham exposure.

For flow cytometry analysis with an Accuri C6 system (BD Bioscience), 200  $\mu$ l aliquots of the Fluo-4 loaded cell suspensions were transferred to a tube and fluorescence was analysed at with a 488 nm laser and 533/30 nm emission filter. The cytoplasmic calcium concentration of every individual cell was recorded up to 300 seconds at room temperature ( $22 \pm 0.5^\circ\text{C}$ ) before, during, and after exposure. The exposure coil was switched on by a computer at the indicated time points and generated a 50 Hz sine wave with a magnetic flux density of 2.5 mT. Measurements obtained by flow cytometry were analysed by FlowJo. A fluorescence intensity of 10% above basal cytoplasmic value was selected and plotted as the mean fluorescence value measured at every second. To compare mean fluorescence intensities during sham (>30 measurements) or LF EMF (>81 measurements) exposure, the average fluorescence intensity was calculated.

#### *Quantitative real-time PCR*

RNA was isolated from PLB-985 cells by a spin-column purification using the Qiagen RNeasy Mini Kit (Qiagen) according to manufacturer's protocol. RNA yield was quantified with a Nanodrop ND 1000 spectrophotometer (Thermo Scientific). First strand cDNA was synthesised from 0,5  $\mu$ g RNA with Invitrogen's SuperScript® III Reverse Transcriptase Systems for RT-PCR systems (Invitrogen) in 20  $\mu$ l final volume reaction mix containing 50 ng random primers, 1  $\mu$ l 10 mM dNTPs, 1  $\mu$ l 0.1 M DTT, 4  $\mu$ l 5X first standbuffer, 1  $\mu$ l RNase OUT and 1  $\mu$ l SuperScript III. Quantitative real-time polymerase chain reaction (qPCR) was performed in a 72-well Rotor-Gene 2000 standard qPCR machine (Corbett Research) with Brilliant® SYBR® Green Master Mix (Stratagene) for chemistry detection. Specific primer pairs were designed and tested using a pooled sample (Table 1). Melting curves for each primer pair showed one specific signal and primer efficiency was above 1.6 for all pairs. In addition, amplification products from each primer pair were checked on gel.

For relative quantification of gene expression, three reference genes were measured: RPS13, RPL27 and OAZ. NormFinder and BestKeeper online software was used to determine the best-suited reference genes according to their expression stability during differentiation and exposure. RPS13 and OAZ showed to be unregulated reference genes and were therefore used to normalise all qPCR data. Gene expression was calculated with REST© software according to the following equation.

$$Ratio = \frac{(E_{target})^{\Delta CP_{target(control-exposure)}}}{(E_{ref})^{\Delta CP_{ref(control-exposure)}}} \quad (2)$$

Gene	RefSeq accession numbers	Forward primer (5'-3')	Reverse primer (5'-3')
STIM1	NM_001277961	CTTGTCATGCAGTCCCCTA	CTCGCCCTCTACCAACCTCT
STIM2	NM_001169118	TGCTAAAGATGAGGTTGCTGC	CGTCAGAGTCCCAAAGACT
ORAI1	NM_032790	TTATCGTCTTCGCCGTCCAC	TCCTGTAAGCGGGCAAAGCT
TRPC6	NM_004621	CAGGAAATTGAGGATGACGCT	TTGGACTCGGCACCAGATTG
IP3RT1	NM_001099952	GAGTTTCAGCCCTCAGTGGA	ACGCAGAGTGGTGGGACTA
B-actin	NM_001101	CTGCTGCAATGATGTCATT	TCCTTAATGTCACGCACGATTT
Arp2/3	NM_001278556	TACCAAACATCATCGGAAACATGG	GGCAGGTCCTTTGAATTGACTT
Calmodulin	NM_006888	AAATCCGTGAGGCATTCCGAG	AGTTCTGCTGCACTGATATAACC
CD11b	NM_000632	GCCTTGACCTTATGTCATGGG	GTCATTGCGTTTTCAAGTGCC
OAZ	NM_004152	TAAGTGGCGAACAGTGCTGA	ATGAAGACATGGTCCGGCTCG
RPS13	NM_001017	GCTCTCCTTTCGTTGCCTGA	TAGGGTAAAGCCGACTGGGA
RPL27	NM_000988	TGAAACCTGGGAAGGTGGTG	GCGATCTGAGGTGCCATCAT

**Table 1.** Oligonucleotide sequence of human primers used for quantitative PCR

### Scanning Electron Microscope

After sham or LF EMF exposure for five days, a droplet of the dHL-60 cell suspension in normal culture medium was placed onto a poly-l-lysine coated glass slide. After 30 minutes the cells were rinsed using warm culture medium. The samples were fixed in 2.5% (w/v) glutaraldehyde for 30 minutes and post-fixed in 1% (w/v) osmium tetroxide and washed several times in buffer. The samples were dehydrated in a graded series of ethanol and subsequently critical point dried (CPD) with carbon dioxide in a LEICA EM CPD030. Samples were analyzed at 2 kV at room temperature with a field emission scanning electron microscope (Magellan 400, FEI). Image collection and sample analysis were performed blind. Categorization of cell morphology was done for a minimum of five views per condition, with each view containing eight or more cells. Cell morphology was scored based on the number of microvilli on the cell surface. Cells showing an elongated phenotype, with clear early lamellipodia adhering to the glass substrate were scored as polarised. The spherical cells were scored based on the number of microvilli on the cell surface. The different groups were: No protrusions, 1-10% coverage with some microvilli and ruffles, between 10 to 20% of the cells surface covered with microvilli, or cells which are for 75% or more covered with microvilli.

### Statistical Analysis

The significance of the differences between the calcium mobilization with and without LF EMF exposure was assessed using repeated measures analysis of variance (ANOVA). Difference in mRNA expression between sham and exposure samples were calculated with a two sided Pair Wise Fixed Reallocation Randomisation Test©. Comparison between the distribution of the phenotypes and LF EMF exposure was done with a Pearson's chi-squared test. Statistical significance was indicated with \* at p<0.05, \*\* at p<0.01 and \*\*\* at p<0.001.

## Results

### *Calcium kinetics after short LF EMF exposure*

To examine if a low-frequency electromagnetic field exposure with Immune or a 50 Hz sine wave affects calcium mobilization in human neutrophils, human cell lines HL-60 were differentiated into neutrophil-like cells for four days. Once differentiated, both cell lines represent a controlled *in vitro* system to investigate the influences of LF EMF on cell behaviour. Basal cytoplasmic calcium in resting dHL-60 was recorded for 30 seconds, after which the cells were stimulated with a suboptimal concentration of the chemotactic peptide platelet-activating factor (PAF). The suboptimal concentration of PAF was determined prior to the exposure experiments (Supplementary data). The rise of intracellular calcium induced by PAF was simultaneously measured for 150 seconds in both the sham and exposure samples.

Pre-exposure of dHL-60 cells for 30 minutes to either 5  $\mu$ T 50 Hz or 5  $\mu$ T Immune LF EMFs did not alter the calcium kinetics (Fig. 1). Neither basal cytoplasmic calcium nor the calcium influx after stimulation was significantly different after a short exposure to 5  $\mu$ T LF EMF. 5  $\mu$ T represents the magnetic flux density humans are daily exposed to, and might be too low to influence cells. Therefore calcium mobilization was again measured in dHL-60 after a 30 minutes exposure to 500  $\mu$ T 50 Hz sine waves or 300  $\mu$ T Immune (Fig. 2). Increasing the magnetic flux density of pre-exposure up to 500  $\mu$ T did not change the calcium mobilization in dHL-60 cells.

### *Calcium kinetics after long LF EMF exposure*

Exposure of neutrophil-like cells to a LF EMF for a short period of 30 minutes did not affect the kinetics of calcium mobilization, therefore an exposure period of five days was investigated. PLB-985 cells were divided into two groups and differentiated into neutrophil-like cells for five days. The exposure group received a continuous 50 Hz sine wave at 500  $\mu$ T or a continuous Immune at 300 mT, whereas the sham group differentiated under identical conditions but without LF EMF. Figure 3 shows the average calcium kinetics of four independent experiments. Neither 50 Hz nor Immune exposure induced a significant difference in calcium mobilization between the sham and the exposure groups after PAF stimulation (Fig. 3). Furthermore, the same negative results were obtained if calcium influx was induced with another powerful inflammatory mediator, complement factor 5a (C5a) (Supplementary data). To ensure that an initial difference in the calcium concentration before calcium mobilization was not lost by normalization to baseline, raw fluorescent data were also analysed. None of the exposure groups showed a consistent initial difference in the basal cytoplasmic calcium concentration compared to sham (Supplementary data). To exclude the possibility that subtle changes in intracellular calcium concentration induced by LF EMF exposure are quick and reversible and therefore only detectable during exposure, we performed a real-time LF EMF exposure of neutrophil-like cells in a flow cytometric setup (Fig. 4). We did not find any reversible calcium mobilization upon LF EMF exposure, even at a magnetic flux density of 2.5 mT.



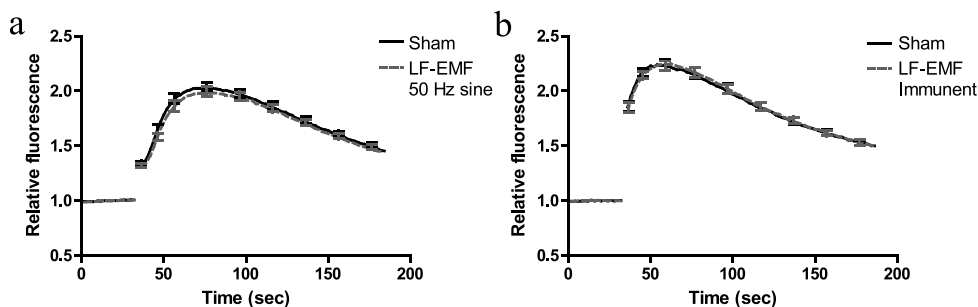


**Figure 1.** Calcium influx in dHL-60 after a 30min exposure to 5 mT LF EMFs. dHL-60 cells were exposed 30min before assay to (a) 50 Hz sine LF EMF of 5 mT (gray line) and sham (black line) or (b) 5 mT Immune LF EMFs (gray line) and sham (black line). Graphs show normalised relative fluorescence intensities representing intracellular calcium content before and after stimulation with 20 nM PAF measured every 2 s. Each line represents the average of three independent experiments of at least 12 individual calcium mobilisation measurements,  $P > 0.05$ . Mean S.E.M of every 20 s.

#### ***mRNA expression of important calcium influx pathway genes after LF EMF exposure***

To determine if LF EMF may affect expression of genes, which are related to the calcium signalling, we analysed a selection of genes by qPCR. Two validated genes, which were stably expressed during differentiation, were used to normalise all samples. After an initial screening (data not shown), nine genes were selected for qPCR analysis. These genes represent important proteins in the calcium-signalling pathway (Supplementary figure 5). Most of the genes selected for qPCR analyses are constitutively expressed in human neutrophils. Figure 5 shows the mRNA expression kinetics of the selected genes during differentiation. Expression of *CD11b* mRNA, a marker for mature neutrophils, was induced already after one day of differentiation by DMSO and showed a maximum hundred-fold up-regulation after two days. *TRPC6*, *IP3RT1*, and *STIM1* mRNA were predominantly expressed at a stable level throughout differentiation of PLB-985 cells. *Calmodulin* and *Orai1* mRNA expression was slightly increased up to 150% compared to undifferentiated cells. Furthermore, *Arp2/3*,  $\beta$ -*actin*, and *STIM2* mRNA expression was increased up till fourfold upon differentiation.

Subsequently potential effects of LF EMF on gene expression levels in fully differentiated PLB-985 cells were determined. Figure 6 shows the normalised gene expression ratio between the sham and exposure group. None of the selected genes showed a significant differential regulation after five days of exposure to 500  $\mu$ T 50 Hz sine waves or 300  $\mu$ T Immune LF EMF.

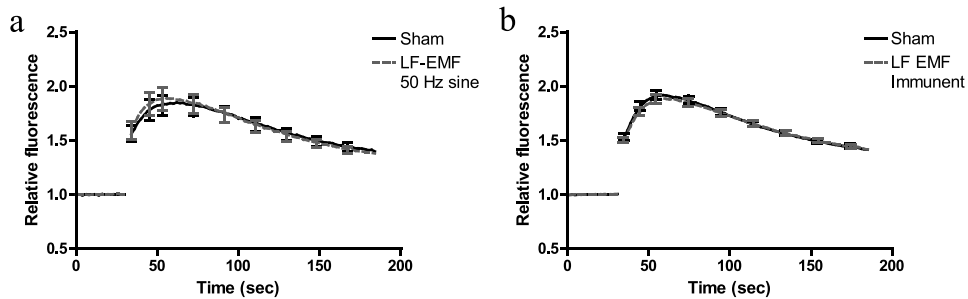


**Figure 2.** Calcium influx in dHL-60 after a 30min exposure to 300 mT and 500 mT LF EMFs. dHL-60 cells were exposed 30min before the assay to (a) 50 Hz sine LF EMF of 500 mT (gray line) and sham (black line) or (b) 300 mT Immune LF EMFs (gray line) and sham (black line). Graphs show normalised relative fluorescence intensities representing intracellular calcium content before and after stimulation with 20 nM PAF measured every 2 s. Each line represents the average of three independent experiments of at least 12 individual calcium mobilisation measurements,  $P > 0.05$ . Mean S.E.M of every 20 s.

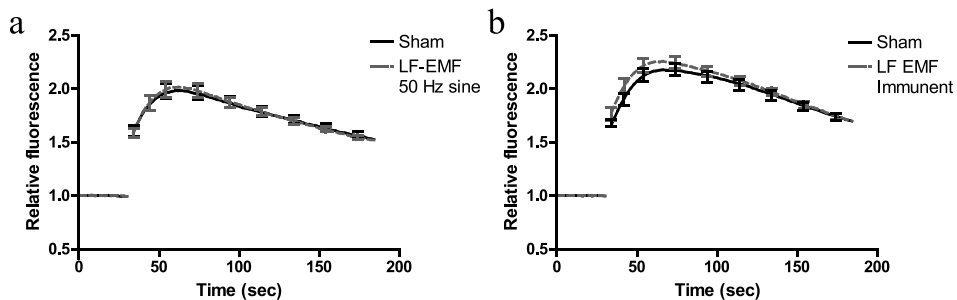


**Figure 3.** Calcium influx in dPLB-985 after five days exposed to 300 mT or 500 mT LF EMFs. PLB-985 cells were exposed for a period of five days during neutrophil differentiation to (a) 50 Hz sine LF EMF of 500 mT (gray line) and sham (black line) or (b) 300 mT Immune LF EMFs (gray line) and sham (black line). Graphs show normalised relative fluorescence intensities representing intracellular calcium content before and after stimulation with 20 nM PAF measured every 2 s. Each line represents the average of four independent experiments of at least 18 individual calcium mobilisation measurements,  $P > 0.05$ . Mean S.E.M of every 20 s.

### *Microvilli analysis after LF EMF exposure by scanning electron microscopy*

Scanning electron microscopy was used to evaluate the morphology of dHL-60 cells after a four-day exposure to sham, 300  $\mu$ T Immune or 500  $\mu$ T 50 Hz LF EMF. An overview of multiple cells showed a variety of cellular phenotypes identifiable in the samples (Fig. 7). Five distinct subpopulations could be detected and used for classification; 1) polarised cells with an early lamellipodium adhered to the glass substrate and spherical cells with 2) no protrusions, 3) up to 10% coverage with some microvilli and ruffles, 4) between 10 to 20% of the cells surface covered with microvilli, or 5) cells almost completely covered with microvilli. Categorization of the cells based on their appearances showed no significant difference in phenotype distribution between the sham and exposure groups (Table 2). Quantification of all individual microvilli is not possible with 2D-SEM images, but detailed images did not reveal alterations in the amount and shape of the microvilli on the cell surfaces after exposure to LF EMF (Fig. 7).

## Discussion

It is still considered controversial whether LF EMF exposure may lead to immune cell modulation or higher incidence of acute lymphoblastic leukaemia<sup>118,119</sup>. A number of studies have identified potential mechanisms by which the non-thermal energy of LF EMF could be transferred to an individual cell or tissue<sup>43,44,106,107,120</sup>. Calcium ions and their intracellular signalling pathways are considered prime candidate targets<sup>121,122</sup>, which is supported by multiple studies that report increase of cytoplasmic calcium mobilization upon LF EMF exposure in T-cells<sup>27-29</sup>, neutrophils<sup>31,123</sup> and osteoblasts<sup>32-34</sup>. An interesting hypothesis by Gartzke and Lange (2002) focuses on the conduction of calcium ions along actin filaments in microvilli as the cellular interaction site for LF EMF<sup>43</sup>. Our study was set out to determine if LF EMF exposure could modulate calcium signalling in human neutrophils. These sensitive immune cells possess numerous microvilli and respond quickly to an infection by a ligand-mediated calcium influx, which induces migration to the site of infection. We were unable to demonstrate a modulatory effect after exposure of neutrophil-like cells to a 50 Hz sine wave or the Immune signal on ligand-induced calcium influx, expression of genes active in the calcium signalling pathway, or the morphology of microvilli on the cell surface.

Neutrophil-like HL-60 cells exposed to 50 Hz sine wave at an environmental relevant magnetic flux density of 5  $\mu\text{T}$ <sup>9</sup> or a hundredfold higher 500  $\mu\text{T}$  did not show an altered calcium influx after an exposure period of 30 minutes. Also exposure to an irregular Immune signal at 5  $\mu\text{T}$  or 300  $\mu\text{T}$  did not evoke a different response. Pre-neutrophilic cell

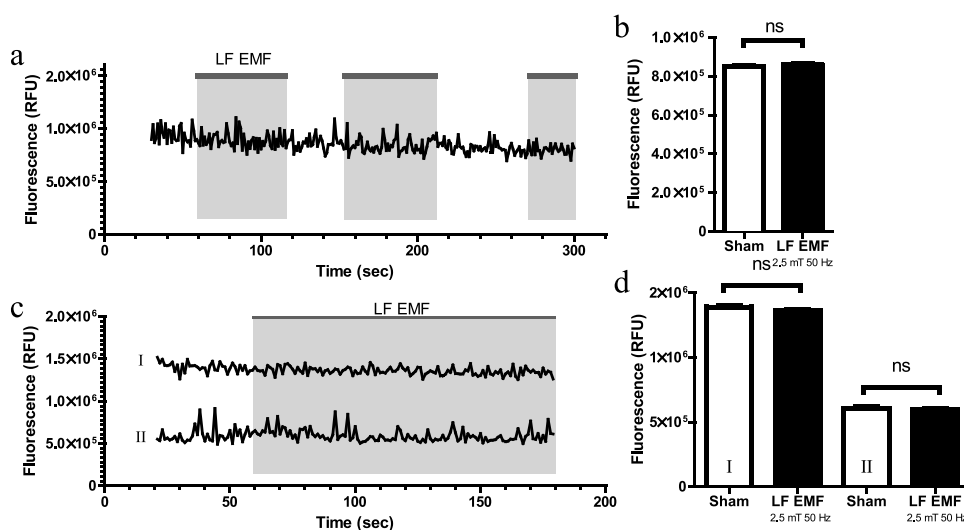


**Figure 4.** Real-time calcium measurements in PLB-985 during LF EMF exposure. Intracellular calcium content was measured in dPLB-985 cells by flow cytometry during sham and 50 Hz sine wave LF EMF exposure at a magnetic flux density of 2.5mT. Three individual samples, ac, were analyzed and fluorescent kinetics were calculated at every time point. Average calcium concentration during sham and LF EMF exposure periods were calculated for each sample b, d (I,II). Mean  $\pm$  S.E.M.

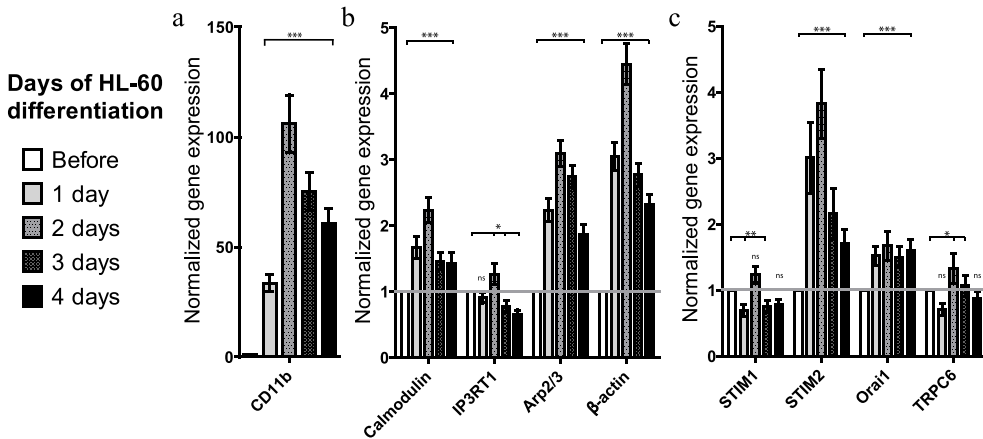


**Figure 5.** mRNA expression kinetics of calcium signalling genes during neutrophil differentiation. Relative gene expression of (a) differentiation marker CD11b, (b) important calcium channel proteins (STIM1, STIM2, Orai1, TRPC6) and (c) calcium signalling pathway proteins (Calmodulin, IP3Receptor type 1) and cytoskeletal components (Arp2/3,  $\beta$ -actin) on subsequent days after induction of differentiation in PLB-985 cells were analyzed by qPCR. Gene expression was normalised to two reference genes (OAZ, RPS13) and expressed as fold induction compared to undifferentiated cells. Mean S.E.M of three individual experiments. \* indicates  $P < 0.05$ , \*\*  $P < 0.01$  and \*\*\*  $P < 0.001$ .

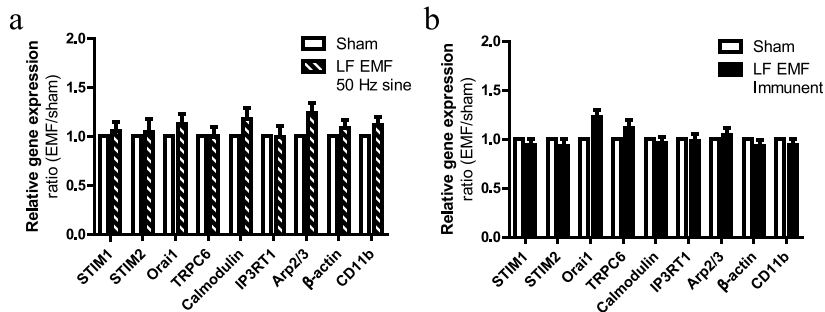


**Figure 6.** mRNA expression of calcium influx genes after five days exposed to LF EMFs. PLB-985 cells were exposed for a period of five days during neutrophilic differentiation to (a) 50 Hz sine LF EMF of 500 mT (stripped bars) and sham (white bars) or (b) 300 mT Immune LF EMF exposure (black bars) and sham (white bars). Gene expression was first normalised to two reference genes and expressed as fold induction compared to sham exposure. Pair Wise Fixed Reallocation Randomization Test  $P > 0.05$ . Mean S.E.M of five individual experiments.

lines such as HL-60 or PLB-985 differentiate during four to five days from free floating promyelocytic cells to fully functional neutrophil-like cells<sup>116</sup>. It is conceivable that an exposure period of 30 minutes is too short to induce significant changes in already differentiated neutrophil-like cells and that a developing neutrophil is more sensitive to LF EMF exposure. Extension of the exposure time from 30 minutes to the full differentiation period of five days was likewise ineffective for both wave forms. These findings indicate that in human neutrophil cell lines, calcium homeostasis related to ligand-induced influx cannot

be modified by LF EMF exposure under the tested conditions. This corroborates earlier studies that were unable to show effects of LF EMF on calcium influx or basal calcium levels in T-lymphocytes<sup>124-126</sup>, thymocytes<sup>127</sup> or neutrophils<sup>125,128</sup>. In contrast, significant effects have been reported for the same cell types<sup>27,31,129-131</sup>. Proper comparison between studies is however hampered by the use of different exposure- or experimental conditions and by the small scale of some experiments<sup>124</sup>. Our approach involved the use of a sensitive fluorescence spectrometer to assay the calcium influx in a time-resolved manner in thousands of cells at the same time, which minimised the large variation normally seen between individual cells<sup>132</sup>. In addition, we used a single wavelength dye called Fluo-4 as a calcium indicator, which is in contrast to the radiometric dye Fura-2, compatible with flow cytometry measurements and undergoes a 40- to 200-fold increase in fluorescence upon binding of calcium<sup>133</sup>. This combination enabled us to measure multiple sham and exposed samples at the same time. We thereby created a reliable assay, since sensitivity and temporal stability of the cellular response is critically temperature dependent<sup>134</sup> as is the decline of the fluorescence in time. The current research was not designed to evaluate the modulatory effect of LF EMF in single cells, which could result in an underestimation of the true effect. This is also shown in a comparative study that tried to reproduce positive results from Lindström et al. (1995). This comparative study was unable to obtain the same reproducible results, but indicated that the large incidence of cells (57% up to 85%) responding to LF EMF found in the Lindström study might be induced by pre-selection of individual cells before investigation<sup>27,124</sup>. So, one possible explanation for the inconsistency between our data and previously reported significant results may be the presence of a specific LF EMF sensitive subgroup in the neutrophil-like population. If this subgroup is relatively small, the subtle changes in fluorescence induced by LF EMF exposure may be obscured by the greater part of the sample. In addition, the influence of LF EMF exposure on calcium signalling might be reversible and therefore only detectable during exposure<sup>130,135,136</sup>. However, our primary data from real-time LF EMF exposure of neutrophil-like cells in a flow cytometric setup did not show any indications for LF EMF modulation of calcium influx. Furthermore, the potential sensitivity to LF EMF may be influenced by cell cycle<sup>137</sup>, cell activation<sup>137,138</sup>, cell morphology<sup>43,139</sup>, cell adhesion<sup>130</sup> or metabolic status<sup>129,140</sup>.

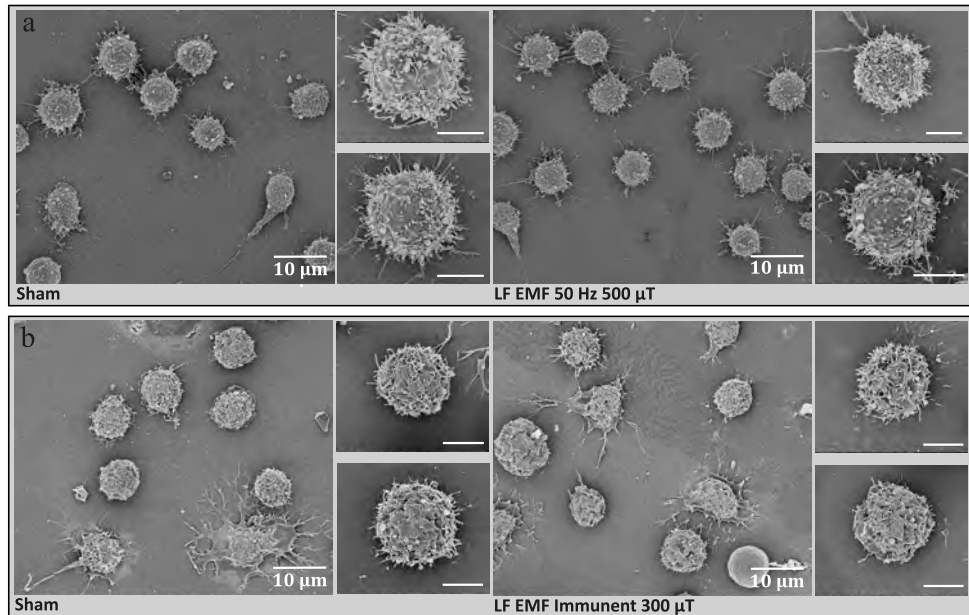


**Figure 7.** Scanning electron microscopy images of dHL-60 after four days of LF EMF exposure. HL-60 cells were exposed for a period of four days during neutrophil differentiation to (a) 50 Hz sine LF EMF of 500 mT with corresponding sham sample or (b) 300 mT Immune LF EMF exposure with corresponding sham sample. Representative overview on the left and detailed images of every group on the right (scale bars are 4 mm).

With this experimental setup we were not able to find significant modulations of ligand-induced calcium influx in human neutrophil cell lines by LF EMF, but these results do not exclude a potential harmful downstream effect after amplification of an initial subtle effect. Calcium serves as a downstream signal that is subsequently propagated and amplified. Small transient perturbations of intracellular calcium may therefore have a long-term effect on gene expression<sup>141,142</sup>. If LF EMF exposure leads to temporarily changes in the calcium homeostasis, gene expression patterns analysis after five days could reveal this. Previous studies have shown gene transcriptional changes induced by LF EMF for intermediate early genes like *CREB*<sup>143</sup>, *c-fos*<sup>131,144,145</sup>, and *c-myc*<sup>146</sup>. These well-characterised primary response genes are quickly upregulated by a rise of intracellular calcium, but it is hard to distinguish which gene regulates which promoter region of a secondary response gene<sup>147</sup>. Intermediate early genes display an interaction network that is broadly overlapping and is too extensive to accurately identify the secondary genes. Primers specific for nine secondary response genes, which encode proteins that play an important role in the calcium signalling and migration pathway of human neutrophils were selected. CD11b is an expression marker for neutrophil differentiation and expression of *CD11b* could indicate altered differentiation of neutrophils by LF EMF, like reported in HL-60 cells<sup>148</sup>. While gene expression kinetics of *CD11b* showed an upregulation of a hundredfold during neutrophil differentiation, we did not detect any changes in the mRNA expression levels of *CD11b* after five days of exposure to any of the two wave forms. Further analysis of the mRNA expression levels focussed on the expression

	Phenotype					Total
	Polarized	0%	~1-10%	>20%	>75%	
Sham	4 (7%)	0 (0.0%)	7 (13%)	18 (32%)	26 (47%)	55
50 Hz sine	8 (19%)	1 (2%)	5 (12%)	14 (33%)	15 (35%)	43

	Phenotype					Total
	Polarized	0%	~1-10%	>20%	>75%	
Sham	15 (28%)	1 (2%)	11 (20%)	10 (19%)	17 (31%)	54
Immune	15 (17%)	2 (2%)	22 (25%)	20 (22%)	30 (34%)	89

**Table 2.** Phenotypical appearance of dHL-60 after exposure to LF EMFs. The cells were categorized in five different phenotypical-groups, depending on how much of cell surface area was covered with microvilli. The number of cells showing a specific phenotype in indicated for every treatment, with the proportion of total between brackets.

of calcium channels and sensors. Endoplasmic reticulum calcium sensors *STIM1*, and paralogue *STIM2*, together with calcium channel *Orai1*, form a dynamic system that mediates ligand induced store-operated calcium entry through TRP channels. Both intracellular calcium<sup>149,150</sup> and reactive oxygen species<sup>151</sup> regulate gene expression levels of these fundamental calcium-signalling proteins. Furthermore, basal cytosolic calcium concentrations are kept within tight limits by *STIM2* via a feedback mechanism<sup>150</sup>. These molecular characteristics make *STIM1*, *STIM2*, *Orai1*, and *TRPC6* interesting genes for qPCR analysis after LF EMF exposure. However, quantitative PCR analysis of these four genes did not show a significant difference in gene expression levels after LF EMF exposure for five days compared to sham exposed cells for both wave forms. These same results were found for *calmodulin*, *IP3 receptor type 1*, *Arp2/3* or  *$\beta$ -actin* mRNA expression levels after LF EMF exposure. All investigated genes did show a small dynamic regulation of gene expression levels during neutrophil differentiation, ranging from a 0.5 decrease for *IP3 receptor* up till 4.5 fold increase for  *$\beta$ -actin* in our cell line. The genes investigated in our study are not previously reported in combination with LF EMF exposure, but the current results are in line with the cytokine gene expression in macrophages<sup>114</sup>, *NF-kB* induction in monocytes<sup>152</sup>, and heat shock protein 70 expression in neutrophil-like cells<sup>153,154</sup>. They also showed no significant effect of LF EMF on expression patterns of cell-specific secondary genes. It is possible that we are not able to notice significant changes of LF EMF, because we make *a priori* assumption with our qPCR analysis about which genes might be modulated by LF EMF. One way to overcome this problem would be to use high-throughput screening by microarray. Though, comprehensive microarray studies addressing the effect of LF EMF reported regulation of only a small percentage of individual genes<sup>155-157</sup>. The responses found ranged from 0.1% to 1% of the assayed genes, with expression fold-changes often below 2.0<sup>158</sup>. Moreover, the genes found to be influenced by LF EMF belong to different signal transduction pathways and perform diverse functions in a cell and thus the risk of conclusions based on false positives cannot

be excluded<sup>159</sup>. Occurrence of false positives is minimised by the use of housekeeping or reference genes. The current use of housekeeping genes like *GAPDH* or *β-actin* to normalise mRNA data is based on the misconception that these genes are constitutively expressed, but for accurate and reliable gene expression analysis, especially in differentiating cells, two or more reference genes are required<sup>160</sup>. The expression patterns of *β-actin*, with over fourfold upregulation during only two days of PLB-985 differentiation, clearly illustrate this. To ensure maximum reliability, we analysed three novel reference genes<sup>161</sup>; *RPL27*, *OAZ*, and *RPS13* and selected the latter two to normalise our qPCR data. Nevertheless, none of the investigated genes showed a significant difference of gene expression levels after LF EMF exposure.

The transduction mechanism for non-thermal EMF is still under debate, with theories concentrating on intracellular calcium, calcium-binding proteins like calmodulin<sup>44</sup>, reactive oxygen species production and redox status<sup>120,162,163</sup>, or cytoskeleton and cell morphology<sup>164,165</sup>. The actin cytoskeleton is sensitive to changes in cytosolic calcium and actin rearrangements are a prerequisite for the dynamic behaviour of migrating neutrophils. In 2002, Gartzke and Lange proposed a theoretical mechanism with microvilli as the site of interaction for LF EMF. Microvillar shape and elongation is regulated by ligand binding, intracellular calcium and oxidative stress<sup>166</sup>, making these dynamic and sensitive protrusions a useful indicator for subtle LF EMF modulations. For this reason, we evaluated the presence and number of microvilli on fully differentiated neutrophil-like cells by scanning electron microscopy. Exposure of HL-60 cells during a five days period of differentiation to a 500 μT 50 Hz sine wave or 300 μT Immune LF EMF did not significantly change the phenotype of the cells. All samples, exposed and sham, showed different phenotypes ranging from smooth cell surfaces to completely being covered by microvilli. Santor et al. (1997) and Tenezzo et al. (2006) did report major changes in microvilli phenotype after LF EMF exposure, but based their conclusions on two individual cells shown in their article<sup>164,165</sup>. An overview of a number of cells in combination with quantitative blinded data analysis of multiple views, like shown in this study, makes a phenotypical characterization analysis of SEM images more reliable.

In summary, *in vitro* LF EMF exposure of 50 Hz sine wave or Immune at an environmental relevant magnetic flux density of 5 μT or peak 500 μT level could not alter calcium signalling in neutrophil cell lines. This was substantiated with gene expression patterns of calcium-signalling related genes. Also the cell morphology with abundant presence of microvilli was not affected by LF EMF exposure. We therefore conclude that under these exposure conditions LF EMF will not adapt cellular neutrophil functions through modulation of calcium signalling pathways.

## Acknowledgements

The authors would like to thank Remco Westerink and Martje de Groot for helpful discussions. The scanning electron microscopy images were obtained with the help of Marcel Giesbers from the Electron microscopy centre Wageningen.



## Supplementary data

Supplementary information online

DOI: 10.1002/bem.21924

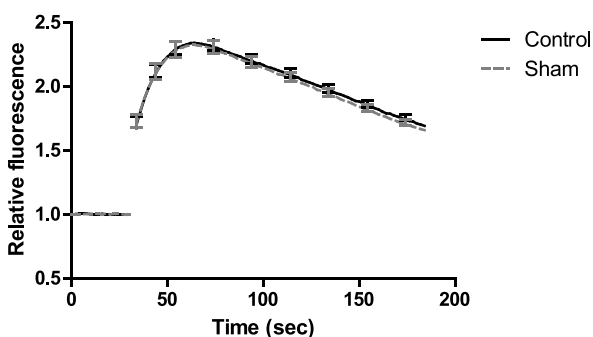


**Figure 1. Calcium influx in dPLB-985 after five days of sham-sham exposure.**

PLB-985 cells were cultured for a period of five days during neutrophilic differentiation in two separate incubators with both an unenergised coil inside (Control; black line and Sham; Grey dotted line). Graphs show normalized relative fluorescence intensities representing the intracellular calcium content before and after stimulation with 20 nM PAF measured every two seconds. Each line represents the average of 3 independent experiments of at least 15 individual calcium mobilization measurements. Mean  $\pm$  S.E.M of every 20 seconds

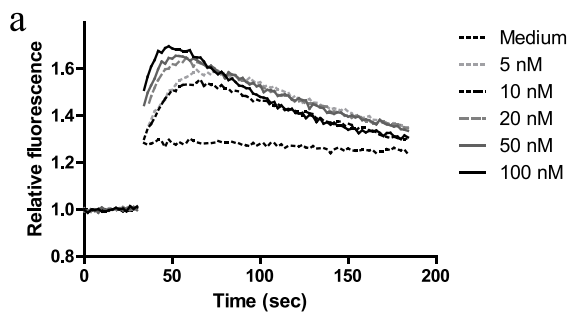


**Figure 2a. Calcium influx in dHL-60 induced with ascending concentration of PAF.**

Calcium influx was induced in differentiated HL-60 cells with PAF at different concentration. Graphs show normalized relative fluorescence intensities representing the intracellular calcium content before and after stimulation with the indicated concentration of PAF and measured every two seconds. Each line represents the average of 2 independent experiments with at least 4 individual calcium mobilization measurements.

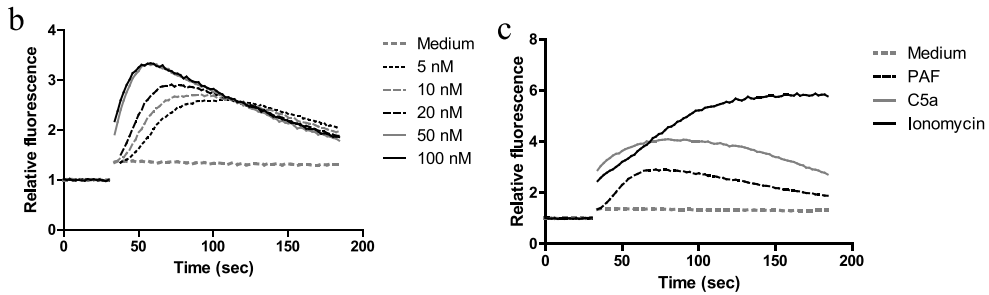


**Figure 2b, c. Calcium influx in dPLB-985 induced with PAF, C5a and ionomycin.**

Calcium influx was induced in differentiated PLB-985 cells with (b) PAF at different concentration or (c) culture medium, 20 nM PAF, 750 nM C5a, 110 nM ionomycin. Graphs show normalized relative fluorescence intensities representing the intracellular calcium content before and after stimulation with the indicated stimulus and measured every two seconds. Each line represents the average of 2 independent experiments with at least 4 individual calcium mobilization measurements.

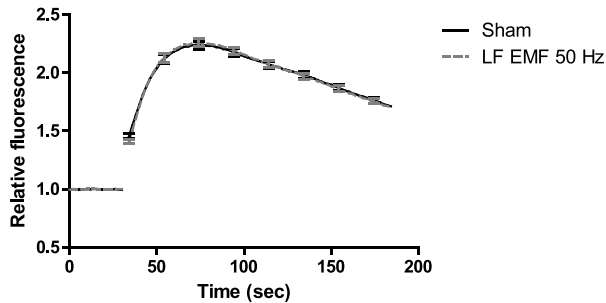


**Figure 3. Calcium influx in PLB-985 after five days exposed to 500  $\mu$ T LF EMF.**

PLB-985 cells were exposed for a period of five days during neutrophil differentiation to 50 Hz sine LF EMF of 500  $\mu$ T (grey line) or sham (black line). Graphs show normalized relative fluorescence intensities representing the intracellular calcium content before and after stimulation with 500 nM C5a measured every two seconds. Each line represents the average of 4 independent experiments with at least 8 individual measurements. Mean  $\pm$ S.E.M of every 20 seconds

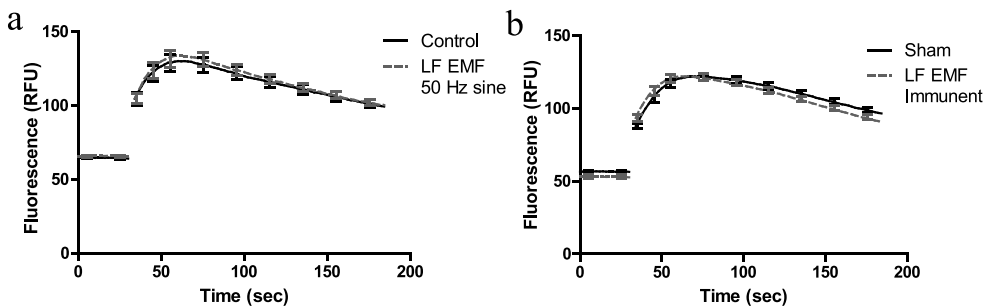


**Figure 4. Calcium influx in dPLB-985 after five days exposed to 300  $\mu$ T or 500  $\mu$ T LF EMF.**

PLB-985 cells were exposed for a period of five days during neutrophilic differentiation to (a) 50 Hz sine LF EMF of 500  $\mu$ T (grey line) and sham (black line) or (b) 300  $\mu$ T Immune LF EMF exposure (grey line) and sham (black line). Graphs show normalized relative fluorescence intensities representing the intracellular calcium content before and after stimulation with 20 nM PAF measured every two seconds. Each line represents the average of 4 independent experiments with at least 18 individual measurements. Mean  $\pm$ S.E.M of every 20 seconds.

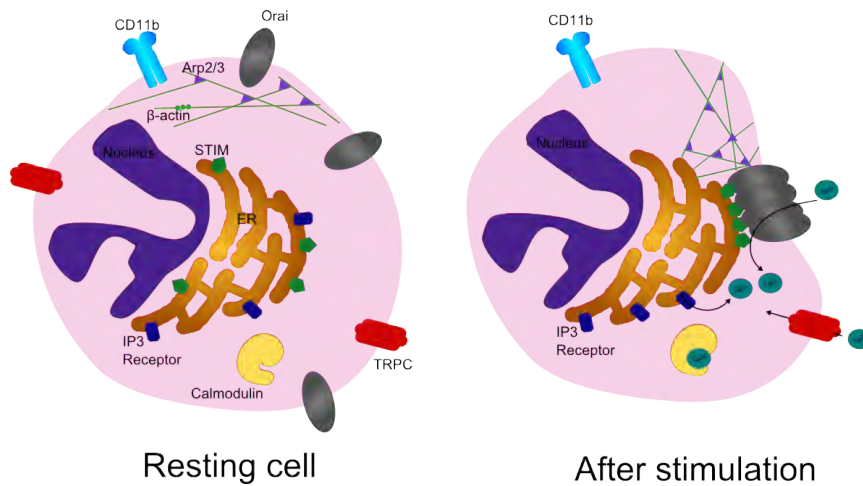
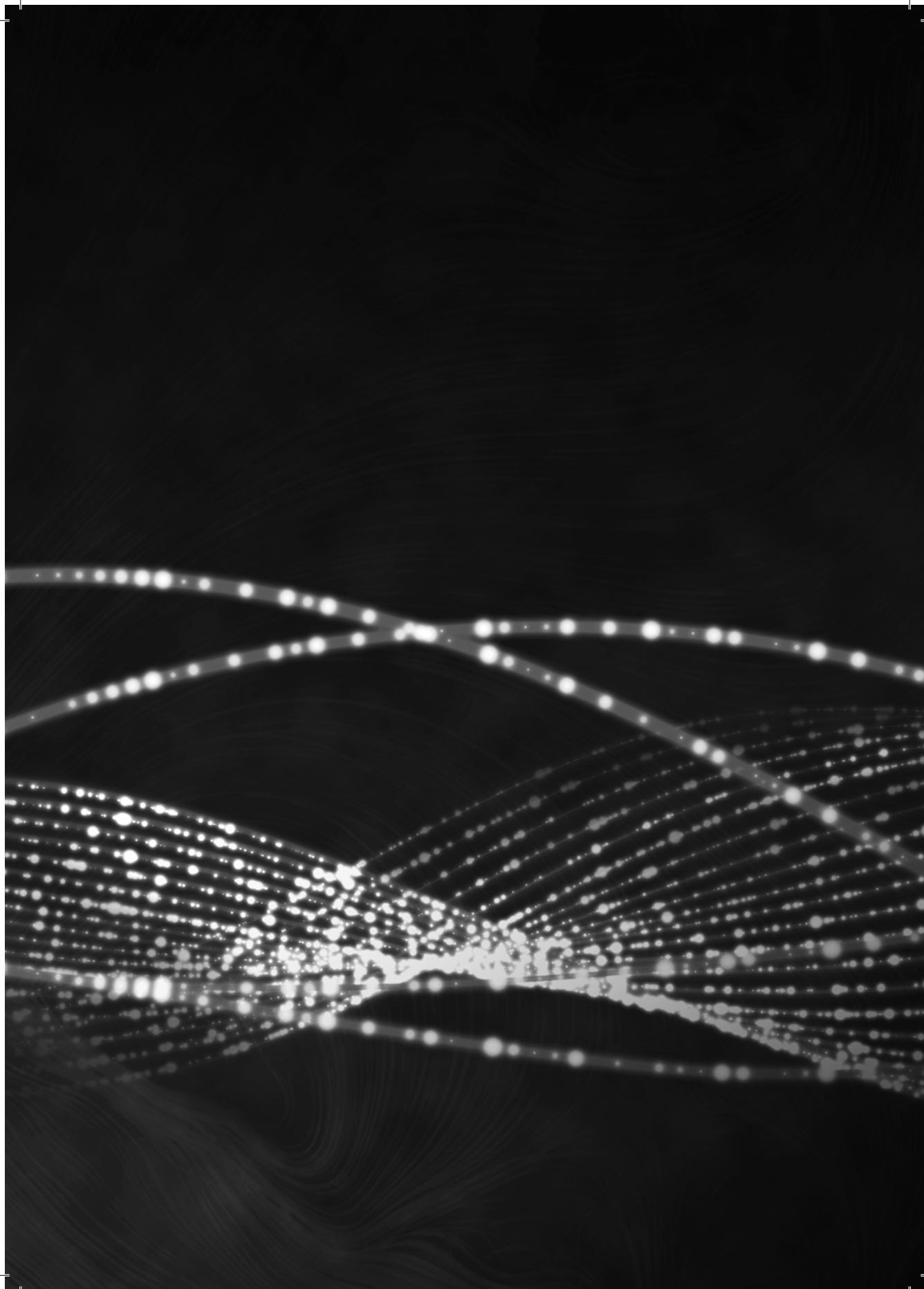


**Figure 5. Schematic drawing of the role of selected genes in the calcium influx pathway**

A neutrophil, characterized by high CD11b expression, stores calcium inside the endoplasmic reticulum (ER). On the membrane of the ER are amongst others IP3 receptors and STIM proteins. Cellular activation via G-protein coupled receptors leads to activation of phospholipase C (PLC), which stimulates the production of inositol 1,4,5-trisphosphate (IP3) and diacylglycerol (DAG) (Not indicated in the figure). IP3 triggers release of calcium from the ER through IP3 receptors. Subsequently, the cytoskeleton consisting filaments of  $\beta$ -actin subunits and Arp2/3 crosslinking proteins redirect the ER towards the outer membrane of the cell. The STIM on the calcium-store membranes communicates with plasma membrane channels (Orai) and TRPCs to release more intracellular stored calcium and regulate an influx of extracellular calcium. To restore the calcium balance after influx, calmodulin binds cytoplasmic calcium ions.



# Chapter 3

---

## **Calcium homeostasis and low-frequency Calcium homeostasis and low-frequency magnetic and electric field exposure: A systematic review and meta-analysis of *in vitro* studies**

L. .A. Golbach, L.A. Portelli, S.R. Terwel, H. F.J. Savelkoul, N. Kuster, R.B.M. de Vries, B.M.L. Verburg-van Kemenade

*Manuscript under review*  
*Journal: Environment International*

## Abstract

Low frequency electromagnetic field (LF MF) exposure is recurrently suggested to induce health effects in society. Therefore, *in vitro* model systems are used to investigate biological effects of exposure. LF MF induced changes of the cellular calcium homeostasis are frequently hypothesised to be the possible target, but this hypothesis is both substantiated and rejected by numerous studies in literature. Despite the large amount of data, no systematic analysis of *in vitro* studies has been conducted to address the strength of evidence for an association between LF MF exposure and calcium homeostasis. Our systematic review, with inclusion of 42 studies, showed evidence for an association of LF MF with internal calcium concentration and calcium oscillation patterns. The oscillation frequency increased and the amplitude reduced, while the percentage of oscillating cells remained constant. The intracellular calcium influx increased (SMD 0.351, 95% CI 0.126, 0.576). Subgroup analysis revealed heterogeneous effects associated with the exposure frequency, magnetic flux density and duration. Similar effects were found to support the presence of MF-sensitive cell types. Nevertheless, there may be a great risk of bias introduced in the included studies, through uncontrolled or not reported exposure conditions, temperature ranges and ambient fields. In addition, mathematical calculations of the parasitic induced electric fields showed to be associated with increased intracellular calcium. Our results demonstrate that LF MF might influence the calcium homeostasis in cells *in vitro*, but the risk of bias and high heterogeneity ( $I^2 > 75\%$ ) weakens our analyses. Therefore any potential clinical implications await further investigation.

## Introduction

Low-frequency magnetic fields (LF MFs) generated by power distribution and usage have led to ever increasing public concerns regarding its potential to induce harmful biological effects. Some of the consequences commonly attributed, at least in part, to LF EMF exposure range from non-specific physical symptoms such as sleep disorders and headaches <sup>167</sup> to very specific ones like childhood Leukaemia <sup>3</sup>, breast cancer and Alzheimer's disease <sup>168</sup>. However, direct evidence supporting an association between exposure and health status appears to be insufficient and inconsistent <sup>4,5,169</sup>.

The concern for the possibility of harmful health effects in combination with scientific curiosity have led to the proposal of multiple potential mechanisms of action of LF MF on biological systems as well as to a large pool of *in vivo* and *in vitro* experimental results <sup>170,171</sup>. A subgroup of these studies have calcium homeostasis modulation by LF MF as a common denominator, with experiments on cell lines and primary cell cultures <sup>31,121,137,172</sup> and with several attempts to explain or predict this interaction in a mechanistic way <sup>41,43,44</sup>. For example, it has been suggested that cationic nature of the calcium ion could make it susceptible for induced electric fields (IEFs) that LF MF generate in solution <sup>43,173</sup>. The biological relevance of this presumed target for LF MF-cell interaction lies within the notion calcium is the most abundant and most pivotal second messenger in the cell. Calcium signalling is crucial for cell function and survival <sup>174,175</sup> and it can act as an intrinsic stressor that indicates cellular damage within minutes after the imposed insult <sup>176,177</sup>. Efficient calcium signalling needs maintenance of calcium homeostasis, requiring cytosolic calcium concentrations to stay low and stable by storage of calcium ions in the endoplasmic reticulum <sup>178</sup>. However, upon activation, calcium is released from these stores into the cytoplasm and an intracellular signalling cascade is initiated. This subsequently regulates a second influx of extracellular calcium from the environment. Hence, calcium signalling results from a complex interplay between activation and inactivation of intracellular and extracellular calcium permeable channels. These fluxes of intracellular calcium can occur in the form of transient increases or repetitive calcium oscillations, which both ultimately lead to altered cell activity <sup>178,179</sup>.

Over time, multiple potential targets of LF MF exposure and multiple mechanisms of interaction were proposed <sup>41,43,44</sup>, however conflicting results to support such theories have been consistently reported. Some of the differences in experimental outcomes might be explained by the use of specific experimental parameters such as signal frequency <sup>180</sup>, IEF <sup>63</sup>, or specific cell type(s) sensitivity to exposures <sup>41,172</sup>. However, apparently conflicting *in vitro* results have obscured the support for any of these theories. On the other hand, further variability might be explained by unaccounted heterogeneity on the apparently controlled LF MF parameters on the exposure systems.

By now, sufficient data are present to systematically investigate the effect of LF MF exposure on calcium homeostasis, therefore we conducted a systematic review and meta-analysis <sup>181</sup>. For this, we first selected a group of *in vitro* studies based on a strict set of quality criterion on both the biological and physical aspects of the reported data. Subsequently, we examined if the effects depend on the use of a particular cell type, type of calcium assay and specificities of magnetic or electric field exposure; frequency, magnitude, duration of exposure. Finally, we examined the reported biological effects in terms of possible differentials in LF MF exposure introduced by unaccounted technical aspects on the exposure systems.

## Methods

### Study identification

The following electronic databases were searched to find any original articles concerning the effect of LF EMFs on calcium in *in vitro* cell cultures (searched up until January 1, 2015): PubMed, Web of Science, Scopus, and EMBASE (via OvidSP). The search strategy was composed of three elements: LF MF, calcium and an element intended to exclude studies on high frequency fields, with a wide range of keywords and combinations adapted for every database/search engine (for full search strategy see Table 1). Furthermore, the reference list of the selected papers and reviews were screened for potentially relevant papers. During the search, no language selection was applied. All inclusion criteria and methods of analysis were specified *a priori* in a protocol.

PubMed	
<b>Calcium</b>	Calcium [MeSH] OR calcium [tiab] OR CA [tiab] OR Ca2+ [tiab]
<b>EMF</b>	(Electromagnetic Fields [mesh] OR (electromagnetic [tiab] AND field [tiab]) OR (electromagnetic [tiab] AND fields [tiab]) OR (electromagnetic [tiab] AND radiation [tiab]) OR (electromagnetic [tiab] AND radiations [tiab]) OR (electromagnetic [tiab] AND irradiation [tiab]) OR (electromagnetic [tiab] AND irradiations [tiab]) OR EMF [tiab] OR EMFs [tiab])
<b>Exclusion</b>	(radio[tiab] OR RF-EMF [tiab] OR RF-EMFs [tiab] OR static [tiab] OR MHz [tiab] OR megahertz [tiab] OR THz [tiab] OR terahertz [tiab])
Web of Science	
<b>Calcium</b>	TS=(calcium OR Ca OR Ca2+)
<b>EMF</b>	TS=((electromagn* near/3 (field* OR *radiation* )) OR EMF OR EMFs)
<b>Exclusion</b>	TS=(radio OR RF-EMF OR RF-EMFs OR static OR MHz OR megahertz OR THz OR terahertz)
Scopus	
<b>Calcium</b>	TITLE-ABS-KEY("calcium") OR TITLE-ABS-KEY ("ca") OR TITLE-ABS-KEY("Ca2+")
<b>EMF</b>	TITLE-ABS-KEY("Electromagnetic Field") OR TITLE-ABS-KEY("Electromagnetic ")
<b>Exclusion</b>	TITLE-ABS-KEY(" radio") OR TITLE-ABS-KEY(" RF-EMF") OR TITLE-ABS-KEY ("MHz") OR TITLE-ABS-KEY(" terahertz") OR TITLE-ABS-KEY(" static")
EMBASE	
<b>Calcium</b>	Exp Calcium/ OR (calcium OR Ca OR Ca2+).ti,ab.
<b>EMF</b>	(Exp electromagnetic field/ OR Exp electromagnetic radiation/ OR ((electromagnetic AND (field OR fields OR radiation OR radiations OR irradiation OR irradiations)) OR EMF OR EMFs).ti,ab.)
<b>Exclusion</b>	(radio OR RF-EMF OR RF-EMFs OR static OR MHz OR megahertz OR THz OR terahertz).ti,ab.



### *Study selection*

The first screening of potentially relevant studies was performed based on title and abstract independently by two investigators (L.A. Golbach and B.M.L. van Kemenade). After screening, full text versions from the remaining papers were obtained if possible. All full text papers were evaluated based on the defined selection criteria by the same two investigators. Possible disagreement between investigators or technical uncertainties in the publications were resolved by a third investigator (L.A. Portelli).

For paper inclusion based on title and abstract, the following criteria were used:

*Exposure:* Only studies applying magnetic fields with frequencies between 1 and 300 Hz, no static magnetic fields.

*Set-up:* The studies should examine the effect of LF MF exposure on animal or human cells in an *in vitro* set-up. Studies that report direct animal exposure with subsequent analysis of individual cells were not included in the analysis, though isolation of cells from a primary source before exposure was included (*ex vivo* set-up). In addition, studies reporting experiments conducted on prokaryotes, algae, or fungi were excluded as well.

*Reporting:* The studies should report primary peer-reviewed data, reviews and meeting abstracts were not included.

For full-text inclusion, the following criteria were used:

*Exposure:* Only studies applying LF MFs with frequencies between 1 and 300 Hz, no static magnetic fields. The exposure systems details needed to be reported in such a way that uncertainty on the exposure parameters could be reasonably quantised therefore allowing for the reproduction of the conditions. A complete description of the assumptions, estimations and calculations performed is found in supplementary note 1 and supplementary table 3.

*Calcium:* The calcium assays reported in the studies should measure actual calcium release, uptake, fluctuations or homeostasis without the use of pharmacological inhibitors. Path-clamp experiments were excluded, since the measurements require short electrical pulses to evoke calcium release. Studies reporting deposition of solid calcium minerals were also excluded.

*Set-up:* The studies should examine the effect of LF MF exposure on animal or human cells in an *in vitro* set-up. Studies that report direct animal exposure with subsequent analysis of individual cells were not included in the analysis, though isolation of cells from a primary source before exposure was included (*ex vivo* set-up). In addition, studies reporting experiments conducted on prokaryotes, algae, or fungi were excluded as well.

*Reporting:* A language restriction was applied, only articles reporting in English were included in the analysis. The studies should report primary peer-reviewed data, so reviews and meeting abstracts were not included, however reviews were used to screen for missing articles. If the full text was not available online, neither through the library nor after contacting the authors, the article was excluded from the analyses.

### *Study characteristics and data extraction*

For each included study, the following data were extracted: official cell type or cell line name, origin of cellular material, type of cells, dependent or independent control/sham groups, exposure frequency, duration and timing of exposure, magnetic flux density, type of calcium assay, batch or single measurements and stimulation of a calcium influx. Bibliographic details of the studies such as corresponding author, journal and year of publication were also retrieved (Table 1 Supplementary data).

From all studies (s), number of events or mean, standard error (SE) or standard deviation (SD) and number of measurements or individual cells (n) of control/sham and exposure groups were recorded. When the data from individual experiments or animals rather than aggregated data were presented<sup>121,129,182</sup> mean and SD were calculated. If data were only available in a graphical representation, values were measured with a digital ruler (Universal Desktop Ruler). Authors were contacted to obtain missing data on sample size, SD or SE. If a value was missing and authors did not respond, an estimate of the sample size was made by mathematical calculations with the SD or SE obtained from the graph(s) and the possible sample sizes reported in the paper. This was only performed for the data extracted from Lisi, 2006<sup>183</sup> and Pilger, 2004<sup>184</sup>. For further specific details regarding these calculations, contact the corresponding author. Two experiments<sup>185,186</sup> and nine papers were excluded from the meta-analysis, as we were unable to obtain the required data<sup>27,125,127,187-192</sup>.

### *Assessment of risk of bias and reporting quality of included studies*

The methodological quality of the included studies was determined using predefined criteria (Supplementary Table 2). For *in vitro* studies, no standard quality assessment tool exists; we therefore developed these criteria ourselves. Two reviewers (L.A. Golbach, B.M.L. van Kemenade) independently scored the selected papers for these criteria. The criteria shown in table 2 were meant to assess the risk of systematic errors due to selection, performance or detection bias. The risk of these different biases was scored with “Low”, “Moderate”, or “High”. When a paper lacked the necessary details to assess the risk, the risk was categorised as “Risk Unknown”. Furthermore, we assessed the lack of reproducibility due to poor or incomplete reports (reporting quality). “No”, “Partly” or “Yes”, indicated the presence (“Yes/Partly”) or absence (“No”) of essential information regarding the study design and experimental controls.

### *Data synthesis and statistical analysis*

First, the type of calcium assay that was used was determined for every paper. From experiments that measured intracellular calcium concentrations with radioactive calcium (<sup>45</sup>Ca) or with a fluorescence dye, the mean, SD/SE and sample size were extracted, to calculate standardised mean differences (SMD). The same was done for studies that described continuous data related to the calcium oscillations. For studies only describing a number of events, the Odds ratio was calculated. If outcomes were measured in independent experiments with different frequencies, magnetic flux density or cell types, then all outcome values were noted. If the outcome of one sample was determined on multiple time points, being a dependent measurement in time, the moment with the largest difference between sham/control and EMF treatment was selected for both the baseline and the stimulation moment. However, if outcomes were determined at different time points using separate independent

samples, all time points were included. When the intracellular calcium concentration of resting cells, and subsequently the concentration during stimulation of a calcium influx was measured under sham and EMF conditions, both outcomes were noted<sup>137,193</sup>. From these double datasets, only data from the stimulated sample were used for the overall analysis.

	Yes	Partly	No	Risk unknown
<i>Is the cell origin and cell type used reported?</i>	Reported	Not clearly reported	Not reported	-
<i>Is the duration of exposure reported?</i>	Reported	Not clearly reported	Not reported	-
<i>Is the frequency of exposure reported?</i>	Reported	Not clearly reported	Not reported	-
<i>Is the magnetic flux density of exposure reported?</i>	Reported	Not clearly reported	Not reported	-
<i>Environmental background magnetic field reported</i>	AC/DC reported	AC or DC reported	Not reported	
<i>Is a sham or dummy coil used for control treatment?</i>	Yes	-	No	Not reported
<i>Is the temperature controlled?</i>	Yes, with SE	Yes, without SE	No	Not reported
<i>Was the exposure blinded?</i>	Yes	-	No	Not reported
<i>Was the exposure randomised?</i>	Yes	-	No	Not reported
<b>Selection Bias</b> <i>Is the cell vitality scored/measured?</i>	Yes	-	No	Not reported
<i>Were the methods the same for control and exposure treatment?</i>	Yes, independent measurements	Dependent measurements	No	-
<i>Were the data measurements randomised?</i>	Yes	-	No	Not reported
<b>Other Bias</b> <i>Was there no industry sponsoring involved</i>	Yes	-	No	-

**Table 2.** Reporting quality and risk of bias scheme.

The SMD, odds ratios and effect sizes were calculated with specialised software, Comprehensive Meta Analysis (CMA version 2.0). Individual effect sizes were pooled to obtain an overall effect size and 95% confidence interval with a random effect size model. Based on the study characteristics of every experiment, subgroups were determined. Subgroup analyses were planned for the following study characteristics: the type of cells used, exposure frequency, magnetic flux density, and duration of the LF MF exposure, and single cell or batch analysis of the intracellular calcium concentration. For the calcium oscillation studies, individual analyses were planned for three types of outcome measures. All subgroups should consist of data from at least three individual papers or five independent experiments. The effect sizes and confidence intervals of the overall analyses and subgroup analyses were displayed in a forest plot. Heterogeneity was calculated in CMA and expressed as  $I^2$ , which is the proportion of variability in a meta-analysis that is explained by between-trial heterogeneity rather than by sampling error<sup>194</sup>. We performed a sensitivity analysis, to assess the robustness of our findings by removing studies in which we made calculated estimates of the mean, SD or N<sup>195</sup>. If the direction of the effect greatly depended on the removed studies, then the results would have to be interpreted with great caution.

#### *Electric and magnetic field exposure assessment*

A thorough survey of the exposure conditions reported in literature was performed to extract all relevant information of the electric and magnetic field exposure parameters at the culture space. Only publications which provided enough explicit or implicit information about their exposure conditions were included in this study. Crosschecks were made between reported and calculated exposure values in order to establish the most accurate parameters of the magnetic and electric field exposure for each report. A complete description of the assumptions, estimations and calculations performed is found in supplementary note 1 and supplementary table 3. Briefly, the signal type, magnitude, spatial distribution and the geometrical characteristics of the culture container were extracted for each exposure condition. Based on this data, maximum and minimum electric and magnetic fields to which cultures were exposed were calculated utilizing the most extreme combination of exposure parameters setting upper boundaries and uncertainties for each exposure condition from the ones reported. In the case of exposures under a microscope, calculations were also made based on the largest radius of the field of view of the specific objective utilised and correction factors were introduced to account for possible artefacts introduced by the metallic objectives on the imposed and induced fields. Additionally, the assessment also included the presence of unshielded parasitic electric fields and artificially generated background magnetic fields which were also combined based on estimated or directly reported values.

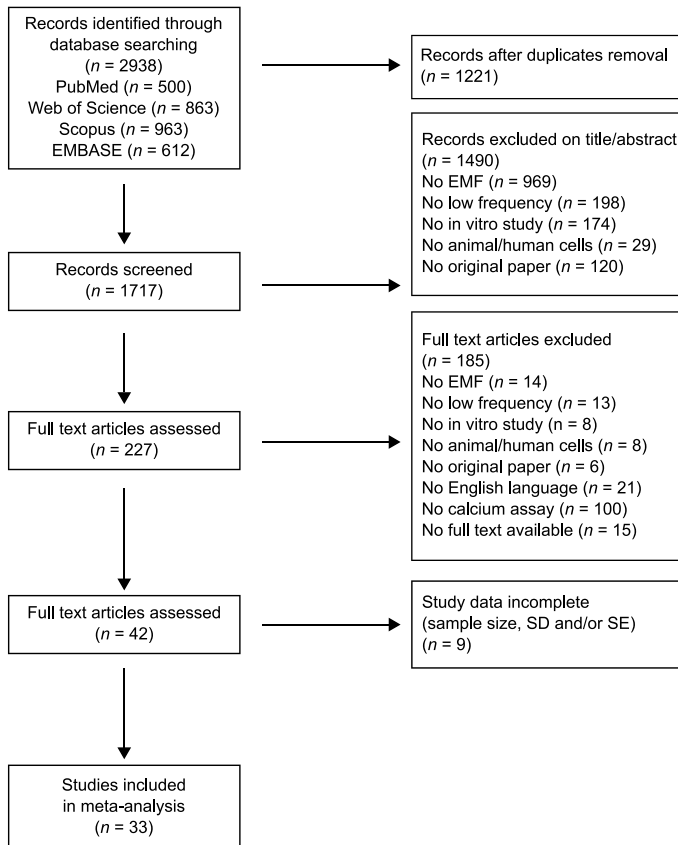


**Figure 1.** Flow diagram of the systematic review protocol illustrating the literature search and exclusion process.

## Results

### *Study selection and characteristics*

The search strategy performed in this paper was designed to retrieve all papers related to LFMF exposure and calcium homeostasis. The search terms were kept broad for every search engine, which led to 1717 potential papers in the initial phase (Fig. 1). From these articles, 1490 articles could already be excluded based on title and abstract, since they did not describe the exposure of cells to magnetic fields. Further investigation of the 227 remaining papers based on their full-text led to inclusion of 42 studies<sup>27,28,60,63,121,124-127,129,136,137,146,182-193,196-212</sup>.

Study characteristics of all included papers are shown in supplementary table 1, including the characteristics of every individual experiment/comparison. These study characteristics varied considerably between the included papers. All *in vitro* experiments included in our study are performed with cells extracted from a multicellular organism. They were either immortalised cell lines, which were established through isolation of cancer cells or induction of mutations, or primary *ex vivo* cell cultures. From the 148 experiments, 72

were performed with cell lines and 76 with primary cells. Mice, rats and humans were the most commonly used species, as only two studies performed experiments with cells from cows<sup>197</sup> and pigs<sup>200</sup>. The EMF exposure characteristics were more diverse: the magnetic flux densities ranged from 40 nT to 22 mT and duration of exposure from a couple of minutes to many days. In almost two-third of the studies, the cells were exposed to 50 or 60 Hz (92 of the 148) and only in 15 experiments a specific calculated calcium resonance frequency was applied. With respect to the timing of exposure, a little over two-third of the experiments was carried out with a calcium measurement during acute exposure (105 of 148).

To examine the effect of EMF exposure, all papers compared EMF-exposed samples to sham exposed ones, however the definition of control/sham differed. To minimise sample variation, a sample or cell was used as its own control in 26 of the experiments and 122 experiments performed independent measurements during or after sham or EMF exposure.

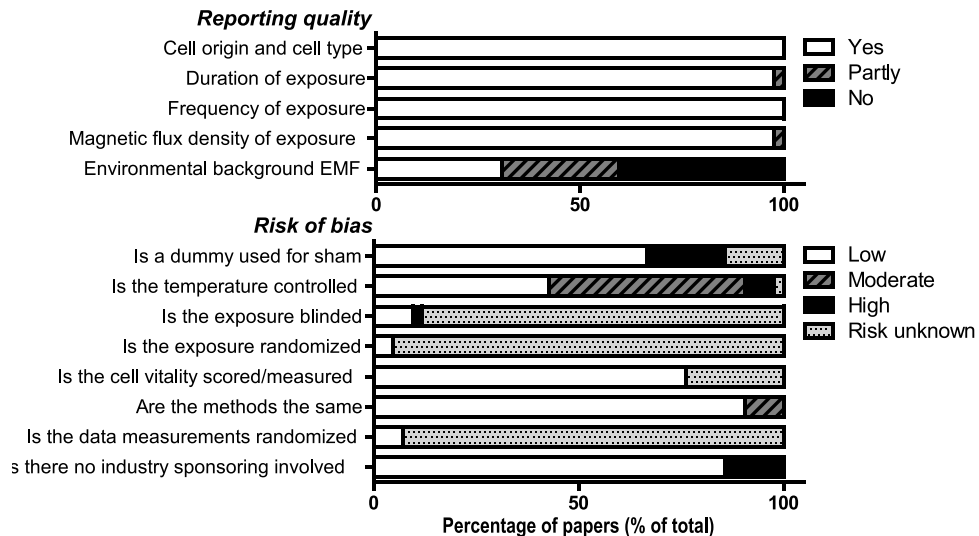


**Figure 2. Reporting quality and risk of bias.** Average score in percentage of all 42 papers. For the reporting quality, papers were scored. “Yes”, “Partly” or “No” indicates the presence or absence of essential study details. For the risk of bias, a “Low”, “Moderate” or “High” risk of bias might be introduced in the studies. If the outcome was not reported or mentioned, the “risk is unknown” and scored accordingly.

### Reporting quality and risk of bias

The reporting quality of all included papers showed large differences (Fig 2). While the cell type, duration, frequency and magnetic flux density were mentioned in all of the papers, only ~30% described the ambient electromagnetic and static fields during the exposure. Moreover, 40% did not mention any values for these environmental fields. Furthermore, our risk of bias assessment showed large or unknown risks. All papers clearly described the frequency and magnetic flux density that was applied to the cells, however only two-third (64.3%) described the use of sham exposure or an unenergised coil for the control condition. One out of ten studies lacked an identical protocol to measure control and LF MF samples and in 78% of the studies the vitality of the cells before or after exposure was

scored. The largest unknown risks are introduced by not reporting blinding of exposure, and randomisation of exposure and measurements. Additionally, although temperature control during exposure was described in more than 90% of all papers, with half of them also reporting the error range, measurements were typically made outside of the culture space which also sets this variable as a possible important artefact. For potential industry sponsoring, 6 of the 42 papers reported a connection or employment at a company, which might increase the risk of biased outcomes.

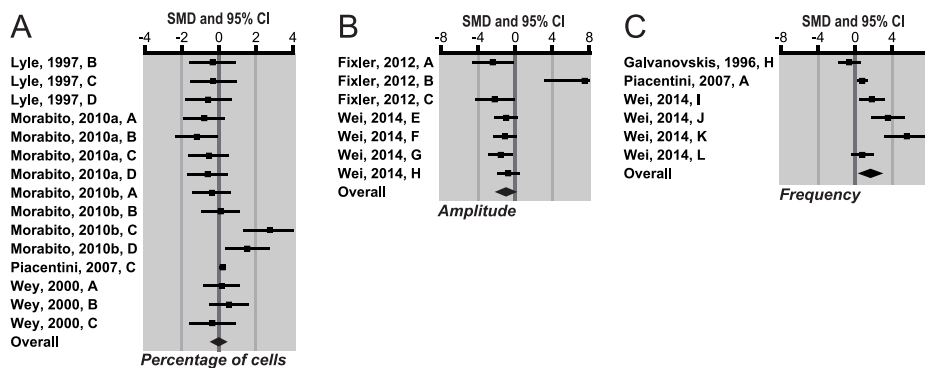


**Figure 3. Influence of LF MF exposure on calcium oscillations.** Forest plot for the three different outcomes regarding calcium oscillations. a) The percentage of cells that showed an altered oscillation pattern during sham/exposure, b) changes in the frequency or c) amplitude of the calcium waves. The forest plot displays the SMD (squares) and 95% confidence interval of the individual studies. The diamond indicates the overall estimate and 95% confidence interval. Meta-analysis

### *Intracellular calcium oscillations*

Twelve papers investigating the effect of LF EMF exposure on calcium oscillations could be included in our meta-analyses. Four of the eleven papers reported dichotomous outcomes, from which one used dependent measurements. This study was not included in our analysis. The other event in the three papers were grouped and odds ratio with a 95% CI was calculated (Supplementary Fig. 1).

In the remaining eight papers, oscillation patterns were measured in 15 experiments, from which only three showed a significantly different oscillation pattern compared to control treatment. The overall effect analysis did not indicate a significant effect of exposure (fig. 3A; SMD -0.007 [-0.392, 0.378];  $n=15$ ;  $s=5$ ). Two studies that together performed seven experiments measured the amplitude of the waves during or after exposure. Three out of seven indicated a statistically significant decrease of amplitude compared to control conditions. The overall effect of these seven experiments showed no effect on the amplitude of calcium oscillations (SMD -0.994 [-2.013, 0.024];  $n=7$ ;  $s=2$ ). The last outcome measure, frequency of the oscillating waves, showed a mixed effect when comparing the six included experiments: five experiments showed an increase and two experiments a neutral effect. Nevertheless, overall analysis showed a statistically significant effect of LF EMF exposure on the frequency of the calcium waves (SMD 1.669 [0.488, 2.849];  $n=6$ ;  $s=3$ ).

### *Intracellular calcium concentration*

Reliable measurements of intracellular calcium concentrations can be performed

with the stable artificial radioisotope  $^{45}\text{Ca}$ , to only measure the entry of calcium from the external medium into the cells. A second approach is the use of chemical fluorescent dyes to quantify the intracellular calcium concentration. These dyes facilitates investigation of potential functions and regulatory mechanisms of calcium in a cell, such as channels and pumps. Of the studies included in our review, 24 investigated the effect of LF MFs on the intracellular calcium concentration using one of the methods described above. We determined the presence of an effect regardless of direction, by expression all differences between control and LF MF exposure as a positive value. This analysis only indicates the presence of an effect, but cannot be used to determine the overall direction or effect size. Subsequently, both positive and negative effects were analysed using their original direction. This second analysis is used to estimate the overall direction and effect size. Our intracellular calcium analyses contained 24 studies with 81 experiments. Overall, the presence of an effect of LF MF exposure on intracellular calcium was shown (SMD 0.914 [0.723, 1.104];  $n=81$ ;  $s=24$ ) (Fig. 4a). Forty-nine of the 81 experiments showed no significant influence of LF MF exposure on the intracellular calcium concentration. In addition, 22 experiments showed an increase in calcium, and ten reported a significant reduction of the intracellular concentration. The overall analysis of all 24 papers indicated that the direction of this effect was positive, with a small significant increase in intracellular calcium by LF MF exposure (SMD 0.351 [0.126, 0.576];  $n=81$ ;  $s=24$ ) (Fig. 4b). Heterogeneity was high ( $I^2= 83\%$ ) and reported standardised mean differences (SMD) ranged from to -10.39<sup>200</sup> to 21.62<sup>198</sup>.

#### ***Subgroup meta-analysis of study characteristics***

The included intracellular calcium studies contained sufficient datasets to perform multiple subgroup comparisons, based on characteristics (supplementary table 1) determined *a priori*. All experiments were combined in subgroups and analysed in two ways. First we determined the presence of an effect and secondly provided an estimate of the effect size and direction. In figure 5, the effect of the different subgroups is shown, expressing the effects in one direction. The lower limits of the confidence intervals of all subgroups were above zero, which indicated the presence of an effect of LF MF exposure for every subgroup. However, the direction and magnitude of these effects differed between subgroups (Fig. 6). A large number of fluorescent calcium indicators are available for *in vitro* studies to investigate intracellular calcium concentrations and calcium mobilization in cells<sup>213</sup>. Intracellular calcium measured with any of the fluorescent calcium dyes showed no significant difference compared to control, both during and after exposure (*Dye-during*; SMD 0.137 [-0.104, 0.378];  $n=23$ ;  $s=5$ ; and *Dye-after*; SMD 0.066 [-0.261, 0.393];  $n=28$ ;  $s=13$ ). The isotope  $^{45}\text{Ca}$ -studies on the other hand, showed a significant increase in intracellular calcium under the influence of LF EMF exposure ( $^{45}\text{Ca}$ ; SMD 1.018 [0.342, 1.694];  $n=30$ ;  $s=6$ ). Comparison of the three techniques showed no significant difference between the effects.

To examine if there is evidence for a specific LF MF feature that explains differences in the effect of LF EMF exposure reported by different groups, all LF MF exposure characteristics were categorised. The frequency, magnetic flux density, and duration of exposure were studied in subgroup analyses. The magnetic flux density was grouped according to exposure limits for LF MF developed by the International Commission on Non-Ionizing Radiation Protection (ICNIRP). Continuous exposure of the human body is allowed to be up to 200  $\mu\text{T}$ , whereas occupational exposure safety limits are at 1 mT<sup>24</sup>.



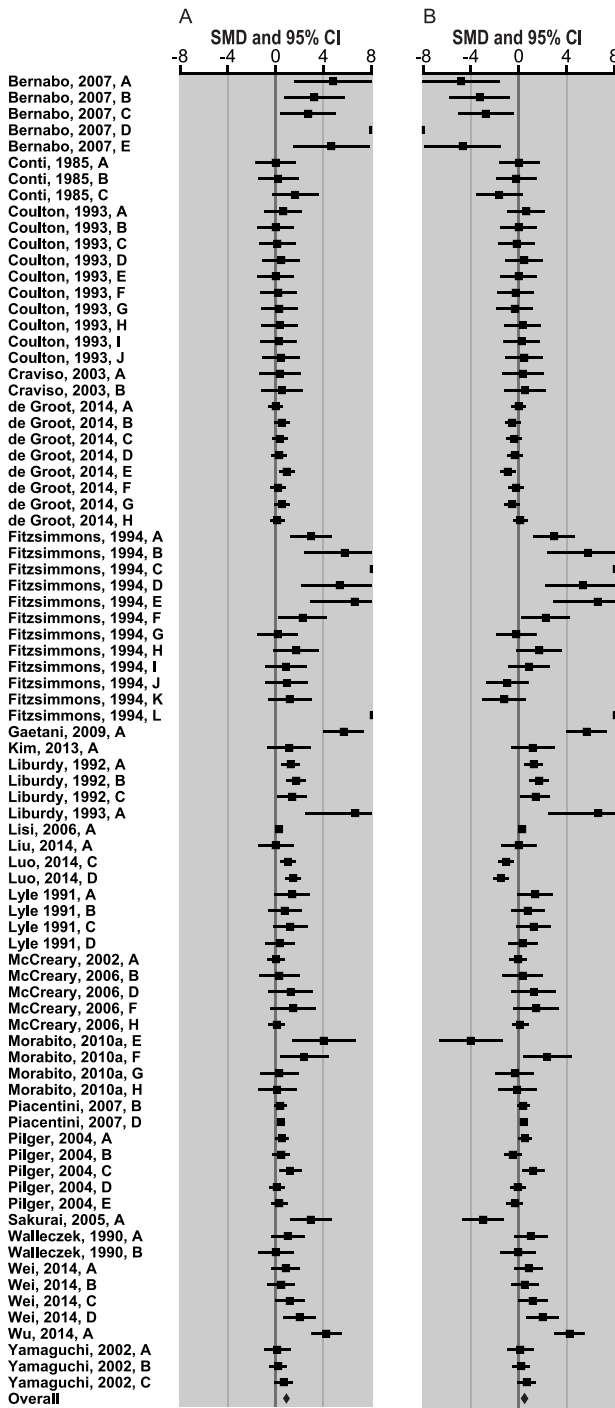


**Figure 4.** Influence of LF EMF exposure on the intracellular calcium concentration. Forest plot of 81 included studies that described intracellular calcium concentrations during or after exposure. a) The presence of an association between LF EMF exposure and intracellular calcium concentrations, and b) the direction of the effects. The forest plot displays the SMD (square) and 95% confidence interval (CI) of individual studies. The diamond at the bottom of the graph indicates the overall estimate and 95% confidence interval.

The different magnetic flux densities demonstrated different effects of LF EMF exposure. Exposure levels up to 200  $\mu\text{T}$  showed a significant increase, while higher exposure levels showed a neutral effect. Comparison of the different subgroups revealed no significant difference between the different exposure levels (<200  $\mu\text{T}$ ; SMD 0.612 [0.199, 1.025]; n=40; s=8, 200-100  $\mu\text{T}$ ; SMD 0.096 [-0.280, 0.472]; n=25; s=11, and >1000  $\mu\text{T}$ ; SMD 0.456 [-0.119, 1.032]; n=16; s=8).

Furthermore, subgroup analysis of the different frequencies indicated a relation between the frequency applied to the cells and intracellular calcium. The different frequencies were grouped based on two theories present in literature. First, electrical power supplies produce MFs with a frequency of 50 or 60 Hz. These power line frequencies are applied the most in the included studies and they did not indicate any effect of LF EMFs on calcium homeostasis (50/60 Hz; SMD 0.054 [-0.190, 0.298]; n=50; s=19). A second extensively investigated frequency during the late 1980s and early 1990s is the ion resonance frequency (IRF) for calcium ions. The original hypothesis by Liboff<sup>214</sup> suggested that calcium ions were activated by a specific combination of frequency and direct current (DC) field. Four papers investigated the existence of the IRF and subgroup analysis showed that this relation might exist, as the subgroup displayed a significant increase in intracellular calcium (IRF; SMD 2.655 [1.293, 4.018]; n=12; s=4). A more detailed investigation of the four individual studies included in this subgroup - Coulton et al. 1993<sup>207</sup>, Lyle et al. 1997<sup>126</sup>, Gaetani et al. 2009<sup>199</sup> and Fitzsimmons et al. 1994<sup>198</sup> - showed that only the latter two showed a significant effect and very pronounced increase of intracellular calcium by LF MF. Interestingly, analysis of papers describing exposure to frequencies other than IRF or 50/60 Hz indicated a small significant increase of intracellular calcium by LF MF exposure, although the effect is less pronounced than shown by the IRF subgroup (Other; SMD 0.205 [0.014, 1.028]; n=19; s=5). Only IRFs showed a significant difference compared to the other two subgroup in our analysis.

The last characteristic of the exposure set-up is exposure duration, ranging from a couple of minutes to many days. Subgroup analysis did not show any significant differences for exposures longer than one hour (1-24 hours; SMD -0.752 [-1.577, 0.073]; n=9; s=2 and >24 hours; SMD -0.046 [-0.559, 0.467]; n=17; s=7). Short exposures up to one hour on the other hand, indicated a significant increase of cellular calcium (SMD 0.657 [0.374, 0.940]; n=55; s=16). This increase after less than 60 minutes of exposure was significantly different from the negative trend reported after an exposure period up to 24 hours. In summary, the magnetic flux density, the frequency applied and duration of exposure might all be EMF characteristics that influence the outcome of the experiments.

The existence of a specific cell type or cellular feature that is susceptible to LF MF exposure is debated in literature<sup>41,43,172</sup>. Our subgroup analysis for the 24 included calcium concentration papers showed a significant difference between the different cell types. Immune cells showed an increased intracellular calcium concentration (Immune; SMD 0.543 [0.226, 0.861]; n=28; s=8), whereas grouping neural cells showed a neutral effect (Neural; SMD -0.235 [-0.521, 0.050]; n=20; s=7). Bone-related cell types also indicated a significant effect (Bone; SMD 1.921 [0.891, 2.951]; n=7; s=2), but caution is required as this subgroup only contained two individual studies. The remaining cell types were grouped together and did not show any effect with LF MF exposure (Other; SMD 0.071 [-0.744, 0.886]; n=18; s=7).

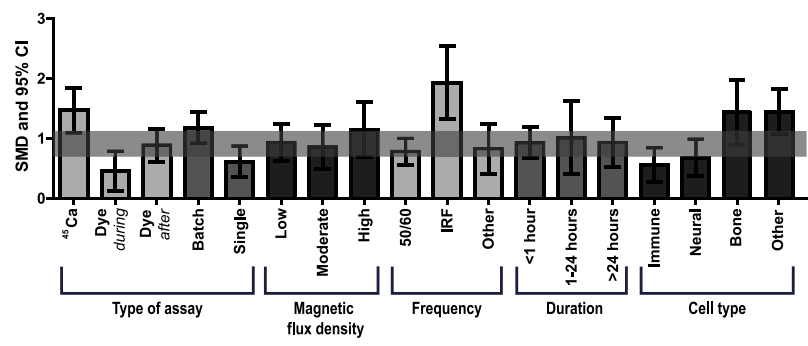


**Figure 5.** Subgroup analyses of the different study characteristics to determine the presence of an effect of LF MF on intracellular calcium. The grey horizontal bar shows the overall effect size and 95% confidence interval. Every vertical bar represents the subgroup SMD and 95% confidence interval. All study effects are reported in one direction (positive) to evaluate the presence of an association. Measurements performed with radioactive calcium (<sup>45</sup>Ca), calcium dyes during acute exposure (Dye during) or after exposure (Dye after) on a batch (Batch) or individual cells (Single), with a magnetic flux density up to 200  $\mu$ T (Low), 200-1000  $\mu$ T (Moderate) or above 1000  $\mu$ T (High). Frequencies were groups based on the frequency, 50/60 Hz (50/60), ion resonance frequency (IRF) and frequencies other (Other) than 50/60 or IRF.

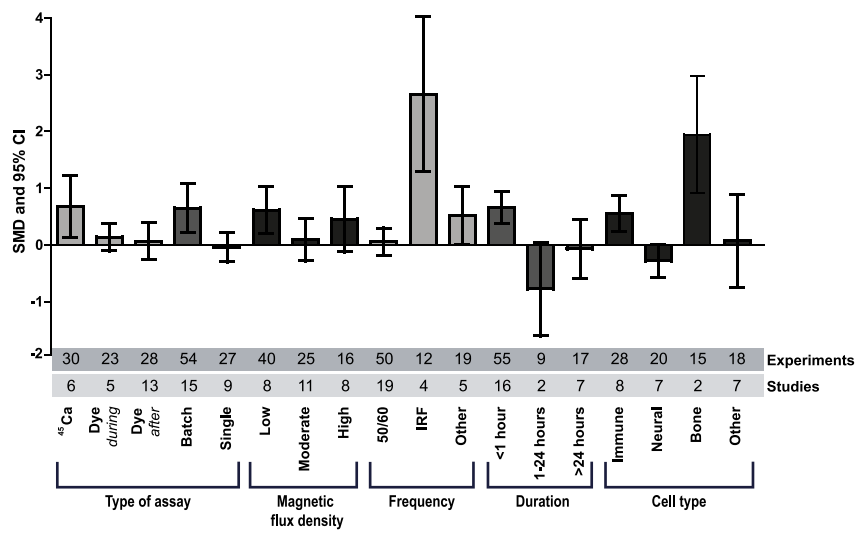


**Figure 6.** Subgroup analyses of the different study characteristics to determine the direction of an effect of LF EMF on intracellular calcium. All studies were reported with their actual effect size and direction, from which a grouped effect size and direction was calculated. Every vertical bar represents the subgroup SMD and 95% confidence interval. The total number of individual studies and experiments in every subgroup is indicated underneath every bar.

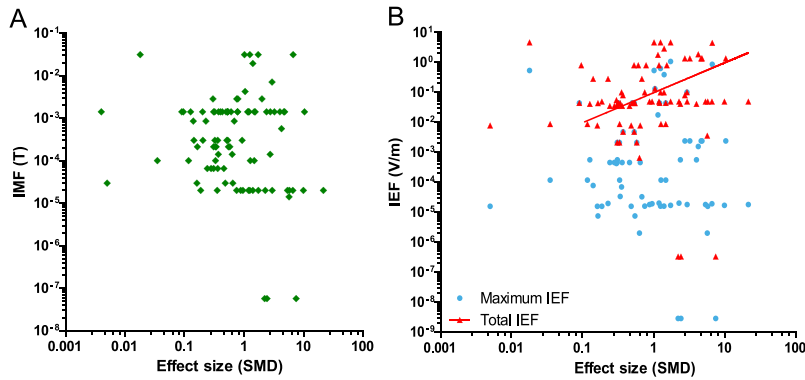


**Figure 7.** Regression plot of the effect sizes versus the imposed magnetic fields and induced electric fields. The calculated effect size (SMD) of every intracellular calcium measurement was plotted against a) the imposed magnetic field (IMF) and b) maximum or total induced electric field (IEF). The maximum IEF was calculated with the IMF values and the total IEF represents the maximum IEF by all means generated by the IMF and parasitic fields. Linear regression was calculated for the latter (line).

### *Magnetic and Electric field exposure assessment*

From the included papers that reported intracellular calcium concentrations during or after exposure, the electric and magnetic fields could be calculated (supplementary table 3). These values were plotted against the effect size, to investigate a correlation between intracellular calcium and these fields. The total magnetic fields to which the cells are exposed is composed of the field generated by the exposure system (IMF) plus the field generated by secondary sources (See supplementary Note 1 for details). Plotting the total magnetic field values against the SMD of intracellular calcium did not show a correlation (Fig. 7a). Furthermore, the calculated IEFs ranged from 0 to 4.62 V/cm, as cells inside one container experience IEFs of different strengths, depending on their distance from the centre and the orientation of the magnetic field. We plotted the maximum electric field, which are generated by the IMF plus the field generated by secondary sources, against the SMD and observed no correlation (Fig. 7b). The calculated total electric field was higher in most experiments as the most significant possible secondary source corresponds to parasitic electric fields. These fields can be generated by a potential drop along the inductance of the coils of the exposure system<sup>215</sup> and were found to be typically unaccounted for in the reviewed literature. Since they could contribute to the total electric field in culture, we also explored the possibility of their presence. Figure 7b indicates that the effect size potentially correlates to the total electric fields, if a linear relation between the two variables is assumed. Though the correlation was very weak, shown by a slope ( $R^2$ ) of  $0.096 \pm 0.037$ .

### *Sensitivity analysis*

With a sensitivity analysis, the robustness of the results of a meta-analysis is assessed. Exclusion of the studies in which mathematical calculations were made to estimate the sample size did not influence the effect size of the overall analysis of intracellular calcium. This showed that our estimates are robust.

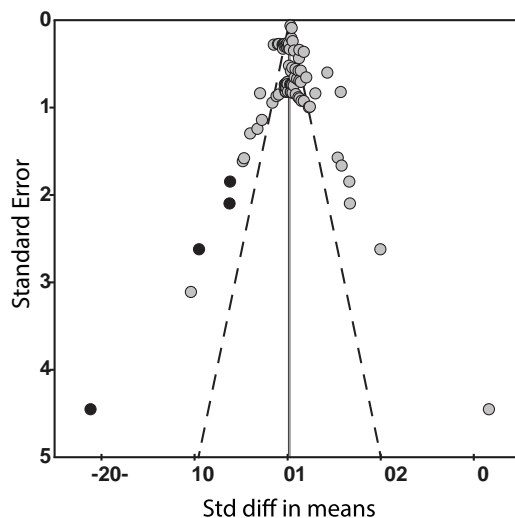


**Figure 8.** Funnel plot. All 81 individual studies (grey circles) that measured intracellular calcium during or after exposure were plotted according to their standard error and standard difference in means (SMD). The 95% confidence interval (dotted black lines) of the overall effect (grey line) is adjusted by the addition of four studies (black circles) and gives a new estimated effect (vertical black line).

### **Publication bias**

In figure 8, a funnel plot is displayed generated from the data in all 24 papers that described intracellular calcium measurements. A trim and fill algorithm<sup>216</sup> estimated the number of missing studies to be four. Adding these four missing studies indicated only a small overestimation of the effect size.

### **Discussion**

An accumulating number of papers is published that report contradicting health effects induced by LF MF exposure. This has led to an even larger rise in papers that aimed to investigate a possible molecular mechanism to explain these effects. This systematic review and the included meta-analyses focussed on modulation of calcium homeostasis by LF MF exposure in an *in vitro* model system. These meta-analyses revealed an association of LF MF exposure with an increased frequency of inherent cellular calcium oscillations. A positive association could also be observed for overall intracellular calcium. However, the effect size and direction of every effect indicated only significant effects for experiments measured with radioactive calcium, experiments that applied frequencies other than 50/60 Hz or a weak magnetic flux density. In addition, experiments performing a short exposure, or which exposed immune or bone cells or a batch of cells showed effects after exposure. Part of these results might be due to inclusion of three papers reporting extremely large effects of LF MF exposure<sup>146,198,200</sup>.

Calcium oscillations represent a naturally occurring process that plays a vital role in intracellular signalling<sup>178</sup>. These short cytoplasmic calcium waves are a common phenomenon in both excitable cells, such as cardio-myocytes and neural cells<sup>217,218</sup>, as well as in non-

excitable cells, like immune, endocrine and endothelial cells <sup>219</sup>. Moreover, calcium oscillations regulate the activation of intracellular proteins <sup>179</sup>. Calcium oscillations are decoded by one or several intracellular molecules that sense the calcium and change their activities accordingly. The different outcome measures of calcium oscillation in our study revealed a heterogeneous effect of LF MF exposure. The percentage of oscillating cells during or after exposure did not change and the amplitude of oscillations remained unaffected. The frequency of the waves on the other hand, was significantly increased. Since the frequency of calcium oscillations determines which downstream proteins are activated <sup>179</sup>, these results suggest that LF EMF exposure may modulate cellular behaviour. Only one of the included studies reported both frequency and amplitude as a study outcome, with effects similar to our estimates <sup>210</sup>; increased frequency in combination with reduced amplitude. Unfortunately, downstream effects of altered oscillations after LF EMF exposure were not investigated in this paper. Recent literature demonstrated that altered cellular behaviour, regulated by the frequency of calcium oscillations, only applies in a situation where the amplitude remains constant <sup>219</sup>. Since frequency, amplitude, and duration of oscillations together determine the ultimate intracellular signalling, we are not able to predict downstream effects of LF EMF exposure from our data and only show an association present in literature.

Calcium oscillations regulate protein activity and gene expression <sup>219</sup>, but in passive cells a stable intracellular calcium concentration is maintained. Cytoplasmic calcium is mainly stored in calcium stores, like the endoplasmic reticulum. Moreover, sodium-calcium exchangers and/or plasma membrane calcium ATPases (PMCA) pump cytoplasmic calcium back into the extracellular milieu without the need of biological stimuli <sup>178</sup>. Our meta-analysis showed an effect of LF MF exposure on the intracellular calcium concentration. However, this analysis should be interpreted with some caution, since the directions of the reported effects differed between studies. Only 25% of the studies reported a significant increase of calcium, whereas 12.5% reported decreased concentrations. Moreover, the overall effect size found was quite small. This suggests that either the effect of LF MF might depend on experimental conditions, or that uncontrolled confounding variables influence the outcomes of the studies <sup>209,220,221</sup>.

Subgroup analysis of the three different methods of analysis for intracellular calcium showed that only the experiments performed with radioactive calcium showed a positive association. Measurements performed with a fluorescent dye, during or after exposure showed a neutral effect. Based on the <sup>45</sup>Ca-measurements we could speculate that LF EMF exposure influences the calcium homeostasis by modulating the calcium uptake or efflux. In accordance with the present results, it has been reported that LF MF exposure induced a rise in inositol 1,4,5-triphosphate (IP3) levels <sup>222</sup>, an increase of protein kinase C (PKC) activity or that it modified the activity of voltage-gated channels <sup>41,203</sup>. All these processes could lead to an altered calcium homeostasis. However, the effects might be compensated by calcium efflux or uptake in intracellular stores, a hypothesis that is supported by the calcium-dye subgroup that measured intracellular calcium after exposure. The cell thereby maintained or restored the intracellular calcium balance after the initial increase, regardless of continuous exposure. Though, if LF MFs changed the influx or efflux of calcium during exposure, this implies that a short difference in the intracellular calcium concentration would be measured, just before the cells readjust their internal balance. Nevertheless, meta-analysis of the

calcium-dye papers that measured during exposure did not substantiate this hypothesis. This contradiction does not strengthen the association found in our study and suggest conflicting outcomes induced by uncontrolled technical parameters, such as temperature<sup>221</sup> or ambient fields<sup>220</sup>.

The study characteristics of the intracellular calcium papers enabled us to investigate the potential presence of specific LF MF exposure features that may be related to the biological effects of LF MFs. Therefore, subgroup analyses were performed based on frequency, magnetic flux density or exposure duration. The existence of a frequency window, which modulates cellular signalling, has been debated<sup>180,223</sup>. However regression plots of all studies did not reveal a specific frequency window (data not shown). The calcium IRF has been hypothesised to move calcium ions in a cell and our meta-analysis showed significant increase of intracellular calcium. This subgroup differed significantly from the other two clustered frequencies. Though, a more detailed investigation of the four individual studies included in the IRF-subgroup revealed that the results are not univocal. Only a few experiments reported a pronounced increase of intracellular calcium by LF MFs, whereas the other experiments showed neutral effects. Power line frequencies of 50 or 60 Hz were reported in 50 of the 81 included studies, and did not display a significant calcium modulation by LF MFs. Interestingly, the use of frequencies other than IRF or 50/60 Hz also indicated increased intracellular calcium by LF MFs, with frequencies ranging from 16 to 120 Hz. These results indicate that the universal exposure frequencies in our daily life, the 50 and 60 Hz, might not explain possible health effects. Rather, an association with other less common frequencies could exist, as well as the possibility of cell adaptation to constant environmental exposure. This second notion is supported by Goodman et al.<sup>224</sup> and Lin et al.<sup>225</sup>, which both showed that chronic exposure of cellular systems could lead to adaptation without the occurrence of any effects *in vitro*. We assessed a similar effect for the exposure duration. Our meta-analysis indicated a significant increase of intracellular calcium concentrations if cells were exposed for no longer than 60 minutes. Increasing the exposure duration from 1 hour up to 24 hours led to reduced intracellular calcium, shown by a not significant trend. Based on this subgroup meta-analysis, we could hypothesise that the biological effect of LF EMFs could depend on the duration of exposure. An initial increase of intracellular calcium by influx or reduced efflux is followed by a period to re-establish the homeostasis after one hour. Eventually the cell returns to a state of balanced calcium level, and is no longer affected by the presence of any exposure.

Biological effects that depend on the strength of the magnetic flux-density have been advocated, each with their own threshold<sup>226,227</sup>. We found an indication for a magnetic flux density related increase of intracellular calcium by LF MF exposure, only related to flux densities of up to 200  $\mu$ T. An association with low level fields could potentially be interpreted as a health risk in normal daily life. However, this specific subgroup contained one study published by Fitzsimmons et al.<sup>198</sup> with extremely high effects at 40 nT LF EMFs, while the other studies show consistent effects with neutral or only minor differences. A flux density of 40 nT is very low, but still too high to represent chronic daily exposure<sup>228,229</sup>. However, such magnitudes could in fact been easily obscured by artefacts introduced by unaccounted secondary sources (see Supplementary figure 2). For these reasons, this subgroup meta-analysis should be interpreted with caution, because the associations might be related to only one included study that influences our estimates. In summary, there are indications that low

level fields with a specific frequency and short duration, influence calcium homeostasis of cells in an *in vitro* model system. However these results are not univocal. A large proportion of studies also contradicted with the association, indicating that the evidence of association is weak.

Selective EMF-sensitivity of different cell types has been postulated. The central nervous system for instance, might be particularly vulnerable since neural function is highly voltage-dependent<sup>41,60</sup>. Immune cells on the other hand, produce free radicals<sup>172</sup> or possess antennae-like phenotype<sup>43</sup> that might make them sensitive to EMF exposure. Furthermore, bone cells not only use calcium as an intracellular second messenger, but also convert calcium ions into a solid extracellular matrix during cartilage and bone production<sup>230</sup>. With our subgroup analysis, we found significant evidence for a cell-type related effect. The intracellular calcium concentration of immune and bone-related cells was increased during or after LF MF exposure. Additionally, neural cells showed a neutral effect with possible decrease in intracellular calcium. These contradictory trends indicate that a possible effect of LF MF exposure might indeed be related to the type of cells. This could explain why a prominent effect of multiple other cell types is calculated, even though the direction and effect size are not significant. We grouped cells with different phenotypes together, but there might exist multiple biological targets of LF MFs, resulting in different interactions and an overall neutral effect. If LF MFs interact with different biological targets, then this could make an overall comparison of all *in vitro* studies less reliable. These results emphasise the importance of investigating different cells types without generalising them in *in vitro* and *in vivo* experiments regarding the mechanism of LF MF exposure.

Finally, we examined if the measured effect sizes were related to the magnetic and electric fields in culture. To calculate these fields, most experiments required assumptions in order to reconstruct the experimental conditions from the information provided in the papers. Errors in the reporting of the physical parameters were commonplace, such as diameter reported as radius, or  $\mu\text{T}$  instead of mT. Some of these discrepancies were detectable and conciliation was possible, others were incomplete beyond reasonable estimation and could not be included in this study. This highlights the importance of thorough experimental setup descriptions. Furthermore, we calculated the maximum fields that cells experience inside cell culture incubators or under a microscope. In the case of exposures under microscopes, it is generally assumed that the IEF is around zero under homogeneous magnetic fields, as the imaging area is in the middle of the magnetic vortex. However, modelling of inhomogeneity in the IMF induced by the presence of microscope parts in close proximity to the culture volume has been shown to introduce significant variations to the maximum IEF (around 37%), spatial gradients of the IMF (> 200%) and dislocation of the vortex<sup>231</sup>. The ranges provided for the magnitude and direction of electric fields in this study correspond to the most informed estimate possible, however real values are case specific and may differ significantly within the ranges provided. Ideally, the total electric field in the culture volume must be measured directly as it comprises the summation of all sources of electric fields and magnetic fields in proximity with the culture container.

For exposure of multiple cells inside culture incubators, we did not account for inhomogeneous exposure of cells, but calculated the maximum fields. However, the strength of electric and magnetic fields depend on the location of the cells within the culture container and the orientation of the magnetic field. For parallel IMF, most of the adhered cells on the



culture plane are exposed to homogeneous fields<sup>64</sup>. However, when the imposed homogeneous magnetic field is perpendicular to the culture plane, the IEF vortex will be located at the centre of the culture surface and its magnitude will grow linearly as a function of the radius<sup>63</sup>. As consequence, about 50% of the cells are exposed to electric fields that range from 0% to 70% of the maximum IEF on the container<sup>64</sup>. This uncertainty becomes even more prominent when the cells are in suspension. Consequently, the IEF that cells actually experience might be smaller than the values reported in our graph, since we plotted the maximum field possible. We did not observe a correlation for the maximum IEF or IMF, but found a weak association with the total IEF. Since the total IEFs is generated by parasitic fields plus the maximum IEF, and IEFs alone did not indicate a relation, we hypothesise that parasitic fields and other exposure system unaccounted parameters greatly influenced the experimental outcomes. These parameters need to be controlled in future experiments to make sure that conclusions are based LF MF exposure and not the existence of parasitic induced electric fields.

Publication biases are an unavoidable part of a systematic review and meta-analysis, but the large number of neutral effects included in our analyses already indicated that this type of bias is less pronounced in LF MF research. Neutral data published on LF MF exposure are valuable and could reduce societal concern regarding the potential health effects of LF MF<sup>232</sup>. Funnel plot of our largest data-set indicated that four papers might be missing from our intracellular calcium analysis, confirming that this type of bias did not strongly affect our overall analysis. However, in our analysis we did not correlate our data to the impact factor of the journals. Neutral data might end up in low-impact journals, whereas significant differences are published in higher journals. This would still be a type of publication bias, but based on our initial funnel plot we expect that our meta-analysis outcomes are not influenced by the absence of a small number of papers.

Performing a meta-analysis of *in vitro* studies could lead to heterogeneity, due to the numerous cell types, assays and culture conditions available for an *in vitro* model system. Our meta-analysis showed a high heterogeneity ( $I^2 > 75\%$ ), which might not only be caused by variation in cell type and cell origin, but also by variation in exposure characteristics such as frequency, magnetic flux density and exposure duration. However, grouping similar papers did not reduce heterogeneity. This is a limitation that necessitates careful interpretation of every meta-analysis. One of the few systematic reviews that also combined experiments performed with *in vitro* cell cultures and LF MF exposure presented a similar heterogeneity;  $I^2 > 88\%$ <sup>233</sup>. Next to heterogeneity, the risk of bias introduced by a lack of blinding, temperature control or cell vitality measurements was substantial. There is no golden standard for *in vitro* experiments, but these factors could confound the outcome<sup>221,234</sup>. Information concerning the use of an identical exposure system for sham treatment was lacking and ambient fields during exposure were poorly described<sup>220</sup>. Owing to the lack of these crucial components in design and reporting quality results should always be interpreted with caution.

For future research regarding the effects of LF MF exposure, it is important to confirm the positive association with intracellular cellular measurements performed with radioactive calcium. Our meta-analysis indicated a positive association, however thorough replication of the <sup>45</sup>Ca experiments would confirm and strengthen our association, or emphasize the presence of outlier studies in literature that conceal the true effect. Our subgroup analyses also indicated a possible interaction related to the use of uncommon frequencies, with a low

magnetic flux density, for a short exposure period. A combination of all these features presents a good experimental design for future research. With an independent collaboration between different research groups technical bias will be minimised. Furthermore, the calcium oscillation experiments revealed a mixed effect depending on the outcome variable. It is advised to investigate this in more detail, in an experimental setup that simultaneously measures frequency, amplitude, calcium content and preferably downstream protein activation during LF MF exposure.

## Supplementary

Supplementary figures and tables are available online.

### Supplementary note 1

#### Imposed Magnetic Field (IMF) and Induced Electric field (IEF) exposure assessment

A thorough survey of the exposure conditions reported in the literature was performed to extract all information of relevance to the electric and magnetic field exposure parameters on the culture space. Only publications which provided enough explicit or implicit information about their exposure conditions were included in this study.

**Signal Type:** The maximum dB/dt presented by each specific signal was utilised for the calculation of the maximum induced electric field in the culture space. For all continuous signals, the maximum dB/dt corresponded to the highest harmonic in the signal. In the case of intermittent signals, the maximum dB/dt resulting from the modulation of the continuous signal was extracted. Intermittent signals which presented modulations which frequency components smaller than the frequency components of the carrier signal (“soft switching”) were treated as continuous signals. In the case of sinusoidal signals which were explicitly generated by a dedicated function generator or “synthesised”, the contribution of higher harmonics other than the fundamental frequency was deemed irrelevant. Signals were considered “generic power signals” in cases where information about its higher harmonics was not provided. The definition of “generic power signals” utilised in this study corresponds to the maximum accepted distortion for low- to medium-voltage power systems by the International Electrotechnical Commission (IEC) [1996] which is comprised of a multiple-harmonic signal requiring the consideration of frequency-weighted parameters for the calculation of the maximum electric field induced in the cell medium. For the calculations here presented, the parameters utilised are given in <sup>215</sup> for a homogeneous magnetic field exposure. In the cases where the generation of such sinusoidal was not explicitly specified, both “synthesised” and “generic power signal” categories were assumed. Studies which utilised non-sinusoidal signals were only included where the maximum dB/dt of the signal utilised was specified.

**Signal magnitude:** The imposed magnetic field magnitude reported in the publications reviewed is here and throughout the text reported as “peak” magnitude, that is, one half of the “peak-to-peak” difference in the waveform. In the cases where the signal’s magnitude

reported of the signals was not explicitly specified, both Root-Mean-Square (RMS) and “peak” value were assumed.

**Signal spatial distribution:** Homogeneity of the Imposed Magnetic Field (IMF) is highly dependent on the exposure system geometrical configuration and details. Some of the publications reviewed provide an assessment of the homogeneity of the IMF over the culture volume by direct measurements. However, most of the sizes of the magnetic field sensors utilised were of comparable size to the exposure coil systems or to the culture containers. Furthermore, measurement resolution on the exposed area is many times lacking. This puts in question the ability of such measurements to detect possible gradients generated either by the coil systems or by extra metallic features of the exposure systems (microscope plates, objectives, etc.)<sup>231,235</sup>. For this reason, a measure of the deviation of the reported IMF magnitude was obtained for each exposure configuration in the reviewed literature (usually based on calculations, measurements or estimations at the centre of the exposure system or culture container) and is reported as multipliers (max and min) for the worst-case inhomogeneity on each exposure system.

The homogeneity of the IMF was calculated for each exposure system and its associated culture container over the volume of interest taking into consideration their mutual relative position. For commonly used configurations (round and square single and Helmholtz coils) the results for this calculations are tabulated<sup>236</sup>. However, for other configurations based in round coils (off- center plane coils and solenoids, finite solenoids, multiple coil systems) routines were built in MATLAB R2007a software (Mathworks, Natick, MA) and validated with the on-axes solutions as these require off-axis calculations involve elliptical integrals<sup>237</sup>. The maximum variation of the magnetic field magnitude over the plane of greater area perpendicular to the imposed magnetic field referenced to the value at the centre of the culture container was extracted and is reported as a multiplier (See Table 3 supplementary). The calculation was performed for the designated culture space described for each experiment. In the cases were this space was not explicitly described, estimations were made based on the dimensions and specificities of the exposure systems and their associated culture containers. For arrangements of discrete coils and solenoids homogeneity was assessed inside a coaxial cylinder centred on the exposure location with radius equal to the larger dimension between the radius of the culture container collective volume escribed sphere and 60% the coil radius (default); and a height equal to the larger dimension between the culture containers collective wet volume and 10% of the coil radius (default). For known configurations (Helmholtz coils, Merritt Coils, Maxwell coils, etc.) homogeneity was assessed inside a concentric sphere centred on the culture container collective volume with radius equal to the larger dimension between the radius of the culture container collective volume escribed sphere and 60% the greatest coil radius (default). Default values were assumed in cases where the culture container collective volume was not explicitly specified. Default culture container sizes were also assigned in cases where the culture container sizes were not explicitly specified.

The effect of microscope-induced spatial inhomogeneity was considered by multiplying the IMF signal magnitude of such exposure systems by a factor of 2.33 in order to account for possible asymmetric distortions. Commonly utilised nickel-chrome based coatings and iron

internal components (springs, screws, studs, etc.) commonplace to microscope objectives and other components. Distortions observed could be several millimetres away from the focal plane and detectable only partially by direct measurements, as the gradients generated are often too sharp for conventionally-sized measurement equipment<sup>235</sup>.

All publications report (or imply) the generation of linearly polarised imposed magnetic field.

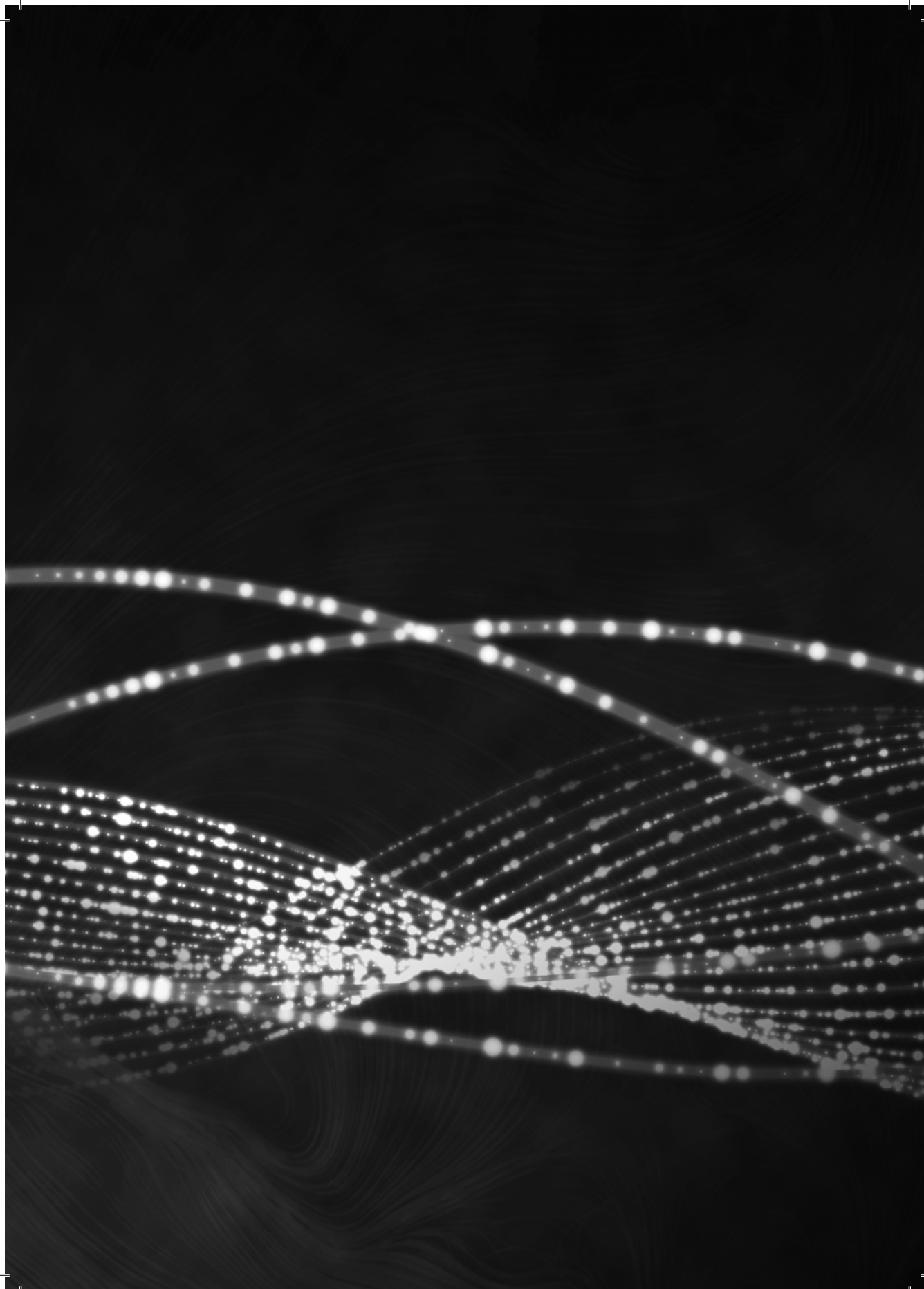
**Perpendicular plane maximum radius:** The radius representing every culture container corresponds to the radius of the maximum inscribed circle on the plane of greatest area perpendicular to the imposed magnetic field on the culture volume. Taking the surface of the culture liquid as reference, the plane of greatest area could then be limited entirely by the container in the case of “perpendicular (I-)” orientations (e.g. Petri dish exposed with an imposed magnetic field perpendicular to its culture treated area) or it could be limited by the container and the liquid surface in the case of “parallel (II)” orientations (e.g. Petri dish exposed with an imposed magnetic field parallel to its culture treated area). For the cases in which the height of the liquid was not explicitly described for conventional culture containers, it was obtained from the maximum standard culture liquid volume to surface area (0.5 ml/cm<sup>2</sup>) which allows the minimum gaseous diffusion of oxygen required by most cells<sup>238</sup>, while for cells under coverslips was set to 0.1 mm from the standard height of the counting chamber of a Neubauer hemocytometer<sup>238</sup>. The radius corresponding to the area observed under 20X, 40X and 100X objectives was also utilised for IEF calculation in the case of cultures which biological effects were recorded while exposed under the microscope for imposed magnetic fields perpendicular to the culture/observation plane (in the case of parallel orientations, the radius would correspond to the height of the liquid instead).

**Induced Electric Field Calculation:** Upper boundaries for the induced electric fields were obtained by the using a simplified form of the Maxwell-Faraday equation, which assumes magnitude and direction homogeneity of the IMF over the culture volume. Maximum and Minimum induced electric fields were calculated by utilizing the most extreme combination of exposure parameters for this expression respectively. In the case of exposures under a microscope, calculations were also made based on the largest radius of the field of view of the specific objective utilised.

**Extra Electric and Magnetic field Artefacts:** The magnitude of the contribution to the total Induced Electric field on the culture space was assessed for secondary electric and magnetic field sources. Other artefacts were considered besides the distortion imposed by metallic hardware close to the culture space which may have a significant influence in the resultant fields:

- a) **Artificially-generated background time-varying magnetic fields:** The total IMF to which the culture space is exposed is composed of the field generated by the exposure system plus that of generated by secondary sources (electrically heated microscope stages, laboratory equipment, adjacent power distribution lines, Incubation systems, etc.). Magnitudes for the secondary sources were obtained from the reviewed literature when available. In the case this information was not available, 240uT was used instead as an upper boundary according to previously surveyed data on biological incubators<sup>220</sup>.

- b) Parasitic electric fields:** The total electric field in the culture space is composed of the IEF by the IMF and also of parasitic electric fields. The latter are generated in the surrounding space by the potential drop along the inductance of the coils making up the exposure system <sup>215</sup> and its contribution to the total electric field in culture could be relevant depending on the specific special distribution and magnitude. Magnitudes for the parasitic electric fields were obtained from the reviewed literature when available. An estimation was made for cases where these values were not provided by dividing the potential drop reported by the diameter of the coil system escribed sphere (in the case the feed point of the coil system was not explicitly detailed). In cases where the potential drop was not provided, it was calculated via ohms law. For this, the coil inductive reactance and resistance were utilised to calculate the total impedance which was then multiplied by the current injected into the coil system. In cases were the wire material was not specified, Cu ( $s = 5.96 \times 10^{-7} \text{S/m}$ ) was assumed. In cases where the wire diameter was not specified and could not be deduced from other provided parameters, 28 AWG (0.32 mm diameter) was assumed. Coils inductances were calculated according to [ARRL] <sup>239</sup> for the cases where direct measurements were not provided and single-layer coil configurations were assumed for the cases in which the coil's system geometry was not sufficiently described. In cases where the height of the coil was not specified, 0.5 cm/100 turns of wire was assumed. In cases where the injected current was not specified, it was calculated depending on the mechanical specifications of each coil system <sup>240</sup> and the maximum IMF generated by the system (obtained as described previously in this section). Finally, an estimate of the upper boundary for the parasitic Electric field inside the medium ( $\epsilon_r = 80$ ) on the culture containers was calculated utilizing the maximum possible parasitic Electric field obtained. A shielding factor of 300 was applied for cases where shielding was applied, but measurements of residual fields were not provided <sup>215</sup>.




# Chapter 4

---

**A novel method to investigate filopodia dynamics during low frequency electromagnetic field exposure**

Lieke A. Golbach, Eline H. Verbon, Norbert C.A. De Ruijter, Huub F.J. Savelkoul, B.M. Lidy Verburg-van Kemenade

*Manuscript in preparation*

The background of the page features a series of glowing, interconnected particle trails that create a sense of depth and movement. These trails are composed of numerous small, bright dots connected by thin lines, forming a complex, web-like structure that curves across the lower half of the page. The overall effect is reminiscent of a network or a dynamic system, fitting the scientific nature of the chapter's title.

## Abstract

Cell protrusions like microvilli and filopodia are suggested to be a potential site of interaction for low frequency electromagnetic field exposure (LF EMF). These protrusions contain dense bundles or actin filaments that possibly transport calcium ions upon exposure to EMF. This might eventually influence cellular function, but initially will influence the dynamics of the actin filaments inside the core. In this study we describe a unique method to investigate the potential effect of exposure on filopodial dynamics. We generated an epithelial cell line (HeLa-80) that stably expresses Lifeact-EGFP with equal expression levels in every cell. Initial experiments showed that Lifeact-EGFP reversibly binds to actin filaments without interfering with cell growth or actin dynamics. Furthermore, HeLa cells showed numerous filopodia that exhibit high dynamic movement, which was diminished upon stimulation with a biological stimuli. Our image analysis quantified filopodia behaviour and showed clear potential to be applied in research to examine the effect of LF EMF exposure on filopodia.



## Introduction

During the past decades, numerous theories have been put forward to explain the potential interaction mechanism of low-frequency electromagnetic fields (LF EMFs) with cells and tissues. These theories hypothesise how non-ionising fields influence cellular processes in order to give reasons for claimed harmful effects of chronic environmental exposure. Epidemiological studies found a weak association between exposure and the development of mild non-specific health issues<sup>1</sup>, but to strengthen or reject such an association sufficient evidence including a biological mechanism is required.

Calcium, one of the most central ions in a cell, has often been suggested as a possible target of LF EMF exposure. Different cellular mechanisms are proposed, ranging from direct interactions with the plasma membrane<sup>38-40</sup> to complex models that predict an interaction by ion-binding proteins<sup>44</sup>. Although different hypothesis are supported by studies performed in T-cells<sup>27-29</sup>, neutrophils<sup>30,31</sup> and osteoblasts<sup>32-34</sup>, other studies also report conflicting observations with neutral effects<sup>124,241</sup>. Furthermore, validating the hypothetical mechanism to disclose the actual cellular interaction showed to be difficult<sup>242</sup>. LF EMF contains low field energy, consequently a cellular mechanism will be required to convert this low energy into a physiological response that involves much higher energies. In regard to this notion, Gartzke and Lange published a hypothesis in 2002<sup>43</sup>. They proposed a theoretical-interaction mechanism that focuses on calcium ion conduction along actin filaments in microvilli. Microvilli are small membrane protrusions with a structural core of dense bundles of cross-linked actin filaments<sup>243</sup>. The theory described a concept in which the actin-filament core of the microvilli functions as a cable-like structure to conduct ionic currents along the filament axis. Although this would theoretically decrease the threshold and permit low level exposure to influence a cell, this theory remains to be proven with an *in vitro* model system.

We aimed to design an *in vitro* model system to examine the possible interaction of LF EMFs with cellular structures such as microvilli. The average diameter of microvilli is only around 50-100 nm and they are 2  $\mu\text{m}$  in length, which enables the use of any light microscopy for time-resolved microscopy. Fortunately, microvilli are not the only antenna-like structures protruding on cell's surface. Filopodia have been observed in a multitude of different cell types and are described as 'antennae' or 'fingers' that cells use to probe their microenvironment. The primary biological role of filopodia seems to be sensing for extracellular cues, both mechanical<sup>244</sup> and chemical<sup>245,246</sup>, accordingly serving as pioneers during cell protrusion. Filopodia are longer and wider compared to microvilli, around 100 to 300 nm in diameter. Electron microscopy analyses showed that the filopodial core is also made up of 15 to 30 tightly-packed long parallel actin filaments<sup>247</sup>. This makes filopodia a perfect alternative for microvilli in light microscopy applications during EMF exposure.

In this study, we describe the design of a novel approach to investigate the theory proposed by Gartzke and Lange. To visualise the filopodia, we stably expressed Lifeact, a small protein that reversibly binds to actin filaments<sup>248</sup>, conjugated with a fluorescent probe. With our approach, we could visualise the dynamic movement of filopodia in epithelial cells during acute LF EMF exposure in a time-resolved manner.

## Material and Methods

### Cell lines

Human embryonic kidney (HEK) 293FT cells and the human cell line HeLa-80 were obtained from ATCC. HEK293FT cells were grown DMEM supplemented with 10% fetal calf serum (FCS) 100 U/ml penicillin and 100 µg/ml streptomycin. HeLa-80 wells were grown in MEM supplemented with 10% fetal calf serum (FCS), 100 U/ml penicillin and 100 µg/ml streptomycin. The cells were cultured at 37°C, 5% CO<sub>2</sub> in a humidified incubator and passaged every 3-4 days.

	Sequence
<b>Lifeact</b>	<u>GATCCGACCATGGGGTGTCCGAGATTTGATCAAGAAATTCGAAAGCATCTCAAAGGAAGAA</u>
<b>Reverse</b>	<u>CCGGTTCCTCCTTTGAGATGCTTTCGAATTTCTTGATCAAATCTGCGACACCCAT</u>

**Table 1.** Sequence of the oligonucleotides. Underlined nucleotides encode the sequence of the Lifeact protein.

### Lentiviral construct

An oligonucleotide encoding the sequence of the Lifeact protein (Table 1) was cloned into a lentiviral vector (Fig. 1). The backbone vector, a pRRLSIN.cPPT.PGK-GFP.WPRE, was a gift from Didier Trono (Addgene plasmid # 12252). Two restriction sites between the PGK-promotor and EGFP sequence were unique for BamHI (GGATCC) and AgeI (ACCGGT) restriction enzymes. The Lifeact-oligonucleotide was designed with the proper overhang for both restriction sites (Table 1). Insertion of the oligonucleotide was confirmed by PCR and subsequent sequencing. The new plasmid was amplified with Maxiprep Endotoxin-free Plasmid Purification kit (Qiagen) according to manufacturer's protocol. Virus particles were produced in HEK293FT cells grown in DMEM containing L-Glutamine with 10% FBS, 100 U/ml penicillin, 100 µg/ml streptomycin, 1x HyClone MEM Amino Acid solution (Gibco), 100 nM Pyruvate, and 100 µg/ml G418 (Sigma-Aldrich). At 70% confluence, the cells were transfected with jetPRIME (Polyplus) with 2 µg DNA; 1 µg of the Lifeact-EGFP containing vector and 0.33 µg pRSV-Rev expression vector, 0.33 µg pMDLg/pRRE (Addgene) and 0.33 µg pMD2.G vector. After a four-hour incubator period, DMEM containing only G418 was added to the cells. The DMEM was replaced the following day and virus particles were harvested 48h and 72h post transfection and stored in 1.5 ml aliquots at -80°C in cryovials.

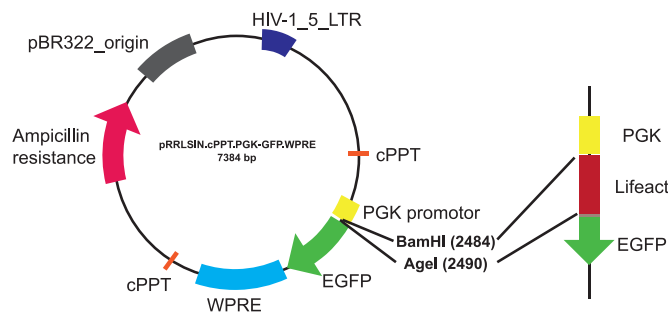


**Figure 1.** Lentiviral backbone and integration of the oligonucleotide encoding Lifeact.

### *Lentiviral transduction*

HeLa cells were seeded onto a 6-well plate and cultured in supplemented MEM medium. After six hours, the medium was removed and replaced by 1.5 ml DMEM containing the virus particles obtained at 72 hours. The medium was supplemented with 1 ml complete MEM medium and incubated at 37°C overnight. The following day, the virus particle containing medium was replaced with 2 ml complete MEM. The cells were kept at 37°C and passaged every 3-4 days. To obtain a cell line from a single cell, transduced HeLa-80 cells were detached with trypsin and resuspended in MEM medium. A serial dilution up till 1 cell/μl medium was made and subsequently 1 μl was added in a clean 96-well culture plate. The presence of only one single cell/well was checked with a microscope and verified by a second observer. All wells containing only a single cell were filled with 100 μl medium and 100 μl conditioned medium. Plates were incubated at 37°C, 5% CO<sub>2</sub> in a humidified incubator. After ten days, clones were checked for fluorescence by microscopy and after one month, the expression of Lifeact was validated by immuno-fluorescence and flow cytometry.

### *Validation of uniform Lifeact expression*

Expression of Lifeact-EGFP was confirmed by flow cytometry. One million HeLa-80 cells per treatment (Normal cells, Transduced cells and single cell colony) were detached with trypsin and resuspended in PBS. From every sample, 20.000 events were recorded by an Accuri C6 flow cytometer (BD Biosciences). Cells showing a normal forward and side scatter (>85% of all events) were gated and the expression intensity of the EGFP was plotted in a histogram.

### *Validation of Lifeact expression by immune-fluorescence*

Transduced HeLa cells were grown onto glass coverslips and incubated at 37°C overnight to adhere. The following day, cells were fixed in 2% paraformaldehyde (PFA) in PBS for 20 minutes. Subsequently, the cells were washed twice with PBS to rinse off the fixation fluid and permeabilised in 0.05% Triton-X100 in PBS. Actin filaments were stained with 1 U/ml phalloidin-Texas Red (Invitrogen) in PBS for 20 minutes. The cells were washed twice with PBS and mounted onto confocal microscopy slides with VectaShield (Vector laboratories). Images were obtained with a Zeiss LSM 510 confocal microscope, equipped with a 488nm Argon laser with a 505-550 nm band pass filter for the EGFP. Phalloidin was visualised with a 543 nm HeNe laser with a 585 nm long pass filter. To confirm co-localisation of both phalloidin and Lifeact-EGFP, a line was drawn in the images and the fluorescence intensity was plotted against the distance of the line.

### *Image acquisition*

Transduced HeLa cells were grown onto microscopy tissue culture dishes containing #1 glass coverslips. The cells were left to adhere overnight at 37°C in a humidified incubator containing 5% CO<sub>2</sub>. The next day, the cells were starved in DMEM medium (without phenol red) for two hours prior to imaging. Images of Lifeact-EGFP were obtained with a spinning disk confocal microscope (Andor Revolution on a Nikon Ti Eclipse) equipped with autofocus (PFS3), piezo stage (ASI XY- LE), and sensitive Electron-Multiplying-CCD camera (Andor iXon888, 1024x1024, 13x13). Lifeact-EGFP expressing cells were excited with a 488 nm Argon laser at 5% and emission passing a 510/40 nm band pass filter was detected at 11 frames / minute. Cells were imaged for 15 minutes at controlled conditions of 37°C ±0.1

sample temperature (Tokai Hit), with continuous 5% CO<sub>2</sub> flow to minimise any (additional) stresses. To analyse the influence of an extracellular growth factor, 10 ng/ml EGF (Gibco) diluted in pre-warmed DMEM without phenol red was added to the cells.

### *ImageJ analysis*

A macro was designed for ImageJ, to perform automatic and user-independent analysis of the fluorescence intensity and associated actin dynamics. First, images from multiple time points were stacked together in z-stack and a band pass filter was applied. Small structures were enhanced up to 5 pixels, whereas large structures were reduced to 10 pixels. Outlier-pixels were removed (radius of 3) with a custom build-in plugin part of ImageJ. The resulting images were thresholded with a Triangle threshold<sup>249</sup>. The appearance of new fluorescence was calculated according to the method described by Van der Honing et al.; New pixels divided by the total amount of pixels times 100<sup>250</sup>. The total amount of pixels corresponds with the new pixels plus the pixels that were present in both images.

## Results and discussion

### *Validation of uniform Lifeact-EGFP expression*

The Lifeact peptide has proved to be a convenient, non-toxic F-actin probe and has been used to image F-actin in diverse organisms such as mice, plants and filamentous fungi<sup>248,251-253</sup>. To analyse the dynamics of filopodia containing long bundles of actin filaments during LF EMF exposure in a time-resolved manner, the filopodia were visualised through expression of Lifeact-EGFP. Lifeact-EGFP can be expressed with the use of transient transfections or stable expression by lentiviral transduction. To prevent the harmful effects of transient transfections and to minimise cell-to-cell variation, we selected the latter in combination with clonal expansion. We constructed a personalised Lifeact-EGFP lentiviral vector through insertion of an oligonucleotide encoding the first 17 aa residues of yeast ABP140 fused to EGFP<sup>248</sup> under the control of the phosphoglycerate kinase 1 (PGK) promoter. It was shown that PKG and elongation factor-1 alpha (EF1 $\alpha$ ) govern high-level gene expression compared to conventional cytomegalovirus (CMV) in cells from the human hematopoietic lineages as well as derived hematopoietic cell lines<sup>254</sup>. A PGK promoter enables the use of the same procedure to innate immune cells in future research. The lentiviral plasmid was incorporated into lentiviral particles and HeLa-80 cells were transduced. When delivered as viral particle, the transgene is integrated into the host genome, providing stable, long-term expression of the target gene.

Expression of the Lifeact-EGFP protein was checked by flow cytometry before and after transduction (Fig. 2a). HeLa-80 cells did not show high auto-fluorescence and before transduction. Once transduced, a mixed population formed, with different expression levels of Lifeact-EGFP depending on both the place and number of insertions of the lentiviral DNA in the genome. Half of the cells showed a fluorescent intensity above that of non-transduced cells. The clonal expanded cells that were generated from one single cell, showed very uniform expression levels in all of the cells. This expression showed to be stable and not to interfere with any biological process, as after six months of cell proliferation and propagation *in vitro*, the expression is still uniform (Fig. 2b). This is important, because lentiviruses insert their DNA at a seemingly random location on one of the host chromosomes. Not all mutations

will significantly affect the proliferation of the cell. However, if the insertion occurs in an essential gene or a gene that is involved in cellular replication or programmed cell death, the insertion may compromise the viability of the cell or immortality of the cell <sup>255,256</sup>.

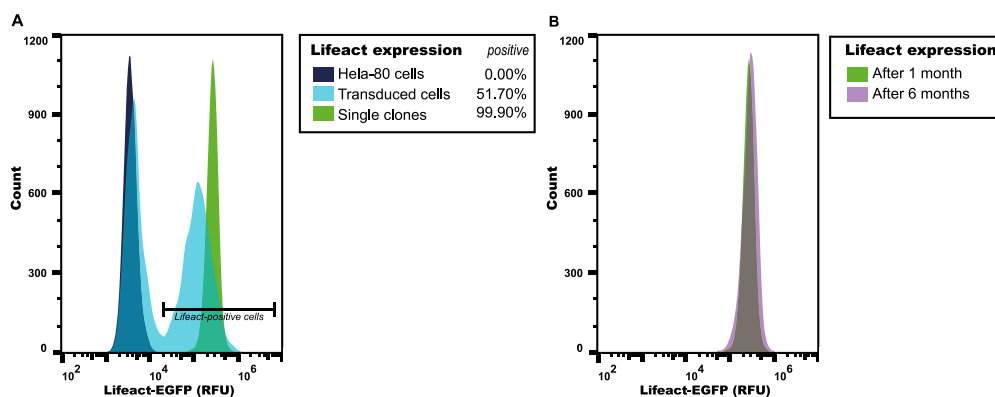


**Figure 2.** Flow cytometry analysis of the expression of Lifact-EGFP. Fluorescence intensity was measured in untreated HeLa-80 cells (dark blue), HeLa-80 cells ten days after transduction with lentiviral particles (light blue) and HeLa-80 cells transduced with Lifact-EGFP and grown from a single cell for one month (green). Percentage of cells showing green fluorescence above the indicated threshold are shown behind every sample group.

Clonal expansion of one single transduced cell was time-consuming, however subsequent stable expression ensured equal expression levels of Lifact-EGFP in every individual cell. As a result, this stable expression will make it possible to compare fluorescence intensities from multiple cells without compensating for the initial expression level. Furthermore, we selected clones that showed low expression levels to prevent interference of Lifact-EGFP with cellular functions. In 2001, Van der Honing et al. reported that high levels of Lifact expression in Arabidopsis resulted in subtle alterations of the actin filament dynamics within root hair cells <sup>250</sup>. In addition, transfection of Rat-2 fibroblasts with Lifact-mGFP induced an increase of filopodial extensions that was not seen in untransfected cells <sup>257</sup>. Thus, some cell types and tissues may be more sensitive to alterations in F-actin dynamics caused by these labelling tools.

### *Lifact-EGFP expression pattern in HeLa-80 cells*

To investigate the expression pattern of our Lifact-EGFP, HeLa-80 cells from the heterogeneous population were counterstained with a TexasRed fluorophore conjugated to phalloidin, a protein that selectively binds to actin filaments. Figure 3a shows that Lifact-EGFP expression is not present in all the cells, whereas phalloidin stained the actin filaments of every cell. The actin filaments are mainly present in the cell cortex, a cross-linked network of actin that lies directly underneath the plasma membrane and in the cell protrusions <sup>258</sup>. We did not see any adverse effects of Lifact-EGFP on cell spreading or cell adhesion compared to not transduced cells, like reported for  $\beta$ -actin-GFP fusion proteins <sup>259</sup>. Moreover, the phalloidin staining in red and Lifact-EGFP in green nicely co-localise in our cells, shown by the yellow pixels in the overlay (Fig. 3b). This co-localisation was also confirmed by the intensity plot of a cross-section of the cells that showed peak fluorescent regions at the same distances (Fig. 3c).

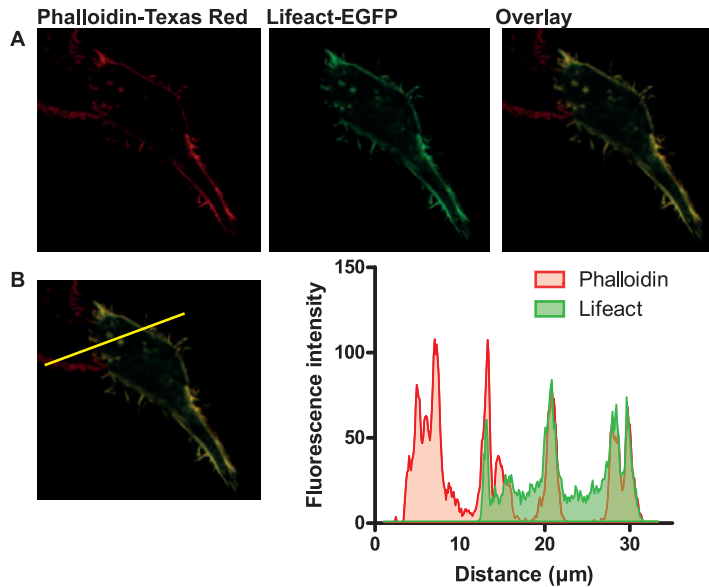


**Figure 3. Expression patterns of Lifeact-EGFP and phalloidin.**

a) Actin filaments were stained with phalloidin in HeLa-80 cells that were transduced with Lifeact-EGFP. An overlay of both images showed co-localised expression in yellow. b) Additionally, co-localisation was measured in a small cross section of the image (yellow line) and fluorescence intensity was plotted against the distance of the line. Peaks of intensity in both images indicated co-localisation of phalloidin and Lifeact-EGFP.

Even though the intensity plot showed clear co-localisation of Lifeact-EGFP and phalloidin, a higher fluorescent intensity was observed in the cytoplasmic region of the Lifeact cells compared to phalloidin staining. Lifeact-EGFP is expressed by the cells and secreted into the cytoplasm where it reversibly binds to actin filaments. Phalloidin proteins also selectively bind to actin filaments, but unbound proteins are removed by subsequent washing steps. Thus probably a small portion of the unbound Lifeact-proteins generates a low intensity fluorescence in the cytoplasm. However, the fluorescence intensity is four times lower than that of the actin filaments and will therefore not affect our analysis.

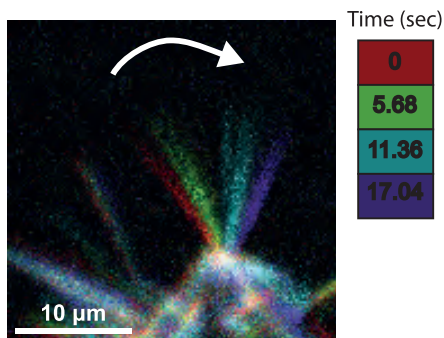


**Figure 4. Time-resolved projection of four images of a single filopodium.** Images were taken every 5.68 seconds of a HeLa-80 cell expressing Lifeact-EGFP. A cropped section of the original images was combined in a color-coded projection. The colours of the filopodia indicate the time points at which the images were obtained.

### ***Time-resolved imaging of filopodial dynamics***

Filopodia act as antennae for a cell to probe the surrounding environment, they explore the surrounding topography and detect extracellular chemicals<sup>245,246</sup>. Therefore, filopodia contain receptors for diverse signalling and extracellular matrix molecules. Without an external stimulus and liquid environment, the movement of filopodia is random<sup>260</sup>. A similar movement is seen in our HeLa-80 cells that stably expressed Lifeact-EGFP. They moved their filopodia randomly through the extracellular environment without the need of any stimulus in the culture medium. By time-resolved imaging, we obtained images with 5.68 seconds intervals for 15 minutes to determine the moving speed of random filopodia movement. Initial experiments showed that the tip of the filopodia travelled around 3.235  $\mu\text{m}$  per 5.68 seconds, which corresponds to  $\sim 550$  nm/s (Fig. 4). In literature, spatiotemporal movement of filopodia has only been measured in terms of extension and retraction rates. Extension rates of a filopodium are reported in the range of  $\sim 30$  nm/s in Dictyostelium cells<sup>261</sup> to 500 nm/s in mouse cortical neurons<sup>261</sup>, which indicates that these rates are depending on the cell type. Moreover, filopodia not only extend and retract, but also move laterally as they sense their environment. Unfortunately, the quick movement of the filopodia restricted acquisition of images at multiple planes with a spinning disk microscope, also referred to as a Z-stack. As a result, filopodia will move out of the focal plane and/or appear if they make a vertical movement between the different stacks. Therefore, the acquisition speed of the microscope is limiting the spatial resolution of our images. Nevertheless, there was frequent movement at a thin cross section of a cell in time, which might be influenced by an external stressor like EMF exposure. Therefore, an image analysis macro for ImageJ was designed to measure the activity of the filopodia and actin filaments. We adapted a method previously published by Van Bruaene et al.<sup>262</sup> and Van der Honing et al.<sup>250</sup> to determine the dynamics of microtubules and actin cytoskeleton in Arabidopsis root hairs. First, a time sequence of images was combined into a stack. Due to the movement of the cell protrusions, substantial noise is introduced that degrades filopodial contrast. To enhance the contrast between the filopodia and the background, a band pass filter was applied. Subsequently, the filopodia were segmented with a Triangle threshold<sup>249</sup>. Every time frame was compared to the subsequent and previous one. Expression of Lifeact in both images was indicated in yellow, new fluorescence signals were shown in green and pixels that disappeared were highlighted in red (Fig. 5).

Despite the fact that confocal systems block out-of-focus light and achieve depth discrimination by the use of a limiting pinhole detector, we still recorded substantial amounts of noise. This might be prevented if a Z-stack was obtained, from which a maximum intensity project could be calculated<sup>263</sup>. This popular method compares all of the pixel values at a given (x,y) position in the stack, and chooses the brightest of these pixel values for the projection. As a result, maximum projections emphasise details in fluorescence images<sup>263,264</sup>. The noise in our images limited our possibilities to segment fine structures, such as the filopodia from the background. Ideally, every individual filopodium should result in a segmented line that is attached to the base of the cell cortex. We tested multiple noise-correction methods, but to no avail. In addition, also local threshold software designed by Gabriel Landini et al. to cope with intensity variations within images, did not result in proper segmentation of our images. Therefore we applied a band-pass filter that enhanced smaller structures, but also clustered neighbouring filopodia together instead of highlighting individual protrusions. The incomplete segmentation might be solved in future research, by increasing the brightness of

fluorescence. Our Lifeact protein was conjugated to only one EGFP fusion protein, however in-frame fusion of multiple fluorescent proteins will enhance the spectral output. Trimeric enhanced yellow fluorescence protein (EYFP) construct created by Genove et al. displayed a 12-fold higher fluorescence output than a single EFYP<sup>265</sup>.

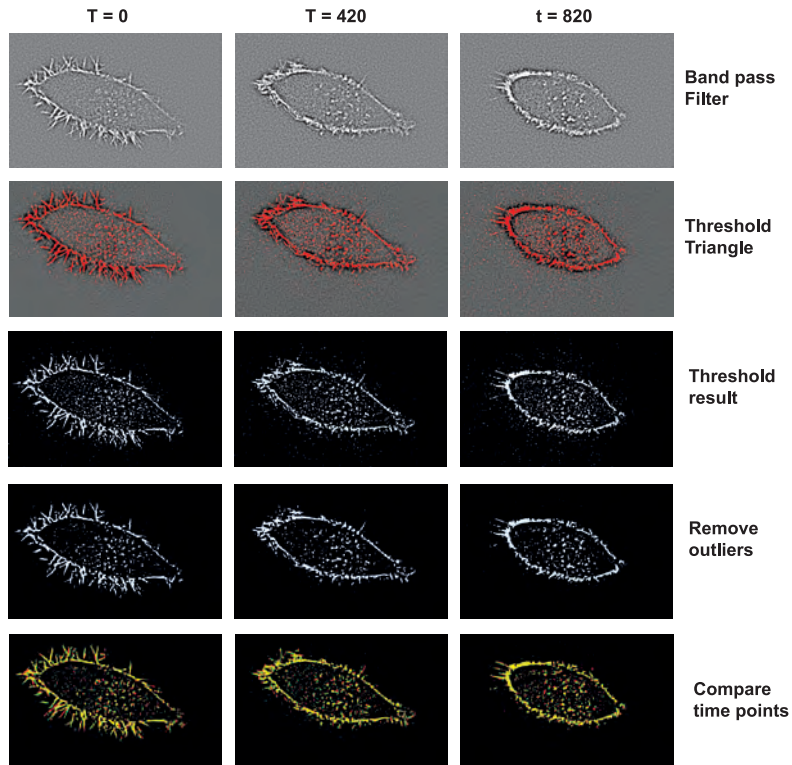


**Figure 5. Image analysis in ImageJ.**

See material and method section for complete description of the different steps.

### ***Filopodial dynamics during epidermal growth factor (EGF) stimulation***

Finally, we investigated if our current method is able to reveal changes in the filopodia dynamics. Images were obtained for 820 seconds of one focal plane of HeLa-80 cells that expressed Lifeact-EGFP. After 270 minutes, which corresponds with 49 images, 10 ng/ml EGF was added to the cells. Image acquisition continued for an additional 550 seconds. Analysis of the dynamics of the filopodia, the cell cortex and small intracellular clusters of actin filaments showed that without EGF, the number of newly appearing pixels is stable in time (Fig. 6). Addition of EGF on the other hand, rapidly reduced the movement. The filopodia were retracted and moved less quickly compared to the unstimulated situation. Two minutes after the addition of EGF, a new equilibrium was reached when the cell had retracted almost all protrusions and started to migrate. Our method was able to detect major changes of the filopodia induced by EGF. Subsequent experiments showed that our observations were related to EGF stimulation, and not the addition of a liquid, because cells stimulated with



PBS showed no significant change in their filopodial dynamics (Fig. 7). EGF is a very potent stimulator of both elongation and retraction of filopodia. It has been shown that filopodia are enriched with EGF receptors (EGFR). Moreover, Tsu et al. reported that the elongation and retraction rate increase up to 30% in CL1-10 lung cancer cells after addition of EGF, which suggests more vigorous actin activities in the cells induced by EGF<sup>266</sup>. Eventually, EGF will trigger coordinated cell migration leading to the formation of a lamellipodium.

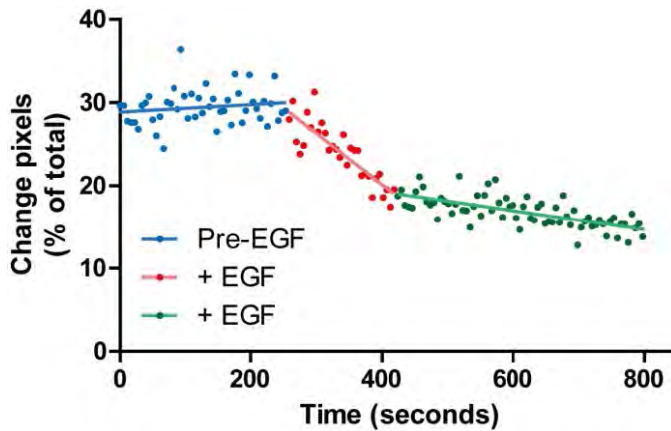


**Figure 6.** Dynamics of the filopodia and actin cell's cortex before and during EGF stimulation. Images were obtained from an individual Lifeact-EGFP expressing HeLa-80 for 15 minutes every ~5.5 seconds (150 images). The dynamics of the actin filaments was calculated by image analysis and expressed as the number of pixels that changed between two subsequent images. The graph was divided into three phases; before EGF stimulation (blue), immediately after EGF stimulation (red) and after two minutes of EGF stimulation (green).

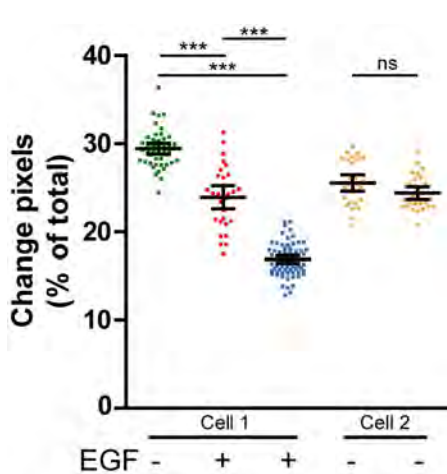
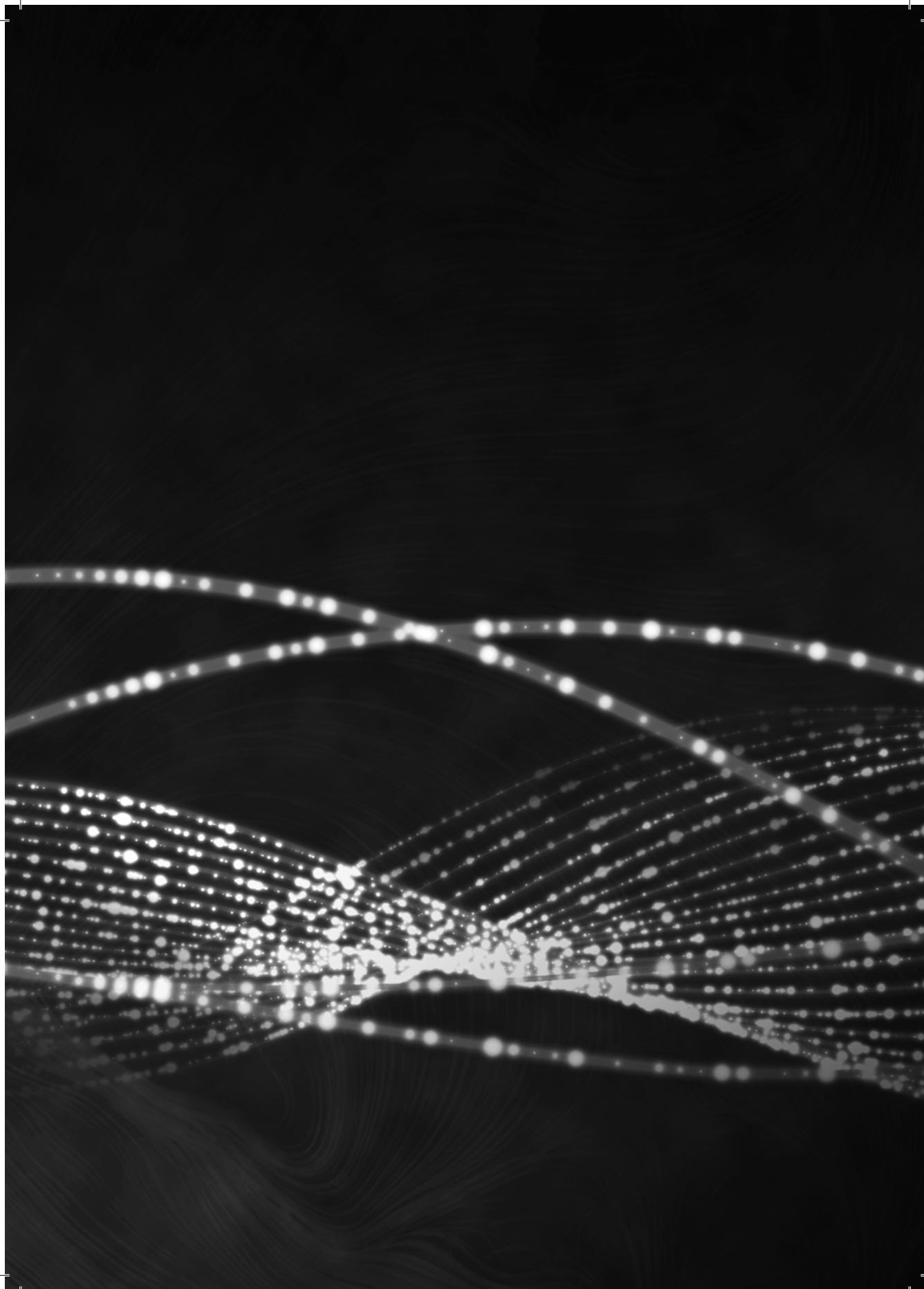


**Figure 7.** Dynamics of the filopodia and actin cell's cortex. Images were obtained from two individual Lifeact-EGFP expressing HeLa-80 every ~5.5 seconds up to 15 minutes (150 images). The dynamics of the actin filaments was calculated by image analysis and expressed as the number of pixels that changed between two subsequent images. The cells were stimulated (cell 1) or left unstimulated (cell 2). The measurements of the EGF stimulated cells were divided into three phases; before EGF stimulation (blue), immediately after EGF stimulation (red) and after two minutes of EGF stimulation (green). The measurements of the unstimulated cells (yellow) were obtained in the first time frame 0 to 5 minutes (left) and after stimulated with PBS (right). Graph shows mean with 95% CI of all measurements (dots), ns = not significant and \*\*\*  $p < 0.01$ .

In 2002, Gartzke and Lange<sup>43</sup> suggested in their theoretical paper a potential site of interaction for LF EMF exposure. Cell protrusions, like microvilli, possess the property to function as antenna and facilitate ion conductivity along their actin-filament core. In their extensive review, they elaborate on the potential interaction, however they did not describe an experimental design suited to investigate their theory *in vitro*. Moreover, subsequent articles published by Gartzke and Lange mainly focus on the role of actin filaments as potential calcium stores<sup>267</sup>. Numerous proteins regulate actin filament (de)polymerisation, many of which are dependent on calcium. These proteins for instance cap the barbed ends of actin filaments, to prevent elongation<sup>268,269</sup> or nucleate actin assembly<sup>270</sup> to facilitate branching. In this study, we extrapolated the original theoretical site of interaction from microvilli to other cell protrusions, the filopodia. We created an epithelial cell line with stable expression of a Lifeact-EGFP and generated a clonal expansion of individual cells. Uniformity of the clones and expression patterns of Lifeact-EGFP were validated by flow cytometry and by immunostaining. Our image analysis was able to quantify the altered dynamics of the filopodia and actin cortex upon EGF stimulation. However, we expect the potential effect of LF EMF exposure on filopodia to be more subtle than EGF stimulation, due to the low level energy. Preliminary experiments of fixed samples did not reveal any alteration in the shape or number of the filopodia (data not shown), but the effect of exposure might be underestimated in these experiments, because we compared different cells. Filopodia are dynamic and motile protrusions that respond to very sensitive changes in the cell's environment. Therefore, many, be it subtle, between-cell variations in the number of filopodia, in their length and their orientation might be expected after LF EMF exposure. A reversible or only a short term effect of EMF exposure will not be detected in fixed samples. Our current method will resolve these issues and is therefore suited to examine the potential effects of LF EMFs during and after exposure. It will provide information about the behaviour of the filopodia with spatiotemporal resolution.





# Chapter 5

---

## Effects of 50 Hz electromagnetic field exposure on epithelial cell migration during wound healing

Lieke A. Golbach, Marcela M. Fernandez-Gutierrez, Tomas H.M. Strooband, Huub F.J. Savelkoul, B.M. Lidy Verburg-van Kemenade

*Manuscript in preparation*

## Abstract

*In vivo* wound-healing is the orchestrated process of clot formation, inflammation, cell migration and proliferation, and tissue remodelling. It is initiated when the integrity of an epithelial barrier is compromised. Scratch assays are the *in vitro* orthologue of wound healing that enable measurements of mainly the migration phase. This type of assay is extensively used to screen potential novel migration enhancers or to investigate the effect of inhibitory drugs. Low frequency electromagnetic field (LF EMF) exposure is suggested to influence the migration of cells. In this study we tested this hypothesis by pre-exposure of cells to moderate level fields (500  $\mu$ T) with a continuous 50 Hz sine wave. Exposure was followed by a scratch assay with high-throughput image acquisition in combination with a custom-designed analysis macro for ImageJ. To ensure that the assay will detect either stimulated or inhibited migration, it was validated with epidermal growth factor (EGF) stimulation and pharmacological inhibition with cytochalasin-D and EHop-016. Pre-exposure of the cells for 18 hours to the LF EMFs did not change the migration speed or wound closure compared to sham treatment. However, initial experiments of a short 2-hour exposure indicated increased cell migration, but this effect was abolished when the scratch was almost closed. Our data suggest that short pre-exposure influences epithelial migration speed, and that this effect is dependent on the exposure duration. Longer chronic exposure might lead to cellular adaption, without any effects on migration.

## Introduction

The ability of individual cells to actively migrate, either directionally or randomly, is an important aspect already at the first stages of life<sup>271</sup>. Later in life, cell migration is involved in important physiological processes in the development and maintenance of multicellular organisms. The migration process is driven by a tightly orchestrated signalling pathway that reorganises the actin cytoskeleton. Actin assembly drives formation of a leading edge and changes a cell's polarity. Subsequently, the leading edge starts to move forward, while the tail of the cell is retracted, which results in movement of cells in a particular direction to a specific location.

Cell migration is also involved in wound healing. Wound healing is a complex, multicellular process that involves the coordinated efforts of several cell types including keratinocytes, fibroblasts, endothelial cells, macrophages, and platelets<sup>272,273</sup>. The primary function of the epithelial layer is to serve as a protective barrier against the environment. Loss of integrity of the skin causes disruption of blood vessels and extravasation of blood constituents. The assembly of a blood clot re-establishes haemostasis and provides a provisional extracellular matrix for cell migration. The platelets in the wound secrete several mediators of wound healing, such as platelet-derived growth factor, that attract and activate macrophages and fibroblasts. After the inflammation phase, the keratinocytes initiate re-epithelisation, only a couple of hours after injury. Several chemokines and growth factors have been shown to influence keratinocyte migration, like EGF, TGF- $\beta$ , GM-CSF, IL-1 $\beta$  and IL-6<sup>274</sup>.

Inside the wound, it has been demonstrated that endogenous electric fields play a central role in promoting cell shape changes and directing migration<sup>275,276</sup>. Many epithelial cells, including human keratinocytes, have the ability to detect electric fields of this magnitude and respond with directed migration. Moreover, *in vitro* exposure to small electrical fields could induce reorientation of human corneal epithelial cells<sup>277</sup>, fibroblasts<sup>278</sup> and keratinocytes<sup>279</sup>. Recently, possible interactions with low level electromagnetic fields are debated (EMF)<sup>211</sup>. The current daily exposure to EMFs produced by household appliances and power lines leads to increased concern in our society.

In the present study, we examined the influence low level and low frequency EMF (LF EMF) (500  $\mu$ T, 50 Hz) exposure on the migration of epithelial cells with the use of a scratch assay. In a scratch assay, a wound is introduced by scratching cells grown in a monolayer. The cells at the wound edge polarise and migrate into the wound space, without the need of chemoattractants. We performed time-laps microscopy of the scratch assays to observe the behaviour of cells after exposure. Analysis of the images was done with an automatic image-analysis method developed for this study. Our method is not susceptible to user-dependent errors and it performs blinded analyses. We demonstrate that 18 hours pre-exposure to 50 Hz EMFs does not affect the migration rate of the epithelial cells *in vitro*.

## Material and Methods

### *Cell culture*

Human oral gingival carcinoma cell line (Ca9-22) was routinely cultured in complete medium containing DMEM supplemented with 10% fetal bovine serum (FBS), 25 mM HEPES, L-glutamine (2 mM), streptomycin (100 µg/ml) and penicillin (100 U/ml). The cells were cultured at  $37\pm 0.2^\circ\text{C}$  in a humidified atmosphere containing 5%  $\text{CO}_2$  and passaged every three to four days.

For the migration assay, the cells were detached from the tissue culture flask and diluted to 35,000 cells in 100 µL complete medium. Subsequently, 100 µL was added to every well of a 96 well plate and the cells were left to adhere for 18 hours in the incubator. After incubation, the medium was removed and 100 µL per well of starvation medium containing DMEM without phenol red, and supplemented with 25 mM HEPES, L-glutamine (2 mM), streptomycin (100 µg/ml) and penicillin (100 U/ml) was added. The cells were incubated for two hours in the starvation medium and then the nuclei were stained for 20 minutes with 2 µg/ml Hoechst before the scratching and migration assay was performed.

### *Exposure system*

Cell pre-exposure was done in the middle of a specialised custom-made exposure system by Immument BV<sup>280,281</sup>. The coil fits inside a standard cell culture incubator to ensure optimal cell culture conditions with  $37\pm 0.2^\circ\text{C}$  and 5%  $\text{CO}_2$ . The cell culture flasks were placed in the central region of the coils, perpendicular to the vertical magnetic field lines. The copper wire coil is wound on a double co-axial cylinder with an inner (65 turns; Ø 184 mm) and outer cylinder (2 times 8 turns; Ø 400 mm) of polymethyl methacrylate (PMMA). All positional parameters are optimised together to achieve a high homogeneity in the exposure area of <0.4%. The system is connected to a signal generator with pre-programmed signals. The LF EMF wave used was a 50 Hz sine wave. The resulting magnetic signal B (t) is measured using a Gauss/Tesla meter with sensitive probe (Model 5180, F.W. Bell). A magnetic flux density of 500 µT was used. Two identical cell culture incubators with an identical exposure coil inside were used and randomly assigned to be active or sham for each experiment, to eliminate any effects induced by the internal environment of one of the incubators. Background AC levels at the place of exposure and sham-exposure were less than 0.2 µT and ambient DC fields were 10 µT.

### *Cell exposure*

Prior to every migration assay, a 96-well plate from BD Falcon™ was cut in half mechanically, between column 6 and 7. The two halves were joined together during cell seeding and imaging. LF EMF or sham exposure was performed simultaneously in two identical cell culture incubators at  $37\pm 0.2^\circ\text{C}$  in a humidified atmosphere containing 5%  $\text{CO}_2$ . Before exposure, the two halves of the 96-well plate were separated and one half of the plate was placed in the middle of the LF EMF coil and the other in the sham coil. For both groups, culture conditions were kept identical. After exposure, both halves of the plate were joined again and treated as one single 96-well plate during the subsequent protocol. For the short, two-hour exposure, cells were exposed during the starvation period. For the long-term exposure, the cells were exposed to 50 Hz sine waves during the adherence period, 18 hours,



and subsequent 2-hours starvation period. These two exposure periods were selected based on the current notion that acute and chronic exposure<sup>172,201,282</sup> might alter diverse cellular functions.

#### *Scratching and migration assay*

After Hoechst staining of the nuclei, a horizontal scratch was made with a sterile scratch tool (Peira Scientific Instruments, Belgium). All 96 wells of one joined plate were scratched simultaneously. The cells were washed two times with sterile PBS, to remove detached cells and excess dye. Subsequently, 100  $\mu$ L starvation medium was added to every well supplemented with inhibitors or stimuli. To inhibit or reduce cell migration, 5  $\mu$ M EHop-016 or 1  $\mu$ M cytochalasin-D was added. To promote cell migration, 6 ng/ml epidermal growth factor (EGF) was added. The cell culture plate was placed into the acclimated chamber (37°C and 5% CO<sub>2</sub>) of the BD Pathway 855 Bioimaging System (BD Biosciences) for image acquisition. Hoechst images were obtained with a 350 nm laser, and emission was recorded at 461 nm with a 4x magnification. Bright field was recorded by sample illumination of white light. In total, 18 images per well were taken over a time course of ~5.5 hours.

#### *Data analysis*

Initial Hoechst and bright field images were acquired at 16-bit and taken every 18 minutes. The Hoechst-stained nucleus images were used to analyse the migration speed and the bright field images served as a visual control for cell vitality. The Hoechst images were analysed with a custom-designed macro developed in ImageJ (Macro code present as supplementary data file), as existing plug-in and codes did not suit our needs or were unable to segment the scratch from the cells. Figure 1 shows a schematic overview of our macro. First the macro combines all images taken from one well together in a stack with only one dimension, time. Then the 16-bit images were scaled back to 8-bit and cropped to allow analysis of the complete stack at once. To enhance the contrast of the cells, we use a mathematical technique that finds edges in images. Subsequently, the maximum pixel intensity with a radius of 4 was applied to smooth the monolayer of cells and cover areas with lower fluorescent intensity, like the cytoplasm of the cells. The scratch and monolayer of cells is then separated, with a triangle threshold. The converted mask is inverted and the white area is calculated by the software, generating a table with the scratch area per image. This analysis is performed blinded, to prevent the introduction of any user-dependent bias.

#### *Statistics*

Data were analysed using GraphPad Prism 5.0 (GraphPad Software). Differences between treatments were analysed using repeated-measures two-way ANOVA with post-hoc Bonferroni correction. The number of individual experiments, group mean and SEM are indicated in the legend. Statistical significance was accepted at  $p < 0.05$ .

## **Results**

#### *Image analysis of the scratch area*

Scratch assays represent a two-dimensional wound healing, which can be visualised by fluorescence microscopy in a time-resolved manner. Both the sham and EMF treated

samples were imaged at the same time, with a maximum of 48 samples per group. In our setup, every 19 minutes images of the bright field and stained nucleus were taken of all 96-wells (Fig. 1). To translate the 8-bit fluorescent images of the scratch to an actual area value, an analysis macro in ImageJ was designed (Fig. 2). In short, 8-bit images of the labelled cells were cropped to reduce the file size. The nuclei were brightly fluorescent, whereas the surrounding cytoplasm did not emit fluorescent light. To highlight the sharp change in intensity between the nucleus and the cytoplasm, a Sobel edge detector was applied. The natural edges in the image led to bright lines around every nucleus. A value that corresponded with the maximum pixel intensity of a circle with a radius of four pixels was assigned to every pixel, to merge all nuclei into a uniform monolayer.

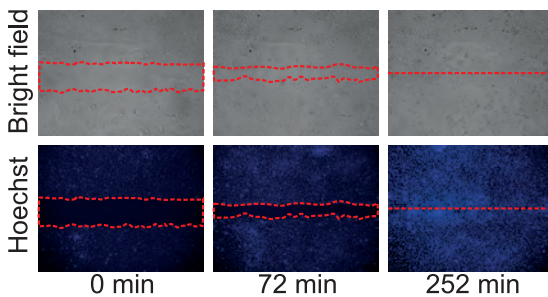


**Figure 1. Overview of three images obtained with our high-throughput microscope setup.**

Before the assay, epithelial cells are grown in monolayer and stained with Hoechst, to visualise their nucleus. Subsequent, a scratch is introduced, which mimics a wound. Migration of the cells is then imaged for 5.5 hours and images are taken every 19 minutes of the bright field and fluorescent channel. The red line indicates the scratch area created in the monolayer.

As a result, the contrast between the scratch and the cell layer became large enough to segment both areas with a Triangle threshold. This threshold was calculated for every individual image and subsequently the binary mask was inverted. Finally, the scratch area was analysed by counting the number of white pixels in every frame, which represents the migration speed for every individual well. The analysis was performed in a blinded manner, without the introduction of a user-defined threshold or area.

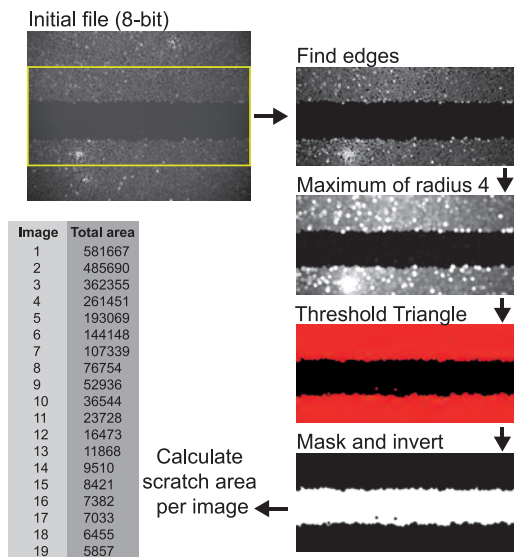


**Figure 2. Overview of the ImageJ macro designed for our scratch assays.**

The 8-bit fluorescent images are cropped, edges are enhanced and smoothed. Subsequently, the image is thresholded and inverted. The area of the scratch is calculated for every time point of a single well.

### Validation of the migration speed

An automatic imaging and analysis tool is ideal to prevent user-introduced bias. However, we needed to establish that epithelial cell migration in our setup could be influenced by environmental factors. As a baseline, we used cell migration in cell culture medium without any additions. Cell migration was stimulated with EGF (6 ng/ml) and inhibition was induced with two different cytoskeleton inhibitors. Cytochalasin-D (1  $\mu$ M) blocked actin depolymerisation, whereas EHop-016 (5  $\mu$ M) inhibited the upstream activators of actin-filament formation, namely *rac1-3*<sup>283</sup>. Figure 3 shows that epithelial migration can be enhanced or decreased when the cells are incubated with the different chemicals. EGF stimulation significantly enhanced cell migration and led to complete closure of the scratch 200 minutes after the initial scratch. Of the two inhibitors, cytochalasin D showed to be more effective in reducing the cell migration. Already at the start of the experiment, this pharmacological inhibitor slowed down cell migration significantly. EHop-016 on the other hand, displayed a reduction after 200 minutes, compared to the medium control. Based on these results, we selected EGF and cytochalasin-D for further experiments.

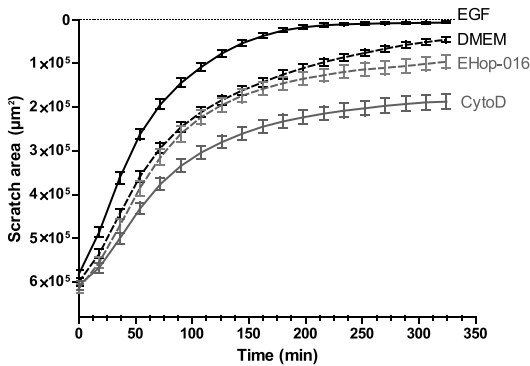


**Figure 3. Effect of different treatments on migration speed.**

Epithelial cell migration was assessed with a scratch assay. The cells were incubated in DMEM, DMEM supplemented with EGF, EHop-16 or cytochalasin-D (CytoD) for 5.5 hours during imaging to evaluate pharmacological inhibition or promotion of migration. The area of the scratch was calculated every 19 minutes. Mean  $\pm$  SEM of at least 45 individual scratches measured in three individual experiments.

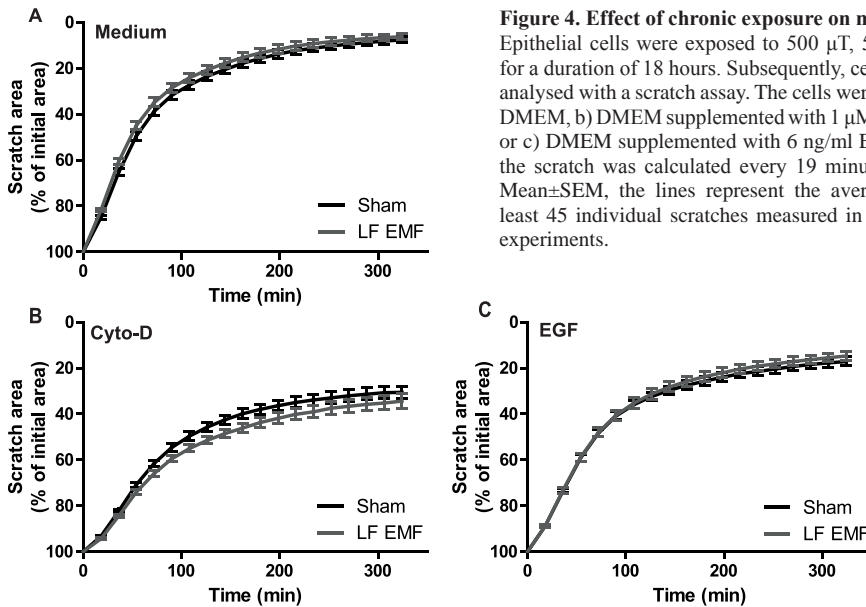
### Effect of chronic 50 Hz EMF exposure

The cells were exposed to a 50 Hz sine wave, with a magnetic flux density of 500  $\mu$ T for 18 hours. The exposure was applied before the cell migration assay was performed and the data from three individual experiments were combined. For the DMEM treated cells, no significant difference was observed in the migration speed and wound closure after exposure (Fig. 4a). Moreover, both groups required more than 5.5 hours to completely close the gap. Addition of EGF to selected samples only enhanced migration speed, without revealing a significant difference between sham and LF EMF exposed cells (Fig. 4b). Furthermore, inhibition of actin polymerisation during migration did not significantly change migration in the LF EMF treated samples compared to sham (Fig. 4c). Hence, chronic LF EMF exposure was unable to influence epithelial migration in the presence of minimal culture medium, with or without EGF or cytochalasin-D.

### Effect of acute two-hour EMF exposure

Chronic exposure might lead to adaptation of the cell, which subsequently does not respond to the exposure or showed altered migration. For this reason, we also included an experiment with a minimised exposure period of two hours just before imaging (Figure

5). Cells exposed to 50 Hz sine wave EMF at a magnetic flux density of 500  $\mu\text{T}$  showed significant increased cell migration after 90 minutes (Fig. 5a). This enhanced migration speed continued up to 216 minutes, after which the migration speed slowed down as the gap is almost closed. Sham exposed cells showed different kinetics, but an equal gap size after 5.5 hours. The remaining gap size of sham exposure was  $7.45\% \pm 1.19$  and  $4.08\% \pm 0.89$  for EMF treated samples. This enhanced migration after EMF exposure was completely abolished when EGF was added to the medium (Fig. 5b). EGF stimulated cell migration, but did not reveal differences between the two groups.



## Discussion

In this study we show that *in vitro* cell migration is not altered by LF EMF exposure. We applied a 500  $\mu\text{T}$  field of a continuous 50 Hz sine wave for two and 18 hours, before creating a wound in the monolayer of the cells. We used time-lapse microscopy to measure the influence of exposure during the wound healing process. Furthermore, the results of every experiment were independently calculated with an automatic analysis protocol. While pharmacological inhibition or biological stimulation could alter the migration speed, pre-exposure for 18 hours to LF EMF did not alter the migration speed significantly at any moment in the wound-healing process. A two-hour exposure on the other hand, showed significant increase of cell migration during the wound healing, but after 5.5 hours the effect of exposure was not detected any more.

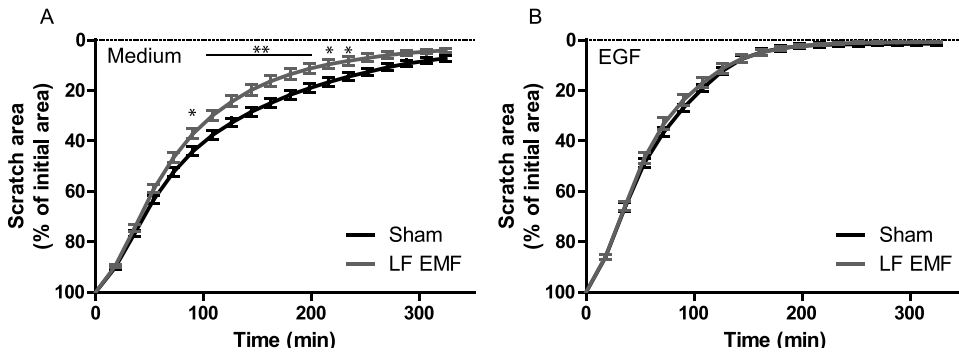


**Figure 5.** Effect acute exposure on migration speed. Epithelial cells were exposed to 500  $\mu$ T, 50 Hz LF EMFs for a duration of two hours. Subsequently, cell migration was analysed with a scratch assay. The cells were incubated in a) DMEM or b) DMEM supplemented with EGF (6 ng/ml). The area of the scratch was calculated every 19 minutes, a/b) Normalized Mean $\pm$ SEM, the lines represent the average value of at least 15 individual scratches measured in one individual experiments.

*In vitro* wound healing assays are widely used for research in biology and medicine<sup>284</sup>. Cells on the edges of an artificial wound migrate towards the wound area, allowing quantification of the *in vitro* healing process. Visualisation occurs by time-lapse microscopy, a powerful method to directly observe and characterise the migratory behaviour of cells. With this method, the influence of different culture conditions, different biological stimuli, novel small molecules or environmental factors can be investigated. Conventional data analysis of the migration speed and scratch closure are done by manual cell tracking. This is a labour-intensive method that is susceptible to user-dependent errors regarding the determination of the "edge" of the wound<sup>285</sup>. Therefore in this study, we developed an application of automatic migration tracking of a monolayer of cells. Automatic tracking of scratch areas is not a new phenomenon, but every type of software or programming code is only applicable to a certain type of data. For our data set, already published open source methods by Glass et al.<sup>286</sup> (Mitobo) and Bise et al.<sup>287</sup> were unsuitable, since they did not segment the scratched area in our images properly. This was probably due to uneven illumination and staining of only a small portion of a single cell, the nucleus. Furthermore, the method of Bise et al. was not designed to process a large number of images, making it unsuitable for high-throughput applications. For this reason we developed our own image analysis. Through enhancing sharp changes in intensity with a Sobel edge filter<sup>288</sup>, we highlighted the transition between the nucleus and the rest of the cells. By calculating the maximum pixel intensity for a small radius, we subsequently enlarged the highlighted cell area and joined neighbouring cells into one coherent monolayer. The image was then thresholded with a triangle algorithm<sup>249</sup>. In this approach, a line is constructed between the maximum and the lowest value of the grey level histogram. The threshold cut-off is the point of maximum distance between the line and the histogram. This technique was particularly effective as our monolayer of cells produced a weak peak in the grey level histogram, also shown by similar images other groups that segmented different cells types, tissues and cellular structures<sup>289-291</sup>. The different segmentation and enhancement steps were combined in a small macro compatible with ImageJ (Fig. 2), to ensure automatic and unbiased analysis of every image. Our macro prevented user-dependent

biases regarding the outcomes. As a result we could perform both image acquisition and data analysis blinded.

The assay was validated with the use of a stimulatory growth factor and two pharmacological inhibitors. We observed that wound-healing is hampered when actin polymerisation or pivotal cytoskeleton regulator proteins were inhibited. The migration speed was reduced and a scratch remained present, even after 12 hours. On the other hand, compared to only culture medium, EGF was able to increase migration speed immediately after addition. Substantial levels of EGF are found in wound fluid of patients with small burn injuries<sup>292</sup>. This locally produced growth factor is secreted by platelets, macrophages, and wound fibroblasts<sup>293</sup> and it showed the potential to accelerate delayed wound healing in clinical applications<sup>294</sup>. EGF-receptors are expressed by many types of cells including skin keratinocytes, fibroblasts, vascular endothelial cells, and epithelial cells. They are located on the plasma membrane and cluster together on the leading edge upon activation, to promote protrusions, directing cell migration and consequently healing of the wound. Since EGF promotes cell migration, EGF production and activation of the receptors is suggested as a potential mechanism for the beneficial effects of pulsed EMFs<sup>211,295</sup>.

To minimise the inter assay variation in our study, we applied an unconventional approach. By mechanically separating the microscopy tissue culture plate into two equal parts, we ensured that our samples were subjected to identical environments during imaging. Temperature has a ubiquitous impact on all cells. It not only affects enzymatic activities at the molecular level, but also affects mechanical properties at subcellular level<sup>296,297</sup>. A thermodynamic study of rabbit skeletal muscles showed that polymerization was enhanced at increasing temperatures<sup>298</sup>. Moreover, cells modulate their adhesive state depending on the temperature, as cell adhesion is dramatically reduced at room- or lower temperatures compared with physiological temperatures<sup>299</sup>. Hartmann-Petersen et al. demonstrated that temperature of the medium profoundly influenced cell motility recorded by time-lapse microscopy<sup>300</sup>. Additionally, they showed that cell dissociation procedures, seeding density, time of cultivation, and substrate concentrations affect cellular speed significantly. So, temperature is an important experimental variable and thereby also a confounding factor in *in vitro* wound-healing assays. With our experimental design, we minimised the confounding effect of temperature, which strengthens our outcome and might explain contradictory reports by other research groups.

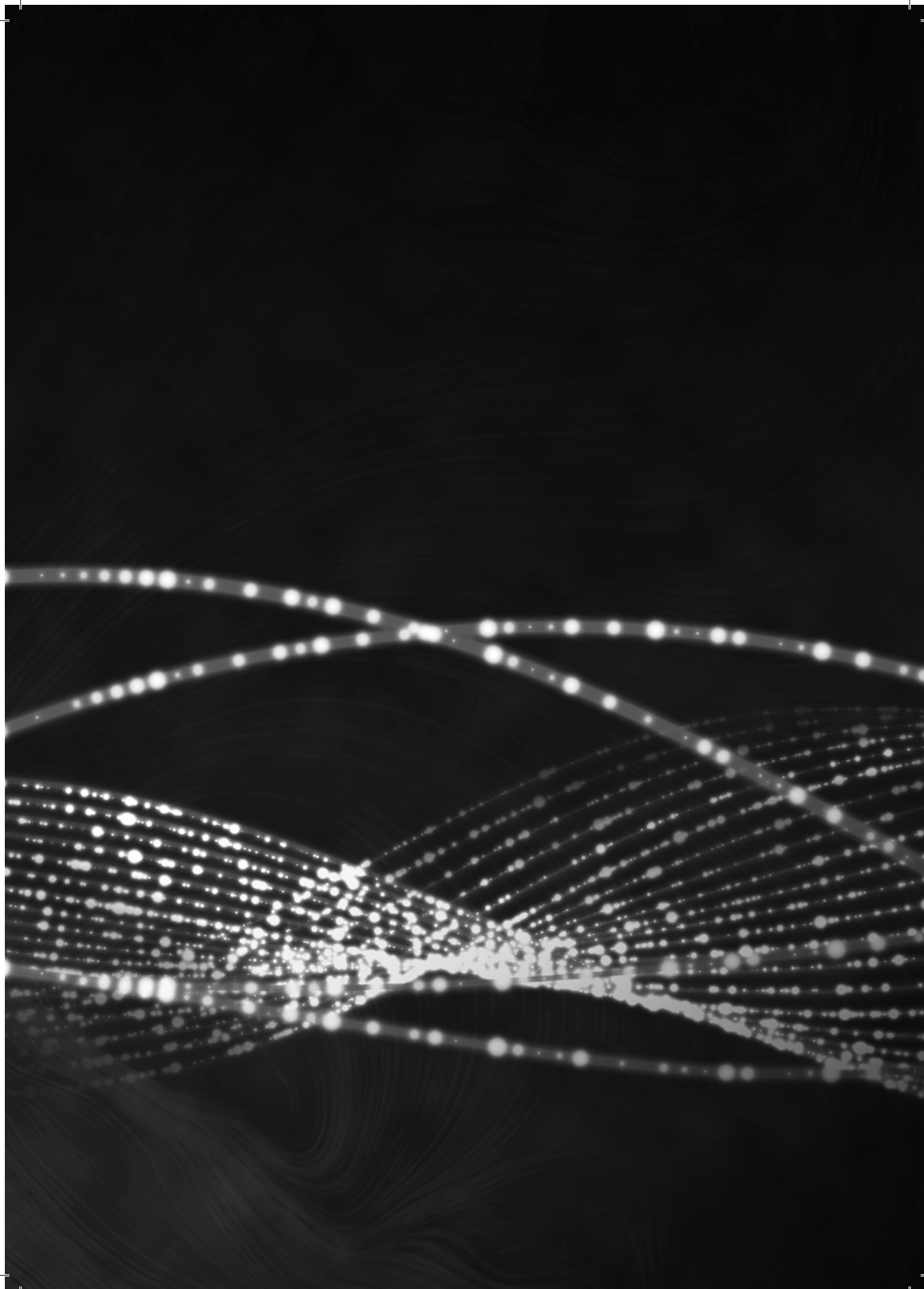
LF EMF exposure was applied for two or 18 hours to a monolayer of epithelial cells. Only the experiment of short two hours exposure showed altered cell migration during subsequent time-lapse microscopy. However, even though we analysed up to 15 individual scratches at the same time, it is still premature to draw final conclusions as also small intra assay variations were observed between separate experiments measured after an 18-hour exposure period. Altered migration speed after an exposure period of two hours, but unaffected kinetics after 18 hours of exposure might indicate that cellular adaptation occurs. Cellular adaptation to a stressor is suggested previously by Goodman et al.<sup>224</sup>, when they determined that only a brief exposure modulated protein expression in neutrophils. A few years later, Lin et al.<sup>225</sup> confirmed these results and suggested that chronic exposure of cellular systems could lead to adaptation without the occurrence of any harmful effects. Our exposure system was designed to deliver a homogeneous, well-characterised EM field inside a cell culture incubator. The system is unable to apply exposure during microscopy imaging. For this

reason, we are unable to detect any short and reversible interactions that eventually led to adaptation. Additional experiments are required to examine the effect of both 2-hours and acute exposure on cell migration and wound healing.

EMF-induced effects on migration have shown to be both beneficial and harmful. The therapeutic potential of pulsed EMFs on skin lesions has been demonstrated with rats<sup>301</sup>. In addition, human clinical studies highlighted that pulsed EMF (PEMFs) can reduce healing time as well as diminish the rate of recurrence of venous leg ulcers<sup>302,303</sup>. The *in vitro* studies however show conflicting reports that corroborate the beneficial effects, as cell migration was increased<sup>304,305</sup>, but also showed no effects by EMF exposure<sup>306</sup>. The outcomes varied among the studies, possibly due to different treatment protocols or frequencies applied.

There is both experimental *in vitro* and clinical *in vivo* evidence supporting the beneficial effects of electromagnetic fields. This effect is strongly related to the use of specific pulsed EMFs that are produced by custom-made devices. Pulsed EMF does not represent chronic exposure in our modern society. Low frequency fields are generated by our mobile phones, wireless routers, tablets, laptops, high voltage power lines and mobile phone base-stations. The increasing use of electronics and wireless communication systems has made our lives easier, but recently people worry about potential adverse health effects induced by chronic exposure to these electromagnetic fields. However, there is yet inadequate evidence to confirm the impact of these fields on human health. We were interested in the potential effect of environmentally relevant wave forms and found no clear indications that chronic exposure influences cells *in vitro*. Moreover, this study investigated an exposure level of 500  $\mu\text{T}$ , which is 1000-times higher than normal ambient exposure levels<sup>229</sup>. A guideline limit with a magnetic flux density of 200  $\mu\text{T}$  is published by the International Commission on Non-Ionizing Radiation Protection (ICNIRP)<sup>24</sup>. For occupational exposure, the safety limits are at 1000  $\mu\text{T}$ . A magnetic flux density of 500  $\mu\text{T}$  was selected based on the ICNIRP guidelines, however replicating our experiments with low level fields, up to 5  $\mu\text{T}$ , is highly recommended for future research.

In summary, we designed an automatic image analysis protocol, to investigate the influence of LF EMF (50 Hz, 500  $\mu\text{T}$ ) on *in vitro* wound healing. The image acquisition and analysis were performed blinded to prevent user-dependent biases. Long term exposure did not influence cell migration, but initial data that showed enhanced migration speed after a short 2-hours exposure awaits confirmation.





# Chapter 6

---

## **Low-Frequency Electromagnetic Field Exposure Enhances Extracellular Trap Formation by Human Neutrophils through the NADPH Pathway**

Lieke A. Golbach, Marleen H. Scheer, Jan J.M. Cuppen, Huub F.J. Savelkoul, B.M. Lidy Verburg-van Kemenade

*Published in Journal of Innate Immunity  
Volume 7 (2015)*

## Abstract

Low-frequency electromagnetic fields (LF EMFs) are abundantly present in modern society and the potential biological consequences of exposure to these fields are under intense debate. Immune cells are suggested as possible target cells, though a clear mechanism is lacking. Considering their crucial role in innate immune activation, we selected an *ex vivo* exposure setup with human neutrophils, to investigate a possible correlation between neutrophil extracellular traps (NETs) formation and LF EMF exposure. Our study shows that formation of NETs is enhanced by LF EMF exposure. Enhanced NET formation leads to increased antimicrobial properties, as well as damage to surrounding cells. We found that LF EMF-induced NET formation is dependent on the NADPH-oxidase pathway and production of reactive oxygen species (ROS). Additionally, LF EMF exposure does not influence autophagy and PAD4 activity. Our study provides a mechanism by which exposure to LF EMFs could influence the innate immune system.

## Introduction

Environmental exposure to low-frequency electromagnetic fields (LF EMFs) produced by household appliances, communication equipment and power lines is increasing. Consequently, societal concern regarding potential adverse health effects of chronic exposure to LF EMFs is rising<sup>307</sup>. Reported effects of LF EMFs on biological systems range from harmful interactions<sup>120</sup>, to beneficial effects<sup>308</sup>. No precise mechanism of action of LF EMFs has yet been elucidated, although immune cell activation through receptor interactions, calcium mobilisation and free radical production has been suggested<sup>172</sup>. Mechanistic studies to elucidate the biological response to LF EMF exposure so far mainly focussed on macrophages and monocytes<sup>163,172,308</sup>. Neutrophils on the other hand, were not studied extensively in this context. Neutrophils however, fulfil a key role in the innate immune system by rapid eradication of invading pathogens via several strategies. They quickly migrate towards an infection, and dominate the infected site already after a couple of minutes<sup>309</sup>. They are highly reactive, mobile and sensitive cells, which makes them putative targets to investigate possible cell modulation by LF EMF exposure<sup>172</sup>.

Initially phagocytosis of pathogens and degranulation of lytic enzymes were considered to be the only two antimicrobial strategies neutrophils used, but in 2004 a third special defence mechanism was described: neutrophil extracellular trap (NET) formation<sup>66</sup>. During NET formation, nuclear DNA is mixed with antimicrobial proteins to release an antimicrobial extracellular trap that captures and destroys extracellular microbes. Recent studies showed the importance of NADPH-oxidase activity and consequential ROS formation that triggers dissociation of the peptide complexes, which contain the antimicrobial proteins<sup>75,310</sup>. Subsequently, peptidylarginine deiminase 4 (PAD4)<sup>311</sup> decondensates the chromatin, followed by disintegration of the nuclear envelope through autophagy to facilitate intermingling of these antimicrobial peptides with chromosomal DNA<sup>80</sup>. These findings underscore that NET formation involves specific signal transduction pathways and is tightly regulated to ensure a well-balanced innate immune response. NET formation requires an active NADPH-oxidase complex to generate large amounts of superoxide ( $O_2^-$ ) that are rapidly dismutated to hydrogen peroxide ( $H_2O_2$ ). Chronic granulomatous disease patients highlight the importance of functional NADPH oxidase activity, since these patients fail to maintain phagocytosis or generate NETs<sup>312</sup>. Even though NET formation involves activation of intracellular signalling pathways that have been linked to effects of LF EMFs, such as ROS production and NADPH-oxidase activation<sup>52,313</sup>, a correlation between NET formation by neutrophils and LF EMF exposure has not yet been studied. In an *ex vivo* experimental setup we show that LF EMF exposure is able to enhance NET formation in neutrophils for which the NADPH-pathway and subsequent ROS production are essential. These NETs are able to capture and kill bacteria, as well as damage epithelial cells, thereby indicating that NET formation by neutrophils is a vital but also delicately regulated process, which may be modulated by LF EMF exposure. Our study provides a reliable mechanism by which exposure to LF EMFs could influence the innate immune system.

## Material and Methods

### *Neutrophil isolation and neutrophil extracellular trap formation*

Blood of healthy donors, which were not taking any medication, was used. Ethical permission for all donations was obtained from a local ethical committee (number NL.44545.091.13) and a written consent was obtained from each donor. Blood was layered onto a discontinuous Percoll density gradient (1.079 g/ml and 1.098 g/ml) and centrifuged at 1200 x g for 10 minutes. Red blood cells were lysed and the remaining neutrophils were washed and with RMPI (detailed method in supplementary note 1). Cell purity was ~98% or higher determined by flow cytometry. To induce NET formation,  $0.1 \times 10^6$  neutrophils were seeded in black/clear 96-well plates and left to adhere for one hour with or without diphenyleiodonium chloride (DPI) (0.5  $\mu$ M, 5.0  $\mu$ M), Wortmannin (100 nM), Cl-Amidine (200  $\mu$ M) or Cytochalasin D (20  $\mu$ M). NET formation was induced by the addition of 50 nM PMA. Cells were exposed to either 300  $\mu$ T LF EMF or sham. Extracellular DNA was quantified with Sytox Green 1, 2, 3 and 4 hours after stimulation (1  $\mu$ M, 5 minute) with a spectrofluorometer (ex 504 nm/em 515 nm).  $O_2^-$  production was determined 60 minutes after stimulation with 1 mg/ml NBT as described earlier<sup>314</sup>.

### *RNA FISH of neutrophils and bacteria*

LF EMF exposure and sham neutrophils ( $0.2 \times 10^6$ ) on glass slides were stimulated with 50 nM PMA for three hours. Living cells were stained with 1 ng/ml Hoechst and 1  $\mu$ M Sytox-Green for 5 minutes. For immunohistochemistry, *Escherichia coli* JM109 bacteria (multiplicity of infection: 6) were added after 30 minutes of PMA stimulation. After three hours, cells and bacteria were fixed in 4% PFA and stained with 16S-Alexa488 (1  $\mu$ g/100  $\mu$ l) and 0.5  $\mu$ M Sytox Green (detailed method in supplementary note 2). Images were taken with an EVOS® FL System and Leica LSM 510.

### *Bacterial killing assay by NETs*

Neutrophils were stimulated with medium or 50 nM PMA. After 4 hours, the NETs were removed by vigorously shaking for 5 minutes at 300 rpm and the supernatant was centrifuged for 5 minutes at 500 x g. To determine bacterial killing by NETs,  $0.5 \times 10^6$  *E.coli* JM109 bacteria were incubated for 3 hours in: either RMPI-1640, supernatant from unstimulated neutrophils (Sup) or supernatant from stimulated neutrophils containing NETs (NETs). PMA concentrations were kept equal for each condition (50nM). To release captured bacteria, after 3 hours samples were incubated with 100 U/ml DNase I for 15 minutes. Serial dilutions in sterile PBS were placed on Lysogeny broth agar plates and the surviving bacteria were enumerated and normalised to the bacterial survival in RMPI-1640. Experiments were performed with three independent donors in three independent experiments. Due to large variations between individual experiments with the same experimental outcomes, only one of the three experiments is presented with mean CFU  $\pm$  SEM of five individual agar plates.

### *Endothelial cell vitality and caspase 3/7 activities after NET treatment*

Cells from the human gingival carcinoma cell line Ca9-22 were seeded in 96-well plates to reach 90% confluence. RMPI-1640, supernatant or NETs were added. Cell viability was determined by MTS tetrazolium formation (P3580 Promega protocol) and apoptosis

induction by caspase-3 and -7 activities (Caspase-Glo® 3/7 Assay Promega) at the indicated time points.

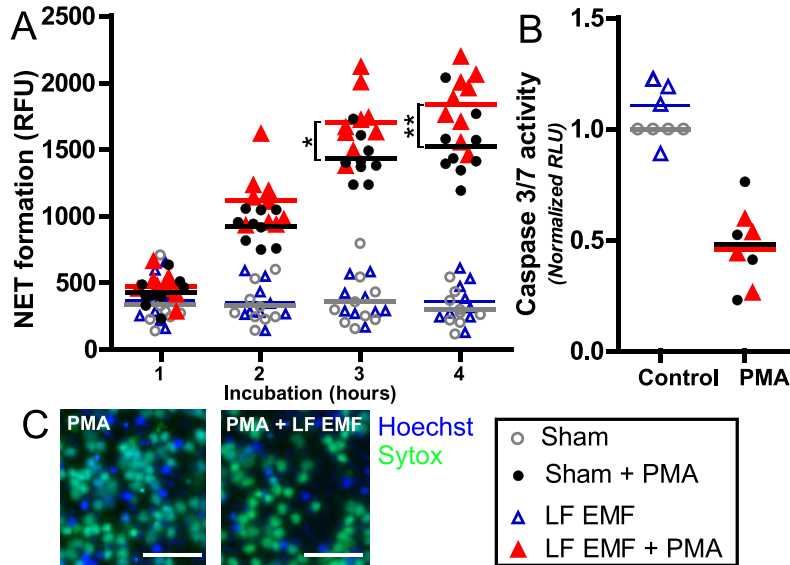


**Figure 1. LF EMF exposure enhances NET formation.**

**a)** Human neutrophils were stimulated with 50 nM PMA (● / ▲) or left unstimulated (○ / □) in the absence (sham; ○ / ●) or presence of LF EMF (▲ / □). Group mean (line) of all 9 individual donors (dots), \*  $p < 0.05$ , \*\*  $p < 0.01$ . **b)** Caspase-3 and -7 activity. Group means (lines) of all 4 individual donors (dots). **c)** Microscopic image of extracellular DNA (SYTOX Green) and nuclear DNA (Hoechst blue; see online version for colours). Scale bar = 100 μm.

#### *LF EMF Exposure system*

Cell exposure was performed with a custom-made exposure system (Immunent BV, Veldhoven, The Netherlands), which fits inside a standard cell culture incubator to ensure optimal cell culture conditions with  $37 \pm 0.2^\circ\text{C}$  and 5%  $\text{CO}_2$ . An irregular combination of four block waves, described in <sup>114</sup>, with frequencies of 320, 730, 880, and 2600 Hz was applied at a magnetic field intensity of 300 μT. Sham treatment consisted of identical culture conditions, with a unenergised coil in a second identical incubator.

#### *Statistics*

Data were analysed using GraphPad Prism 5.0 (GraphPad Software). Gaussian distribution was checked, and differences between sham and LF EMF groups were analysed using repeated-measures two-way ANOVA with post-hoc Bonferroni correction. Differences between CFU were analysed using one-way ANOVA with post-hoc Bonferroni correction. The number of individual donors (n), group mean and SEM are indicated in the legend. Statistical significance was accepted at  $p < 0.05$ .

## Results and Discussion

### *Effect of LF EMF exposure on ex vivo NET formation*

Human neutrophils were isolated from blood of healthy volunteers (n=9) and exposed to LF EMFs or sham in the absence or presence of 50 nM PMA, a potent NET formation inducer. Although, mean total exposure during a normal day does not get above 5  $\mu\text{T}$ <sup>9</sup>, we selected 300  $\mu\text{T}$  as it exceeds the general exposure safety limit of 200  $\mu\text{T}$ , but is well below the occupational exposure limit of 1 mT<sup>24</sup>. After one, two, three and four hours, the extracellular DNA content was quantified with Sytox Green. Figure 1a shows that NET formation induced by PMA significantly increased by ~25% after four hours, if the cells were simultaneously exposed to LF EMFs. Both the LF EMF and sham exposed cells showed clear cloud-like structures after selective DNA staining (Fig 1c). Without PMA stimulation, LF EMF was not able to induce NET formation by itself.

To eliminate the possibility that increased fluorescence intensity was the result of an alternative pathway leading to apoptotic cells with a compromised membrane, caspase 3 and 7 activity were determined after LF EMF exposure (Fig. 1b). Caspase cleavage is not involved in NET formation and was shown to be actively blocked by PMA stimulation<sup>315</sup>. These results exclude the potential induction of apoptosis by LF EMF exposure, which has previously been suggested<sup>120 316</sup>.

### *Consequences of LF EMF enhanced NET formation in vitro*

The prime role of NET formation by neutrophils is to combat invading pathogens. They trap and immobilise pathogens to prevent spreading towards other tissues and facilitate killing by other immune cells, such as macrophages. Moreover, pathogens can be killed by the antimicrobial peptides bound to the DNA strands<sup>66</sup>. As LF EMF enhanced NET release by stimulated neutrophils, we investigated the effect of these NETs on bacterial killing. There are various assays to investigate the killing capacity of NETs. Most research groups block phagocytosis with a high concentration of cytochalasin D, to exclusively investigate killing by NET formation. However, cytochalasin D has been proven to reduce or even completely prevent NET formation<sup>317,318</sup>. On the other hand, LF EMF exposure is linked to reduced bacterial growth<sup>319</sup>, which would make it difficult to distinguish between the effect of EMF on neutrophils or bacteria. Therefore, we adopted a functional method that involves the isolation of NETs from neutrophils and subsequent incubation with bacteria<sup>320</sup>. This protocol allowed us to solely investigate bacterial killing upon various concentrations of NETs. As shown in figure 2a, three hours incubation of bacteria with NETs significantly reduced subsequent bacterial survival in a concentration-dependent manner, compared to medium control. Fluorescence *in situ* hybridisation showed bacterial entrapment in the released DNA threads of the neutrophils (Fig. 2c). Furthermore, complete digestion by DNase I did not significantly increase the amount of CFUs (Fig 2b), demonstrating that released NETs do not only entrap but also kill microbes. Together, these data show that increasing amounts of NETs correlate with decreased bacterial survival. This implies that LF EMF enhanced NET formation is capable of eliminating more invading pathogens.

However, NET formation is a double edge sword, since the cytotoxic effects of NETs are not limited to foreign pathogens. NETs represent a diverse range of cryptic self-epitopes that can lead to autoimmune diseases like systematic lupus erythematosus<sup>321</sup> and

arthritis<sup>322</sup>. Furthermore, collateral damage to host's own endothelial and epithelial cells was also described<sup>320</sup>. Our data support this report, since we were able to show cell damage as a result of NET release. We visualised cellular damage by incubating a monolayer of oral epithelial cells with isolated NETs. After four hours, cell vitality measured by MTS formation was not affected, but after 16 hours cell vitality was significantly reduced (Fig. 2d). Furthermore, already after five hours of incubation with NETs, increased caspase 3 and 7 activity is detected in the epithelial cells (Fig. 2e). After 20 hours, caspase activity was significantly increased, compared to medium or the supernatant of unstimulated neutrophils, showing that enhanced NET formation leads to apoptosis of epithelial cells. This indicates that enhanced NET formation by LF EMF is a risky strategy that may contribute to microbial killing as well as increased host cell damage.

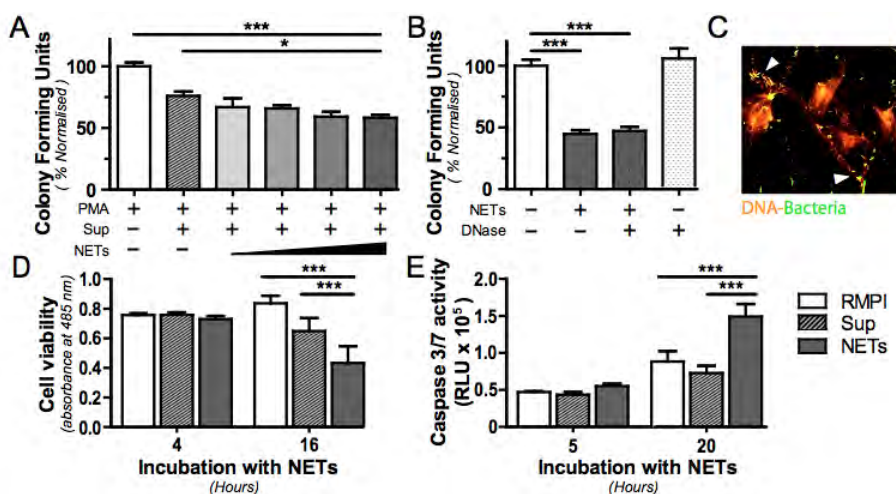


**Figure 2.** Killing of microbes and damage of oral epithelial cells by NETs. Bacterial survival after 3 h of incubation with medium, supernatant of unstimulated neutrophils (Sup) or NETs in increasing concentrations (a) and surviving colonies after DNase treatment (b). Graphs show representative data from three independent experiments. Mean CFU  $\pm$  SEM of five individual agar plates. c RNA FISH of bacteria (green) trapped in DNA filaments (orange; see online version for colours). d MTS formation activity in oral epithelial cells after incubation with RPMI, supernatant (Sup) or NETs. e Caspase-3 and -7 activity by oral epithelial cells after incubation with RPMI, supernatant (Sup) or NETs. Means  $\pm$  SEM of quadruplicate measurements of 2 independent donors, \*  $p < 0.05$ , \*\*  $p < 0.001$ .

### ***Molecular mechanism of LF EMF increased NET formation***

PMA (dose-dependent up to 15 nM, Supplementary Fig. 1a) is a potent inducer of NET formation and increasing the PMA concentration to 100 nM did not induce more NETs (Supplementary Fig. 1b). PMA mimics a pathogenic stimulation in neutrophils by intracellular protein kinase C (PKC) activation<sup>323</sup>. Interestingly, even at 50 nM of PMA, LF EMF exposure showed a synergistic effect on NET formation (Fig 1a), suggesting that LF EMF modulates the PMA-induced signalling pathway downstream of PKC activation.

To further unravel the molecular mechanism by which LF EMF is increasing PMA-stimulated NET formation, we investigated possible signalling pathways preceding actual NET release. Within 30 minutes after PMA stimulation, neutrophils undergo profound and significant morphological changes, characterised by immediate cell flattening, adherence and

massive vacuolisation<sup>324</sup>. This process is an interplay between autophagy, the cytoskeleton, superoxide production and histone citrullination<sup>315</sup>, and by using selective inhibitors for each of these cellular pathways, contributing signalling pathways were identified. The importance of a functional cytoskeleton has already been emphasised shortly after the first discovery of NETs<sup>318</sup>, but a recent report uncovered the physiological mechanisms. The actin cytoskeleton acts as a temporal store for cytoplasmic neutrophil elastase, to gradually increase the nuclear concentration of elastase, eventually leading to histone citrullination<sup>317</sup>. We found that cytochalasin D was able to block this process under LF EMF and sham conditions, which shows that LF EMF enhanced NET formation also requires an active cytoskeleton.

When autophagy was inhibited with PI3K inhibitor Wortmannin, only a small reduction in NET formation was observed (Figure 2d). These data must be interpreted with caution, as altered NET formation by Wortmannin is difficult to detect with cell-impermeable dyes like Sytox. Upon autophagy inhibition, the neutrophils undergo a type of cell death characterised by hallmarks of apoptosis, leading to membrane rupture<sup>315</sup>.

Further downstream of the NET formation pathway is PAD4 activation. Histone citrullination by PAD4 is considered to promote NET formation through chromatin decondensation, thereby facilitating intermingling of antimicrobial peptides with chromosomal DNA. PAD4 activity is calcium-dependent and crucial for NET formation induced by living bacteria<sup>325</sup> and the pro-inflammatory cytokine TNF $\alpha$ <sup>326</sup>. However, Neeli et al. showed that PMA induces activation of PKC $\alpha$ , which inhibits PAD4 histone citrullination without interfering with the cell's capacity to release NETs<sup>323</sup>. Interestingly, this research group also demonstrated that stimulation of neutrophils with PMA and calcium-ionophore led to more extensive NET release. We hypothesised that if LF EMF enhances PAD4 activity, resulting in increased NET formation, this would be inhibited with a PAD4 inhibitor. When neutrophils were pre-incubated with 200  $\mu$ M of the PAD4 inhibitor Cl-amidine, no changes in NET formation were observed, indicating that LF EMF does not enhance PAD4 activity. These results are further corroborated by the ability of PAD4 overexpression to induce NET formation even in non-immune cells<sup>327</sup>. Therefore, if LF EMF exposure increases PAD4 activity, LF EMF exposure alone would have induced enhanced NET formation, which we did not detect at any of the indicated time points.

### ***Role of NADPH-oxidase in enhanced NET formation***

Previous studies have established that PMA-induced NET formation requires an active NADPH oxidase complex to generate large amounts of superoxide ( $O_2^-$ ) that are rapidly converted inside the cell to hydrogen peroxide ( $H_2O_2$ ) by dismutation. The crucial role of NADPH oxidase in NET formation is illustrated in chronic granulomatous disease patients with dysfunctional NADPH oxidase activity as they fail to generate NETs<sup>312</sup>. In addition, pharmacological inhibition of NADPH oxidase activity by diphenyliodonium (DPI) in healthy neutrophils resulted in complete inhibition of NET formation. Oxidative stress with free radical production is one of the proposed mechanisms by which LF EMF exposure affects cellular behaviour<sup>52,172</sup>. Neutrophils exposed to 50 Hz electromagnetic fields showed increased ROS production and free radical production<sup>52</sup>. We used DPI to investigate if LF EMF exposure influenced NET formation in a NADPH-dependent manner (Fig. 3b). In accordance to other studies, DPI completely blocked PMA stimulated NET formation. Moreover, LF EMF enhanced NET formation was also completely abolished if the



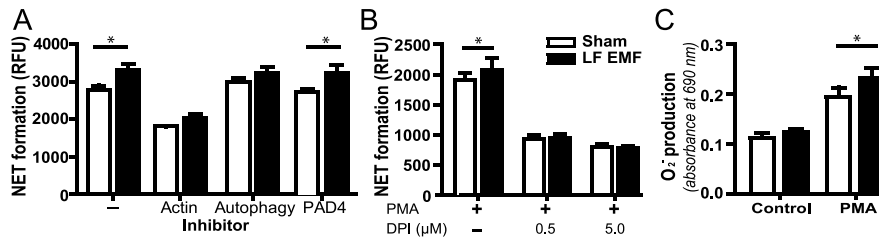


**Figure 3.** Exposure to LF EMF enhances NET formation via NADPH oxidase and ROS. a NET formation induced by PMA (-) was blocked with the use of the indicated inhibitors. Means  $\pm$  SEM of 3 independent donors. b Neutrophils stimulated with 50 nM PMA, supplemented with 0, 0.5 or 5.0  $\mu$ M DPI. Means  $\pm$  SEM of 6 independent donors. c Intracellular O<sub>2</sub><sup>-</sup> production by neutrophils. Means  $\pm$  SEM of four independent donors, \*  $p < 0.05$ .

neutrophils were pre-incubated with DPI. This indicates that LF EMF enhanced NET formation acts via a NADPH-oxidase dependent mechanism and does not activate an alternative pathway, as found for uric acid<sup>328</sup> or ionomycin induced NET formation<sup>329</sup>. These results were further substantiated by analysis of O<sub>2</sub><sup>-</sup> production 60 minutes after PMA stimulation, which showed significant increase of O<sub>2</sub><sup>-</sup> production by LF EMF exposure compared to PMA stimulation alone (Fig. 3c). For monocytes<sup>54</sup> and macrophages<sup>163</sup>, small increases in ROS production, in the range of 1.2 to 1.5 fold were observed when LF EMF was applied to the cells. In these studies, activation of the NADPH-oxidase complex by PMA was no prerequisite to achieve significant differences in ROS production. We observed a different effect, since stimulation of the intracellular pathway appeared to be required. One mechanism for increased ROS production by LF EMF could be enhanced NADPH-oxidase activity or elevated protein expression levels. The backbone of this enzyme is the cell membrane-bound cytochrome *b558*, which consists of two subunits gp91phox and p22phox. Frahm et al. showed that while TPA, an analogue of PMA, induced a transient increase of gp91phox protein expression after two hours, 50 Hz EMF exposure was able to achieve a similar upregulation already after 15 minutes<sup>163</sup>. Since the effect of LF EMF was only detectable after stimulation with PMA, priming of neutrophils could occur. This phenomenon is also observed when neutrophils are exposed to a low concentration of granulocyte-macrophage colony-stimulating factor, before oxidative burst stimulation<sup>330</sup>. The neutrophils are shortly brought to a state of enhanced responsiveness that is reflected by increased activity upon further addition of a potent stimulus, like PMA. We therefore suggest that the synergistic effect of LF EMF and PMA might be the result of short-term priming of neutrophils by LF EMF exposure.

## Conclusion

This is the first study to show that LF EMF exposure is able to significantly enhance NET formation *ex vivo*. Cellular activation by PMA was needed, since LF EMF exposure alone was not able to promote NET formation. The pathways involved in PMA stimulated NET formation are partly known<sup>331</sup> and with the use of selective pharmacological inhibitors, we demonstrated that the NADPH-pathway is crucial for LF EMF enhanced NET formation, possibly by upregulated ROS production. These data provide a basic mechanism of action on immune cells to explain potential health effects of LF EMFs generated by household appliances and power lines.

## Supplementary

### Note 1

#### *Human neutrophil isolation*

Blood from healthy volunteers was collected in lithium-heparin tubes (BD Vacutainer). The neutrophils were purified using a discontinuous Percoll density gradient. From the whole blood, 2 ml was layered on top of two times 3 ml layers of 1.079 g/ml and 1.098 g/ml Percoll in 0.15 M NaCl, followed by centrifugation at 150 x g for 8 minutes without brakes. Subsequently the tubes were centrifuged a second time at 12000 x g for 10 min without brakes. The neutrophil layer was isolated and red blood cells were lysed in lysis buffer, containing 155 mM  $\text{NH}_4\text{Cl}$ , 10 mM  $\text{KHCO}_3$ , 110  $\mu\text{M}$   $\text{Na}_2\text{-EDTA}$  and 2.5% (w/v) bovine serum albumin. Neutrophils were washed in RPMI-1640 and resuspended in phenol red-free RPMI-1640 supplemented with L-glutamine (2 mM), streptomycin (100  $\mu\text{g}/\text{ml}$ ) and penicillin (100 U/ml). Cell purity was ~98% or higher.

### Note 2

#### *FISH Immunohistochemistry*

Isolated neutrophils ( $0.2 \times 10^6$ ) were placed onto  $\varnothing$  22 mm glass slides and stimulated with 50 nM PMA. After 30 minutes, *E.coli* JM109 bacteria at an MOI of 6 were added and incubated at 37 °C. After three hours, cells and bacteria were fixed in 4% paraformaldehyde. The slides were stained with 16S-Alexa488 probe. The 16S probe (1.0  $\mu\text{g}$ ) is diluted in 100  $\mu\text{l}$  hybridisation buffer (20 mM TRIS-HCL, pH 7.4, 0.9 M NaCl, 0.1% (w/v) SDS) and added to every slide. The slides were incubated for four hours at 50°C, washed in FISH washing buffer (20 mM TRIS-HCL, pH 7.4, 0.9 M NaCl) for 20 minutes at 50°C. Three washing steps with PBS were performed, after which the slides were stained with 0.5  $\mu\text{M}$  Sytox orange for 5 minutes and embedded in VectaShield. Images were obtained with a Zeiss 510 CLSM.

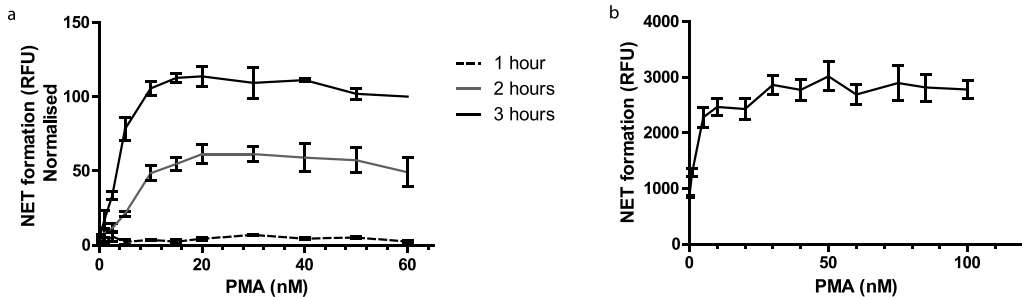
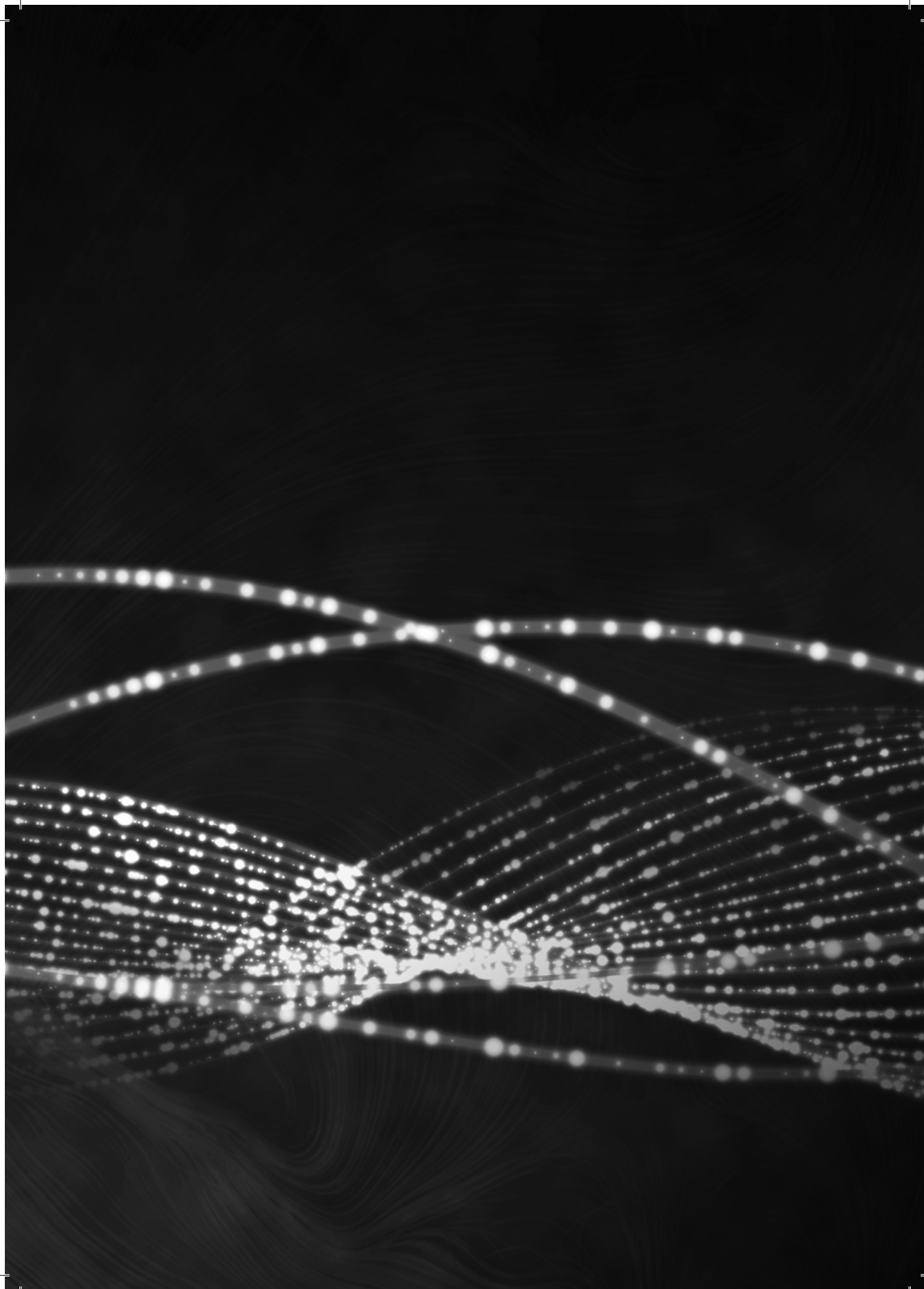


**Figure 1.** Neutrophils release an increasing amount of NETs when incubated with increasing concentrations of PMA. Human neutrophils were stimulated with various concentrations of PMA for 1, 2, 3 hours. NET formation was quantified with 1  $\mu\text{M}$  Sytox Green. a) The lines represent the mean  $\pm$  SEM normalised (to 60 nM PMA) NET formation of three individual donors. b) NET release upon various concentrations of PMA after 4 hours. The line represents the mean  $\pm$  SEM NET formation of one individual donor measured in triplicate.

Increased NET formation by LF EMF exposure



# Chapter 7

---

**EHop-016, a small molecule inhibitor for Rac1-3,  
induces extracellular trap formation in human neutrophils  
via PAD4 activation**

Lieke A. Golbach, Huub F.J. Savelkoul, B.M. Lidy Verburg-van Kemenade

*Submitted to FEBS Letters*

## Abstract

EHop-016 is a small molecule inhibitor, designed to interact with Rac 1, 3 and Cdc42, thereby inhibiting cell motility and cancer metastasis. *In vivo* studies showed that EHop-016 has potential as an anti-cancer compound to block metastasis. Here we show that EHop-016 induces neutrophil extracellular traps formation (NETs), a process characterised by release of long DNA/histone fibres coated with anti-microbial enzymes. Contrary to microbial stimulation, activation of NETs by EHop-016 was independent of reactive oxygen species (ROS) generation and NADPH oxidase activity. Instead, PAD4 activity was pivotal for EHop-induced NET release and led to citrullination of histone H3.

## Introduction

Neutrophils are key players in the innate immune response against invading microbes. They engulf microbes for intracellular killing or release antimicrobial peptides to facilitate extracellular killing<sup>332</sup>. Recent investigations highlighted a novel third killing mechanism, called neutrophil extracellular trap (NET) formation or NETosis<sup>333</sup>. During NETosis, nuclear DNA decondensates, the nuclear envelope collapses and the untangled DNA is mixed with antimicrobial peptides from the granules in a process that only takes two to three hours. Eventually, the cell membrane ruptures and the NETs are released into the extracellular environment. NET formation is a novel type of cell death, with distinct hallmarks, such as loss of the nuclear membrane, disappearance of cytoplasmic organelles, and its independence of caspase activity<sup>78</sup>.

Since the discovery of NET formation, many researchers have investigated the signalling pathways involved in NET formation. NADPH oxidase activation and subsequent reactive oxygen species (ROS) production were the first pathways linked to NET release<sup>78</sup>. NETosis requires an active NADPH oxidase complex to generate large amounts of superoxide anions ( $O_2^-$ ), which are rapidly dismutated to hydrogen peroxide ( $H_2O_2$ ). Fuchs et al. showed that this process was blocked with a pharmacological inhibitor of NADPH, diphenyleneiodonium (DPI). In addition, chronic granulomatous patients without functional NADPH oxidases, fail to maintain phagocytosis or form NETs<sup>79</sup>. Subsequent research has recognised autophagy as another pivotal pathway<sup>80</sup>, as well as activation of peptidylarginine deiminase 4 (PAD4). Upon activation of the NET formation pathway, active PAD4 enzymes catalyse the conversion of arginine residues of histones to citrulline. PAD4 operates together with elastase, which is released from granules and subsequently partially degrades specific histones to decondensate the DNA<sup>82</sup>. The relevance of PAD4 during NET formation was shown with PAD4-null mice, which failed to produce NETs<sup>81,311</sup>. Fundamental research already showed that the actin cytoskeleton is indispensable for NET release, since inhibition of filament polymerisation by cytochalasin D resulted in reduced NET formation<sup>334</sup>.

The importance of different cellular pathways is often determined with the use of small molecule inhibitors that block specific proteins of a pathway. One of these small molecule inhibitors, EHop-016, was designed to interact with Rac1 and 3<sup>335</sup>. Rac1, 2 and 3, together with RhoA and Cdc42, are the three major proteins involved in cytoskeletal reorganisation<sup>336</sup>. EHop-016 was proposed to serve as targeted novel therapy to reduce the migration of cancer cells that exhibit enhanced Rac-expression, which was shown to promote metastasis *in vivo*. Rac proteins are small GTPases responsible for regulation of the actin cytoskeleton and generation of ROS by NADPH oxidases<sup>337</sup>. Since both NADPH oxidase and the cytoskeleton are crucial for NET release, we investigated the suspected inhibitory effect of EHop-016 in human neutrophils. Interestingly, we show in this study that EHop-016 does not inhibit NET formation, but in contrast induced NETs. Subsequent experiments revealed a pivotal role for PAD4 activation and histone 3 citrullination upon EHop-016 stimulation.

## Material and Methods

### *Neutrophil isolation and neutrophil extracellular trap formation*

Neutrophils were isolated from blood of healthy volunteers. Ethical permission was obtained from a local ethical committee (No. NL.44545.091.13) and a written consent was obtained from each donor. Blood was layered onto a discontinuous Percoll density gradient (1.079 g/ml and 1.098 g/ml) and centrifuged at 1200 x g for 10 minutes. Red blood cells were carefully lysed for 5 minutes in lysis buffer, containing 155 mM NH<sub>4</sub>Cl, 10 mM KHCO<sub>3</sub>, 110 μM Na<sub>2</sub>-EDTA and 2.5% (w/v) BSA and remaining neutrophils were washed with RPMI. Cell purity was ~98% or higher determined by flow cytometry. To induce NET formation, 0.1 x 10<sup>6</sup> neutrophils were seeded in black/clear 96-well plates and left to adhere for one hour at 37°C with or without diphenyleneiodonium chloride (DPI) (0.5 μM, 5.0 μM), wortmannin (100 nM), Cl-amidine (20 μM, 200 μM), L-name (3 μM, 30 μM), NF-κB inhibitor (481406), p38 inhibitor (SB2035810, 10 μM), MEK1/2 inhibitor (U0126, 10 μM), necrostatin-1 (10 μM, Santa Cruz Biotechnology, Santa Cruz, CA, USA), z-VAD-fmk (10 μM) and cytochalasin D (1 μM, 10 μM). NET formation was induced by the addition of various concentrations of EHop-016 (Sigma-Aldrich). Medium without a stimulus was used as a negative and 50 nM PMA as a positive control. In addition, cells were stimulated with NSC23766 (50 μM, 100 μM) and/or ML-141 (200 nM, 800 nM). Spontaneous and maximum NET formation differed between donors, like reported by Fuchs et al.<sup>78</sup>, therefore comparisons between treatments were made with neutrophils from the same donors. Extracellular DNA was quantified with 1 μM Sytox Green for five minutes with a spectrofluorometer (excitation at 504 nm/emission 515 nm).

### *ROS production*

ROS production was determined by real-time chemiluminescence (H<sub>2</sub>O<sub>2</sub> and O<sub>2</sub><sup>-</sup> production) and nitroblue tetrazolium (NBT) assay (O<sub>2</sub><sup>-</sup> production). For the luminescence assay, neutrophils resuspended in RPMI were seeded in a white 96-well plate (0.1\*10<sup>6</sup>) and incubated for one hour at 37°C. Subsequently, 50 μl of luminol (10 mM) in 0.2 M borate buffer (pH 9.0) and 50 μl stimuli were added. The chemiluminescence emission was measured with a multimode micro plate reader every minute at 37°C. O<sub>2</sub><sup>-</sup> production was determined 90 minutes after stimulation with 1 mg/ml NBT as described earlier<sup>314</sup>. In short, 100 μl cell suspensions, containing 0.1\*10<sup>6</sup> neutrophils in RPMI, were seeded in a clear 96-well plate and incubated for one hour at 37°C, followed by addition of RPMI containing the NBT and different stimuli. The plates were incubated for 60 minutes at 37°C in a humidified incubator with 5% CO<sub>2</sub>. Cells were fixed in 70% ethanol and air-dried. The reduced formazan was dissolved in 120 μl KOH (2 M), and cells were lysed with 140 μl dimethyl sulphoxide. The reduction of NBT was measured at 690 nm with a 414 nm reference filter using a multimode micro plate reader.

### *Caspase 3/7 activity*

Apoptosis induction by caspase-3 and -7 activities was measured according to the manufacturer's protocol (Caspase-Glo® 3/7 Promega). In short, neutrophils were seeded in a white 96-well plate and stimulated with medium, Actinomycin-D (10 μg/ml), 50 nM PMA or EHop-016, like described above for the NET formation assay. Two hours after stimulation,



caspase-Glo reagent was added to every well at a 1:1 ratio. The plate was incubated 30 minutes at room temperature and luminescence was measured with a multimode micro plate reader.

#### *Immunocytochemistry*

To stain NETs,  $0.1 \times 10^6$  neutrophils were adhered to an 18 x 18 mm cover slip and stimulated with medium, 50 nM PMA or various concentrations EHop-016. After three hours, the cells were fixed in 4% paraformaldehyde in PBS and permeabilised with 0.05 % Triton X-100. The cells were incubated for one hour with a primary elastase antibody (ab21595, 1:200). After three subsequent washing steps with PBS containing 5% serum, a 1:1000 dilution of the goat-anti-rabbit-Alexa 633 (A21071, Molecular probes) was added and incubated for one hour. The secondary staining was followed by a five minutes staining of extracellular DNA and cell nucleus with 0.1  $\mu$ M Sytox green. Slides were embedded in VectaShield and the images were obtained with a Zeiss 510 CLSM.

#### *Elastase assay*

Isolated neutrophils were resuspended in RPMI, seeded in a 96-well plate at a density of  $0.1 \times 10^6$  cells/well and incubated for one hour at 37°C. Subsequently, neutrophils were stimulated with medium, 50 nM PMA or 1  $\mu$ M, 5  $\mu$ M, 10  $\mu$ M EHop-016. After three hours, NETs were isolated by gently shaking (300 rpm) for 5 minutes, followed by removal of the supernatant containing NETs. The amount of elastase released was calculated compared to complete cell and granula lysis with 0.1% Triton X-100. The supernatant was diluted 1:1 with 200  $\mu$ M elastase substrate (N-(Methoxysuccinyl)-Ala-Ala-Pro-Val 4-nitroanilide) and incubated for 30 minutes at room temperature. The optical density was measured at 405 nm with a plate reader.

#### *H3-cit western blot*

Isolated neutrophils were resuspended in RPMI, seeded in a 12-well plate at a density of  $1 \times 10^6$  cells/well and left to adhere for 1.5 hour at 37°C in 5% CO<sub>2</sub> in control medium with or without 200 $\mu$ M Cl-amidine. Subsequently, neutrophils were stimulated with vehicle control, 50 nM PMA or 10  $\mu$ M EHop-016 to induce NET formation. After one hour, the medium was removed and the cells were resuspended in 20  $\mu$ L PBS with 1X Laemmli buffer. Samples were separated on a polyacrylamide gel and proteins were transferred to nitrocellulose membranes. The membranes were stained with Ponceau S to visualise protein loading in every lane. Subsequently, the membranes were blocked with 5% milk in TBS and stained with 1  $\mu$ g/ml  $\alpha$ H3cit R2-R8- R17 antibody (ab5103) overnight at 4°C. The membranes were washed in TBS with 0.1% Tween and incubated with the secondary antibody, polyclonal goat anti-rabbit HRP (P0448, DAKO) for one hour at room temperature. HRP activity was detected using a chemiluminescence reagent (WesternBright ECL).

#### *Statistics*

Data were analysed using GraphPad Prism 5.0 (GraphPad Software). Differences between the different treatments were analysed using on-way ANOVA or repeated-measure two-way ANOVA with post hoc Bonferroni correction when multiple comparison were made. The numbers of individual donors (n), group means and SEM are indicated in the legend. Statistical significance was accepted at  $p < 0.05$ .

## Results

### *EHop-016 induced NET-like structures*

We aimed to investigate the role of cytoskeleton reorganisation during NET formation, with the use of EHop-016, an inhibitor for Rac1 and Rac3<sup>283</sup>. Addition of increasing concentrations of EHop-016 followed by PMA stimulation did not significantly influence the amount of NETs released (Fig. 1a). A high fluorescence intensity was measured when 5 or 10  $\mu$ M of EHop-016 alone were added (Fig. 1b). The identity of the NETs was confirmed by fluorescence microscopy, which showed clear cloud-like structures of extracellular stained DNA (Fig. S1) in a concentration-dependent manner (Fig. S2). Since these results were contradictory with our primary hypothesis, we examined the composition of the released NET-like structures by immunocytochemistry. Figure 2 shows that elastase is present in the cytoplasm of resting neutrophils, presumably in the antimicrobial granules. However, after a three-hour stimulation with 50 nM PMA, elastase co-localises with the DNA fibres. A similar pattern is observed for EHop-016 stimulated cells, indicating that the released NET-like structures contain DNA fibres with elastase proteins. These results were substantiated by colorimetric assay of the elastase release (Fig. S3).

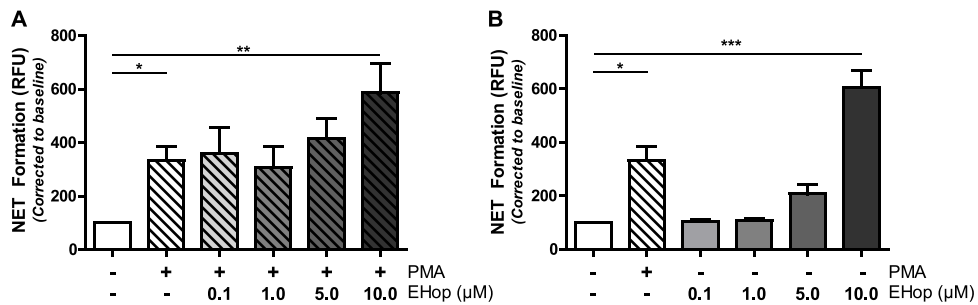


**Figure 1. EHop-016 induces NET-like structures without the need of PMA stimulation.** a) Human neutrophils were stimulated with medium, 50 nM PMA or various concentrations of EHop-016 diluted in RMPI. b) NET formation was induced with 50 nM PMA in the absence or presence of increasing concentrations EHop-016. Extracellular DNA concentration was quantified after three hours with 1  $\mu$ M Sytox-green. Graphs mean  $\pm$  SEM of three independent donors, ns = not significant, \*  $p < 0.05$ , \*\*  $p < 0.01$ .

### *Caspase 3/7 activity*

The  $IC_{50}$  of EHop-016 has been established at 1.1  $\mu$ M in cancer cell lines, but cytotoxicity is predicted at concentrations above 5 mM<sup>338</sup>. Active caspases 3 and 7 were detected two hours after induction of NET formation with 10  $\mu$ M EHop-016, as well as in the cells incubated with actinomycin-D (Fig. 3a), but due to the short lifespan of isolated neutrophils, also unstimulated cells show high caspase activity. PMA stimulated cells showed a small decrease compared to medium controls. Interestingly, features of classical apoptosis like blebbing or DNA fragmentations were not detected in the EHop-016 treated samples. To investigate this in more detail, the cells were pre-incubated with an apoptosis inhibitor z-VAD-fmk, and necrosis inhibitor, necrostatin-1 (nec-1). Figure 3b shows that both PMA and EHop-016 induced NETosis was not inhibited by z-VAD-fmk or nec-1. In addition, apoptosis induction by actinomycin-D appeared to inhibit spontaneous NET formation and did not lead to increased DNA staining after possible membrane rupture.

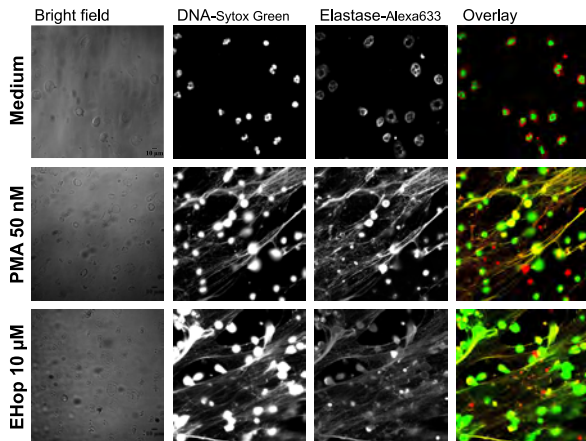


**Figure 2. Immunofluorescence of NET-associated elastase.** a) Human neutrophils were adhered to cover slides and stimulated with medium, 50 nM PMA or 10  $\mu$ M EHop-016 for three hours, followed by fixation in 4% PFA. After fixing, the cells were immunolabelled with antibody to elastase, detected with an Alexa 633-conjugated secondary antibody (red) and subsequently DNA was stained with 1  $\mu$ M Sytox-green (green). No red fluorescence was observed when neutrophils were incubated without the primary elastase antibody. Images are representative of three independent experiments.

### Related small molecule inhibitors for Rac1 and Cdc42 do not induce NETs

To elucidate the possible mechanism of interaction of EHop-016, we examined NETosis after incubation with other cytoskeleton inhibitors. EHop-016's structure was based on the structure of NSC23766, a small molecule inhibitor that inhibits Rac1. Furthermore, 10  $\mu$ M EHop-016 also reduced Cdc42 activity by 74% in cancer cell lines<sup>338</sup>. If EHop-016 induced NET formation through inhibition of Rac1 or Cdc42, we should reproduce these results with similar inhibitors.

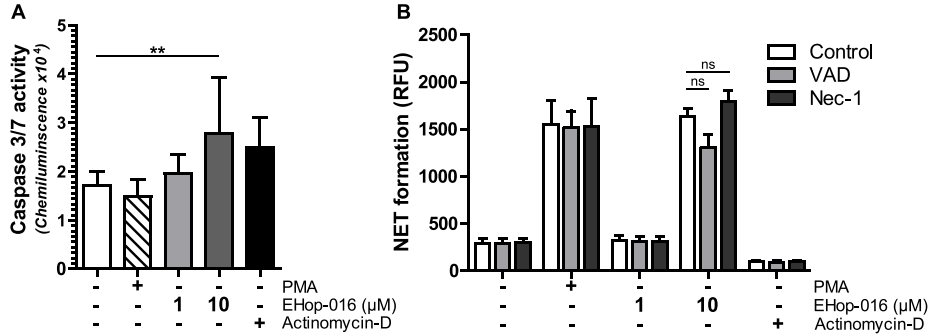


**Figure 3. Limited apoptosis and necrosis induction by EHop-016.** a) Human neutrophils were stimulated with medium, 50 nM PMA, 1  $\mu$ M or 10  $\mu$ M EHop-016 or 10 ng/ml actinomycin-D diluted in RPMI. After two hours, caspase 3/7 activity was determined with a chemiluminescence assay. Graph mean  $\pm$  SEM of three independent donors. b) To determine the role of apoptosis and necrosis, cells were pre-incubated with 10  $\mu$ M z-VAD-fmk (VAD), 10  $\mu$ M Necrostatin-1 (Nec-1) or vehicle control (Control) for one hour, followed by stimulation with medium, 50 nM PMA, 1  $\mu$ M or 10  $\mu$ M EHop-016 or 10 ng/ml actinomycin-D. Extracellular DNA concentration was quantified after three hours with 1  $\mu$ M Sytox-green. Graph mean  $\pm$  SEM of three independent donors, ns = not significant, \*\*  $p < 0.01$ .

Neutrophils were incubated with 200 and 800 nM ML 141 ( $IC_{50}$ =200 nM), a Cdc42 inhibitor.

The effect of Rac1 inhibition was tested with 50 and 100  $\mu\text{M}$  NSC23766 ( $\text{IC}_{50}=50 \mu\text{M}$ ), as well as a combination of both inhibitors (Fig. 4). None of the inhibitors showed a similar effect, suggesting that EHop-016 interacts with other proteins to achieve NET release.

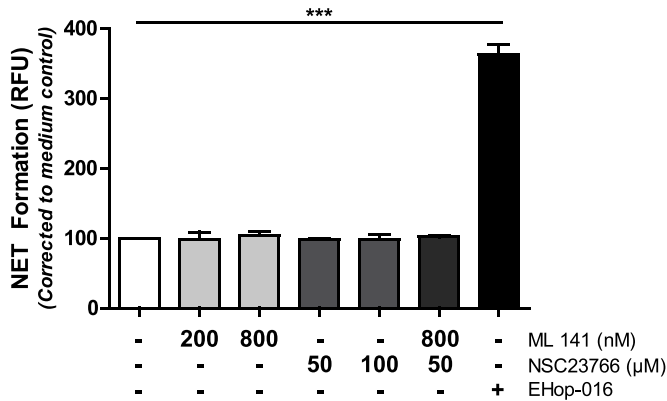


**Figure 4. Mimicking the effect of EHop-016 induced NET formation with other small molecule inhibitors.** Human neutrophils were incubated with medium, ML 141 (Cdc42 inhibitor) NSC23766, (Rac1 inhibitor) or a combination of both inhibitors for three hours. A positive control, 10  $\mu\text{M}$  EHop-016 was used. Extracellular DNA was quantified after three hours with 1  $\mu\text{M}$  Sytox-green. Graph mean  $\pm$  SEM of two independent donors, \*\*\*  $p < 0.001$ .

#### *EHop-016 NET formation does not require ROS production*

PMA-induced NET release requires activation of NADPH oxidase, however we observed no enhanced ROS production after the addition of 0.1, 1, 5 or 10  $\mu\text{M}$  EHop-016 (Fig. 5a). As expected, PMA-stimulated cells produced large amounts of ROS. Real-time measurements of  $\text{H}_2\text{O}_2$  and  $\text{O}_2^-$  production by chemiluminescence (Fig. 5b) showed that already after 25 minutes PMA-induced  $\text{H}_2\text{O}_2$  and  $\text{O}_2^-$  production is at its maximum, whereas EHop-016 induced no  $\text{H}_2\text{O}_2$  and  $\text{O}_2^-$  production at all. These results indicate that EHop-016 signals in a NADPH oxidase and ROS independent manner.

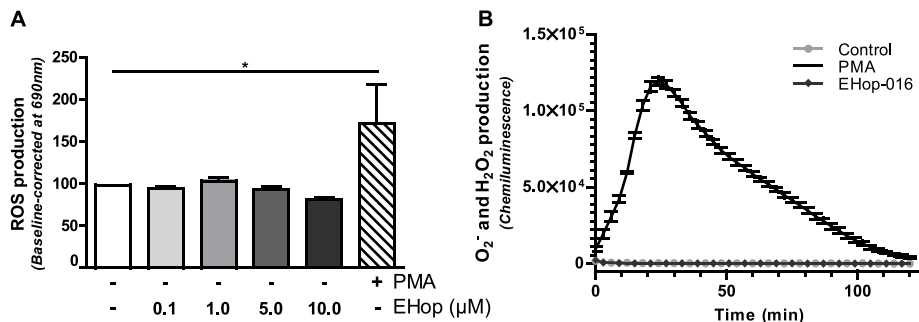


**Figure 5. Oxygen radical production induced by EHop-016 or PMA.** Human neutrophils were incubated in medium containing NBT and stimulated with various concentrations of EHop-016 or 50 nM PMA to induce ROS production. After 90 minutes, the cells were fixed and the amount of ROS produced was measured by optical density at 690 nm. Graph mean  $\pm$  SEM of two independent donors, \*  $p < 0.05$ . b) Real-time radical oxidant production was measured with a chemiluminescence assay. Neutrophils were diluted in luminol, supplemented with vehicle control, 50 nM PMA or 10  $\mu\text{M}$  EHop-016.  $\text{O}_2^-$  and  $\text{H}_2\text{O}_2$  production was determined every three minutes by luminescence intensity. Graph mean  $\pm$  SEM of triplicate measurements of one donor as a representative of three independent experiments.

#### *PAD4 activation is essential for EHop-016 induced NET formation*

Primary cell cultures of neutrophils have a short life-span<sup>339</sup>, therefore we investigate the possible signalling pathways activated by EHop-016 with other pharmacological inhibitors. First, NADPH oxidase activity was blocked by pre-treatment with DPI (Fig. 6a). PMA induced NET formation was decreased and completely inhibited by respectively 0.5 and 5  $\mu$ M DPI, but EHop-016 NET formation remained similar. Furthermore, inhibition of autophagy with wortmannin (100 nM) did not significantly reduce NET formation in either PMA or EHop-016 stimulated cells (Fig. 6b). Pre-treatment of the cells with inhibitors specific for an alternative NET-formation pathway via CXC ligand binding and intracellular phosphorylation of MEK1/2 (10  $\mu$ M U0126) and p38 (10  $\mu$ M SB20358) (Fig. 6c) or NF- $\kappa$ B activation (481406 Calbiochem) (Fig. 6d) did not show any differences. Nevertheless, blocking actin polymerisation with cytochalasin-D reduced NET formation in both PMA and EHop-016 stimulated cells by ~40 to 60%. Finally, PAD4 inhibition with Cl-amidine resulted in decreased NET formation in EHop-016 stimulated cells (Fig. 6f). These results indicate that, blocking the cytoskeleton, or PAD4 activation significantly reduced EHop-016 induce NET formation.

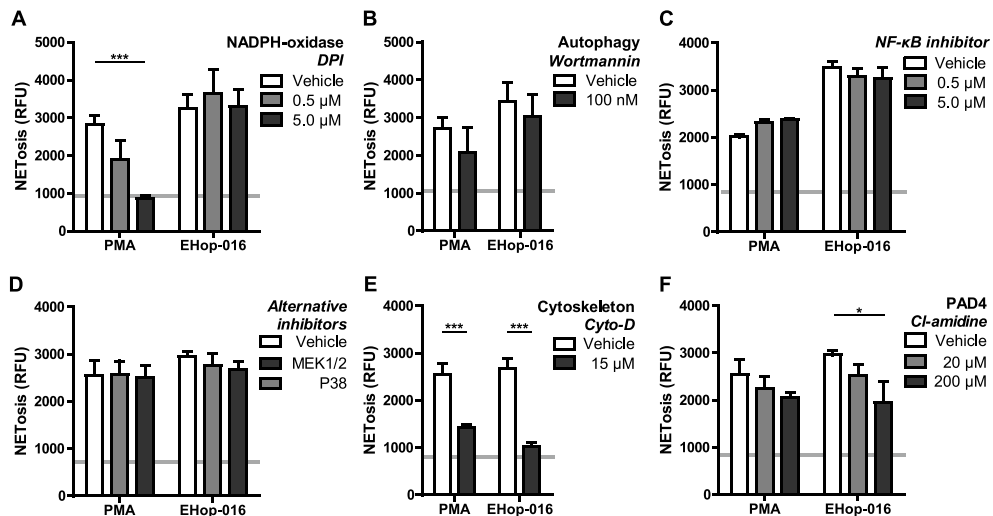


**Figure 6. Inhibition of EHop-016 induced NET formation.** Human neutrophils were pre-incubated for one hour with inhibitors for different elements of the NET formation pathways. Subsequently, NET formation was stimulated with 50 nM PMA or 10  $\mu$ M EHop-016. After three hours, the extracellular DNA concentration was quantified with 1  $\mu$ M Sytox-green. Graphs mean  $\pm$  SEM of four independent donors (n=4) unless stated otherwise, \* p<0.05, \*\*\* p<0.001. a) NADPH oxidase activity was inhibited with 0.5  $\mu$ M or 5.0  $\mu$ M DPI (n=7) and b) autophagy was inhibited with 100 nM Wortmannin or vehicle control before NET formation (n=5). Involvement of the alternative NET formation pathways was examined by pre-incubation of the cells with c) 10 or 50 nM NF- $\kappa$ B inhibitor (481406) or d) 10  $\mu$ M P38 inhibitor (SB2035810) or 10  $\mu$ M MEK1/2 inhibitor (U0126). e) Cytoskeleton reorganisation and actin polymerisation were inhibited with 15  $\mu$ M cytochalasin-D and f) PAD4 activity was inhibited by the addition of 20 or 200  $\mu$ M Cl-amidine before the induction of NET formation.

### *EHop-016 induces histone 3 citrullination*

Since PAD4 converts amino acid arginine into citrulline before NET release, we examined the presence of citrullinated histone 3 by Western blot (Fig. 7). After 1.5 hour of stimulation, citrullinated histone 3 was detected in the PMA samples. When the cells were incubated with 10  $\mu$ M EHop-016, also citrullinate histone 3 was detected. This expression was diminished when the cells were pre-incubated with Cl-amidine.

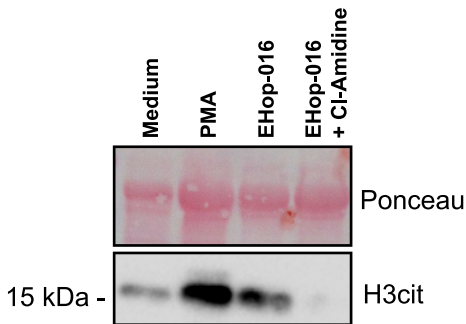


**Figure 7. Histone 3 citrullination by EHop-016.**

Citrullinated histone 3 (H3cit) was detected by Western blot in cell lysates of human neutrophils stimulated with vehicle control, 50 nM PMA, 10  $\mu$ M EHop-016. Protein loading was checked by Ponceau S staining. To block histone modifications, neutrophils were pre-incubated for one hour with Cl-amidine, a PAD4 inhibitor. Graph of one donor as a representative of three independent experiments.

## Discussion

Many small molecule inhibitors are initially designed to interact with one specific protein or cellular pathway, but subsequent research can reveal multiple unpredicted interactions. For EHop-016, an inhibitor of Rac1 and 3, reduced migration of metastatic cancer cell lines was demonstrated<sup>338</sup>. Here we discovered that EHop-016 also induces NET formation in human neutrophils. This was unexpected, since we hypothesised that inhibition of cytoskeleton rearrangements would reduce NET formation. EHop-016 induced NETs consist of long extracellular DNA fibres, coated with elastase. Furthermore, NETosis did not require ROS production, in contrast to NETosis induced by PMA or live microbes<sup>66,329</sup>. Our study moreover showed that PAD4 activity was required for EHop-016 induced NET formation, which was corroborated by EHop-016 promoted citrullination of histone 3.

Normally during PMA-stimulated NET formation, a functional NADPH oxidase complex prevents caspase cleavage<sup>340</sup> and promotes cell survival<sup>315,318</sup>. In contrast to our expectations, we measured both NET formation and caspase 3/7 activity in EHop-016 stimulated neutrophils and no ROS generation. The latter corroborates results of Parker et al., who showed that the requirement of NADPH oxidase activity and subsequent ROS production differed depending on the type of stimulus<sup>329</sup>. Pre-treatment of neutrophils with a necrosis or apoptosis inhibitor showed that EHop-016-induced NET release independent of both pathways. Consequently, caspase cleavage might occur simultaneously to NET formation, however to confirm a possible heterogeneous effect, further research is required.

EHop-016 stimulates NET formation, without the need of microbes or PMA. There are two possible explanations for this phenomenon. Either EHop-016 interacts selectively with its predicted cellular targets or the inhibitor interacts with other cellular proteins. EHop-016 was originally designed to interact with Rac1 and 3, through binding inside the

guanine nucleotide exchange factor (GEF) pocket of these proteins<sup>338</sup>. EHop-016 showed specificity at concentrations of  $\geq 5 \mu\text{M}$  and at higher concentrations, Cdc42 activity was also inhibited. Pharmacological mimicking with ML 141<sup>341</sup>, a specific Cdc42 inhibitor or Rac1 inhibition with NSC23766 did not result in NET formation. Rac2 comprises >96% of all Rac proteins in human neutrophils<sup>342</sup>, whereas mouse neutrophils have equivalent expression levels of Rac1 and Rac2. Knockdown studies showed that only Rac2 is essential for NET formation in mice<sup>343</sup>. Unfortunately, the initial EHop-016 study did not investigate an interaction of EHop-016 with Rac2<sup>338</sup>. Nevertheless, since inhibition of either Cdc42 or Rac1 did not result in increased NET formation, we propose that EHop-016 might interact with another protein that plays a pivotal role during NET formation.

NET formation is only recently acknowledged as an orchestrated cellular process, and therefore knowledge regarding the precise intracellular pathways and proteins involved is now evolving<sup>331</sup>. In our study, induction of ROS generation by EHop-016 was excluded and NADPH oxidase activity was not required. Next to this, we observed citrullinated histone 3 after stimulation with EHop-016, which depended on PAD4 activity. Increased activity of PAD4 could promote NET formation, as shown by overexpression of PAD4 in fibroblasts which stimulated the release of NET-like structures<sup>327</sup>. PAD4 activity is dependent on binding of calcium ions, however, in our study, EHop-016 did not induce a rise of cytoplasmic calcium (data not shown). Alternatively, it can be hypothesized that EHop-016 can directly interact with PAD4 to increase its activity. A similar interaction was reported for anti-PAD4 autoantibodies, which strikingly increased the catalytic efficiency of PAD4 by 500-fold by means of decreasing the enzyme's requirement for calcium<sup>344</sup>, making it independent of a transient calcium rise.

In summary, we show that EHop-016 induces NET formation in human neutrophils. EHop-016 was initially designed to reduce mammary tumour growth and inhibit metastatic cancers<sup>335</sup>. Also Castillo-Pichardo et al. recommended future research to evaluate the potential interaction of EHop-016 with other cells, like immune cells. We observe EHop induced NETS that display all characteristic hallmarks, but do not require ROS generation and rely on PAD4 activation.

## Authorship

L.G. carried out most of experimental work and data analysis and contributed to interpretation of the data and preparation of the manuscript. H.S. contributed to the experimental design, interpretation of the data and preparation of the manuscript. L.K. contributed to the experimental design, analysis and interpretation of the data and preparation of the manuscript.

## Acknowledgments

This work was supported by the Dutch organisation for health research and development, ZonMw (grant number 85300006).

## Supplementary data

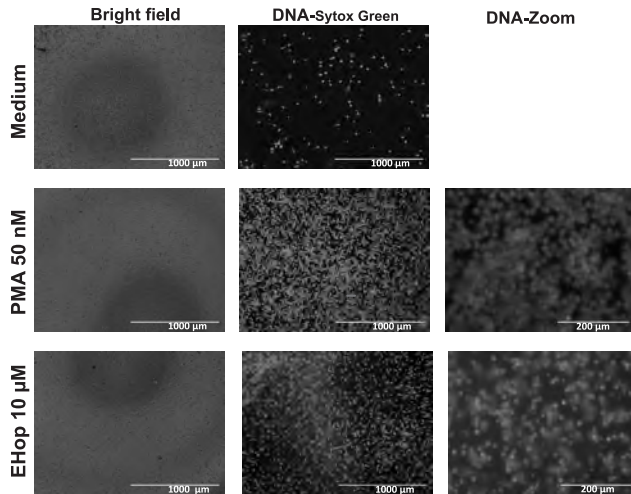


**Figure 1.** NET formation induced by medium, EHop-016 or PMA. Human neutrophils were stimulated with medium, 10 μM EHop-016 or 50 nM PMA for three hours. Subsequently, only extracellular DNA was stained with 1 μM Sytox-green for 5 minutes. Images were obtained with a EVOS microscope at 20x. Scale bar is 1000 μm for the overview images and 200 μm for the zoomed images.

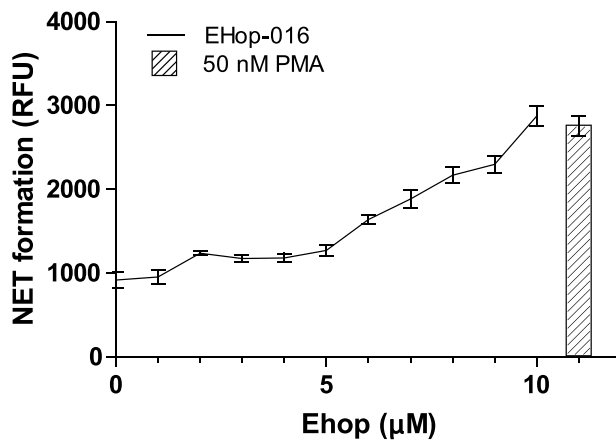


**Figure 2.** Concentration dependent NET formation by EHop-016. Human neutrophils were stimulated with RMPI (0 μM) or various concentrations of EHop-016 diluted in RMPI. 50 nM PMA was included as a reference and positive control. Extracellular DNA concentration was quantified after three hours with 1 μM Sytox-green. Graphs mean ± SEM quadruplicate measurements of a single donor.



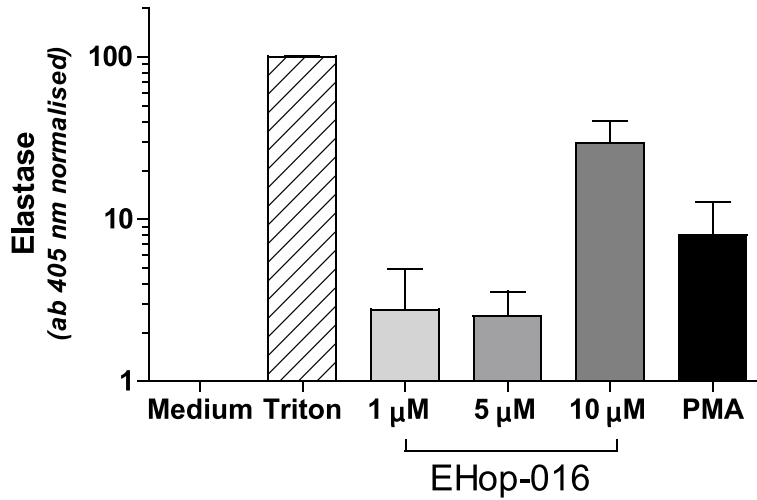
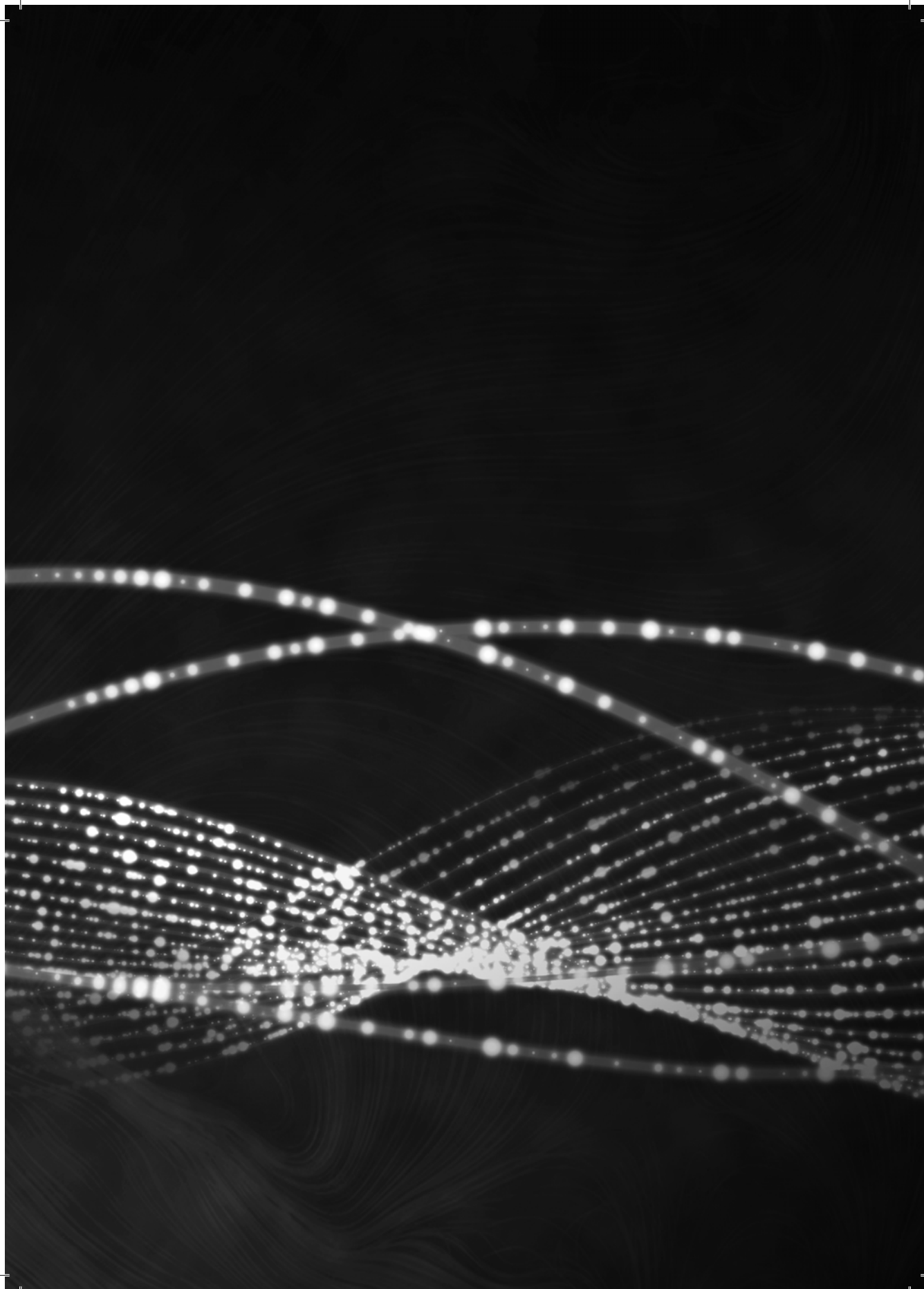


**Figure 3.** Elastase release upon stimulation. Human neutrophils were stimulated 1, 5, 10  $\mu\text{M}$  EHop-016 diluted or 50 nM PMA in RPMI. Stimulation of the cells without stimuli (medium) was used to determine spontaneous release and set to 0%. Maximum elastase release was determined by cell lysis with 0.5% Triton X-100 and set to 100%. After three hours, the supernatant was removed and incubated with the elastase substrate ((N- (Methoxysuccinyl)-Ala-Ala-Pro-Val 4-nitroanilide, Sigma) for 30 minutes. Substrate conversion was determined at 405nm absorption. Graphs mean  $\pm$  SEM duplo measurements of a single donor.




# Chapter 8

---

## General discussion

Lieke A. Golbach

The background of the page is a dark, almost black, space filled with a complex network of glowing white and light grey lines and dots. These elements form a series of overlapping, wavy patterns that create a sense of depth and movement, reminiscent of a data visualization or a network diagram. The lines are thin and delicate, while the dots are small and bright, scattered along the paths of the lines. The overall effect is a futuristic and technical aesthetic.

The aim of this thesis was to assess the effect of low frequency electromagnetic field exposure in an *in vitro* model system. Neutrophils are indispensable cells of our body's innate immune system, but also a cell type that displays a very short lifespan. They appear to be an overlooked immune cell type in literature about the effect of EMFs, nevertheless we selected this cell type for our studies. Neutrophils generate large amounts of oxidants to combat microbes and require a healthy calcium homeostasis for almost every cellular function. Neutrophils respond within seconds to chemokines and migrate towards the site of infection through activation of several highly orchestrated intracellular pathways. Calcium ions and ROS generation are both suggested as a possible molecular targets of EMF exposure, which makes this neglected cell a perfect model system to evaluate the possible effects of EMF exposure and elucidate a potential intracellular mechanism. In this general discussion, I will consider the limitations and challenges of our work and compare our findings to current literature. I will focus on the approach used in our systematic review, and discuss in more detail the intracellular pathways and clinical relevance of neutrophil extracellular traps. Finally, I will reflect on the different approaches of our studies and discuss the statistical significance versus the biological relevance of our findings.

### Systematic review in a broader perspective

It is a major achievement to produce a bias-free experiment, but the second, crucial stage is to synthesise the evidence fairly. An adequate discussion should contain the principal findings, the strengths and weaknesses of the study, these strengths and weaknesses in relation to other studies and the meaning of the study with unanswered questions and future research<sup>345</sup>. Nevertheless, many papers seem to be primarily written to “sell” the paper and to a lesser extent to structure the evidence, leading to cherry-picking and unjustified conclusions. Not only the discussion section of an original article might be biased and incomplete, many scientific reviews also lack a complete overview of the current knowledge. Systematic reviews are conducted to overcome all of these challenges. Originally used in medical sciences in the 1970s to examine the effectiveness of health-care interventions and to support evidence-based medicine, nowadays systematic reviews have infiltrated into a wide range of disciplinary fields<sup>346-348</sup>. Their transparency and rigorous method to generate a robust, empirically derived answer to a research question would make them ideal to evaluate current literature on EMF. However, despite growing interest in the use of systematic reviews and the extensive meta-analyses of epidemiology data regarding childhood leukaemia and EMF, to date these methods are rarely used to evaluate *in vivo* and *in vitro* effects of electromagnetic field exposure.

Performing a systematic review and maybe even more importantly a meta-analysis is challenging, especially with studies that report *in vitro* experiments<sup>233,349,350</sup>. *In vitro* experiments allow for more standardised procedures to test a specific interaction, nevertheless we found that the different exposure conditions and experimental protocols used to evaluate the calcium homeostasis during EMF exposure hampered a proper comparison. To partly overcome this problem, we needed to group frequencies and different cell types together, and categorise magnetic flux densities and exposure durations. Consequently, this could lead to underestimation of the true effect as a very specific EMF characteristics may be crucial to determine a biological response<sup>180,223</sup>.

*Confounding factors; Temperature and ambient fields*

We grouped papers describing exposure to calcium ion resonance frequency (IRF) together. Furthermore, papers using 50/60 Hz were grouped, as well as all remaining frequencies. The existence of frequency windows is controversial, but our subgroup analysis indicated an association between the IRF and increased intracellular calcium. This correlation was not supported by studies of Coulton et al.<sup>207</sup> and Lyle et al.<sup>126</sup>, because they applied IRFs and did not detect differences after exposure. This is interesting observation as one of the included studies by Fitzsimmons et al. reported an effect size of 21 after exposure to IRFs<sup>198</sup>. These large differences between values are difficult to trust and suggest the presence of confounding factors that affect experimental outcomes. In our systematic review, we estimated the risk of bias introduced by two main confounders, ambient temperature and background electromagnetic fields. The temperature of the cells during exposure and/or the calcium assay was controlled in 90% of all studies, however only 42% reported a narrow error range. For most ion channels, thermal energy affects the rate of conformational transitions by 2-to-5 fold per 10°C<sup>351-354</sup>. For calcium channels, it is reported that an increase in temperature reduced the amplitude of the calcium influx of voltage-gated calcium channels<sup>353,355</sup> and lowers the probability of IP3 calcium channels to open<sup>356</sup>. This occurs not only in response to the ambient temperature<sup>134</sup>, but also to quick temperature changes<sup>357</sup>. In addition, generation of high level LF EMFs consequently results in temperature increase due to power dissipation. Therefore lack of an adequate narrow-ranged temperature control could result in a difference between two samples that might not be due to the EMF exposure. The risk of bias becomes even larger when studies also did not report the use of an unenergised or sham coil (35% of all papers). Ideally, the perfect control condition has the same power dissipation in the field windings as present EMF exposure<sup>358</sup>. In line with this, custom-built microscopy coils<sup>359</sup> and complete *in vitro* exposure systems are designed<sup>215</sup>. Nevertheless, these specialised systems are expensive and designing them requires an expertise-level way beyond the capability of most molecular biologists. In our systematic review, only four of the 42 papers described sham exposure by keeping the power dissipation equal and cancelling the EMFs with antiphase waves. The other 23 used a coil without a current flowing through. This is similar to the way we conducted our experiments. Although this might not be the perfect control condition, it will certainly minimise the risk of bias compared to no coil at all.

Environmental exposure, and in particular not controlling for it, is the second largest factor that could introduce a risk of bias. When examining the effects of LF EMF exposure, ambient fields that are produced inside cell culture incubators need to be known. Interestingly, a paper published by Portelli et al. is the only report that scientifically investigates the role of ambient fields<sup>220</sup>. They thoroughly examined the ambient fields in 21 incubators and showed that these fields range from 0.15 µT up to 240 µT. When considering our systematic review, only 15 of the 42 included papers reported an ambient electromagnetic field and only half mentioned a value for the static magnetic field. These statistics are frightening, as it resembles investigating the effect of smoking cigarettes on lung function, without controlling for passive smoking. James Lin, a member of ICNIRP and editor at Bioelectromagnetics called Portelli's paper a "game changer" that might explain the huge degree of variation reported between *in vitro* experiments. He stated that given the potential confounding of unspecified incubator fields, it seemed only reasonable to reassess the data and re-evaluate the validity of any conclusions to date, both positive and negative<sup>360</sup>. Controlling all environmental

confounding factors in a study might be impossible, but critically assessing the risk of bias would strengthen the evidence of studies and reflect unbiased research.

#### *Access and transparency of data*

Obtaining all data required to perform a meta-analysis of our included studies (**chapter 3**) was not without a struggle. We were unable to get a full-text version of 15 of the 227 papers that were included in our initial full-text evaluation phase. Furthermore, thirteen of the 42 included papers neglected to report a standard error, standard deviation or sample size for every experiment. These values are indispensable for the mathematical calculation of the effect size and confidence interval. Nevertheless after contacting every resource still nine papers were missing one or more of these values. In addition, we needed to use the sample mean of several experiments, whereas ideally the mean and error range of every individual experiment should be calculated. It is of course nearly impossible to report every single experiment, since it would make articles tediously long and vague with regard to the main and secondary research findings. However, recent efforts have tried to encourage researchers to make raw data, experimental protocols, and analytical codes available<sup>361,362</sup>. Making data available through a specialised network or supplementary files could benefit not only the reproducibility and clarity of research in general, but also make systematic reviews and meta-analysis like ours stronger. According to Heather Piwowar in 2009, 45% of authors published biological gene-expression microarray intensity values together with their paper<sup>363</sup>. This was a six fold increase compared to 2001, which looks promising. However, when it comes to other types of data sets, only 47 of the 500 analysed papers by Alsheikh-Ali et al. deposited their full primary data sets<sup>364</sup>. Accordingly, depending on the type of data, researchers either provide or rarely share their data. Fortunately, despite the risk of bias and the difficulty to obtain the required data, we were able to perform a meta-analysis.

#### *Radioactive isotopes (<sup>45</sup>Ca) versus fluorescent calcium dyes*

Our meta-analysis suggests a small interaction of LF EMFs with calcium oscillation patterns and intracellular calcium concentrations. The latter contained the most data, as it was performed on 81 individual experiments reported in 24 papers. This meta-analysis suggested a complex association of exposure and calcium homeostasis. Experiments performed with radioactive calcium isotopes showed a significant increase of intracellular calcium, whereas experiments executed with fluorescent dyes did not indicate the same association. This might be the result of two different measurements that are compared. In an assay with radioactive calcium (<sup>45</sup>Ca), cells are incubated in medium containing <sup>45</sup>Ca during exposure or sham treatments. The <sup>45</sup>Ca in the extracellular medium will be transported through calcium channels or passively move across the cell membrane. The cell balances the calcium influx, by extrusion of calcium ions, which are predominantly not radioactive. After the treatment, all extracellular medium is removed and the amount of radioactive calcium ions inside the cells is measured. Therefore, a <sup>45</sup>Ca assay primarily measures calcium uptake and passive influx. Fluorescent dyes on the other hand, are membrane permeable and only become fluorescent when they are hydrolysed inside the cell. Once hydrolysed, some dye-molecules bind to the calcium ions in the cytoplasm and others remain unbound in the cytosol. When the intracellular calcium concentration rises, through either passive influx, release from the calcium stores or opening of calcium channels in the cell membrane, the remaining

dye-molecules bind to calcium ions and their fluorescence intensity increases. While a  $^{45}\text{Ca}$ -assay mainly represents the influx and accumulation of calcium ions via transport from the extracellular medium to the cytoplasm over time, fluorescent dyes quantify the actual calcium concentration at a certain moment in time. So these two assays measure two fundamentally different processes that both describe intracellular calcium homeostasis

Suppose the effect of LF EMF exposure is acute, for instance by opening calcium channels<sup>41</sup> or increasing membrane permeability<sup>38-40</sup>, then it could also quickly be restored by the cell. Pumps and exchangers get activated and remove calcium from the cytoplasm to compensate the small influx. This theory could explain the neutral effect obtained with the calcium dye compared to the  $^{45}\text{Ca}$  assay in our meta-analysis. However, if LF EMFs increase the calcium influx, seen by an accumulation of more radioactive calcium ions, then this should also be visible by an increase of fluorescence during acute exposure. This “*dye-during*” subgroup included all values with the largest possible difference between sham and LF EMF during the whole exposure period. Overall, this subgroup contained 23 individual experiments reported in five papers, but meta-analysis did not indicate a significant increase. This additional analysis did not support the hypothesis of a short influx and subsequent re-establishment of homeostasis and provides no clarification for the conflicting results reported in literature.

#### *From counts per minute (CPM) to nanomolar calcium*

The biological relevance of the measured calcium influx with radioactive isotopes is neglected in most papers, despite the fact that this is crucial stage for correct interpretation of results. For example, none of the included studies<sup>63,121,129,198,200,206,212</sup> converted the measured radioactivity (counts per minutes; abbreviated to CPM) into actual calcium concentrations. Calculation of the actual calcium influx is not difficult, if all cellular and physical parameters are known.

A quick calculation: the radioactivity of a sample, expressed in disintegrations per minute or DPM, largely depends on the efficiency of the scintillation counter as  $\text{DPM} = \text{CPM} \times \text{efficiency}$ . At an efficiency of 100%, measuring 10  $\mu\text{L}$  of 5  $\mu\text{Ci/ml}$  will give  $1.11 \cdot 10^5$  DPM and the same amount of CPM, because of a universal conversion factor. However, the efficiency of liquid scintillation counter is lower than 100% for  $^{45}\text{Ca}$ <sup>365</sup>, therefore count rate does not universally equate to dose rate. None of the articles reported an efficiency or correlation between radioactivity (Ci) and CPM. I therefore use 5  $\mu\text{Ci/ml}$ , and 78047 CPM/10  $\mu\text{l}$  as reported in calculations of Villarroya et al<sup>366</sup>. This corresponds with an efficiency of 14.22%. When considering the article of Robert Liburdy<sup>63</sup>, the difference between the EMF and control samples was 2211.6 CPM. The samples were incubated in 3  $\mu\text{Ci/ml}$  in 1 mM non-radiative calcium ( $^{40}\text{Ca}$ ). Correcting the 7804.7 CPM/nmol  $^{40}\text{Ca}$  for the lower radioactivity gives 4682.8 CPM/nmol calcium (3/5). Hence an increase of 2211.6 CPM after exposure corresponds with 427.27 pmol calcium in the total sample. If I assume that this calcium is taken up equally by all cells, linear in time and I ignore the extrusion or storage of the radioactive calcium, this gives 0.0472 fmol/cell, which is  $\sim 28.5$  million individual calcium ions. These ions are taken up in 3600 seconds, giving an influx of  $\sim 7900$  ions per second. This same calculation can be done for every article, estimating the amount of calcium ions flowing into the cell during one second is between 7900 and one million ions (Table 1). On average, 8.000 to 100.000 ions flow through a calcium channel, depending on the type of channel<sup>367</sup>. From this calculation and the other CPM values reported in the papers included in our meta-

analysis, I estimate that between 1 and 125 channels open every second during EMF exposure. Our maximum value of 125 corresponds perfectly with values reported by Brasen et al. They simulated that around 100 to 150 calcium channels open during the first second of calcium stimulation<sup>368</sup>. A typical mammalian cell has a diameter of roughly 20  $\mu\text{m}$  and a volume of  $\sim 5$  pL. The internal calcium concentration of a typical cell is 100 nM, corresponding with roughly  $3 \times 10^5$  calcium ions. Adding 7900 will give a global concentrations of 103 nM, whereas influx of one million ions will increase the internal concentration to 432 nM. The actual increase in concentration might differ, because these inflowing calcium ions will quickly be buffered by proteins like calmodulin<sup>369</sup>, calcineurin and S100 proteins<sup>370</sup>. Our values are of course estimates that generalise several cell type specific phenotypes, but they do give an indication of the calcium concentration that correlates with the radioactive count that is measured.

Our subgroup meta-analysis indicated an increase of influx according to the  $^{45}\text{Ca}$ -papers, whereas the calcium dyes studies did not support this notion. The recent advantage of enhanced resolution to detect intracellular calcium signals has led to the discovery of calcium puffs, which are local calcium signals that arise from the opening of tightly clustered inositol trisphosphate receptor/channels (IP3R) on the ER. These blibs remain in a small confined cytoplasmic region of the cell and have an amplitude of 15 nM – 300 nM<sup>371</sup>. From these studies we can conclude that calcium dyes would be sensitive enough to detect a small local influx of calcium. Nevertheless, the results of our meta-analysis did not show an increase of intracellular calcium during LF EMF exposure. This could be explained in two ways. One, the  $^{45}\text{Ca}$ -assays are not more sensitive, but the experiments are performed with bias. Either confounding factors or selection bias could contribute to increased calcium concentrations in the exposure group, if an experiment is performed without proper controls or blinding. The second explanation for this difference might be that the calcium dye-experiments were not performed in such a way that they could detect subtle differences. Tiny influxes like blibs can only be measured with Fluo4 at an imaging rate of at least 7.5 Hz<sup>372</sup>. Furthermore, detection of small changes in calcium was limited by the location of the confocal plane relative to the event<sup>373</sup>, so conventional microscopy measurements might overlook these small changes. Regardless of which explanation might be correct, it would be interesting to combine the blib-detection method with acute LF EMF exposure and investigate the calcium mobilisation process during exposure.

#### *Biological relevance of an altered calcium concentration*

Regarding the CPM calculations, an important question remains: would the calculated increase be of biological relevance for an immune cell and eventually our health? The resting intracellular calcium concentration in a neutrophil ranges between 40-100 nM<sup>374-376</sup>. Upon activation by receptor cross-linking<sup>377</sup>, chemotactic molecules<sup>374,376</sup>, interferon gamma<sup>375</sup> or even nanosecond electrical fields<sup>378</sup> captive calcium is released and calcium channels open. This process leads to elevation of the calcium concentrations up to 200-900 nM. A rise of 3 nM is very small and probably not relevant, even though we did not evaluate possible accumulation. Additional research is required to determine the biological relevance. On the other hand, an elevation of 332 nM induced by exposure will activate the intracellular signalling cascade. Pettit et al. showed that a peak of  $385 \pm 145$  nM calcium triggered rapid changes in cell morphology and facilitated spreading<sup>379</sup>. An elevation of 160 nM calcium even promotes the activity of gelsolin, a calcium-binding protein that prevents



polymerisation of actin by capping the filaments<sup>268</sup>. These studies suggest that some of the calculated elevation (between 3 nM and 332 nM) of cytoplasmic calcium induced by LF EMF exposure will influence cellular behaviour and function *in vitro*. However, this conclusion must be interpreted with caution, since we based our estimates on the reported CPM values. There might be a large risk of bias introduced by inaccurate experimental design and/or measurements.

#### *Conventional reviews versus Systematic reviews on effects of LF EMF exposure*

We are the first to report a systematic review and meta-analysis on the influence of EMF exposure on calcium homeostasis, although in earlier reviews other research groups combined literature to try and identify a site of interaction. In 2013, Martin Pall published a review on the substantial evidence for an interaction of EMF and voltage-gated calcium channels<sup>41</sup>. His conclusions are far more univocal and also simplistic compared to our paper, but Pall's review lacks some crucial components compared to a systematic review. The articles in this review were selected based on the evidence presented in them without an unbiased literature search. Conclusions were thus drawn from only a small percentage of the available literature. This was neither acknowledged nor reported in the paper. A total of 23 studies showed activation of voltage-gated channels by EMFs, which was concluded to provide substantial evidence for these channels to be a direct target of EMF. However, Platano et al. reported that GSM modulated radiofrequency did not influence the Ba<sup>2+</sup> current through voltage-gated calcium channels (VGCC)<sup>241</sup>. The same neutral effects were found in resting neuroblastoma cells<sup>380</sup> and PC12 cell lines<sup>381</sup>. This evidence contradicts with Pall's review and therefore questions the selection process of the papers. A second misunderstanding is that static magnetic fields, electrical fields and electromagnetic fields are all combined to support the theory. Voltage-gated channels are activated by changes in electrical membrane potential near the channel. Applying an electrical field will obviously induce a calcium influx. Furthermore, fields with frequencies of 0 Hz (static) 50 Hz, 60 Hz and 1100 MHz were examined. The physical properties of these fields are very different, yet they all showed an effect during exposure. If the effect of exposure would be so universal, it is unexpected that also neutral data are published in literature. It therefore appears that a selection bias was introduced by only selecting data that substantiated the theory. This in combination with a lack of understanding the nature of voltage-gated channels makes the review of Pall biased.

Last year, Mattsson and Simkó published a review evaluating 41 papers that studied the effects of ELF EMF on oxidative response in *in vitro* studies<sup>382</sup>. To combine the different studies, they used a "grouping" tool, which categorised relevant culture conditions, the cell type and the main outcome. An interesting approach, which was not employed to perform a comprehensive review, but to investigate the presence of an EMF sensitive cell type or EMF-characteristic related effects. This approach has similarities with our systematic approach, but it overlooks some essential elements that could make the set-up and outcome stronger. The inclusion and exclusion criteria are not mentioned in the approach and outcomes section. Studies that reported inappropriate, or unsatisfactory experimental conditions were excluded from the analysis. However, the criteria to define exclusion were not described, nor was it reported how many papers failed to meet these criteria. We experienced that defining exclusion and inclusion criteria for *in vitro* studies is challenging. In clinical trial research, randomised controlled double-blind clinical trials are the gold standard of a high quality

method. The same quality control is now slowly drifting to animal experiments and recently the gold standard publication checklist was published by Hooijmans et al.<sup>383</sup>. Unfortunately, such guidelines or a golden standard is not yet determined for *in vitro* experiments. Nevertheless, describing criteria used in a systematic approach makes the review transparent and unbiased and improves the quality of reporting. Future systematic review processes could benefit from these considerations and criteria.

We performed a complete meta-analysis with subgroup analyses of primary data that were extracted from articles, from supplementary data and through e-mail contact with authors. It was a laborious process, in which we were unable to obtain the required data of nine papers. Mattsson and Simkó avoided this problem by not reporting continuous outcomes, but making dichotomous outcome variables. A study was categorised positive if an effect of EMF was shown and negative if the influence of EMFs was not significant. A threshold for significance is not described, but probably a p-value smaller than 0.05 is used to discriminate between positive and neutral outcomes. When comparing the grouped analysis of oxidative stress with our systematic review of the calcium mobilisation, some resemblances and differences appear. Regarding an EMF sensitive cell type, no clear trend indicating a specific cell type dependent EMF effect was reported from the overall effect. Dividing the data set in immune relevant and other cell types however did indicate that immune cells might be more susceptible for EMF (91% positive outcomes versus 77%). We reported a similar association in our meta-analysis with a smaller effect size of  $0.543 \pm 0.318$ . Therefore it might be that immune cells have specific phenotypes that make them more susceptible to EMF exposure. The grouped analysis of the magnetic flux densities showed a pronounced effect of flux densities above 1 mT, as 93% of all oxidative stress outcomes were positive. Our association for the calcium mobilisation was not that strong, however we did find a trend towards more intracellular calcium with both low and very higher magnetic flux density. The correlation between a higher field strength and larger effects is for most researchers considered plausible, whereas low levels fields are advocated to be the environmental source that initiates health issues<sup>384,385</sup>. Furthermore, the observation that acute exposure, <60 minutes, influenced ROS production more than exposures longer than one hour is in agreement with our meta-analysis. An exposure duration of less than 60 minutes was associated with an increased calcium concentration in the cells, while longer exposures did not significantly alter calcium levels in the cells. Cellular adaptation to constant exposure could explain these observations. In the early 90's, Goodman et al.<sup>224</sup> and Lin et al.<sup>225</sup> showed that chronic exposure of cellular systems could lead to adaptation without the occurrence of any harmful effects. Unfortunately, more experimental evidence or a biological theory to support these two papers and our observation is lacking.

Grouping different experiments together and making the outcomes dichromatic bears limitations for the interpretation. It is not possible to discriminate if the response is heterogeneous. A significant reduction or increase of ROS will both be categorised as “positive”, and merging them will mask the true effect. We observed this phenomenon clearly in our two different meta-analysis, which first indicated an effect for every subgroup, but subsequently showed that the direction and ultimate effect size were smaller. We also observed this in our analysis of the different outcome measurements of the calcium oscillation. The percentage of oscillating cells did not indicate a significant effect, whereas the other two outcome measures showed increased frequency and reduced amplitude of the oscillations

during or after LF EMF exposure. Mattsson and Simkó did report the direction of the effect size in their last figure, but without confidence interval due to the dichotomy of the values. It would be interesting to analyse the data included in the grouped review with continuous values. This will give an effect size with a confidence interval and direction for every included experiment. With this information, a meta-analysis and maybe a subgroup analysis could be performed to further unravel the strength of evidence for an oxidative response to LF EMF exposure.

In summary, the last few years different attempts to pool and group present literature on LF EMF exposure dealt with the analysis in different ways. Investigating a potential mechanism of EMF exposure and forming a plausible conclusion through analysis of already published research brings up many challenges. Therefore, we decided to apply a systematic approach according to the guidelines in the Cochrane handbook for systematic reviews of interventions. We collaborated with the systematic review centre for laboratory animal experimentation (SYRCLE) and learned from their expertise. Like mentioned above, there has been no validated guidelines or check list for reporting *in vitro* studies on LF EMF exposure. Compared to numerous experimental protocols that are available for researchers, the number of guidelines for reporting are very limited. For *in vitro* studies on experimental dental research, a check-list and guideline has been published<sup>386</sup>, which described the need for reporting allocation, randomisation as well as the proper hypothesis. These guidelines are supplemented with additional criteria, such as sample size calculations and the meaningfulness of differences, by Krithikadatta et al.<sup>387</sup>. These guidelines could easily be standardised for *in vitro* LF EMF research to make research transparent and less biased. Generalizing protocols ensures unbiased comparison and hopefully reduces the uncertainty many investigators now experience when they read contrasting results of fellow researchers.

### Neutrophil extracellular traps in a broader perspective

Neutrophils are sensitive, dynamic cells that are indispensable for our immune system and in this thesis we used neutrophils as a model cell for our *in vitro* and *ex vivo* experiments. Until one decade ago, attention was mainly focused towards understanding the phagocytic uptake, intracellular degradation of antimicrobial peptides and release of these peptides in an acute inflammatory response towards invading microbes. In 2004, Brinkmann and colleagues described a previously unappreciated behaviour of human neutrophils; neutrophil extracellular trap (NET) formation<sup>333</sup>. These NETs consisted of DNA, histones and antibacterial peptides such as elastase, myeloperoxidase (MPO) and lactotransferrin<sup>388</sup>. Microscopic observations have showed that NETs trap gram-positive and negative bacteria<sup>74,333</sup>, and bind to fungi<sup>76,388</sup>. Subsequent studies showed pivotal roles for NADPH oxidase<sup>75</sup>, ROS production<sup>389</sup>, the cytoskeleton<sup>310</sup> and the supporting function of PAD4<sup>81</sup> and calcium mobilisation<sup>390</sup>.

The NETosis pathway can be influenced by environmental factors such as temperature<sup>391</sup>, oxygen<sup>392</sup> and high level LF EMF exposure (**chapter 6**). We were the first to show an interaction of LF EMF exposure on NET release, apparently induced via enhanced ROS production. This enhanced release is a double-edged sword, as physiological amounts of NETS are important to combat pathogens, but excessive generation of NETs is associated with severe tissue damage<sup>393</sup> and development of autoimmune diseases<sup>394,395</sup>. We acknowledged these positive and negative consequences and investigated both mechanism in **chapter 6**, to get a comprehensive overview of the potential effects *in vivo*.

#### *Limitations of our in vitro NET formation study*

Extrapolation of data obtained in an *in vitro* model system to an *in vivo* situation is complex and our study has a few limitations that will make it even more difficult. The experiments were performed with neutrophils isolated from blood of healthy volunteers on the day of the experiment. The protocol required a Percoll density-gradient centrifugation step and subsequent lysis of any remaining red blood cells. Every step in the protocol could activate the neutrophils, because these sensitive cells respond to temperature changes<sup>396,397</sup>, adhesion surfaces<sup>398</sup> or endotoxins<sup>399</sup>. Human promyelocyte cell lines like HL-60 could also produce NETs<sup>81,400</sup> and this could overcome unwanted activation through separation. However the use of an immortalised cell line makes translation from the *in vitro* to the *in vivo* situation even more complex. HL-60 are neutrophil-like-cells that display almost all neutrophilic functions, but could never completely substitute *ex vivo* neutrophils<sup>401,402</sup>. For this reason we optimised a quick and high-throughput protocol that enabled isolation of large numbers of neutrophils from whole blood, while at the same time cellular behaviour is not strongly influenced in subsequent experiments<sup>403,404</sup>. Polysaccharides, such as Ficoll 400 or Dextran T 500, have been reported to greatly modify neutrophilic properties<sup>404-406</sup>, due to their adhesive nature. We selected a Percoll gradient isolation, which is preferred for cell migration assay<sup>404</sup> and superoxide release<sup>403</sup>. Furthermore, with our *ex vivo* model system we investigated the effect of LF EMF exposure during PMA-stimulated NET formation in a tissue culture plate. This experimental design was therefore not influenced by additional effects of exposure on the bacteria growth<sup>407</sup> or endothelial function. This approach is the strength of our *in vitro/ex vivo* model system, but also its weakness. Our setup is lacking the complex architecture of tissues and interactions with different cell types that *in vivo* modulate the immune response. We investigated killing of bacteria by the NETs, while *in vivo* captured bacteria are cleared by macrophages<sup>408</sup>. Furthermore, interaction of platelets with adhered neutrophils leads to intravascular NET release<sup>77</sup>. Lack of these cellular networks minimises the possibility to directly extrapolate our data.

Secondly, we performed bacterial killing with harmless commensal bacteria that are routinely used in many laboratories; the JM109 strain of *E.coli*. We found that NETs reduce the number of surviving bacteria in a concentration dependent manner. These results are relevant since Parker et al., showed that *E.coli* bacteria induce NET release *in vitro*<sup>75</sup>. However our *E.coli* strain did not develop mechanisms to facilitate evasion. Certain pathogens developed expression of extracellular DNases, as a result of a host-pathogen co-evolutionary arms race. For instance, *Streptococcus pneumoniae* expresses EndA, a DNase, on its surface that digests the DNA scaffold structure of NETs<sup>409,410</sup>. In addition, *Staphylococcus aureus* and *Vibrio cholerae* evade entrapment by NETs through secretion of different nucleases<sup>73,411</sup>. So, many pathogens have armed themselves to circumvent getting trapped by the fibrous structures of NETs. To extrapolate our *in vitro* data, a more biological relevant, and therefore pathogenic microbe should be used.

#### *Extrapolation of our in vitro study*

An extrapolation can only be made if we ignore the limitations of our *in vitro* model system and interpret the results with caution. We observed an increase in the amount of NETs of 20% after LF EMF exposure. The number of surviving bacteria depends on the amount of NETs in the medium, which correlated with a linear regression equation. From this equation I

calculated that an increase of 20%, compared to sham treated cells, would reduce the number of surviving bacteria with 3.4% from 56.71% to 53.27%. On the other hand, epithelial damage was observed as a collateral effect of NET release. If we assume that the NETs are not cleared by other immune cells, 20% more NETs would result in a 9.6% reduction of cell vitality of the surrounding tissue according to our own *in vitro* cell vitality assays. Despite these estimates, translation of the results into proportional changes provides no information on the overall effect, since the changes are not conclusive regarding their biological relevance. Our study only highlights the capacity of preformed NETs to trap and kill microbes and I can only speculate on their potential contribution to host defence. Nevertheless, the next step in our speculations would be exploring a possible *in vivo* challenge with LF EMF exposure.

Quickly after the discovery of NETs, numerous studies reported immunohistochemical staining of NET formation *in vivo*<sup>388,412</sup>. Antibody staining against MPO, histones and neutrophil elastase quantifies NET release in various tissues<sup>413</sup>. In addition, different studies measured damage of lung epithelial cells<sup>414</sup>, veins<sup>415</sup> and liver tissue<sup>416</sup> caused by NET release. New high-tech imaging techniques are combined with conventional approaches to enable dynamic observations of NET formation, without the need of fixing tissues<sup>413</sup>. Application of this knowledge to our research question could cast light on the potential beneficial or harmful effect of high level LF EMF exposures. Injection of LPS mimics pathogenesis of severe sepsis and does not activate the phagocytosis pathway. This would bring us one step closer to evaluating the effect of LF EMF exposure on solely NET formation. However, with this setup we would completely ignore the interaction of exposure with other tissues, which is not a realistic approach. Both low and high level fields penetrate through the skin, tissues and organs of every organism, but also diminish exponentially with distance from the source. The interaction of LF EMFs on NET formation could only be explored *in vivo*, when keeping in mind other possible interactions of LF EMF exposure.

#### *Future experiments*

For future experiments, an *in vivo* challenge would not be our first recommendation, because our *ex vivo* experimental design should first to be optimised. Currently, our *ex vivo* experimental setup limits initial translation to a biological relevant situation. First of all, we applied a LF EMF with a magnetic flux density of 300  $\mu\text{T}$  to our cells, for four hours. This 300  $\mu\text{T}$  field is above the threshold of 200  $\mu\text{T}$  for environmental exposure that is published as safe by the International Commission on Non-Ionizing Radiation (ICNIR)<sup>24</sup>. A field of 300  $\mu\text{T}$  corresponds with blow drying hair or using an electrical razor continuously for four hours. A more relevant magnetic flux density around 0.1-10  $\mu\text{T}$ , or a shorter duration would better resemble exposure in daily life. Furthermore, using a 50/60 Hz frequency that optionally contains deviation frequencies<sup>384</sup>, would make translation and recommendations for health more reliable, since this is more related to power-network exposure. These changes were implemented in our experiments that investigated the role of calcium mobilisation after exposure in **chapter 2**. In this study, we did not observe any differences in calcium mobilisation, gene expression pattern or phenotype of the microvilli after exposure to both low and high level fields. Using environmental relevant exposure levels has also been advocated by Schmid et al. of the IT'IS foundation in a publication last year<sup>417</sup>. Environmental relevant exposure levels and frequency enables extrapolation of *in vitro* work with fewer variables.

A second improvement for our experimental design would be the use of stimuli that

resemble a true invasion of microbes. We induced NET formation through addition of phorbol 12-myristate 13-acetate (PMA), which mimics receptor activation through upregulation of diacyl-glycerol (DAG). Neutrophils engage in NET formation upon activation by interleukin 8 (IL-8)<sup>72</sup>, different types of gram-positive and negative bacteria<sup>73-75</sup>, parasites<sup>68</sup>, fungi<sup>76</sup>, and activated platelets<sup>77</sup>, so more biological relevant infection model are available. We initially focussed only on NET formation and selected PMA, because intact microbes initiate not only NETs, but mostly phagocytosis and intracellular killing. An alternative and also more relevant stimulus could be LPS, which are lipopolysaccharides of the outer membrane of gram-negative bacteria. Unfortunately, LPS did not induce NET formation in our *ex vivo* setup. A phenomenon that is also reported by different research groups<sup>77,80</sup>, but also proven otherwise by others<sup>333,334</sup>. This contradiction in literature might be due to the inability of LPS to promote NADPH oxidase activity and only prime the cells to an oxidative burst (reviewed in 418). PMA has the advantage over microbes that it induces NET formation in more reproducible way, with a small intra-experimental variation. Minor standard errors and reproducible results are required to detect subtle differences. However, re-evaluating the data, it might be possible to detect an increase by LF EMF with different stimuli, because the increase of NETs was around 20%. To minimise phagocytosis, large sized microbes, like *Candida albicans* hyphae or extracellular aggregates of *Mycobacterium bovis* could be used, as Sheppard et al. showed that microbe size determines which pathway is activated in neutrophils<sup>419</sup>. In summary, a more physiological stimulus and environmental relevant exposure characteristics would be our advice for future research.

#### *The functionality of neutrophil extracellular traps*

When NET formation was reported for the first time, sceptics argued that it was not a vital process, but rather a type of necrosis. This was also our first assumption when we administrated EHop-016 to block the actin cytoskeleton during NET formation (**chapter 7**). Though, apoptosis and necrosis both display hallmarks different from “NETosis”. NETotic cells do not externalise phosphatidylserine (PS) before plasma membrane rupture, nor show membrane blebbing or nuclear chromatic condensation. Normally the caspase activity is relatively low in resting neutrophils and only initiated by spontaneous apoptosis. Activation of the NET formation pathway does not increase caspase cleavage. All these phenotypes indicate that NET formation is the result of a completely different cell signalling pathway, leading to cell death (reviewed in 420). Furthermore, pharmacological inhibition of apoptosis by z-VAD-FMK, which blocks caspase activity, did not inhibit PMA-induced NET formation according to Remijsen et al.<sup>80</sup>. The same group also observed an identical effect with necrostatin-1, a necrosis inhibitor. The contradiction in our EHop-016 study was that the response of neutrophils to EHop-016 was probably two-sided, because Z-VAD-FMK consistently reduced NET formation slightly. Furthermore, caspase 3/7 activity was detected in the samples. Discrimination between both subgroups is difficult, since cells collapse and “disappear” after NET release. For this reason, Annexin-V or TUNEL staining examined by flow cytometry would not separate apoptotic from NETotic cells. In addition, cytotoxicity or cell vitality assays rely on the notion that apoptosis compromises cell membrane integrity, shown by release of lactate dehydrogenase (LDH) or staining with vital dyes, such as trypan blue or propidium iodide. Pilsczek et al. reported that NETotic neutrophils release the same amount of LDH as lysed cells<sup>74</sup>. Therefore, none

of these methods would discriminate between apoptosis or NET formation in a single cell assay. Our recommendation for further *in vitro* experiments, to strengthen our results, would be an immunofluorescence staining of activated caspase. This will confirm the presence of both apoptotic as well as NET releasing cells after EHop-016 stimulation.

Critics of NETosis also have doubts concerning the functionality of MPO outside the cells<sup>421</sup>. The MPO enzyme alone lacks antimicrobial activity and rather serves as an essential catalyst. It oxidises chloride ions ( $\text{Cl}^-$ ) in the presence of hydrogen peroxide ( $\text{H}_2\text{O}_2$ ) to generate HOCl, a highly antimicrobial product. Within a phagosome,  $\text{H}_2\text{O}_2$  is provided by the NADPH oxidase complex and dismutated into HOCl. Given the rapid dissipation of  $\text{H}_2\text{O}_2$  during NET formation, this source will be long gone, when a cell releases NETs. Neighbouring phagocytes or NOX protein expressing cells could provide the required oxidants<sup>422,423</sup>. The addition of  $\text{H}_2\text{O}_2$  *in vitro* activates microbial killing of NETs through MPO, indicating a functional complex<sup>424</sup>. However, oxidant production and secretion is predominantly a signal for oxidative stress of non-phagocytic cells (reviewed in 48) and not a cooperative anti-inflammation mechanism. Therefore, oxidant production by neighbouring cells does not provide a convincing explanation. The validity of NE and MPO binding to NETs on the other hand, is verified by immunofluorescence<sup>75</sup>, western blot<sup>310</sup> and transmission electron microscopy<sup>333</sup>. Moreover, Papayannopoulos et al. showed that both enzymes translocate into the nucleus and cooperatively enhance chromatin decondensation<sup>82</sup>. Inhibition of MPO or NE reduced NET formation *in vitro*<sup>82,425</sup>. Moreover MPO-deficient donors completely fail to produce NETs<sup>426</sup>. Nevertheless, presence of the enzymes does not validate functional activity. In my opinion, MPO and NE might be bound to the DNA, because in earlier stages of NET formation these enzymes assist nuclear decondensation. NE partially degrades core histones during NET formation and MPO promotes a relaxed chromatin state. Therefore, the primary function of both enzymes is histone modifications and subsequently they are released with the NETs due to their strong residual interaction with DNA<sup>427</sup>. This hypothesis is substantiated by reports that showed that histones are potent antibiotics that killed bacteria at nanomolar concentrations far more effectively than most other anti-microbial peptides<sup>428</sup>. Moreover, Saffarzadeh et al. discovered that the core histones, but not MPO or NE, also play a dominant role in collateral damage of endothelial cells<sup>393</sup>. This might explain why NETs do kill bacteria, and also why extracellular MPO and NE do not comprise functional antimicrobial activity *in vitro*. Accordingly, I reason that the enzymatic activity of MPO and NE are required inside the cell during NET formation, whereas histones are the true killers once the NETs are released.

### *Healthy criticism*

The discovery of NETs is a great example of healthy distrust of existing views, when Brinkmann et al. re-evaluated a previously unappreciated behaviour of human neutrophils *in vitro*, namely their capacity to extrude DNA, histones, and some granular proteins<sup>333</sup>. Healthy or constructive criticism is essential for good research, as it forces researchers to take a step back, think about their work and evaluate the outcomes. I think that this is practiced too little, especially for EMF research. Many of the papers included in our systematic review (**chapter 3**) lacked proper controlling of environmental factors, as discussed earlier. Next to that, some of the articles with the largest effect sizes, were performed with a rather small sample size. If an effect is that dominant, it can easily be detected in repeated experiments,

which would eliminate possible confounding factors. For instance, Lindström et al. reported response rates of >80% to LF EMF exposure<sup>27</sup>, but examined only 24 cells in their study. Repetition of these experiments by Wey et al. with sham exposure, controlled temperature, randomisation, blinding and a sample size of 250 did not confirm the results<sup>124</sup>. A critical look at Lindström's experimental design gives the impression that the responses might be not associated with EMF exposure, but with the moment of exposure. If sham exposure is always applied during the initial four minutes of imaging, chances are that differences are observed in the subsequent four minutes during exposure<sup>182,429,430</sup>. Unfortunately, Lindström's experimental design is not exceptional in EMF research. Continuous efforts, critical review and healthy scepticism are required with both EMF research and NET formation studies, to prevent publication of incomplete or biased studies.

### **Bottom-up versus top-down approaches in LF EMF research**

In this thesis we investigated the potential influences of LF EMF exposure on cellular behaviour, with the use of an *in vitro* model system. In order to induce beneficial or harmful health effects, EM fields need to interact with cells or tissues in the body. For *in vitro* research, both bottom-up or top-down approaches can be used. The *in vitro* bottom-up design requires a mechanism of interaction or biological target and subsequently determines the effect for the cell's behaviour, from target to cellular function. A top-down approach first determines the effect on the whole cell and then zooms in on suspected candidate targets. We used both strategies to evaluate the potential effects of LF EMF exposure.

#### *Calcium and filopodia measurements with a bottom-up approach*

Our investigation of the calcium mobilisation in **chapter 2** and the filopodia dynamics in **chapter 4** both were designed with a bottom-up method. LF EMFs contains low field energy, so a cellular mechanism might be required to convert this low energy into a physiological response that requires much higher energies. Our suspected potential targets initially based on a theory by Gartzke and Lange, were the calcium ions inside the cell and the microvilli on the outside of neutrophils<sup>43</sup>. Gartzke and Lange proposed a theoretical interaction mechanism that focussed on calcium ion conduction along actin filaments in microvilli. Microvilli are small membrane protrusions with a structural core of dense bundles of cross-linked actin filaments. The theory describes a concept in which the thermal energy evoked by LF EMFs is not enough to influence ions like calcium by itself, but the actin-filament core of microvilli is hypothesised to function as a cable-like structure to allow calcium propagation into the cytoplasm. The cable-like conductance of actin filaments better conducts ionic currents along the filament axis than through the surrounding salt solution<sup>431</sup>. In this way, calcium ions may enter the cytoplasm via the actin filaments, when the energy of the EM field promotes simultaneous jumps of the ions along the filament in the same direction, instead of random Brownian motions.

This theory published in 2002 still needs to be proven *in vitro*, as well as lacks experimental evidence that shows that this calcium transport eventually leads to alter gene expression or cellular behaviour. When applying the ion-conductance theory to the data presented in **chapter 2**, we did not find supportive evidence for this theory. We did not observe changes in gene expression patterns after exposure and even after five days of exposure, expression levels were still unaltered. Furthermore, the phenotype and number of microvilli



was not altered after exposure. Our data did not substantiate the theory, even though microvilli could be a plausible target, because they are important microdomains for calcium influxes. Brasen et al. predicted that the presence of microvilli or wrinkles enhanced the local calcium concentration from 2.5 to 25  $\mu\text{M}$ , compared to a spherical cell. This would only occur close to the plasma membrane, as the internal calcium concentration at the centre of both cell types was equal. They propose that these local microdomains facilitate local cellular processes, like secretion of granules that require 50 - 100  $\mu\text{M}$ <sup>432</sup> or calpain-1 activation at 10 – 50  $\mu\text{M}$ <sup>433,434</sup>. The high calcium concentrations were predicted to last a very short period of time, since in the simulation the channels opened only for a quarter of a second. So, microvilli themselves might be important features of neutrophils, which enable very short and local activation of proteins. This activation could eventually influence the cell's behaviour. Calcium measurements of the calcium influx in microvilli with fluorescent dyes are impossible. The diameter of a microvillus is around 100 nm and the maximum optical resolution, the minimal distance at which two points can be detected as separate objects, for fluorescence microscopy with a UV laser is 190 nm. Consequently, to validate the proposed mechanism, the concept should be applied to larger structures, like podosomes and filopodia<sup>242</sup>. In **chapter 4**, we describe the development of a method to quantify filopodia dynamics. Visualisation of the actin filaments enabled imaging of these large protrusions during acute LF EMF exposure. A short influx of calcium, like predicted by Brasen et al., would result in activation of calpain-1 and actin depolymerisation, leading to filopodia shortening. These changes in the dimensions are detected, if the resolution in time is high enough. Furthermore, our experimental design and imaging analysis can easily be translated to a system with expression of chameleon, a genetically encoded calcium sensor<sup>435</sup>, which would validate local calcium movement. We initially suspected a subtle change of the calcium concentration in our neutrophil-like-cells induced by EMF exposure (**chapter 2**), but a difference that would still present in the whole cell after stimulation with a chemokine. Consequently, we measured the global calcium influx with Fluo4 and not the fluxes in a specific micro domain of the cell. Our results exclude any major changes in the calcium homeostasis induced by LF EMF exposure, similar to what was predicted from our meta-analysis in **chapter 3**. However, there are techniques available to investigate the validity of ion-conductance and/or feature specific EMF effects in a more sensitive way. Our filopodia-dynamics approach with stable expression of Lifeact or calcium-binding proteins has the potential to achieve this. We were unable to perform these experiments, but with the right combination of novel sensitive approaches, this theory could be rejected or validated with a bottom-up approach.

#### *NET formation and migration in a top-down approach*

With different top-down approaches, we determined the rate of cell migration after LF EMF exposure in **chapter 5**, the formation of neutrophil extracellular traps (NETs) during LF EMF exposure or EHop-016 stimulation (**chapter 6 and 7**). Cell migration is the result of activation of several pathways, eventually leading to cell movement. We initially evaluated the effect of exposure on the migration speed, from where a possible target of EMF could be determined if a difference was observed. With NET release, we determined the amount of release after exposure, and subsequently investigated the possible pathways that could be involved, to pin-point a site of interaction of EMF. Moreover, a similar approach was performed to investigate an interaction of the small molecule inhibitor, EHop-016, with different

intracellular proteins. We initially observed NET formation upon stimulation with EHop-016, and subsequently found a pivotal role for PAD4 activation and histone citrullination.

Enhanced NET formation after LF EMF exposure, is a newly discovered interaction between EMF and innate immune cells described in **chapter 6**. With the use of different pharmacological inhibitors, we eliminated PAD4 and autophagy and established that both the cytoskeleton and the NADPH oxidase complex played a pivotal role. A NBT assay showed that significant amounts of ROS production were produced during LF EMF exposure. An interesting, and not completely new interaction, which is extensively reviewed by Simkó and her group<sup>436</sup>. Nevertheless, even though we could determine a possible target, we did not determine the potential mechanism of interaction. Increased ROS could be the result of enhanced activity of the oxidase complex<sup>56</sup>, prolonged lifetime of free radicals<sup>437</sup> or a completely not yet discovered mechanism. For the first theory, the largest quantity of *in vitro* studies are available in literature, however we did not investigate expression pattern, location or assembly of the NADPH oxidase complex ourselves. The only way to explore a potential mechanism suggested in our paper would be to speculate on the role of NADPH oxidase complex during exposure.

We did not detect enhanced ROS production after exposure when the cells were not simultaneously stimulated with PMA. This outcome substantiates the hypothesis that EMF requires a cellular mechanism to convert the low energy of the fields into a physiological response. This requirement implies a priming effect of the neutrophils. Neutrophils exist in many states of activation that vary from dormant to fully activated, with various intermediate stages. While activation triggers immediate anti-microbial activity in neutrophils, priming enables a more powerful response if the cells first acquire a state of pre-activation. This process was demonstrated for increased virion uptake after cytokine-induced priming<sup>438</sup> and enhanced superoxide anion production after exposure to granulocyte colony-stimulating factor (GCSF)<sup>439</sup>, insulin growth factor I<sup>440</sup> and small amounts of endotoxins, such as LPS<sup>441</sup>. *In vivo*, priming affects the neutrophil cytoskeletal organisation to reduce deformability in order to retain in capillary beds. Integrin and selectins expression is upregulated<sup>442</sup> and proteins are translocated. Accordingly, priming triggers important cellular pathways that prepare a cell for a subsequent encounter with microbes.

From our data, I hypothesise that EMF exposure primes the cells, prior to PMA stimulation. Alternatively EMF exposure may enhance the activity of the NADPH oxidase complex after PMA stimulates its assembly. To fully explain the possible mechanisms, it is essential to understand the cellular pathways of ROS production. In short, activation of the NADPH oxidase is known to be dependent on translocation of the p47phox, p67phox, p40phox, cytosolic complex and Rac2 to the plasma membrane. These cytoplasmic elements associate with p22phox and flavocytochrome b558, also known as NOX2 or gp91phox, which are both located in the membranes of specific granules and secretory vesicles (reviewed in 418). It is less likely that EMF enhances the activity of NADPH oxidases, since we used relatively high concentrations of PMA, around 50 nM. Addition of more PMA to the cells did not result in more NETs, suggesting that the activity of the NADPH oxidases were at their maximum in our experimental setup. This proposes that enhanced activity of NADPH oxidase by exposure is not possible, suggesting that priming by EMF prior to cellular stimulation occurs.

PMA is small molecular that does not interact with extracellular receptors, but activates PKC activity through DAG upregulation. In literature, PMA is described as a poor priming agent at very low concentrations, but also as a very powerful activator<sup>443</sup>. Without EMF, 50 nM PMA is able to induce ROS production and NET formation. This emphasises that priming need to take place before stimulation. The timing of our experiment favours priming of neutrophils by EMFs, since our cells were exposed to LF EMFs one hour before PMA was added to the cells. This priming could occur through two different processes<sup>443</sup>. Other groups have shown that small amount of LPS, G-CSF and IL-8 stimulate translocation of b558 to the membrane<sup>439,444</sup>, whereas TNF $\alpha$  priming results in increased phosphorylation of p47phox and p67phox<sup>445</sup>. Also a combination of both processes was demonstrated after priming with a TLR7/8 agonist<sup>446</sup>. I hypothesise that EMF exposure is a priming agent and subsequent administration of PMA activates the whole cascade of ROS formation and eventually NET release. However, to further investigate the role of NADPH oxidase assembly, subtle analyses of the phosphorylation status of the different subunits should be examined with for instance proteomics, a truly quantitative method to measure protein activity<sup>447</sup>. Furthermore, translocation of the different plasma membrane-bound subunits could be imaged during acute exposure. If priming occurs through EMF exposure, it would be interesting to see if “depriming” also occurs if the EM-field source is eliminated. This process is already observed *in vivo* for PAF<sup>448</sup> and TNF $\alpha$ <sup>449</sup>, whereby the duration of priming greatly depends on the type of the priming agent<sup>450</sup>. However, both theories are speculations and additional research is required to determine the true interaction between LF EMF exposure and NADPH oxidases.

#### *From sample size to biological relevance*

With every experimental design, the initial question a researcher needs to ask is “What to expect?” This is critical in both quantitative and qualitative research regarding the potential effects of LF EMF exposure. Even when a potential target or cellular pathway is already suggested in previous work, it is essential to determine the expected effect size and inter-experimental variance induced by a treatment like EMF exposure. For every study published in this thesis, we have carefully selected our approach and estimated the effects. With the calcium experiments in **chapter 2**, it was a delicate balance between the most sensitive methods versus the ability to process large numbers of samples to obtain a reliable estimate of the true effect. We ended up with a high-throughput analysis, with a low affinity calcium indicator called Fluo4. We expected the effect size to be subtle, less than 10%, but detectable with our setup. We used suboptimal concentrations of the biological stimulus that evoked the calcium influx during the measurement. Some groups suggested that the heterogeneous effects of EMFs depend on the cell cycle<sup>137</sup>, baseline calcium oscillation patterns<sup>27,124</sup>, or origin of the cells. We however, predicted the effect to be uniform among all cells in our population, as we used a cell line that did not proliferate anymore, nor should show calcium oscillations in suspension<sup>451</sup>. With these assumptions and limitations in mind, we determined our final experimental approach that would detect possible changes induced by LF EMF exposure. In our later investigated systematic review in **chapter 3**, an estimated effect size of 0.351 was calculated. According to Cohen’s *d* and SMD equation, this correlates to an increase of 1.755% if the standard deviation of the measurements is 5% of the mean value. A quick power calculation estimates the minimal sample size to be 64, at a power of 0.8 in a two-sided analysis with an alpha of 0.05. This calculation highlights that the expected difference

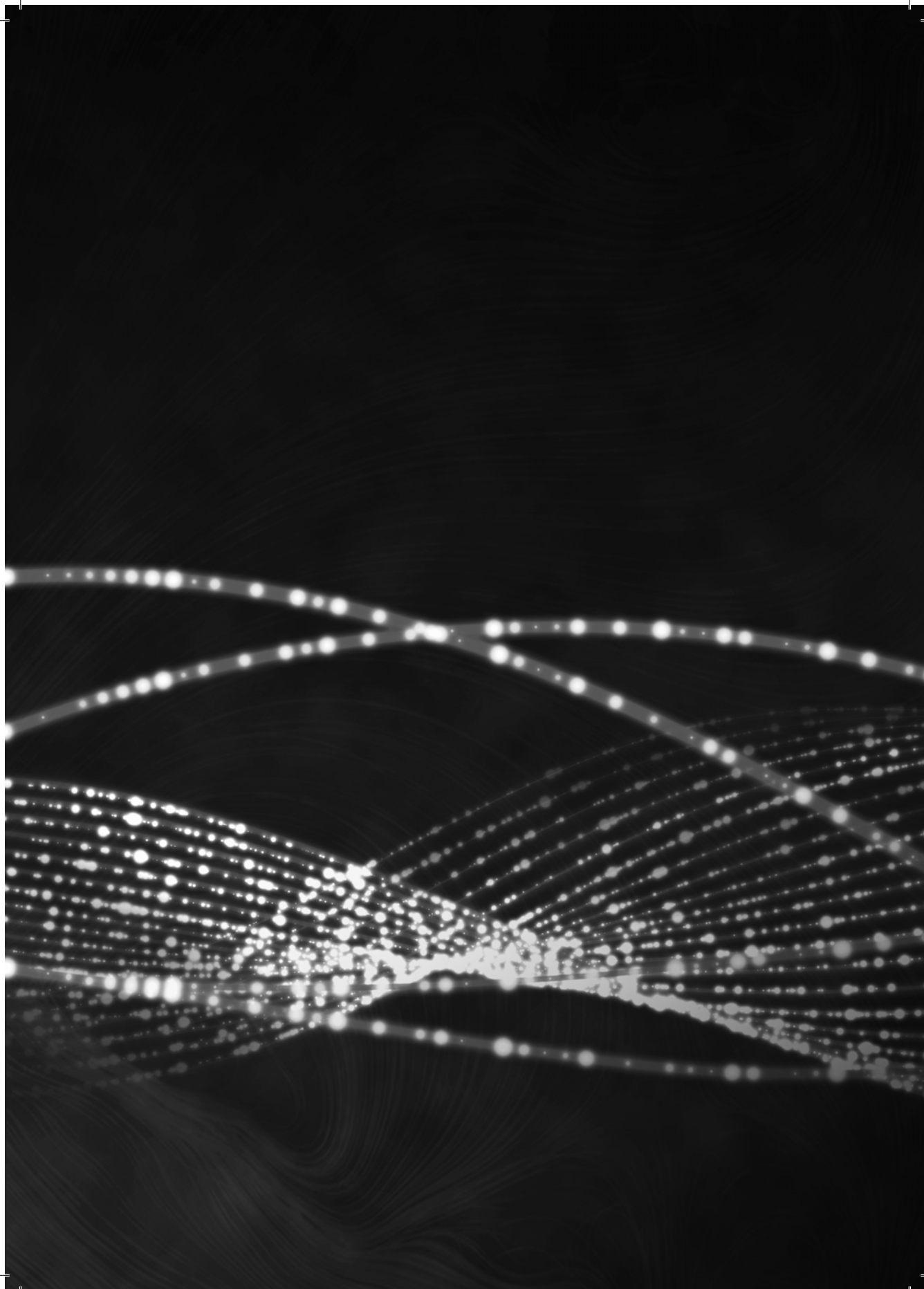
in calcium concentrations induced by LF EMF exposure would be very small and therefore a large sample size is required to strengthen any statistical difference. With a large body of evidence already present in literature, a systematic review generates a good estimation of the expected effect size. Unfortunately, systematic reviews are time-consuming and there might not be enough data available to review every potential mechanism. The importance of sample sizes in clinical trials is already published in 1981 by Lachin<sup>452</sup> and nowadays this is a standard protocol for all human clinical trials and animals experiments. This could be universal for *in vitro* model systems, because even a calculated sample size based on a rough estimate of the effect of LF EMF exposure could strengthen the outcomes reported in every paper

With a sensitive method and a proper sample size, statistical significance will be achieved if effect of a treatment, like EMF exposure exists. However, one of the most common errors in quantitative analyses involves the incorrect interpretation of statistical significance and the related failure to report and interpret effect sizes. Once a potential mechanism is indicated, the study goal evolves from qualitative research to quantitative research. A large, representative sample size is used in quantitative research to generalise findings to populations. This error often leads to under-interpretation of associated p-values when sample sizes are small and the corresponding effect sizes are large. It leads to an over-interpretation of p-values when sample sizes are large and effect sizes are small (reviewed in 453 and 454). Several statisticians advocate that researchers operate under the false illusion that their p-values test importance and relevance<sup>455,456</sup>, whereas p-values are designed to give a statement about the likelihood of findings being due to chance. In our case, we initially hypothesised that calcium might be affected by EMF exposure, through an interaction with microvilli. However, if we only had assessed calcium mobilisation, we would have been unable to give any biological relevance of an expected effect. Therefore, we examined gene expression patterns and appearance of the microvilli. Moreover, when EMF showed to enhance NET formation, we examined the killing capacity and endothelial damage by NETs. Of course, *in vitro* work is difficult to extrapolate to an *in vivo* situation without making assumptions and understanding the limitations, but by performing additional *in vitro* experiments or calculations, a speculation regarding the biological relevance is permitted. This will not only give depth to a scientific discussion, but also make interpretation easier for everybody not familiar with a particular research field.

	EMF (CPM)	EMF (CPM)	Difference (CPM)	Cell density	CPM/nmol Ca	Fmol per cell	Ions per cell	Time (sec)	Ions per second
<i>Liburdy, 1992, A</i>	12450.5	10238.9	2211.6	1.00*10 <sup>7</sup>	4682.8	0.047	2.84*10 <sup>7</sup>	3600	7900.372
<i>Liburdy, 1992, B</i>	14989.8	10238.9	4750.85	1.00*10 <sup>7</sup>	4682.8	0.101	6.11*10 <sup>7</sup>	3600	16971.19
<i>Liburdy, 1992, C</i>	15336.0	11717.7	3618.29	1.00*10 <sup>7</sup>	4682.8	0.077	4.65*10 <sup>7</sup>	3600	12925.41
<i>Craviso, 2003, A</i>	9051	8557	494	6.33*10 <sup>5</sup>	3121.9	0.250	1.51*10 <sup>8</sup>	900	167269
<i>Craviso, 2003, B</i>	2521	2444	77	6.33*10 <sup>5</sup>	3121.9	0.039	2.35*10 <sup>7</sup>	900	26072.29
<i>Fitzsimmons, 1994, A</i>	11222	4340	6882.8	3.33*10 <sup>6</sup>	2598.7	0.795	4.79*10 <sup>8</sup>	1800	266101.1
<i>Fitzsimmons, 1994, B</i>	23040	7360	15680	3.33*10 <sup>6</sup>	2598.7	1.812	1.09 *10 <sup>9</sup>	1800	606216.2
<i>Fitzsimmons, 1994, C</i>	34501	7360	27141	3.33*10 <sup>6</sup>	2598.7	3.136	1.89 *10 <sup>9</sup>	1800	1049319
<i>Fitzsimmons, 1994, D</i>	22129	7360	14769	3.33*10 <sup>6</sup>	2598.7	1.707	1.03 *10 <sup>9</sup>	1800	570995.4
<i>Fitzsimmons, 1994, E</i>	15965	7360	8605	3.33*10 <sup>6</sup>	2598.7	0.994	5.99 *10 <sup>8</sup>	1800	332684.3
<i>Fitzsimmons, 1994, F</i>	13020	7360	5660	3.33*10 <sup>6</sup>	2598.7	0.654	3.94 *10 <sup>8</sup>	1800	218825.5
<i>Fitzsimmons, 1994, G</i>	1973	2204	-231	3.33*10 <sup>6</sup>	2598.7	-0.027	-1.61*10 <sup>7</sup>	1800	-8930.86
<i>Fitzsimmons, 1994, H</i>	4485	2204	2281	3.33*10 <sup>6</sup>	2598.7	0.264	1.59*10 <sup>8</sup>	1800	88187.45
<i>Fitzsimmons, 1994, I</i>	3283	2204	1079	3.33*10 <sup>6</sup>	2598.7	0.125	7.51*10 <sup>7</sup>	1800	41716.03
<i>Fitzsimmons, 1994, J</i>	1239	2204	-965	3.33*10 <sup>6</sup>	2598.7	-0.112	-6.72*10 <sup>7</sup>	1800	-37308.6
<i>Fitzsimmons, 1994, K</i>	1141	2204	-1063	3.33*10 <sup>6</sup>	2598.7	-0.123	-7.40*10 <sup>7</sup>	1800	-41097.4
<i>Fitzsimmons, 1994, L</i>	25978.3	5923.9	20054.35	3.33*10 <sup>6</sup>	2598.7	2.317	1.40*10 <sup>9</sup>	2400	581502.1
<i>Bernabo, 2007, C</i>	31486.3	36917.3	-5431	2.00*10 <sup>8</sup>	809.0	-0.034	-2.02*10 <sup>7</sup>	3600	-5615.16
<i>Bernabo, 2007, D</i>	67640.2	92946.5	-25306.3	.00*10 <sup>8</sup>	809.0	-0.156	-9.42*10 <sup>7</sup>	7200	-13082.2
<i>Bernabo, 2007, E</i>	88664.2	112234	-23569.8	.00*10 <sup>8</sup>	809.0	-0.146	-8.77*10 <sup>7</sup>	14400	-6092.26
<i>Liburdy, 1993, A</i>	15286.0	10795.8	4490.17	1.00*10 <sup>7</sup>	4682.8	0.096	5.77*10 <sup>7</sup>	3600	16039.98
<i>Walleczek, 1990, A</i>	0.00416	0.00236	0.0018	1.00	7804.7	0.231	1.39*10 <sup>8</sup>	3600	38580.22
<i>Walleczek, 1990, B</i>	0.00107	0.00108	-2.04E-06	1.00	7804.7	0.000	-1.57*10 <sup>5</sup>	3600	-43.6814
<i>Lyle, 1991, A</i>	16619.6	11868.6	4751	1.00*10 <sup>6</sup>	7371.6	0.644	3.88*10 <sup>8</sup>	1800	215625.8
<i>Lyle, 1991, B</i>	22491.8	15551.2	6940.6	1.00*10 <sup>6</sup>	7371.6	0.942	5.67*10 <sup>8</sup>	1800	315001.5
<i>Lyle, 1991, C</i>	37713.2	30911	6802.2	1.00*10 <sup>6</sup>	7371.6	0.923	5.56*10 <sup>8</sup>	1800	308720.2
<i>Lyle, 1991, D</i>	13620.8	10989.8	2631	1.00*10 <sup>6</sup>	7371.6	0.357	2.15*10 <sup>8</sup>	1800	119408.8

**Table 1.**

Calculations of the calcium concentration from the CPM values reported in the papers included in our systematic review (chapter 3).



# Appendix

---

References

Summary

Dankwoord

Acknowledgements



## References

- 1 **Heinrich, S., Thomas, S., Heumann, C., von Kries, R. & Radon, K.** The impact of exposure to radio frequency electromagnetic fields on chronic well-being in young people - A cross-sectional study based on personal dosimetry. *Environ. Int.* 37, 26-30, (2011).
- 2 **Milde-Busch, A., von Kries, R., Thomas, S., Heinrich, S., Straube, A. & Radon, K.** The association between use of electronic media and prevalence of headache in adolescents: results from a population-based cross-sectional study. *Bmc Neurology* 10, (2010).
- 3 **Ahlbom, A. et al.** A pooled analysis of magnetic fields and childhood leukaemia. *British Journal of Cancer* 83, 692-698, (2000).
- 4 **Pedersen, C. et al.** Distance to High-Voltage Power Lines and Risk of Childhood Leukemia - an Analysis of Confounding by and Interaction with Other Potential Risk Factors. *Plos One* 9, (2014).
- 5 **Slusky, D. A., Does, M., Metayer, C., Mezei, G., Selvin, S. & Buffler, P. A.** Potential role of selection bias in the association between childhood leukemia and residential magnetic fields exposure: A population-based assessment. *Cancer Epidemiology* 38, 307-313, (2014).
- 6 **Brenner, D. J. et al.** Cancer risks attributable to low doses of ionizing radiation: Assessing what we really know. *Proc. Natl. Acad. Sci. U. S. A.* 100, 13761-13766, (2003).
- 7 **Saha, S., Woodbine, L., Haines, J., Coster, M., Ricket, N., Barazzuol, L., Ainsbury, E., Sienkiewicz, Z. & Jeggo, P.** Increased apoptosis and DNA double-strand breaks in the embryonic mouse brain in response to very low-dose X-rays but not 50 Hz magnetic fields. *Journal of the Royal Society Interface* 11, 10, (2014).
- 8 **Salford, L. G., Brun, A. E., Eberhardt, J. L., Malmgren, L. & Persson, B. R. R.** Nerve cell damage in mammalian brain after exposure to microwaves from GSM mobile phones. *Environ. Health Perspect.* 111, 881-883, (2003).
- 9 **Bolte, J. F. B. & Eikelboom, T.** Personal radiofrequency electromagnetic field measurements in the Netherlands: Exposure level and variability for everyday activities, times of day and types of area. *Environ. Int.* 48, 133-142, (2012).
- 10 **Ryan, K. L., D'Andrea, J. A., Jauchem, J. R. & Mason, P. A.** Radio frequency radiation of millimeter wave length: Potential occupational safety issues relating to surface heating. *Health Physics* 78, 170-181, (2000).
- 11 **Messias, I. D., Okuno, E. & Colacioppo, S.** Occupational exposure of physical therapists to electric and magnetic fields and the efficacy of Faraday cages. *Revista Panamericana De Salud Publica-Pan American Journal of Public Health* 30, 309-316, (2011).
- 12 **Walker, M. M., Dennis, T. E. & Kirschvink, J. L.** The magnetic sense and its use in long-distance navigation by animals. *Current Opinion in Neurobiology* 12, 735-744, (2002).
- 13 **Okano, H. & Ohkubo, C.** Modulatory effects of static magnetic fields on blood pressure in rabbits. *Bioelectromagnetics* 22, 408-418, (2001).
- 14 **Sert, C., Akti, Z., Sirmatel, O. & Yilmaz, R.** An investigation of the heart rate, heart rate variability, cardiac ions, troponin-I and CK-MB in men exposed to 1.5 T constant magnetic fields. *General Physiology and Biophysics* 29, 282-287, (2010).
- 15 **Leitgeb, N., Cech, R., Schrottner, J., Lehofer, P., Schmidpeter, U. & Rampetsreiter, M.** Magnetic emission ranking of electrical appliances. A comprehensive market survey. *Radiation Protection Dosimetry* 129, 439-445, (2008).
- 16 **Stuchly, M. A. & Lecuyer, D. W.** Electromagnetic-fields around induction-heating stoves. *Journal of Microwave Power and Electromagnetic Energy* 22, 63-69, (1987).
- 17 **Calvente, I., Davila-Arias, C., Ocon-Hernandez, O., Perez-Lobato, R., Ramos, R., Artacho-Cordon, F., Olea, N., Nunez, M. I. & Fernandez, M. F.** Characterization of Indoor Extremely Low Frequency and Low Frequency Electromagnetic Fields in the INMA-Granada Cohort. *Plos One* 9, 9, (2014).
- 18 **Maslanyj, M. P., Mee, T. J., Renew, D. C., Simpson, J., Ansell, P., Allen, S. G. & Roman, E.** Investigation of the sources of residential power frequency magnetic field exposure in the UK Childhood Cancer Study. *Journal of Radiological Protection* 27, 41-58, (2007).
- 19 **Schuz, J., Grigat, J. P., Stormer, B., Rippin, G., Brinkmann, K. & Michaelis, J.** Extremely low frequency magnetic fields in residences in Germany. Distribution of measurements, comparison of two methods for assessing exposure, and predictors for the occurrence of magnetic fields above background level. *Radiation and Environmental Biophysics* 39, 233-240, (2000).
- 20 **Grellier, J., Ravazzani, P. & Cardis, E.** Potential health impacts of residential exposures to extremely low frequency magnetic fields in Europe. *Environ. Int.* 62, 55-63, (2014).



- 21 **Wertheimer, N. & Leeper, E.** Electrical wiring configurations and childhood-cancer. *Am. J. Epidemiol.* 109, 273-284, (1979).
- 22 **Greenland, S., Sheppard, A. R., Kaune, W. T., Poole, C., Kelsh, M. A. & Childhood Leukemia, E. M. F. S. G.** A pooled analysis of magnetic fields, wire codes, and childhood leukemia. *Epidemiology* 11, 624-634, (2000).
- 23 **Greenland, S., Schwartzbaum, J. A. & Finkle, W. D.** Problems due to small samples and sparse data in conditional logistic regression analysis. *Am. J. Epidemiol.* 151, 531-539, (2000).
- 24 **International Commission on Non-Ionizing Radiation, P.** Guidelines for limiting exposure to time-varying electric and magnetic fields (1 Hz to 100 kHz). *Health physics* 99, 818-836, (2010).
- 25 **Ahlbom, A. et al.** Guidelines for limiting exposure to time-varying electric, magnetic, and electromagnetic fields (up to 300 GHz). *Health Physics* 74, 494-522, (1998).
- 26 **Adey, W. R. & Bawin, S. M.** Binding and release of brain calcium by Low-level electromagnetic fields -A Review. *Radio Science* 17, S149-S157, (1982).
- 27 **Lindstrom, E., Lindstrom, P., Berglund, A., Lundgren, E. & Mild, K. H.** Intracellular calcium oscillations in a T-cell line after exposure to extremely-low-frequency magnetic-fields with variable frequencies and flux densities. *Bioelectromagnetics* 16, 41-47, (1995).
- 28 **Mattsson, M. O., Lindstrom, E., Still, M., Lindstrom, P., Mild, K. H. & Lundgren, E.** Ca<sup>2+</sup> (i) rise in Jurkat E6-1 cell lines from different sources as a response to 50 Hz magnetic field exposure is a reproducible effect and independent of poly-L-lysine treatment. *Cell Biol. Int.* 25, 901-907, (2001).
- 29 **Still, M., Lindstrom, E., Ekstrand, A. J., Mild, K. H., Mattsson, M. O. & Lundgren, E.** Inability of 50 Hz magnetic fields to regulate PKC- and Ca<sup>2+</sup>-dependent gene expression in Jurkat cells. *Cell Biol. Int.* 26, 203-209, (2002).
- 30 **Blank, M., Monti, M. G., Pernecco, L., Moruzzi, M. S., Battini, R., Zaniol, P. & Barbiroli, B.** Extremely-low-frequency electromagnetic-fields stimulate activation of protein-kinase-C in HL-60 leukemia-cells by increasing membrane-transport of ca<sup>2+</sup>. *Electricity and Magnetism in Biology and Medicine*, 522-524, (1993).
- 31 **Carson, J. J. L., Prato, F. S., Drost, D. J., Diesbourg, L. D. & Dixon, S. J.** Time-varying magnetic-field increase cytosolic Ca-2+ in HL-60 cells. *American Journal of Physiology* 259, C687-C692, (1990).
- 32 **Zhang, X., Zhang, J., Qu, X. & Wen, J.** Effects of different extremely low-frequency electromagnetic fields on osteoblasts. *Electromagn Biol Med*, 167-177, (2007).
- 33 **Torricelli, P., Fini, M., Giavaresi, G. & Giardino, R.** In vitro osteoinduction of demineralized bone. *Artif Cells Blood Substit Immobil Biotechnol*, 309-315, (1998).
- 34 **Long, Y., Cai, G. P., Guan, Z. C., Liu, H. & Liang, X. D.** Effects of electromagnetic fields on the bioactivities of an osteoblast-like cell line (UMR-106). *Electro- and Magnetobiology*, 237-253, (2000).
- 35 **Rosado, J. A. & Sage, S. O.** The actin cytoskeleton in store-mediated calcium entry. *J. Physiol. - London* 526, 221-229, (2000).
- 36 **Pettit, E. J. & Fay, F. S.** Cytosolic free calcium and the cytoskeleton in the control of leukocyte chemotaxis. *Physiol. Rev.* 78, 949-967, (1998).
- 37 **Zeilhofer, H. U., Vestweber, D., Swandulla, D., Brune, K. & Hallman, R.** E-selectin-induced calcium signalling and adhesion in neutrophil granulocytes. *Naunyn-Schmiedebergs Arch. Pharmacol.* 358, R682-R682, (1998).
- 38 **Durney, C. H., Kaminski, M., Anderson, A. A., Brucknerlea, C., Janata, J. & Rappaport, C.** Investigation of AC-DC magnetic field effects in planar phospholipid-bilayers. *Bioelectromagnetics* 13, 19-33, (1992).
- 39 **Liburdy, R. P., Tenforde, T. S. & Magin, R. L.** Magnetic field-induced drug permeability in liposome vesicles. *Radiation Research* 108, 102-111, (1986).
- 40 **Ramundo-Orlando, A., Morbiducci, U., Mossa, G. & D'Inzeo, G.** Effect of low frequency, low amplitude magnetic fields on the permeability of cationic liposomes entrapping carbonic anhydrase I. Evidence for charged lipid involvement. *Bioelectromagnetics* 21, 491-498, (2000).
- 41 **Pall, M. L.** Electromagnetic fields act via activation of voltage-gated calcium channels to produce beneficial or adverse effects. *Journal of Cellular and Molecular Medicine* 17, 958-965, (2013).
- 42 **Gailey, P. C.** Membrane potential and time requirements for detection of weak signals by voltage-gated ion channels. *Bioelectromagnetics Suppl* 4, 102-109, (1999).
- 43 **Gartzke, J. & Lange, K.** Cellular target of weak magnetic fields: ionic conduction along actin filaments of microvilli. *Am. J. Physiol.-Cell Physiol.* 283, C1333-C1346, (2002).
- 44 **Pilla, A., Fitzsimmons, R., Muehsam, D., Wu, J., Rohde, C. & Casper, D.** Electromagnetic fields as first messenger in biological signaling: Application to calmodulin-dependent signaling in tissue repair.



- Biochimica Et Biophysica Acta-General Subjects* 1810, 1236-1245, (2011).
- 45 **Markov, M. S. & Pilla, A. A.** Weak static magnetic field modulation of myosin phosphorylation in a cell-free preparation: calcium dependence. *Bioelectrochemistry and Bioenergetics* 43, 233-238, (1997).
- 46 **Ludin, A. et al.** Reactive Oxygen Species Regulate Hematopoietic Stem Cell Self-Renewal, Migration and Development, As Well As Their Bone Marrow Microenvironment. *Antioxidants & Redox Signaling* 21, 1605-1619, (2014).
- 47 **Boonstra, J. & Post, J. A.** Molecular events associated with reactive oxygen species and cell cycle progression in mammalian cells. *Gene* 337, 1-13, (2004).
- 48 **Valko, M., Leibfritz, D., Moncol, J., Cronin, M. T. D., Mazur, M. & Telser, J.** Free radicals and antioxidants in normal physiological functions and human disease. *International Journal of Biochemistry & Cell Biology* 39, 44-84, (2007).
- 49 **Feinendegen, L. E.** Reactive oxygen species in cell responses to toxic agents. *Human & Experimental Toxicology* 21, 85-90, (2002).
- 50 **Werner, E., Kandimalla, R., Wang, H. & Doetsch, P. W.** A role for reactive oxygen species in the resolution of persistent genomic instability after exposure to radiation. *Journal of radiation research* 55 Suppl 1, i14, (2014).
- 51 **Park, J. E., Seo, Y. K., Yoon, H. H., Kim, C. W., Park, J. K. & Jeon, S.** Electromagnetic fields induce neural differentiation of human bone marrow derived mesenchymal stem cells via ROS mediated EGFR activation. *Neurochemistry International* 62, 418-424, (2013).
- 52 **Poniedzialek, B., Rzymiski, P., Nawrocka-Bogusz, H., Jaroszyk, F. & Wiktorowicz, K.** The effect of electromagnetic field on reactive oxygen species production in human neutrophils in vitro. *Electromagn. Biol. Med.* 32, 333-341, (2013).
- 53 **Garip, A. I. & Akan, Z.** Effect of ELF-EMF on number of apoptotic cells: Correlation with reactive oxygen species an HSP. *Acta Biologica Hungarica* 61, 158-167, (2010).
- 54 **Lupke, M., Rollwitz, J. & Simko, M.** Cell activating capacity of 50 Hz magnetic fields to release reactive oxygen intermediates in human umbilical cord blood-derived monocytes and in Mono Mac 6 cells. *Free Radical Research* 38, 985-993, (2004).
- 55 **Simko, M., Kriehuber, R., Weiss, D. G. & Luben, R. A.** Effects of 50 Hz EMF exposure on micronucleus formation and apoptosis in transformed and nontransformed human cell lines. *Bioelectromagnetics* 19, 85-91, (1998).
- 56 **Frahm, J., Mattsson, M. O. & Simko, M.** Exposure to ELF magnetic fields modulate redox related protein expression in mouse macrophages. *Toxicology Letters* 192, 330-336, (2010).
- 57 **Scaino, J. C., Mohtat, N., Cozens, F. L., McLean, J. & Thansandote, A.** Application of the radical pair mechanism to free radicals in organized systems: Can the effects of 60 Hz be predicted from studies under static fields? *Bioelectromagnetics* 15, 549-554, (1994).
- 58 **Roy, S., Noda, Y., Eckert, V., Traber, M. G., Mori, A., Liburdy, R. & Packer, L.** The phorbol 12-myristate 13-acetate (PMA)-induced oxidative burst in rat peritoneal neutrophils is increased by a 0.1 mT (60 Hz) magnetic field. *Febs Letters* 376, 164-166, (1995).
- 59 **Hong, M. N., Han, N. K., Lee, H. C., Ko, Y. K., Chi, S. G., Lee, Y. S., Gimm, Y. M., Myung, S. H. & Lee, J. S.** Extremely Low Frequency Magnetic Fields Do Not Elicit Oxidative Stress in MCF10A Cells. *Journal of Radiation Research* 53, 79-86, (2012).
- 60 **de Groot, M. W. G. D. M., Kock, M. D. M. & Westerink, R. H. S.** Assessment of the neurotoxic potential of exposure to 50 Hz extremely low frequency electromagnetic fields (ELF-EMF) in naive and chemically stressed PC12 cells. *Neurotoxicology* 44, 358-364, (2014).
- 61 **Palumbo, R., Capasso, D., Brescia, F., Mita, P., Sarti, M., Bersani, F. & Scarfi, M. R.** Effects on apoptosis and reactive oxygen species formation by Jurkat cells exposed to 50 Hz electromagnetic fields. *Bioelectromagnetics* 27, 159-162, (2006).
- 62 **Parkinson, W. C.** Comments on the use of electromagnetic fields in biological studies. *Calcif. Tissue Int.* 37, 198-207, (1985).
- 63 **Liburdy, R. P.** Calcium signaling in lymphocytes and elf fields - Evidence for an electric-field metric and a site of interaction involving the calcium-ion channel. *Febs Letters* 301, 53-59, (1992).
- 64 **Bassen, H., Litovitz, T., Penafiel, M. & Meister, R.** ELF in vitro exposure systems for inducing uniform electric and magnetic fields in cell culture media. *Bioelectromagnetics* 13, 183-198, (1992).
- 65 **Claassen, L., Smid, T., Woudenberg, F. & Timmermans, D. R. M.** Media coverage on electromagnetic fields and health: Content analysis of Dutch newspaper articles and websites. *Health Risk & Society* 14, 681-696, (2012).
- 66 **Brinkmann, V., Reichard, U., Goosmann, C., Fauler, B., Uhlemann, Y., Weiss, D. S., Weinrauch, Y. & Zychlinsky, A.** Neutrophil extracellular traps kill bacteria. *Science* 303, 1532-1535, (2004).

- 67 **Behnen, M., Leszczyc, C., Moller, S., Batel, T., Klinger, M., Solbach, W. & Laskay, T.** Immobilized Immune Complexes Induce Neutrophil Extracellular Trap Release by Human Neutrophil Granulocytes via Fc gamma RIIIB and Mac-1. *J. Immunol.* 193, 1954-1965, (2014).
- 68 **Guimaraes-Costa, A. B., Nascimento, M. T. C., Froment, G. S., Soares, R. P. P., Morgado, F. N., Conceicao-Silva, F. & Saraiva, E. M.** Leishmania amazonensis promastigotes induce and are killed by neutrophil extracellular traps. *Proc. Natl. Acad. Sci. U. S. A.* 106, 6748-6753, (2009).
- 69 **Arai, Y., Nishinaka, Y., Arai, T., Morita, M., Mizugishi, K., Adachi, S., Takaori-Kondo, A., Watanabe, T. & Yamashita, K.** Uric acid induces NADPH oxidase-independent neutrophil extracellular trap formation. *Biochemical and Biophysical Research Communications* 443, 556-561, (2014).
- 70 **Jerjomiceva, N., Seri, H., Vollger, L., Wang, Y. M., Zeitouni, N., Naim, H. Y. & von Kockritz-Blickwede, M.** Enrofloxacin Enhances the Formation of Neutrophil Extracellular Traps in Bovine Granulocytes. *J. Innate Immun.* 6, 706-712, (2014).
- 71 **Hakkim, A., Fuchs, T. A., Martinez, N. E., Hess, S., Prinz, H., Zychlinsky, A. & Waldmann, H.** Activation of the Raf-MEK-ERK pathway is required for neutrophil extracellular trap formation. *Nature Chemical Biology* 7, 75-77, (2011).
- 72 **Keshari, R. S., Jyoti, A., Dubey, M., Kothari, N., Kohli, M., Bogra, J., Barthwal, M. K. & Dikshit, M.** Cytokines Induced Neutrophil Extracellular Traps Formation: Implication for the Inflammatory Disease Condition. *Plos One* 7, 8, (2012).
- 73 **Seper, A. et al.** Vibrio cholerae Evades Neutrophil Extracellular Traps by the Activity of Two Extracellular Nucleases. *PLoS Pathog.* 9, 15, (2013).
- 74 **Pilszczek, F. H. et al.** A Novel Mechanism of Rapid Nuclear Neutrophil Extracellular Trap Formation in Response to Staphylococcus aureus. *J. Immunol.* 185, 7413-7425, (2010).
- 75 **Parker, H., Draganow, M., Hampton, M. B., Kettle, A. J. & Winterbourn, C. C.** Requirements for NADPH oxidase and myeloperoxidase in neutrophil extracellular trap formation differ depending on the stimulus. *J. Leukoc. Biol.* 92, 841-849, (2012).
- 76 **Bruns, S. et al.** Production of Extracellular Traps against Aspergillus fumigatus In Vitro and in Infected Lung Tissue Is Dependent on Invading Neutrophils and Influenced by Hydrophobin RodA. *PLoS Pathog.* 6, 18, (2010).
- 77 **Clark, S. R. et al.** Platelet TLR4 activates neutrophil extracellular traps to ensnare bacteria in septic blood. *Nature Medicine* 13, 463-469, (2007).
- 78 **Fuchs, T. A., Abed, U., Goosmann, C., Hurwitz, R., Schulze, I., Wahn, V., Weinrauch, Y., Brinkmann, V. & Zychlinsky, A.** Novel cell death program leads to neutrophil extracellular traps. *J. Cell Biol.* 176, 231-241, (2007).
- 79 **Palmer, L. J., Cooper, P. R., Ling, M. R., Wright, H. J., Huissoon, A. & Chapple, I. L. C.** Hypochlorous acid regulates neutrophil extracellular trap release in humans. *Clinical and Experimental Immunology* 167, 261-268, (2012).
- 80 **Remijnsen, Q. et al.** Neutrophil extracellular trap cell death requires both autophagy and superoxide generation. *Cell Research* 21, 290-304, (2011).
- 81 **Wang, Y. M. et al.** Histone hypercitrullination mediates chromatin decondensation and neutrophil extracellular trap formation. *J. Cell Biol.* 184, 205-213, (2009).
- 82 **Papayannopoulos, V., Metzler, K. D., Hakkim, A. & Zychlinsky, A.** Neutrophil elastase and myeloperoxidase regulate the formation of neutrophil extracellular traps. *J. Cell Biol.* 191, 677-691, (2010).
- 83 **Ley, K., Laudanna, C., Cybulsky, M. I. & Nourshargh, S.** Getting to the site of inflammation: the leukocyte adhesion cascade updated. *Nature Reviews Immunology* 7, 678-689, (2007).
- 84 **Brandolini, L., Bertini, R., Bizzarri, C., Sergi, R., Caselli, G., Zhou, D., Locati, M. & Sozzani, S.** IL-1 beta primes IL-8-activated human neutrophils for elastase release, phospholipase D activity, and calcium flux. *J. Leukoc. Biol.* 59, 427-434, (1996).
- 85 **Bengtsson, T., Jaconi, M. E. E., Gustafson, M., Magnusson, K. E., Theler, J. M., Lew, D. P. & Stendahl, O.** Actin dynamics in human neutrophils during adhesion and phagocytosis is controlled by changes in intracellular free calcium. *Eur. J. Cell Biol.* 62, 49-58, (1993).
- 86 **Itagaki, K., Kannan, K. B., Livingston, D. H., Deitch, E. A., Fekete, Z. & Hauser, C. J.** Store-operated calcium entry in human neutrophils reflects multiple contributions from independently regulated pathways. *J. Immunol.* 168, 4063-4069, (2002).
- 87 **Heiner, I., Eisfeld, J. & Luckhoff, A.** Role and regulation of TRP channels in neutrophil granulocytes. *Cell Calcium* 33, 533-540, (2003).
- 88 **Salmon, M. D. & Ahluwalia, J.** Discrimination between receptor- and store-operated Ca<sup>2+</sup> influx in



- human neutrophils. *Cellular Immunology* 265, 1-5, (2010).
- 89 **Prentki, M., Wollheim, C. B. & Lew, P. D.** Ca<sup>2+</sup> homeostasis in permeabilized human neutrophils. Characterization of Ca<sup>2+</sup>-sequestering pools and the action of inositol 1,4,5-triphosphate. *J. Biol. Chem.* 259, 3777-3782, (1984).
- 90 **Smith, I. F. & Parker, I.** Imaging the quantal substructure of single IP3R channel activity during Ca<sup>2+</sup> puffs in intact mammalian cells. *Proceedings of the National Academy of Sciences of the United States of America* 106, 6404-6409, (2009).
- 91 **Misakian, M., Sheppard, A. R., Krause, D., Frazier, M. E. & Miller, D. L.** Biological, physical, and electrical parameters for in-vitro studies with ELF magnetic and electric-fields - A primer. *Bioelectromagnetics*, 1-73, (1993).
- 92 **Evans, J. H. & Falke, J. J.** Ca<sup>2+</sup> influx is an essential component of the positive-feed back loop that maintains leading-edge structure and activity in macrophages. *Proc. Natl. Acad. Sci. U. S. A.* 104, 16176-16181, (2007).
- 93 **Yang, S. Y., Zhang, J. J. L. & Huang, X. Y.** Orai1 and STIM1 Are Critical for Breast Tumor Cell Migration and Metastasis. *Cancer Cell* 15, 124-134, (2009).
- 94 **Weiger, M. C. & Parent, C. A.** Phosphoinositides in chemotaxis. *Sub-cellular biochemistry* 59, 217-254, (2012).
- 95 **Corbalan-Garcia, S., Garcia-Garcia, J., Rodriguez-Alfaro, J. A. & Gomez-Fernandez, J. C.** A new phosphatidylinositol 4,5-bisphosphate-binding site located in the C2 domain of protein kinase C alpha. *J. Biol. Chem.* 278, 4972-4980, (2003).
- 96 **Kunisaki, Y. et al.** DOCK2 is a Rac activator that regulates motility and polarity during neutrophil chemotaxis. *J. Cell Biol.* 174, 647-652, (2006).
- 97 **Macia, E., Partisani, M., Favard, C., Mortier, E., Zimmermann, P., Carlier, M. F., Gounon, P., Luton, F. & Franco, M.** The pleckstrin homology domain of the Arf6-specific exchange factor EFA6 localizes to the plasma membrane by interacting with phosphatidylinositol 4,5-bisphosphate and F-actin. *J. Biol. Chem.* 283, 19836-19844, (2008).
- 98 **Kamimura, Y., Xiong, Y., Iglesias, P. A., Hoeller, O., Bolourani, P. & Devreotes, P. N.** PIP(3)-independent activation of TorC2 and PKB at the cell's leading edge mediates chemotaxis. *Curr. Biol.* 18, 1034-1043, (2008).
- 99 **Le Clainche, C. & Carlier, M. F.** Regulation of actin assembly associated with protrusion and adhesion in cell migration. *Physiol. Rev.* 88, 489-513, (2008).
- 100 **Kwan, W. et al.** Mutant huntingtin impairs immune cell migration in Huntington disease. *J. Clin. Invest.* 122, 4737-4747, (2012).
- 101 **Westerberg, L., Larsson, M., Hardy, S. J., Fernandez, C., Thrasher, A. J. & Severinson, E.** Wiskott-Aldrich syndrome protein deficiency leads to reduced B-cell adhesion, migration, and homing, and a delayed humoral immune response. *Blood* 105, 1144-1152, (2005).
- 102 **Bermudez, D. M., Xu, J. W., Herdrich, B. J., Radu, A., Mitchell, M. E. & Liechty, K. W.** Inhibition of stromal cell-derived factor-1 alpha further impairs diabetic wound healing. *Journal of Vascular Surgery* 53, 774-784, (2011).
- 103 **De la Rosa, G., Yang, D., Tewary, P., Varadhachary, A. & Oppenheim, J. J.** Lactoferrin acts as an alarmin to promote the recruitment and activation of APCs and antigen-specific immune responses. *J. Immunol.* 180, 6868-6876, (2008).
- 104 **Chertov, O., Michiel, D. F., Xu, L. L., Wang, J. M., Tani, K., Murphy, W. J., Longo, D. L., Taub, D. D. & Oppenheim, J. J.** Identification of defensin-1, defensin-2, and CAP37/azurocidin as T-cell chemoattractant proteins released from interleukin-8-stimulated neutrophils. *J. Biol. Chem.* 271, 2935-2940, (1996).
- 105 **De Carlo, F. et al.** Nonionizing Radiation as a Noninvasive Strategy in Regenerative Medicine: The Effect of Ca<sup>2+</sup>-ICR on Mouse Skeletal Muscle Cell Growth and Differentiation. *Tissue Eng. Part A* 18, 2248-2258, (2012).
- 106 **Hendee, S. P., Faour, F. A., Christensen, D. A., Patrick, B., Durney, C. H. & Blumenthal, D. K.** The effects of weak extremely low frequency magnetic fields on calcium/calmodulin interactions. *Biophys. J.* 70, 2915-2923, (1996).
- 107 **Koch, C., Sommarin, M., Persson, B. R. R., Salford, L. G. & Eberhardt, J. L.** Interaction between weak low frequency magnetic fields and cell membranes. *Bioelectromagnetics* 24, 395-402, (2003).
- 108 **Simko, M., Droste, S., Kriehuber, R. & Weiss, D. G.** Stimulation of phagocytosis and free radical production in murine macrophages by 50 Hz electromagnetic fields. *Eur. J. Cell Biol.* 80, 562-566, (2001).
- 109 **Walleczek, J.** Electromagnetic-field effects on cells of the immune system - The role of calcium

- signaling. *Faseb J.* 6, 3177-3185, (1992).
- 110 **Maul-Pavicic, A. et al.** ORA11-mediated calcium influx is required for human cytotoxic lymphocyte  
degranulation and target cell lysis. *Proc. Natl. Acad. Sci. U. S. A.* 108, 3324-3329, (2011).
- 111 **Hauser, C. J., Fekete, Z., Livingston, D. H., Adams, J., Garced, M. & Deitch, E. A.** Major trauma  
enhances store-operated calcium influx in human neutrophils. *J. Trauma-Injury Infect. Crit. Care* 48,  
592-597, (2000).
- 112 **Liu, D., Zhang, J. C., Wu, J. M., Zhang, C. G. & Xu, T.** Altered calcium-induced exocytosis in  
neutrophils from allergic patients. *Int. Arch. Allergy Immunol.* 134, 281-287, (2004).
- 113 **Cuppen, J. J. M., Wiegertjes, G. F., Lobee, H. W. J., Savelkoul, H. F. J., Elmusharaf, M. A.,  
Beynen, A. C., Grooten, H. N. A. & Smink, W.** Immune stimulation in fish and chicken through weak  
low frequency electromagnetic fields. *The Environmentalist* 27, 577-583, (2007).
- 114 **Bouwens, M., de Kleijn, S., Ferwerda, G., Cuppen, J. J., Savelkoul, H. F. J. & Verburg-van  
Kemenade, B. M. L.** Low-frequency electromagnetic fields do not alter responses of inflammatory  
genes and proteins in human monocytes and immune cell lines. *Bioelectromagnetics* 33, 226-237,  
(2012).
- 115 **de Kleijn, S., Bouwens, M., Verburg-van Kemenade, B. M. L., Cuppen, J. J. M., Ferwerda, G. &  
Hermans, P. W. M.** Extremely low frequency electromagnetic field exposure does not modulate toll-  
like receptor signaling in human peripheral blood mononuclear cells. *Cytokine* 54, 43-50, (2011).
- 116 **Collins, S. J., Ruscelli, F. W., Gallagher, R. E. & Gallo, R. C.** Terminal differentiation of human  
promyelocytic leukemia-cells induced by dimethyl-sulfoxide and other polar compounds. *Proc. Natl.  
Acad. Sci. U. S. A.* 75, 2458-2462, (1978).
- 117 **Tucker, K. A., Lilly, M. B., Heck, L. & Rado, T. A.** Sharacterization of a new human-diploid  
myeloid-leukemia cell-line (PLB-985) with granulocytic and monocytic differentiating capacity. *Blood*  
70, 372-378, (1987).
- 118 **Ahlbom, A. et al.** A pooled analysis of magnetic fields and childhood leukaemia. *Br J Cancer* 83, 692-  
698, (2000).
- 119 **McBride, M. L. et al.** Power-frequency electric and magnetic fields and risk of childhood leukemia in  
Canada. *Am. J. Epidemiol.* 149, 831-842, (1999).
- 120 **Wolf, F. I., Torsello, A., Tedesco, B., Fasanella, S., Boninsegna, A., D'Ascenzo, M., Grassi, C.,  
Azzena, G. B. & Cittadini, A.** 50-Hz extremely low frequency electromagnetic fields enhance cell  
proliferation and DNA damage: Possible involvement of a redox mechanism. *Biochim. Biophys. Acta-  
Mol. Cell Res.* 1743, 120-129, (2005).
- 121 **Conti, P., Gigante, G. E., Alesse, E., Cifone, M. G., Fieschi, C., Reale, M. & Angeletti, P. U.** A role  
for Ca<sup>2+</sup> in the effect of very low-frequency electromagnetic-field on the blastogenesis of human-  
lymphocytes. *Febs Letters* 181, 28-32, (1985).
- 122 **Conti, P., Gigante, G. E. & Cifone, M. G.** Effect of electromagnetic fields on two calcium dependent  
biological systems. *Journal of Bioelectricity* 4, 227-236, (1985).
- 123 **Blank, M., Monti, M. G., Pernecco, L., Moruzzi, M. S., Battini, R., Zaniol, P. & Barbiroli, B.**  
*Extremely-low-frequency electromagnetic-fields stimulate activation of protein-kinase-C in HL-60  
leukemia-cells by increasing membrane-transport of ca<sup>2+</sup>.* (San Fransico Press, 1993).
- 124 **Wey, H. E., Conover, D. P., Mathias, P., Toraason, M. & Lotz, W. G.** 50-Hertz magnetic field and  
calcium transients in Jurkat cells: results of a research and public information dissemination (RAPID)  
program study. *Environ. Health Perspect.* 108, 135-140, (2000).
- 125 **Garciasancho, J., Montero, M., Alvarez, J., Fonteriz, R. I. & Sanchez, A.** Effects of extremely-low-  
frequency electromagnetic-fields on ion-transport in several mammalian-cells. *Bioelectromagnetics* 15,  
579-588, (1994).
- 126 **Lyle, D. B., Fuchs, T. A., Casamento, J. P., Davis, C. C. & Swicord, M. L.** Intracellular calcium  
signaling by Jurkat T-lymphocytes exposed to a 60 Hz magnetic field. *Bioelectromagnetics* 18, 439-  
445, (1997).
- 127 **Nishimura, I., Yamazaki, K., Shigemitsu, T., Negishi, T. & Sasano, T.** Linearly and circularly  
polarized, 50 Hz magnetic fields did not alter intracellular calcium in rat immune cells. *Industrial  
Health* 37, 289-299, (1999).
- 128 **Belton, M., Prato, F. S., Rozanski, C. & Carson, J. J. L.** Effect of 100 mT Homogeneous  
Static Magnetic Field on Ca<sup>2+</sup> (c) Response to ATP in HL-60 Cells Following GSH Depletion.  
*Bioelectromagnetics* 30, 322-329, (2009).
- 129 **Walleczek, J. & Liburdy, R. P.** Nonthermal 60 Hz sinusoidal magnetic-field exposure enhances  
Ca-45(2+) uptake in rat thymocytes - dependence on mitogen activation. *Febs Letters* 271, 157-160,  
(1990).



- 130 **Galvanovskis, J., Sandblom, J., Bergqvist, B., Galt, S. & Hamnerius, Y.** Cytoplasmic Ca<sup>2+</sup> oscillations in human leukemia T-cells are reduced by 50 Hz magnetic fields. *Bioelectromagnetics* 20, 269-276, (1999).
- 131 **Karabakhtsian, R., Broude, N., Shalts, N., Kochlatyi, S., Goodman, R. & Henderson, A. S.** Calcium is necessary in the cell response to EM Fields. *FEBS Lett.* 349, 1-6, (1994).
- 132 **Staljanssens, D., De Vos, W. H., Willems, P., Van Camp, J. & Smaghe, G.** Time-resolved quantitative analysis of CCK1 receptor-induced intracellular calcium increase. *Peptides* 34, 219-225, (2012).
- 133 **Gee, K. R., Brown, K. A., Chen, W. N. U., Bishop-Stewart, J., Gray, D. & Johnson, I.** Chemical and physiological characterization of fluo-4 Ca<sup>2+</sup>-indicator dyes. *Cell Calcium* 27, 97-106, (2000).
- 134 **Harper, J. L. & Daly, J. W.** Store-operated calcium channels in HL-60 cells - Effects of temperature, differentiation and loperamide. *Life Sci.* 67, 651-662, (2000).
- 135 **Shahidain, R., Mullins, R. D. & Sisken, J. E.** Calcium spiking activity and baseline calcium levels in ROS 17/2.8 cells exposed to extremely low frequency electromagnetic fields (ELF EMF). *Int J Radiat Biol.* 241-248, (2001).
- 136 **Fixler, D., Yitzhaki, S., Axelrod, A., Zinman, T. & Shainberg, A.** Correlation of magnetic AC field on cardiac myocyte Ca<sup>2+</sup> transients at different magnetic DC levels. *Bioelectromagnetics* 33, 634-640, (2012).
- 137 **McCreary, C. R., Dixon, S. J., Fraher, L. J., Carson, J. J. L. & Prato, F. S.** Real-time measurement of cytosolic free calcium concentration in Jurkat cells during ELF magnetic field exposure and evaluation of the role of cell cycle. *Bioelectromagnetics* 27, 354-364, (2006).
- 138 **Hwang, Y. H. et al.** Intracellular Ca<sup>2+</sup> Mobilization and Beta-hexosaminidase Release Are Not Influenced by 60 Hz-electromagnetic Fields (EMF) in RBL 2H3 Cells. *Korean J. Physiol. Pharmacol.* 15, 313-317, (2011).
- 139 **Hassan, N., Chatterjee, I., Publicover, N. G. & Craviso, G. L.** Numerical study of induced current perturbations in the vicinity of excitable cells exposed to extremely low frequency magnetic fields. *Physics in Medicine and Biology* 48, 3277-3293, (2003).
- 140 **Tuinstra, R., Goodman, E. & Greenebaum, B.** Protein kinase C activity following exposure to magnetic field and phorbol ester. *Bioelectromagnetics* 19, 469-476, (1998).
- 141 **Werlen, G., Belin, D., Conne, B., Roche, E., Lew, D. P. & Prentki, M.** Intracellular Ca<sup>2+</sup> and the regulation of early response gene-expression in HL-60 myeloid-leukemia cells. *J. Biol. Chem.* 268, 16596-16601, (1993).
- 142 **Hardingham, G. E., Chawla, S., Johnson, C. M. & Bading, H.** Distinct functions of nuclear and cytoplasmic calcium in the control of gene expression. *Nature* 385, 260-265, (1997).
- 143 **Zhou, J. L., Yao, G. D., Zhang, J. S. & Chang, Z. L.** CREB DNA binding activation by a 50-Hz magnetic field in HL60 cells is dependent on extra- and intracellular Ca<sup>2+</sup> but not PKA, PKC, ERK, or p38 MAPK. *Biochemical and Biophysical Research Communications* 296, 1013-1018, (2002).
- 144 **Lahijani, M. S., Farivar, S. & Khodaeian, M.** Effects of 50 Hz electromagnetic fields on the histology, apoptosis, and expression of c-Fos and beta-Catenin on the livers of preincubated white leghorn chicken embryos. *Electromagnetic Biology and Medicine* 30, 158-169, (2011).
- 145 **Rao, S. & Henderson, A. S.** Regulation of c-fos is affected by electromagnetic fields. *J. Cell. Biochem.* 63, 358-365, (1996).
- 146 **Liburdy, R. P., Callahan, D. E., Harland, J., Dunham, E., Sloma, T. R. & Yaswen, P.** Experimental-evidence for 60-Hz magnetic-fields operating through the signal-transduction cascade - effects on calcium influx and c-myc messenger-rna induction. *Febs Letters* 334, 301-308, (1993).
- 147 **Fambrough, D., McClure, K., Kazlauskas, A. & Lander, E. S.** Diverse signaling pathways activated by growth factor receptors induce broadly overlapping, rather than independent, sets of genes. *Cell* 97, 727-741, (1999).
- 148 **Chang, H. H., Oh, P. Y., Ingber, D. E. & Huang, S.** Multistable and multistep dynamics in neutrophil differentiation. *BMC Cell Biol.* 7, 1-11, (2006).
- 149 **Lioudyno, M. I., Kozak, J. A., Penna, A., Safrina, O., Zhang, S. L., Sen, D., Roos, J., Stauderman, K. A. & Cahalan, M. D.** Orai1 and STIM1 move to the immunological synapse and are up-regulated during T cell activation. *Proc. Natl. Acad. Sci. U. S. A.* 105, 2011-2016, (2008).
- 150 **Brandman, O., Liou, J., Park, W. S. & Meyer, T.** STIM2 is a feedback regulator that stabilizes basal cytosolic and endoplasmic reticulum Ca<sup>2+</sup> levels. *Cell* 131, 1327-1339, (2007).
- 151 **Chaudhari, S., Wang, Y. X., Ding, M., Ding, Y. F., Yuan, J. & Ma, R.** Prolonged high glucose treatment increased STIM1/Orai1 protein expression and enhanced store-operated Ca<sup>2+</sup> entry in human glomerular mesangial cells. *Faseb J.* 27, (2013).

- 152 **Miller, S. C., Haberer, J., Venkatachalam, U. & Furniss, M. J.** NF-kappa B or AP-1-dependent  
reporter gene expression is not altered in human U937 cells exposed to power-line frequency magnetic  
fields. *Radiation Research* 151, 310-318, (1999).
- 153 **Morehouse, C. A. & Owen, R. D.** Exposure to low-frequency electromagnetic fields does not alter  
HSP70 expression or HSF-HSE binding in HL60 cells. *Radiation Research* 153, 658-662, (2000).
- 154 **Jorquera, G., Juretic, N., Jaimovich, E. & Riveros, N.** Membrane depolarization induces calcium-  
dependent upregulation of Hsp70 and Hmxo-1 in skeletal muscle cells. *Am. J. Physiol.-Cell Physiol.*  
297, C581-C590, (2009).
- 155 **Lupke, M., Frahm, J., Lantow, M., Maercker, C., Reniondini, D., Bersani, F. & Simko, M.**  
Gene expression analysis of ELF-MF exposed human monocytes indicating the involvement of the  
alternative activation pathway. *Biochim. Biophys. Acta-Mol. Cell Res.* 1763, 402-412, (2006).
- 156 **Huwiler, S. G., Beyer, C., Fröhlich, J., Hennecke, H., Egli, T., Schurmann, D., Rehrauer, H. &  
Fischer, H. M.** Genome-wide transcription analysis of *Escherichia coli* in response to extremely low-  
frequency magnetic fields. *Bioelectromagnetics* 33, 488-496, (2012).
- 157 **Luceri, C. et al.** Extremely low-frequency electromagnetic fields do not affect DNA damage and gene  
expression profiles of yeast and human lymphocytes. *Radiation Research* 164, 277-285, (2005).
- 158 **McNamee, J. P. & Chauhan, V.** Radiofrequency Radiation and Gene/Protein Expression: A Review.  
*Radiation Research* 172, 265-287, (2009).
- 159 **Vanderstraeten, J. & Verschaeve, L.** Gene and protein expression following exposure to  
radiofrequency fields from mobile phones. *Environmental health perspectives* 116, 1131-1135, (2008).
- 160 **Kozera, B. & Rapacz, M.** Reference genes in real-time PCR. *Journal of Applied Genetics* 54, 391-  
406, (2013).
- 161 **de Jonge, H. J. et al.** Evidence based selection of housekeeping genes. *PLoS One* 2, e898, (2007).
- 162 **Poniedzialek, B., Rzymiski, P., Nawrocka-Bogusz, H., Jaroszyk, F. & Wiktorowicz, K.** The effect of  
electromagnetic field on reactive oxygen species production in human neutrophils in vitro. *Electromagn  
Biol Med.* 333-341, (2013).
- 163 **Frahm, J., Mattsson, M. O. & Simko, M.** Exposure to ELF magnetic fields modulate redox related  
protein expression in mouse macrophages. *Toxicol. Lett.* 192, 330-336, (2010).
- 164 **Santoro, N., Lisi, A., Pozzi, D., Pasquali, E., Serafino, A. & Grimaldi, S.** Effect of extremely low  
frequency (ELF) magnetic field exposure on morphological and biophysical properties of human  
lymphoid cell line (Raji). *Biochim. Biophys. Acta-Mol. Cell Res.* 1357, 281-290, (1997).
- 165 **Tenuzzo, B., Chionna, A., Panzarini, E., Lanubile, R., Tarantino, P., Di Jeso, B., Dwikat, M. &  
Dini, L.** Biological effects of 6 mT static magnetic fields: A comparative study in different cell types.  
*Bioelectromagnetics* 27, 560-577, (2006).
- 166 **Reid, G. G., Edwards, J. G., Marshall, G. E., Sutcliffe, R. G. & Lee, W. R.** Microvilli elongate in  
response to hydrogen peroxide and to perturbations of intracellular calcium. *Exp. Cell Res.* 236, 86-93,  
(1997).
- 167 **Schreier, N., Huss, A. & Roosli, M.** The prevalence of symptoms attributed to electromagnetic field  
exposure: a cross-sectional representative survey in Switzerland. *Sozial-und Pravent.* 51, 202-209,  
(2006).
- 168 **Davanipour, Z. & Sobel, E.** Long-term exposure to magnetic fields and the risks of Alzheimer's  
disease and breast cancer: Further biological research. *Pathophysiology : the official journal of the  
International Society for Pathophysiology / ISP* 16, 149-156, (2009).
- 169 **Liebl, M. P., Windschmitt, J., Besemer, A. S., Schaefer, A.-K., Reber, H., Behl, C. & Clement, A.  
M.** Low-frequency magnetic fields do not aggravate disease in mouse models of Alzheimer's disease  
and amyotrophic lateral sclerosis. *Scientific Reports* 5, (2015).
- 170 **Prato, F. S.** Non-thermal extremely low frequency magnetic field effects on opioid related behaviors:  
Snails to humans, mechanisms to therapy. *Bioelectromagnetics*, n/a-n/a, (2015).
- 171 **Barnes, F. S. & Greenebaum, B.** The Effects of Weak Magnetic Fields on Radical Pairs.  
*Bioelectromagnetics* 36, 45-54, (2015).
- 172 **Simko, M. & Mattsson, M. O.** Extremely low frequency electromagnetic fields as effectors of cellular  
responses in vitro: Possible immune cell activation. *J. Cell. Biochem.* 93, 83-92, (2004).
- 173 **Lednev, V. V.** Possible mechanisms for the influence of weak magnetic-fields on biological-systems.  
*Bioelectromagnetics* 12, 71-75, (1991).
- 174 **Missiaen, L. et al.** Abnormal intracellular Ca<sup>2+</sup> homeostasis and disease. *Cell Calcium* 28, 1-21,  
(2000).
- 175 **Khan, A. A., Soloski, M. J., Sharp, A. H., Schilling, G., Sabatini, D. M., Li, S. H., Ross, C. A.  
& Snyder, S. H.** Lymphocyte apoptosis: Mediation by increased type 3 inositol 1,4,5-trisphosphate



- receptor. *Science* 273, 503-507, (1996).
- 176 **Steenbergen, C., Murphy, E., Levy, L. & London, R. E.** Elevation in cytosolic free calcium-concentration early in myocardial-ischemia in perfused rat-heart. *Circulation Research* 60, 700-707, (1987).
- 177 **Jeschke, M. G., Gauglitz, G. G., Song, J. Q., Kulp, G. A., Finnerty, C. C., Cox, R. A., Barral, J. M., Herndon, D. N. & Boehning, D.** Calcium and ER stress mediate hepatic apoptosis after burn injury. *Journal of Cellular and Molecular Medicine* 13, 1857-1865, (2009).
- 178 **Berridge, M. J., Bootman, M. D. & Roderick, H. L.** Calcium signalling: Dynamics, homeostasis and remodelling. *Nat. Rev. Mol. Cell Biol.* 4, 517-529, (2003).
- 179 **Smedler, E. & Uhlen, P.** Frequency decoding of calcium oscillations. *Biochimica Et Biophysica Acta-General Subjects* 1840, 964-969, (2014).
- 180 **Niu, Z. Q., Hou, J. Q., Wang, H. B., Zhang, H., Yan, J., Lu, Z. Y., Guo, G. Z., Wang, C. M. & Lin, H.** The window bioeffects of electromagnetic waves. *Chinese Journal of Biomedical Engineering*, 126-132, (2003).
- 181 **Lau, J., Ioannidis, J. P. A. & Schmid, C. H.** Quantitative synthesis in systematic reviews. *Ann. Intern. Med.* 127, 820-826, (1997).
- 182 **Galvanovskis, J., Sandblom, J., Bergqvist, B., Galt, S. & Hamnerius, Y.** The influence of 50-Hz magnetic fields on cytoplasmic Ca<sup>2+</sup> oscillations in human leukemia T-cells. *Science of the Total Environment* 180, 19-33, (1996).
- 183 **Lisi, A. et al.** Extremely low frequency electromagnetic field exposure promotes differentiation of pituitary corticotrope-derived AtT20 D16V cells. *Bioelectromagnetics* 27, 641-651, (2006).
- 184 **Pilger, A., Ivancsits, S., Diem, E., Steffens, M., Kolb, H. A. & Rudiger, H. W.** No effects of intermittent 50 Hz EMF on cytoplasmic free calcium and on the mitochondrial membrane potential in human diploid fibroblasts. *Radiation and Environmental Biophysics* 43, 203-207, (2004).
- 185 **Sakurai, T., Koyama, S., Komatsubara, Y., Jin, W. & Miyakoshi, J.** Decrease in glucose-stimulated insulin secretion following exposure to magnetic fields. *Biochemical and Biophysical Research Communications* 332, 28-32, (2005).
- 186 **Liu, D.-D., Ren, Z., Yang, G., Zhao, Q.-R. & Mei, Y.-A.** Melatonin protects rat cerebellar granule cells against electromagnetic field-induced increases in Na<sup>+</sup> currents through intracellular Ca<sup>2+</sup> release. *Journal of Cellular and Molecular Medicine* 18, 1060-1070, (2014).
- 187 **Tonini, R., Baroni, M. D., Masala, E., Micheletti, M., Ferroni, A. & Mazzanti, M.** Calcium protects differentiating neuroblastoma cells during 50 Hz electromagnetic radiation. *Biophysical Journal* 81, 2580-2589, (2001).
- 188 **Lee, S. H., Lee, H. S., Lee, M. K., Lee, J. H., Kim, J. D., Park, Y. S., Lee, S. Y. & Lee, H. Y.** Enhancement of tissue type plasminogen activator (tPA) production from recombinant CHO cells by low electromagnetic fields. *Journal of Microbiology and Biotechnology* 12, 457-462, (2002).
- 189 **Hwang, Y. H. et al.** Intracellular Ca Mobilization and Beta-hexosaminidase Release Are Not Influenced by 60 Hz-electromagnetic Fields (EMF) in RBL 2H3 Cells. *Korean J Physiol Pharmacol* 15, 313-317, (2011).
- 190 **Grande, D. A., Magee, F. P., Weinstein, A. M. & McLeod, B. R.** The effect of low-energy combined ac and dc magnetic-fields on articular-cartilage metabolism. *Annals of the New York Academy of Sciences* 635, 404-407, (1991).
- 191 **Oh, S. J., Lee, M. K., Lee, S. H., Lee, J. H., Kim, D. J., Park, Y. S. & Lee, H. Y.** Effect of electromagnetic fields on growth of human cell lines. *Journal of Microbiology and Biotechnology* 11, 749-755, (2001).
- 192 **Conti, P., Gigante, G. E. & Cifone, M. G.** Effect of electromagnetic fields on two calcium dependent biological systems. 4, 227-236, (1985).
- 193 **Luo, F.-L., Yang, N., He, C., Li, H.-L., Li, C., Chen, F., Xiong, J.-X., Hu, Z.-A. & Zhang, J.** Exposure to extremely low frequency electromagnetic fields alters the calcium dynamics of cultured entorhinal cortex neurons. *Environmental research* 135, 236-246, (2014).
- 194 **Higgins, J. P. T. & Thompson, S. G.** Quantifying heterogeneity in a meta-analysis. *Statistics in Medicine* 21, 1539-1558, (2002).
- 195 **Baker, R. & Jackson, D.** A new approach to outliers in meta-analysis. *Health Care Management Science* 11, 121-131, (2008).
- 196 **Lindstrom, E., Mild, K. H. & Lundgren, E.** Analysis of the T cell activation signaling pathway during ELF magnetic field exposure, p56(lck) and Ca<sup>2+</sup> (i)-measurements. *Bioelectrochemistry and Bioenergetics* 46, 129-137, (1998).
- 197 **Craviso, G. L., Chatterjee, I. & Publicover, N. G.** Catecholamine release from cultured bovine



- adrenal medullary chromaffin cells in the presence of 60-Hz magnetic fields. *Bioelectrochemistry* 59, 57-64, (2003).
- 198 **Fitzsimmons, R. J., Ryaby, J. T., Magee, F. P. & Baylink, D. J.** Combined magnetic-fields increased net calcium flux in bone-cells. *Calcif. Tissue Int.* 55, 376-380, (1994).
- 199 **Gaetani, R. et al.** Differentiation of human adult cardiac stem cells exposed to extremely low-frequency electromagnetic fields. *Cardiovascular Research* 82, 411-420, (2009).
- 200 **Bernabo, N., Tettamanti, E., Pistilli, M. G., Nardinocchi, D., Berardinelli, P., Mattioli, M. & Barboni, B.** Effects of 50 Hz extremely low frequency magnetic field on the morphology and function of boar spermatozoa capacitated in vitro. *Theriogenology* 67, 801-815, (2007).
- 201 **Morabito, C., Guarnieri, S., Fano, G. & Mariggio, M. A.** Effects of Acute and Chronic Low Frequency Electromagnetic Field Exposure on PC12 Cells during Neuronal Differentiation. *Cellular Physiology and Biochemistry* 26, 947-958, (2010).
- 202 **Kim, H. J., Jung, J., Park, J. H., Kim, J. H., Ko, K. N. & Kim, C. W.** Extremely low-frequency electromagnetic fields induce neural differentiation in bone marrow derived mesenchymal stem cells. *Experimental Biology and Medicine* 238, 923-931, (2013).
- 203 **Piacentini, R., Ripoli, C., Mezzogori, D., Azzena, G. B. & Grassi, C.** Extremely low-frequency electromagnetic fields promote in vitro neurogenesis via upregulation of Ca(v)1-channel activity. *Journal of Cellular Physiology* 215, 129-139, (2008).
- 204 **Loschinger, M., Thumm, S., Hammerle, H. & Rodemann, H. P.** Induction of intracellular calcium oscillations in human skin fibroblast populations by sinusoidal extremely low-frequency magnetic fields (20 Hz, 8 mT) is dependent on the differentiation state of the single cell. *Radiation Research* 151, 195-200, (1999).
- 205 **Yamaguchi, D. T., Huang, J., Ma, D. F. & Wang, P. K. C.** Inhibition of gap junction intercellular communication by extremely low-frequency electromagnetic fields in osteoblast-like models is dependent on cell differentiation. *Journal of Cellular Physiology* 190, 180-188, (2002).
- 206 **Craviso, G. L., Poss, J., Lanctot, C., Lundback, S. S., Chatterjee, I. & Publicover, N. G.** Intracellular calcium activity in isolated bovine adrenal chromaffin cells in the presence and absence of 60 Hz magnetic fields. *Bioelectromagnetics* 23, 557-567, (2002).
- 207 **Coulton, L. A. & Barker, A. T.** Magnetic-fields and intracellular calcium - Effects on lymphocytes exposed to conditions for cyclotron-resonance. *Physics in Medicine and Biology* 38, 347-360, (1993).
- 208 **Morabito, C., Rovetta, F., Bizzarri, M., Mazzoleni, G., Fano, G. & Mariggio, M. A.** Modulation of redox status and calcium handling by extremely low frequency electromagnetic fields in C2C12 muscle cells: A real-time, single-cell approach. *Free Radical Biology and Medicine* 48, 579-589, (2010).
- 209 **McCreary, C. R., Thomas, A. W. & Prato, F. S.** Factors confounding cytosolic calcium measurements in Jurkat E6.1 cells during exposure to ELF magnetic fields. *Bioelectromagnetics* 23, 315-328, (2002).
- 210 **Wei, J., Sun, J., Xu, H., Shi, L., Sun, L. & Zhang, J.** Effects of extremely low frequency electromagnetic fields on intracellular calcium transients in cardiomyocytes. *Electromagn Biol Med*, (2014).
- 211 **Wu, X. et al.** Weak Power Frequency Magnetic Field Acting Similarly to EGF Stimulation, Induces Acute Activations of the EGFR Sensitive Actin Cytoskeleton Motility in Human Amniotic Cells. *PLoS One* 9, (2014).
- 212 **Lyle, D. B., Wang, X. H., Ayotte, R. D., Sheppard, A. R. & Adey, W. R.** Calcium uptake by leukemic and normal T-lymphocytes exposed to low frequency magnetic fields. *Bioelectromagnetics* 12, 145-156, (1991).
- 213 **Thomas, D., Tovey, S. C., Collins, T. J., Bootman, M. D., Berridge, M. J. & Lipp, P.** A comparison of fluorescent Ca<sup>2+</sup> indicator properties and their use in measuring elementary and global Ca<sup>2+</sup> signals. *Cell Calcium* 28, 213-223, (2000).
- 214 Liboff, A. R., Rozek, R. J., Sherman, M. L., McLeod, B. R. & Smith, S. D. in *Journal of Bioelectricity* Vol. 6 13-22 (1987).
- 215 **Schuderer, J., Oesch, W., Felber, N., Spat, D. & Kuster, N.** In vitro exposure apparatus for ELF magnetic fields. *Bioelectromagnetics* 25, 582-591, (2004).
- 216 **Duval, S. & Tweedie, R.** Trim and fill: A simple funnel-plot-based method of testing and adjusting for publication bias in meta-analysis. *Biometrics* 56, 455-463, (2000).
- 217 **Wu, F., Wei, G. Z., Li, W. J., Liu, B., Zhou, J. J., Wang, H. C. & Gao, F.** Low extracellular K<sup>+</sup> increases intracellular Ca<sup>2+</sup> oscillation and injury by activating the reverse mode Na<sup>+</sup>-Ca<sup>2+</sup> exchanger and inhibiting the Na<sup>+</sup>, K<sup>+</sup> ATPase in rat cardiomyocytes. *International Journal of Cardiology* 140, 161-168, (2010).
- 218 **Wang, X. S. & Gruenstein, E. I.** Mechanism of synchronized Ca<sup>2+</sup> oscillations in cortical neurons.



- 219 *Brain Research* 767, 239-249, (1997).
- 220 **Song, S., Li, J., Zhu, L., Cai, L., Xu, Q., Ling, C., Su, Y. & Hu, Q.** Irregular Ca<sup>2+</sup> Oscillations Regulate Transcription via Cumulative Spike Duration and Spike Amplitude. *J. Biol. Chem.* 287, 40246-40255, (2012).
- 221 **Portelli, L. A., Schomay, T. E. & Barnes, F. S.** Inhomogeneous background magnetic field in biological incubators is a potential confounder for experimental variability and reproducibility. *Bioelectromagnetics* 34, 337-348, (2013).
- 222 **Butler, J. M., Johnson, J. E. & Boone, W. R.** The heat is on: room temperature affects laboratory equipment-an observational study. *J. Assist. Reprod. Genet.* 30, 1389-1393, (2013).
- 223 **Korzhsleptsova, I. L., Lindstrom, E., Mild, K. H., Berglund, A. & Lundgren, E.** Low-frequency MFs increased inositol 1,4,5-trisphosphate levels in the Jurkat cell-line. *Febs Letters* 359, 151-154, (1995).
- 224 **Pilla, A. A., Muehsam, D. J., Markov, M. S. & Siskin, B. F.** EMF signals and ion/ligand binding kinetics: prediction of bioeffective waveform parameters. *Bioelectrochemistry and Bioenergetics* 48, 27-34, (1999).
- 225 **Goodman, R., Wei, L. X., Bumann, J. & Shirleyhenderson, A.** Exposure to electric and magnetic (EM) fields increases transcripts inHL-60 cells - Does adaptation to EM fields occur. *Bioelectrochemistry and Bioenergetics* 29, 185-192, (1992).
- 226 **Lin, H., Blank, M., Jin, M. & Goodman, R.** Electromagnetic field stimulation of biosynthesis: Changes in c-myc transcript levels during continuous and intermittent exposures. *Bioelectrochemistry and Bioenergetics* 39, 215-220, (1996).
- 227 **Blackman, C. F., Benane, S. G. & House, D. E.** Evidence for direct effect of magnetic-fields on neurite outgrowth. *Faseb J.* 7, 801-806, (1993).
- 228 **Zhang, Y., Ding, J. & Duan, W.** A study of the effects of flux density and frequency of pulsed electromagnetic field on neurite outgrowth in PC12 cells. *Journal of Biological Physics* 32, 1-9, (2006).
- 229 **van Tongeren, M., Mee, T., Whatmough, P., Broad, L., Maslanyj, M., Allen, S., Muir, K. & McKinney, P.** Assessing occupational and domestic ELF magnetic field exposure in the UK Adult Brain Tumour Study: Results of a feasibility study. *Radiat. Prot. Dosim.* 108, 227-236, (2004).
- 230 **Bolte, J. F. B., Baliatsas, C., Eikelboom, T. & van Kamp, I.** Everyday exposure to power frequency magnetic fields and associations with non-specific physical symptoms. *Environ. Pollut.* 196, 224-229, (2015).
- 231 **Meghji, S.** Bone remodeling. *British Dental Journal* 172, 235-242, (1992).
- 232 **Chatterjee, I., Hassan, N., Craviso, G. L. & Publicover, N. G.** Numerical computation of distortions in magnetic fields and induced currents in physiological solutions produced by microscope objectives. *Bioelectromagnetics* 22, 463-469, (2001).
- 233 **Siegrist, M. & Cvetkovich, G.** Better negative than positive? Evidence of a bias for negative information about possible health dangers. *Risk Anal.* 21, 199-206, (2001).
- 234 **Adams, J. A., Galloway, T. S., Mondal, D., Esteves, S. C. & Mathews, F.** Effect of mobile telephones on sperm quality: A systematic review and meta-analysis. *Environ. Int.* 70, 106-112, (2014).
- 235 **Blackman, C. F., Benane, S. G. & House, D. E.** The influence of temperature during electric- and magnetic-field-induced alteration of calcium-ion release from in vitro brain tissue. *Bioelectromagnetics* 12, 173-182, (1991).
- 236 **Publicover, N. G., Marsh, C. G., Vincze, C. A., Craviso, G. L. & Chatterjee, I.** Effects of microscope objectives on magnetic field exposures. *Bioelectromagnetics* 20, 387-395, (1999).
- 237 **Frix, W. M., Karady, G. G. & Venetz, B. A.** Comparison of calibration systems for magnetic field measurement equipment. *IEEE Trans. Power Deliv.* 9, 100-106, (1994).
- 238 **Montgomery, D. B. & Terrell, J.** *Some useful information for design of aircore solenoids.* (Air Force Office of Scientific Research, United States Air Force, 1961).
- 239 **Freshney, R.** *The Culture of Animal Cells: A Manual of Basic Technique and Specialized Applications.* (Wiley-Blackwell, 2010).
- 240 **Newington, C. T.** *The ARRL Handbook for Radio Communications 2003.* Vol. 80 (American Radio Relay League, 2002).
- 241 **Olivares-Galvan, J. C., Campero-Littlewood, E., Escarela-Perez, R., Magdaleno-Adame, S. & Blanco-Briset, E.** Coil Systems to Generate Uniform Magnetic Field Volumes. *Excerpt from the Proceedings of the COMSOL* 13, 7, (2010).
- 242 **Platano, D., Mesirca, P., Paffi, A., Pellegrino, M., Liberti, M., Apollonio, F., Bersani, F. & Aicardi, G.** Acute exposure to low-level CW and GSM-modulated 900 MHz radiofrequency does not affect Ba<sup>2+</sup> currents through voltage-gated calcium channels in rat cortical neurons. *Bioelectromagnetics* 28,

- 599-607, (2007).
- 242 **Funk, R. H. W. & Monsees, T. K.** Effects of electromagnetic fields on cells: Physiological and  
therapeutical approaches and molecular mechanisms of interaction. *Cells Tissues Organs* 182, 59-78,  
(2006).
- 243 **Bartles, J. R.** Parallel actin bundles and their multiple actin-bundling proteins. *Curr. Opin. Cell Biol.*  
12, 72-78, (2000).
- 244 **Galbraith, C. G., Yamada, K. M. & Galbraith, J. A.** Polymerizing actin fibers position integrins  
primed to probe for adhesion sites. *Science* 315, 992-995, (2007).
- 245 **Gallo, G. & Letourneau, P. C.** Regulation of growth cone actin filaments by guidance cues. *J.*  
*Neurobiol.* 58, 92-102, (2004).
- 246 **Geraldo, S. & Gordon-Weeks, P. R.** Cytoskeletal dynamics in growth-cone steering. *J. Cell Sci.* 122,  
3595-3604, (2009).
- 247 **Lewis, M. A. & Murray, J. D.** Analysis of dynamic and stationary pattern formation in the cell cortex.  
*J. Math. Biol.* 31, 25-71, (1992).
- 248 **Riedl, J. et al.** Lifeact: a versatile marker to visualize F-actin. *Nat. Methods* 5, 605-607, (2008).
- 249 **Zack, G. W., Rogers, W. E. & Latt, S. A.** Automatic measurement of sister chromatid exchange  
frequency. *J. Histochem. Cytochem.* 25, 741-753, (1977).
- 250 **van der Honing, H. S., van Bezouwen, L. S., Emons, A. M. C. & Ketelaar, T.** High Expression  
of Lifeact in Arabidopsis thaliana Reduces Dynamic Reorganization of Actin Filaments but does not  
Affect Plant Development. *Cytoskeleton* 68, 578-587, (2011).
- 251 **Berepiki, A., Lichius, A., Shoji, J. Y., Tilsner, J. & Read, N. D.** F-Actin Dynamics in Neurospora  
crassa. *Eukaryot. Cell* 9, 547-557, (2010).
- 252 **Era, A. et al.** Application of Lifeact Reveals F-Actin Dynamics in Arabidopsis thaliana and the  
Liverwort, Marchantia polymorpha. *Plant and Cell Physiology* 50, 1041-1048, (2009).
- 253 **Spracklen, A. J., Fagan, T. N., Lovander, K. E. & Tootle, T. L.** The pros and cons of common actin  
labeling tools for visualizing actin dynamics during Drosophila oogenesis. *Dev. Biol.* 393, 209-226,  
(2014).
- 254 **Salmon, P., Kindler, V., Ducrey, O., Chapuis, B., Zubler, R. H. & Trono, D.** High-level transgene  
expression in human hematopoietic progenitors and differentiated blood lineages after transduction  
with improved lentiviral vectors. *Blood* 96, 3392-3398, (2000).
- 255 **Recchia, A. et al.** Retroviral vector integration deregulates gene expression but has no consequence on  
the biology and function of transplanted T cells. *Proc. Natl. Acad. Sci. U. S. A.* 103, 1457-1462, (2006).
- 256 **Cesana, D., Sgualdino, J., Rudilosso, L., Merella, S., Naldini, L. & Montini, E.** Whole  
transcriptome characterization of aberrant splicing events induced by lentiviral vector integrations.  
*Journal of Clinical Investigation* 122, 1667-1676, (2012).
- 257 **Silvan, U., Jockusch, B. M. & Schoenenberger, C. A.** in *Organisation of Chromosomes* Vol. 90  
*Advances in Protein Chemistry and Structural Biology* (ed R. Donev) 151-177 (Elsevier Academic  
Press Inc, 2013).
- 258 **Roubinet, C., Tran, P. T. & Piel, M.** Common Mechanisms Regulating Cell Cortex Properties during  
Cell Division and Cell Migration. *Cytoskeleton* 69, 957-972, (2012).
- 259 **Feng, Z. Q., Chen, W. N., Lee, P. V. S., Liao, K. & Chan, V.** The influence of GFP-actin expression  
on the adhesion dynamics of HepG2 cells on a model extracellular matrix. *Biomaterials* 26, 5348-5358,  
(2005).
- 260 **Planchon, T. A., Gao, L., Milkie, D. E., Davidson, M. W., Galbraith, J. A., Galbraith, C. G.  
& Betzig, E.** Rapid three-dimensional isotropic imaging of living cells using Bessel beam plane  
illumination. *Nat. Methods* 8, 417-U468, (2011).
- 261 **Schirenbeck, A., Bretschneider, T., Arasada, R., Schleicher, M. & Faix, J.** The Diaphanous-related  
formin dDia2 is required for the formation and maintenance of filopodia. *Nat. Cell Biol.* 7, 619-U624,  
(2005).
- 262 **Van Bruaene, N., Joss, G. & Van Oostveldt, P.** Reorganization and in vivo dynamics of microtubules  
during arabidopsis root hair development. *Plant Physiol.* 136, 3905-3919, (2004).
- 263 **Brown, D. G. & Riederer, S. J.** Contrast-to-Noise ratios in maximum intensity projection images.  
*Magn. Reson. Med.* 23, 130-137, (1992).
- 264 **Cox, G.** Equipment for mass storage and processing of data. *Methods Enzymol.* 307, 29-55, (1999).
- 265 **Genove, G., Glick, B. S. & Barth, A. L.** Brighter reporter genes from multimerized fluorescent  
proteins. *Biotechniques* 39, 814-+, (2005).
- 266 **Hsu, T. H., Liao, W. Y., Yang, P. C., Wang, C. C., Xiao, J. L. & Lee, C. H.** Dynamics of cancer cell  
filopodia characterized by super-resolution bright-field optical microscopy. *Opt. Express* 15, 76-82,



- (2007).
- 267 **Lange, K. & Gartzke, J.** A critical comparison of the current view of Ca signaling with the novel  
concept of F-actin-based Ca signaling. *Crit. Rev. Eukaryot. Gene Expr.* 16, 307-365, (2006).
- 268 **Gremm, D. & Wegner, A.** Gelsolin as a calcium-regulated actin filament-capping protein. *Eur. J.*  
*Biochem.* 267, 4339-4345, (2000).
- 269 **Kuhlman, P. A., Hughes, C. A., Bennett, V. & Fowler, V. M.** A new function for adducin - Calcium  
calmodulin-regulated capping of the barbed ends of actin filaments. *J. Biol. Chem.* 271, 7986-7991,  
(1996).
- 270 **Young, C. L., Feierstein, A. & Southwick, F. S.** Calcium Regulation of Actin Filament Capping and  
Monomer Binding by Macrophage Capping Protein. *J. Biol. Chem.* 269, 13997-14002, (1994).
- 271 **Weston, J. A.** The migration and differentiation of neural crest cells. *Advances in morphogenesis* 8,  
41-114, (1970).
- 272 **Goldfinger, L. E., Hopkinson, S. B., deHart, G. W., Collawn, S., Couchman, J. R. & Jones, J. C.**  
**R.** The alpha 3 laminin subunit, alpha 6 beta 4 and alpha 3 beta 1 integrin coordinately regulate wound  
healing in cultured epithelial cells and in the skin. *J. Cell Sci.* 112, 2615-2629, (1999).
- 273 **Nguyen, B. P., Ren, X. D., Schwartz, M. A. & Carter, W. G.** Ligation of integrin alpha(3)beta(1) by  
laminin 5 at the wound edge activates Rho-dependent adhesion of leading keratinocytes on collagen. *J.*  
*Biol. Chem.* 276, 43860-43870, (2001).
- 274 **Barrientos, S., Stojadinovic, O., Golinko, M. S., Brem, H. & Tomic-Canic, M.** Growth factors and  
cytokines in wound healing. *Wound Repair Regen.* 16, 585-601, (2008).
- 275 **Nuccitelli, R.** A role for endogenous electric fields in wound healing. *Current Topics in Developmental*  
*Biology, Vol 58* 58, 1-+, (2003).
- 276 **Messerli, M. A. & Graham, D. M.** Extracellular Electrical Fields Direct Wound Healing and  
Regeneration. *Biol. Bull.* 221, 79-92, (2011).
- 277 **Zhao, M., McCaig, C. D., AgiusFernandez, A., Forrester, J. V. & ArakiSasaki, K.** Human corneal  
epithelial cells reorient and migrate cathodally in a small applied electric field. *Curr. Eye Res.* 16, 973-  
984, (1997).
- 278 **Sun, S., Wise, J. & Cho, M.** Human fibroblast migration in three-dimensional collagen gel in response  
to noninvasive electrical stimulus - I. Characterization of induced three-dimensional cell movement.  
*Tissue Eng.* 10, 1548-1557, (2004).
- 279 **Fang, K. S., Ionides, E., Oster, G., Nuccitelli, R. & Isseroff, R. R.** Epidermal growth factor receptor  
relocalization and kinase activity are necessary for directional migration of keratinocytes in DC electric  
fields. *J. Cell Sci.* 112, 1967-1978, (1999).
- 280 **Bouwens, M., de Kleijn, S., Ferwerda, G., Cuppen, J. J., Savelkoul, H. F. J. & Verburg-van**  
**Kemenade, B. M. L.** Low-frequency electromagnetic fields do not alter responses of inflammatory  
genes and proteins in human monocytes and immune cell lines. *Bioelectromagnetics* 33, 226-237,  
(2012).
- 281 **de Kleijn, S., Bouwens, M., Verburg-van Kemenade, B. M. L., Cuppen, J. J. M., Ferwerda, G. &**  
**Hermans, P. W. M.** Extremely low frequency electromagnetic field exposure does not modulate toll-  
like receptor signaling in human peripheral blood mononuclear cells. *Cytokine* 54, 43-50, (2011).
- 282 **Dicarlo, A. L., Hargis, M. T., Penafiel, L. M. & Litovitz, T. A.** Short-term magnetic field exposures  
(60 Hz) induce protection against ultraviolet radiation damage. *Int. J. Radiat. Biol.* 75, 1541-1549,  
(1999).
- 283 **Montalvo-Ortiz, B. L., Castillo-Pichardo, L., Hernandez, E., Humphries-Bickley, T., De La Mota-**  
**Peinado, A., Cubano, L. A., Vlaar, C. P. & Dharmawardhane, S.** Characterization of EHOP-016,  
Novel Small Molecule Inhibitor of Rac GTPase. *J. Biol. Chem.* 287, 13228-13238, (2012).
- 284 **Liang, C. C., Park, A. Y. & Guan, J. L.** In vitro scratch assay: a convenient and inexpensive method  
for analysis of cell migration in vitro. *Nat. Protoc.* 2, 329-333, (2007).
- 285 **Treloar, K. K. & Simpson, M. J.** Sensitivity of Edge Detection Methods for Quantifying Cell  
Migration Assays. *Plos One* 8, (2013).
- 286 **Glass, M., Moeller, B., Zirkel, A., Waechter, K., Huettelmaier, S. & Posch, S.** Cell migration  
analysis: Segmenting scratch assay images with level sets and support vector machines. *Pattern*  
*Recognition* 45, 3154-3165, (2012).
- 287 **Bise, R., Kanade, T., Yin, Z. & Huh, S.-i.** Automatic cell tracking applied to analysis of cell migration  
in wound healing assay. *Conference proceedings : ... Annual International Conference of the IEEE*  
*Engineering in Medicine and Biology Society. IEEE Engineering in Medicine and Biology Society.*  
*Annual Conference* 2011, 6174-6179, (2011).
- 288 **Kanopoulos, N., Vasanthavada, N. & Baker, R. L.** Design of an image edge detection filter using the

- Sobel operator. *IEEE J. Solid-State Circuit* 23, 358-367, (1988).
- 289 **Fleisch, M. C., Maxwell, C. A., Kuper, C. K., Brown, E. T., Barcellos-Hoff, M. H. & Costes, S. V.** Intensity-based signal separation algorithm for accurate quantification of clustered centrosomes in tissue sections. *Microscopy Research and Technique* 69, 964-972, (2006).
- 290 **Nilufar, S., Morrow, A. A., Lee, J. M. & Perkins, T. J.** FiloDetect: automatic detection of filopodia from fluorescence microscopy images. *BMC Syst. Biol.* 7, 12, (2013).
- 291 **Kobel, S. A., Burri, O., Griffa, A., Girotra, M., Seitz, A. & Lutolf, M. P.** Automated analysis of single stem cells in microfluidic traps. *Lab on a Chip* 12, 2843-2849, (2012).
- 292 **Grayson, L. S., Hansbrough, J. F., Zapatasirvent, R. L., Dore, C. A., Morgan, J. L. & Nicolson, M. A.** Quantitation of cytokine levels in skin graft donor site wound fluid. *Burns* 19, 401-405, (1993).
- 293 **Schultz, G., Rotatori, D. S. & Clark, W.** EGF and TGF-alpha in wound healing and repair. *J. Cell. Biochem.* 45, 346-352, (1991).
- 294 **Hori, K., Sotozono, C., Hamuro, J., Yamasaki, K., Kimura, Y., Ozeki, M., Tabata, Y. & Kinoshita, S.** Controlled-release of epidermal growth factor from cationized gelatin hydrogel enhances corneal epithelial wound healing. *Journal of Controlled Release* 118, 169-176, (2007).
- 295 **Tepper, O. M. et al.** Electromagnetic fields increase in vitro and in vivo angiogenesis through endothelial release of FGF-2. *Faseb J.* 18, 1231-+, (2004).
- 296 **Machu, T. K., Dillon, G. H., Huang, R., Lovinger, D. M. & Leidenheimer, N. J.** Temperature: An important experimental variable in studying PKC modulation of ligand-gated ion channels. *Brain Res.* 1086, 1-8, (2006).
- 297 **Fujita, F., Uchida, K., Takaishi, M., Sokabe, T. & Tominaga, M.** Ambient Temperature Affects the Temperature Threshold for TRPM8 Activation through Interaction of Phosphatidylinositol 4,5-Bisphosphate. *J. Neurosci.* 33, 6154-6159, (2013).
- 298 **Asakura, S., Taniguchi, M. & Oosawa, F.** Mechano-chemical behaviour of F-actin. *J. Mol. Biol.* 7, 55-&, (1963).
- 299 **Rico, F., Chu, C., Abdulreda, M. H., Qin, Y. J. & Moy, V. T.** Temperature Modulation of Integrin-Mediated Cell Adhesion. *Biophys. J.* 99, 1387-1396, (2010).
- 300 **Hartmann-Petersen, R., Walmod, P. S., Berezin, A., Berezin, V. & Bock, E.** Individual cell motility studied by time-lapse video recording: Influence of experimental conditions. *Cytometry* 40, 260-270, (2000).
- 301 **Patino, O., Grana, D., Bolgiani, A., Prezzavento, G., Mino, J., Merlo, A. & Benaim, F.** Pulsed electromagnetic fields in experimental cutaneous wound healing in rats. *The Journal of burn care & rehabilitation* 17, 528-531, (1996).
- 302 **Stiller, M. J., Pak, G. H., Shupack, J. L., Thaler, S., Kenny, C. & Jondreau, L.** A portable pulsed electromagnetic field (PEMF) device to enhance healing of recalcitrant venous ulcers: a double-blind, placebo-controlled clinical trial. *British Journal of Dermatology* 127, 147-154, (1992).
- 303 **Ieran, M., Zaffuto, S., Bagnacani, M., Annovi, M., Moratti, A. & Cadossi, R.** Effect of low frequency pulsing electromagnetic fields on skin ulcers of venous origin in human: a double-blind study. *Journal of Orthopaedic Research* 8, 276-282, (1990).
- 304 **Huo, R., Ma, Q. L., Wu, J. J., Chin-Nuke, K., Jing, Y. Q., Chen, J. A., Miyar, M. E., Davis, S. C. & Li, J.** Noninvasive Electromagnetic Fields on Keratinocyte Growth and Migration. *J. Surg. Res.* 162, 299-307, (2010).
- 305 **Iorio, R., Bennato, F., Mancini, F. & Colonna, R. C.** ELF-MF transiently increases skeletal myoblast migration: Possible role of calcpain system. *Int. J. Radiat. Biol.* 89, 548-561, (2013).
- 306 **An, G. Z. et al.** Effects of Long-Term 50Hz Power-Line Frequency Electromagnetic Field on Cell Behavior in Balb/c 3T3 Cells. *Plos One* 10, 13, (2015).
- 307 Feychting, M., Ahlbom, A. & Kheifets, L. in *Annual Review of Public Health* Vol. 26 *Annual Review of Public Health* 165-189 (Annual Reviews, 2005).
- 308 **Akan, Z., Aksu, B., Tulunay, A., Bilsel, S. & Inhan-Garip, A.** Extremely Low-Frequency Electromagnetic Fields Affect the Immune Response of Monocyte-Derived Macrophages to Pathogens. *Bioelectromagnetics* 31, 603-612, (2010).
- 309 **Nathan, C.** Neutrophils and immunity: challenges and opportunities. *Nat. Rev. Immunol.* 6, 173-182, (2006).
- 310 **Metzler, K. D., Goosmann, C., Lubojemska, A., Zychlinsky, A. & Papayannopoulos, V. A.** Myeloperoxidase-Containing Complex Regulates Neutrophil Elastase Release and Actin Dynamics during NETosis. *Cell Reports* 8, 883-896, (2014).
- 311 **Li, P. X., Li, M., Lindberg, M. R., Kennett, M. J., Xiong, N. & Wang, Y. M.** PAD4 is essential for antibacterial innate immunity mediated by neutrophil extracellular traps. *J. Exp. Med.* 207, 1853-1862,



- (2010).
- 312 **Palmer, L. J., Cooper, P. R., Ling, M. R., Wright, H. J., Huissoon, A. & Chapple, I. L. C.** Hypochlorous acid regulates neutrophil extracellular trap release in humans. *Clin. Exp. Immunol.* 167, 261-268, (2012).
- 313 **Rollwitz, J., Lupke, M. & Simko, M.** Fifty-hertz magnetic fields induce free radical formation in mouse bone marrow-derived promonocytes and macrophages. *Biochim. Biophys. Acta-Gen. Subj.* 1674, 231-238, (2004).
- 314 **Choi, H. S., Kim, J. W., Cha, Y. N. & Kim, C.** A quantitative nitroblue tetrazolium assay for determining intracellular superoxide anion production in phagocytic cells. *Journal of Immunoassay & Immunochemistry* 27, 31-44, (2006).
- 315 **Remijsen, Q. et al.** Neutrophil extracellular trap cell death requires both autophagy and superoxide generation. *Cell Research* 21, 290-304, (2011).
- 316 **Pang, L. J., Traitcheva, N., Gothe, G., Gomez, J. A. C. & Berg, H.** ELF-electromagnetic fields inhibit the proliferation of human cancer cells and induce apoptosis. *Electromagn. Biol. Med.* 21, 243-248, (2002).
- 317 **Metzler, K. D., Goosmann, C., Lubojemska, A., Zychlinsky, A. & Papayannopoulos, V.** A Myeloperoxidase-Containing Complex Regulates Neutrophil Elastase Release and Actin Dynamics during NETosis. *Cell Reports* 8, 883-896, (2014).
- 318 **Neeli, I., Dwivedi, N., Khan, S. & Radic, M.** Regulation of Extracellular Chromatin Release from Neutrophils. *J. Innate Immun.* 1, 194-201, (2009).
- 319 **Inhan-Garip, A., Aksu, B., Akan, Z., Akakin, D., Ozaydin, A. N. & San, T.** Effect of extremely low frequency electromagnetic fields on growth rate and morphology of bacteria. *Int. J. Radiat. Biol.* 87, 1155-1161, (2011).
- 320 **Saffarzadeh, M., Juenemann, C., Queisser, M. A., Lochnit, G., Barreto, G., Galuska, S. P., Lohmeyer, J. & Preissner, K. T.** Neutrophil Extracellular Traps Directly Induce Epithelial and Endothelial Cell Death: A Predominant Role of Histones. *PLoS One* 7, (2012).
- 321 **Liu, C. L., Tangsomboonvisit, S., Rosenberg, J. M., Mandelbaum, G., Gillespie, E. C., Gozani, O. P., Alizadeh, A. A. & Utz, P. J.** Specific post-translational histone modifications of neutrophil extracellular traps as immunogens and potential targets of lupus autoantibodies. *Arthritis Res. Ther.* 14, (2012).
- 322 **Pratesi, F. et al.** Antibodies from patients with rheumatoid arthritis target citrullinated histone 4 contained in neutrophils extracellular traps. *Ann. Rheum. Dis.* 73, 1414-1422, (2014).
- 323 **Neeli, I. & Radic, M.** Opposition between PKC isoforms regulates histone deimination and neutrophil extracellular chromatin release. *Frontiers in immunology* 4, 38, (2013).
- 324 **Hakkim, A., Fuchs, T. A., Martinez, N. E., Hess, S., Prinz, H., Zychlinsky, A. & Waldmann, H.** Activation of the Raf-MEK-ERK pathway is required for neutrophil extracellular trap formation. *Nat. Chem. Biol.* 7, 75-77, (2011).
- 325 **Li, P. X., Li, M., Lindberg, M. R., Kennett, M. J., Xiong, N. & Wang, Y. M.** PAD4 is essential for antibacterial innate immunity mediated by neutrophil extracellular traps. *J. Exp. Med.* 207, 1853-1862, (2010).
- 326 **Wang, Y. M. et al.** Histone hypercitrullination mediates chromatin decondensation and neutrophil extracellular trap formation. *J. Cell Biol.* 184, 205-213, (2009).
- 327 **Leshner, M., Wang, S., Lewis, C., Zheng, H., Chen, X. A., Santy, L. & Wang, Y.** PAD4 mediated histone hypercitrullination induces heterochromatin decondensation and chromatin unfolding to form neutrophil extracellular trap-like structures. *Frontiers in immunology* 3, 307, (2012).
- 328 **Arai, Y., Nishinaka, Y., Arai, T., Morita, M., Mizugishi, K., Adachi, S., Takaori-Kondo, A., Watanabe, T. & Yamashita, K.** Uric acid induces NADPH oxidase-independent neutrophil extracellular trap formation. *Biochem. Biophys. Res. Commun.* 443, 556-561, (2014).
- 329 **Parker, H., Draganow, M., Hampton, M. B., Kettle, A. J. & Winterbourn, C. C.** Requirements for NADPH oxidase and myeloperoxidase in neutrophil extracellular trap formation differ depending on the stimulus. *J. Leukoc. Biol.* 92, 841-849, (2012).
- 330 **Weisbart, R. H., Kwan, L., Golde, D. W. & Gasson, J. C.** Human GM-CSF primes neutrophils for enhanced oxidative-metabolism in response to the major physiological chemoattractants. *Blood* 69, 18-21, (1987).
- 331 **Goldmann, O. & Medina, E.** The expanding world of extracellular traps: not only neutrophils but much more. *Frontiers in immunology* 3, 420, (2012).
- 332 **Nathan, C.** Neutrophils and immunity: challenges and opportunities. *Nature Reviews Immunology* 6, 173-182, (2006).

- 333 **Brinkmann, V., Reichard, U., Goosmann, C., Fauler, B., Uhlemann, Y., Weiss, D. S., Weinrauch, Y. & Zychlinsky, A.** Neutrophil extracellular traps kill bacteria. *Science* 303, 1532-1535, (2004).
- 334 **Neeli, I., Dwivedi, N., Khan, S. & Radic, M.** Regulation of Extracellular Chromatin Release from Neutrophils. *J. Innate Immun.* 1, 194-201, (2009).
- 335 **Castillo-Pichardo, L. et al.** The Rac Inhibitor EHop-016 Inhibits Mammary Tumor Growth and Metastasis in a Nude Mouse Model. *Translational oncology* 7, 546-555, (2014).
- 336 **Kaibuchi, K., Kuroda, S. & Amano, M.** Regulation of the cytoskeleton and cell adhesion by the Rho family GTPases in mammalian cells. *Annual Review of Biochemistry* 68, 459-486, (1999).
- 337 **Jyoti, A. et al.** Interaction of Inducible Nitric Oxide Synthase with Rac2 Regulates Reactive Oxygen and Nitrogen Species Generation in the Human Neutrophil Phagosomes: Implication in Microbial Killing. *Antioxidants & Redox Signaling* 20, 417-431, (2014).
- 338 **Montalvo-Ortiz, B. L., Castillo-Pichardo, L., Hernandez, E., Humphries-Bickley, T., De La Mota-Peynado, A., Cubano, L. A., Vlaar, C. P. & Dharmawardhane, S.** Characterization of EHop-016, Novel Small Molecule Inhibitor of Rac GTPase. *J. Biol. Chem.* 287, 13228-13238, (2012).
- 339 **Khwaja, A. & Tatton, L.** Caspase-mediated proteolysis and activation of protein kinase C delta plays a central role in neutrophil apoptosis. *Blood* 94, 291-301, (1999).
- 340 **Wilkie, R. P., Vissers, M. C. M., Dragnow, M. & Hampton, M. B.** A functional NADPH oxidase prevents caspase involvement in the clearance of phagocytic neutrophils. *Infection and Immunity* 75, 3256-3263, (2007).
- 341 **Hong, L. et al.** Characterization of a Cdc42 Protein Inhibitor and Its Use as a Molecular Probe. *J. Biol. Chem.* 288, 8531-8543, (2013).
- 342 **Heyworth, P. G., Bohl, B. P., Bokoch, G. M. & Curnutte, J. T.** Rac translocates independently of the neutrophil NADPH oxidase components p47phox and p67phox. Evidence for its interaction with flavocytochrome b(558). *J. Biol. Chem.* 269, 30749-30752, (1994).
- 343 **Lim, M. B. H., Kuiper, J. W. P., Katchky, A., Goldberg, H. & Glogauer, M.** Rac2 is required for the formation of neutrophil extracellular traps. *J. Leukoc. Biol.* 90, 771-776, (2011).
- 344 **Darrach, E., Giles, J. T., Ols, M. L., Bull, H. G., Andrade, F. & Rosen, A.** Erosive Rheumatoid Arthritis Is Associated with Antibodies That Activate PAD4 by Increasing Calcium Sensitivity. *Sci. Transl. Med.* 5, 9, (2013).
- 345 **Docherty, M. & Smith, R.** The case for structuring the discussion of scientific papers. *Br. Med. J.* 318, 1224-1225, (1999).
- 346 **Pai, M., Zwerling, A. & Menzies, D.** Systematic review: T-cell-based assays for the diagnosis of latent tuberculosis infection: An update. *Ann. Intern. Med.* 149, 177-184, (2008).
- 347 **Kelishadi, R., Poursafa, P. & Jamshidi, F.** Role of environmental chemicals in obesity: a systematic review on the current evidence. *Journal of environmental and public health* 2013, 896789, (2013).
- 348 **Mann, J. J. et al.** Suicide prevention strategies - A systematic review. *JAMA-J. Am. Med. Assoc.* 294, 2064-2074, (2005).
- 349 **Navas-Acien, A., Silbergeld, E. K., Streeter, R. A., Clark, J. M., Burke, T. A. & Guallar, E.** Arsenic exposure and type 2 diabetes: A systematic review of the experimental and epidemiologic evidence. *Environ. Health Perspect.* 114, 641-648, (2006).
- 350 **Finnema, K. J., Ozcan, M., Post, W. J., Ren, Y. J. & Dijkstra, P. U.** In-vitro orthodontic bond strength testing: A systematic review and meta-analysis. *Am. J. Orthod. Dentofac. Orthop.* 137, 615-U108, (2010).
- 351 **Rodriguez, B. M., Sigg, D. & Bezanilla, F.** Voltage gating of shaker K<sup>+</sup> channels - The effect of temperature on ionic and gating currents. *J. Gen. Physiol.* 112, 223-242, (1998).
- 352 **Pusch, M., Ludewig, U. & Jentsch, T. J.** Temperature dependence of fast and slow gating relaxations of ClC-O chloride channels. *J. Gen. Physiol.* 109, 105-116, (1997).
- 353 **Peloquin, J. B., Doering, C. J., Rehak, R. & McRory, J. E.** Temperature dependence of Ca-v 1.4 calcium channel gating. *Neuroscience* 151, 1066-1083, (2008).
- 354 **Rosen, A. D.** Temperature modulation of calcium channel function in GH(3) cells. *Am. J. Physiol.-Cell Physiol.* 271, C863-C868, (1996).
- 355 **Allen, T. J. A.** Temperature dependence of macroscopic L-type calcium channel currents in single guinea pig ventricular myocytes. *J. Cardiovasc. Electrophysiol.* 7, 307-321, (1996).
- 356 **Haeri, H. H., Hashemianzadeh, S. M. & Monajjemi, M.** Temperature effects on the stochastic gating of the IP3R calcium release channel: a numerical simulation study. *J. Biol. Syst.* 17, 817-852, (2009).
- 357 **Cavalié, A., McDonald, T. F., Pelzer, D. & Trautwein, W.** Temperature-induced transitory and steady-state changes in the calcium current of guinea pig ventricular myocytes. *Pflugers Arch.* 405, 294-296, (1985).



- 358 **Kirschvink, J. L.** Uniform magnetic fields and double- wrapped coil systems: Improved techniques for  
the design of bioelectromagnetic experiments. *Bioelectromagnetics* 13, 401-411, (1992).
- 359 **Capstick, M., Schar, P., Schuermann, D., Romann, A. & Kuster, N.** ELF exposure system for live  
cell imaging. *Bioelectromagnetics* 34, 231-239, (2013).
- 360 **Lin, J. C.** Reexamining Biological Studies of Effect of Low-Frequency Electromagnetic Field  
Exposure on Cells in Culture. *Ieee Microwave Magazine* 15, 26+, (2014).
- 361 **Baggerly, K.** Disclose all data in publications. *Nature* 467, 401-401, (2010).
- 362 **Hrynaskiewicz, I., Norton, M. L., Vickers, A. J. & Altman, D. G.** Preparing raw clinical data for  
publication: guidance for journal editors, authors, and peer reviewers. *Br. Med. J.* 340, 6, (2010).
- 363 **Piwowar, H. A.** Who Shares? Who Doesn't? Factors Associated with Openly Archiving Raw Research  
Data. *Plos One* 6, 13, (2011).
- 364 **Alsheikh-Ali, A. A., Qureshi, W., Al-Mallah, M. H. & Ioannidis, J. P. A.** Public Availability of  
Published Research Data in High-Impact Journals. *Plos One* 6, (2011).
- 365 **Sansom, B. F. & Taylor, P. J.** A Simple Device for the Scintillation Counting of Aqueous Solutions of  
Calcium-45 and other bold italic beta-Emitting Isotopes. *Nature* 211, 626-&, (1966).
- 366 **Villarroya, M., Lopez, M. G., Cano-Abad, M. F. & Garcia, A. G.** Measurement of Ca<sup>2+</sup> entry using  
45Ca<sup>2+</sup>. *Methods in molecular biology (Clifton, N.J.)* 312, 135-145, (2006).
- 367 **Wang, S. Q., Song, L. S., Lakatta, E. G. & Cheng, H. P.** Ca<sup>2+</sup> signalling between single L-type  
Ca<sup>2+</sup> channels and ryanodine receptors in heart cells. *Nature* 410, 592-596, (2001).
- 368 **Brasen, J. C., Olsen, L. F. & Hallett, M. B.** Cell surface topology creates high Ca<sup>2+</sup> signalling  
microdomains. *Cell Calcium* 47, 339-349, (2010).
- 369 **Means, A. R. & Dedman, J. R.** Calmodulin - An intracellular calcium receptor. *Nature* 285, 73-77,  
(1980).
- 370 **Schafer, B. W. & Heizmann, C. W.** The S100 family of EF-hand calcium-binding proteins: Functions  
and pathology. *Trends Biochem.Sci.* 21, 134-140, (1996).
- 371 **Bootman, M., Niggli, E., Berridge, M. & Lipp, P.** Imaging the hierarchical Ca<sup>2+</sup> signalling system in  
HeLa cells. *J. Physiol.-London* 499, 307-314, (1997).
- 372 **Thomas, D., Lipp, P., Tovey, S. C., Berridge, M. J., Li, W. H., Tsien, R. Y. & Bootman, M. D.**  
Microscopic properties of elementary Ca<sup>2+</sup> release sites in nonexcitable cells. *Curr. Biol.* 10, 8-15,  
(2000).
- 373 **Hillson, E. J. & Hallett, M. B.** Localised and rapid Ca<sup>2+</sup> micro-events in human neutrophils:  
Conventional Ca<sup>2+</sup> puffs and global waves without peripheral-restriction or wave cycling. *Cell  
Calcium* 41, 525-536, (2007).
- 374 **Chen, L. W. & Jan, C. R.** Mechanisms and modulation of formyl-methionyl-leucyl-phenylalanine  
(fMLP)-induced Ca<sup>2+</sup> mobilization in human neutrophils. *Int. Immunopharmacol.* 1, 1341-1349,  
(2001).
- 375 **Aas, V., Larsen, K. & Iversen, J. G.** IFN-gamma induces calcium transients and increases the  
capacitative calcium entry in human neutrophils. *J. Interferon Cytokine Res.* 18, 197-205, (1998).
- 376 **Brown, G. B. & Roth, J. A.** Comparison of the response of bovine and human neutrophils to various  
stimuli. *Vet. Immunol. Immunopathol.* 28, 201-218, (1991).
- 377 **Ngzikorski, J., Andersson, R., Patarroyo, M. & Andersson, T.** Calcium signaling capacity of the  
CB11b/CD18 integrin on human neutrophils. *Exp. Cell Res.* 195, 504-508, (1991).
- 378 **White, J. A., Blackmore, P. F., Schoenbach, K. H. & Beebe, S. J.** Stimulation of capacitative calcium  
entry in HL-60 cells by nanosecond pulsed electric fields. *J. Biol. Chem.* 279, 22964-22972, (2004).
- 379 **Pettit, E. J. & Hallett, M. B.** Release of 'caged' cytosolic Ca<sup>2+</sup> triggers rapid spreading of human  
neutrophils adherent via integrin engagement. *J. Cell Sci.* 111, 2209-2215, (1998).
- 380 **Sonnier, H., Kolomytkin, O. V. & Marino, A. A.** Resting potential of excitable neuroblastoma cells in  
weak magnetic fields. *Cell. Mol. Life Sci.* 57, 514-520, (2000).
- 381 **Obo, M., Konishi, S., Otaka, Y. & Kitamura, S.** Effect of magnetic field exposure on calcium  
channel currents using patch clamp technique. *Bioelectromagnetics* 23, 306-314, (2002).
- 382 **Mattsson, M.-O. & Simko, M.** Grouping of Experimental Conditions as an Approach to Evaluate  
Effects of Extremely Low-Frequency Magnetic Fields on Oxidative Response in in vitro Studies.  
*Frontiers in public health* 2, 132, (2014).
- 383 **Hooijmans, C., de Vries, R., Leenaars, M. & Ritskes-Hoitinga, M.** The Gold Standard Publication  
Checklist (GSPC) for improved design, reporting and scientific quality of animal studies GSPC versus  
ARRIVE guidelines. *Laboratory Animals* 45, 61-61, (2011).
- 384 **de Vocht, F.** "Dirty electricity": what, where, and should we care? *J. Expo. Sci. Environ. Epidemiol.* 20,  
399-405, (2010).



- 385 **Havas, M.** Electromagnetic hypersensitivity: Biological effects of dirty electricity with emphasis on  
diabetes and multiple sclerosis. *Electromagn. Biol. Med.* 25, 259-268, (2006).
- 386 **Faggion, C. M., Jr.** Guidelines for reporting pre-clinical in vitro studies on dental materials. *The  
journal of evidence-based dental practice* 12, 182-189, (2012).
- 387 **Krithikadatta, J., Gopikrishna, V. & Datta, M.** CRIS Guidelines (Checklist for Reporting In-vitro  
Studies): A concept note on the need for standardized guidelines for improving quality and transparency  
in reporting in-vitro studies in experimental dental research. *Journal of conservative dentistry : JCD*  
17, 301-304, (2014).
- 388 **Urban, C. F., Ermert, D., Schmid, M., Abu-Abed, U., Goosmann, C., Nacken, W., Brinkmann, V.,  
Jungblut, P. R. & Zychlinsky, A.** Neutrophil Extracellular Traps Contain Calprotectin, a Cytosolic  
Protein Complex Involved in Host Defense against *Candida albicans*. *PLoS Pathog.* 5, 18, (2009).
- 389 **Nishinaka, Y., Arai, T., Adachi, S., Takaori-Kondo, A. & Yamashita, K.** Singlet oxygen is essential  
for neutrophil extracellular trap formation. *Biochemical and Biophysical Research Communications*  
413, 75-79, (2011).
- 390 **Gupta, A. K., Giaglis, S., Hasler, P. & Hahn, S.** Efficient Neutrophil Extracellular Trap Induction  
Requires Mobilization of Both Intracellular and Extracellular Calcium Pools and Is Modulated by  
Cyclosporine A. *Plos One* 9, 12, (2014).
- 391 **Kawata, J., Kikuchi, M. & Saitoh, H.** Genomic DNAs in a human leukemia cell line unfold after cold  
shock, with formation of neutrophil extracellular trap-like structures. *Biotechnol. Lett.* 36, 241-250,  
(2014).
- 392 **Khawaja, A. A., Pericleous, C., Thomas, L. W., Ashcroft, M., Porter, J. C. & Giles, I.** Hypoxia  
increases neutrophil extracellular trap formation and adhesion to endothelial cells. *Immunology* 143,  
118-118, (2014).
- 393 **Saffarzadeh, M., Juenemann, C., Queisser, M. A., Lochnit, G., Barreto, G., Galuska, S. P.,  
Lohmeyer, J. & Preissner, K. T.** Neutrophil Extracellular Traps Directly Induce Epithelial and  
Endothelial Cell Death: A Predominant Role of Histones. *Plos One* 7, (2012).
- 394 **Liu, C. L., Tangsomboonvisit, S., Rosenberg, J. M., Mandelbaum, G., Gillespie, E. C., Gozani,  
O. P., Alizadeh, A. A. & Utz, P. J.** Specific post-translational histone modifications of neutrophil  
extracellular traps as immunogens and potential targets of lupus autoantibodies. *Arthritis Research &  
Therapy* 14, (2012).
- 395 **Pratesi, F. et al.** Antibodies from patients with rheumatoid arthritis target citrullinated histone 4  
contained in neutrophils extracellular traps. *Annals of the Rheumatic Diseases* 73, 1414-1422, (2014).
- 396 **Youssef, P. P., Mantzioris, B. X., Robertsthomson, P. J., Ahern, M. J. & Smith, M. D.** Effects of ex  
vivo manipulation on the expression of cell adhesion molecules on neutrophils. *J. Immunol. Methods*  
186, 217-224, (1995).
- 397 **Glasser, L. & Fiederlein, R. L.** The effect of various cell separation procedures on assays of  
neutrophil function. A critical appraisal. *American Journal of Clinical Pathology* 93, 662-669, (1990).
- 398 **Laurent, F., Benoliel, A. M., Capo, C. & Bongrand, P.** Oxidative metabolism of polymorphonuclear  
leukocytes: modulation by adhesive stimuli. *J. Leukoc. Biol.* 49, 217-226, (1991).
- 399 **Haslett, C., Guthrie, L. A., Kopaniak, M. M., Johnston, R. B. & Henson, P. M.** Modulation  
of multiple neutrophil functions by preparative methods or trace concentrations of bacterial  
lipopolysaccharide. *Am. J. Pathol.* 119, 101-110, (1985).
- 400 **Kawakami, T., He, J., Morita, H., Yokoyama, K., Kaji, H., Tanaka, C., Suemori, S.-i., Tohyama,  
K. & Tohyama, Y.** Rab27a Is Essential for the Formation of Neutrophil Extracellular Traps (NETs) in  
Neutrophil-Like Differentiated HL60 Cells. *Plos One* 9, (2014).
- 401 **Ashkenazi, A. & Marks, R. S.** Luminol-dependent chemiluminescence of human phagocyte cell  
lines: comparison between DMSO differentiated PLB 985 and HL 60 cells. *Luminescence* 24, 171-177,  
(2009).
- 402 **Gee, D. J., Wright, L. K., Zimmermann, J., Cole, K., Soule, K. & Ubowski, M.** Dimethylsulfoxide  
exposure modulates HL-60 cell rolling interactions. *Biosci. Rep.* 32, 375-382, (2012).
- 403 **Venaille, T. J., Misso, N. L. A., Phillips, M. J., Robinson, B. W. S. & Thompson, P. J.** Effects of  
different density gradient separation techniques on neutrophil function  
*Scand. J. Clin. Invest.* 54, 385-391, (1994).
- 404 **Sroka, J., Kordecka, A., Wlosiak, P., Madeja, Z. & Korohoda, W.** Separation methods for isolation  
of human polymorphonuclear leukocytes affect their motile activity. *Eur. J. Cell Biol.* 88, 531-539,  
(2009).
- 405 **Chien, S., Simchon, S., Abbott, R. E. & Jan, K. M.** Surface adsorption of dextrans of human red cell  
membrane. *J. Colloid Interface Sci.* 62, 461-470, (1977).



- 406 **Vanosselaer, N., Herman, A. G. & Rampart, M.** Dextran sulphate inhibits neutrophil emigration and  
neutrophil-dependent plasma leakage in rabbit skin. *Agents Actions* 38, C51-C53, (1993).
- 407 **Inhan-Garip, A., Aksu, B., Akan, Z., Akakin, D., Ozaydin, A. N. & San, T.** Effect of extremely low  
frequency electromagnetic fields on growth rate and morphology of bacteria. *Int. J. Radiat. Biol.* 87,  
1155-1161, (2011).
- 408 **Farrera, C. & Fadeel, B.** Macrophage Clearance of Neutrophil Extracellular Traps Is a Silent Process.  
*J. Immunol.* 191, 2647-2656, (2013).
- 409 **Moon, A. F., Gaudu, P. & Pedersen, L. C.** Structural characterization of the virulence factor nuclease  
A from *Streptococcus agalactiae*. *Acta Crystallogr. Sect. D-Biol. Crystallogr.* 70, 2937-2949, (2014).
- 410 **Beiter, K., Wartha, F., Albiger, B., Normark, S., Zychlinsky, A. & Henriques-Normark, B.** An  
endonuclease allows *Streptococcus pneumoniae* to escape from neutrophil extracellular traps. *Curr.*  
*Biol.* 16, 401-407, (2006).
- 411 **Berends, E. T. M., Horswill, A. R., Haste, N. M., Monestier, M., Nizet, V. & von Kockritz-  
Blickwede, M.** Nuclease Expression by *Staphylococcus aureus* Facilitates Escape from Neutrophil  
Extracellular Traps. *J. Innate Immun.* 2, 576-586, (2010).
- 412 **Buchanan, J. T., Simpson, A. J., Aziz, R. K., Liu, G. Y., Kristian, S. A., Kotb, M., Feramisco, J. &  
Nizet, V.** DNase expression allows the pathogen group A streptococcus to escape killing in neutrophil  
extracellular traps. *Curr. Biol.* 16, 396-400, (2006).
- 413 **Tanaka, K. et al.** In Vivo Characterization of Neutrophil Extracellular Traps in Various Organs of a  
Murine Sepsis Model. *Plos One* 9, 14, (2014).
- 414 **Bosmann, M., Grailer, J. J., Ruemmler, R., Russkamp, N. F., Zetoune, F. S., Sarma, J. V.,  
Standiford, T. J. & Ward, P. A.** Extracellular histones are essential effectors of C5aR- and C5L2-  
mediated tissue damage and inflammation in acute lung injury. *FASEB J.* 27, 5010-5021, (2013).
- 415 **Brill, A., Fuchs, T. A., Savchenko, A. S., Thomas, G. M., Martinod, K., De Meyer, S. F., Bhandari,  
A. A. & Wagner, D. D.** Neutrophil extracellular traps promote deep vein thrombosis in mice. *J.*  
*Thromb. Haemost.* 10, 136-144, (2012).
- 416 **McDonald, B., Urrutia, R., Yipp, B. G., Jenne, C. N. & Kubes, P.** Intravascular Neutrophil  
Extracellular Traps Capture Bacteria from the Bloodstream during Sepsis. *Cell Host Microbe* 12, 324-  
333, (2012).
- 417 **Schmid, G. & Kuster, N.** The Discrepancy Between Maximum In Vitro Exposure Levels and Realistic  
Conservative Exposure Levels of Mobile Phones Operating at 900/1800 MHz. *Bioelectromagnetics* 36,  
133-148, (2015).
- 418 **Sheppard, F. R., Kelher, M. R., Moore, E. E., McLaughlin, N. J. D., Banerjee, A. & Silliman, C.  
C.** Structural organization of the neutrophil NADPH oxidase: phosphorylation and translocation during  
priming and activation. *J. Leukoc. Biol.* 78, 1025-1042, (2005).
- 419 **Branzk, N., Lubojemska, A., Hardison, S. E., Wang, Q., Gutierrez, M. G., Brown, G. D. &  
Papayannopoulos, V.** Neutrophils sense microbe size and selectively release neutrophil extracellular  
traps in response to large pathogens. *Nature Immunology* 15, 1017-1025, (2014).
- 420 **Gabelloni, M. L., Trevani, A. S., Sabatte, J. & Geffner, J.** Mechanisms regulating neutrophil survival  
and cell death. *Semin. Immunopathol.* 35, 423-437, (2013).
- 421 **Nauseef, W. M.** Nyet to NETs? A pause for healthy skepticism. *J. Leukoc. Biol.* 91, 353-355, (2012).
- 422 **Babior, B. M.** The NADPH oxidase of endothelial cells. *IUBMB Life* 50, 267-269, (2000).
- 423 **Kooy, N. W., Royall, J. A., Ye, Y. Z., Kelly, D. R. & Beckman, J. S.** Evidence for in vivo  
peroxynitrite production in human acute lung injury. *Am. J. Respir. Crit. Care Med.* 151, 1250-1254,  
(1995).
- 424 **Parker, H., Albrett, A. M., Kettle, A. J. & Winterbourn, C. C.** Myeloperoxidase associated with  
neutrophil extracellular traps is active and mediates bacterial killing in the presence of hydrogen  
peroxide. *J. Leukoc. Biol.* 91, 369-376, (2012).
- 425 **Akong-Moore, K., Chow, O. A., von Kockritz-Blickwede, M. & Nizet, V.** Influences of Chloride and  
Hypochlorite on Neutrophil Extracellular Trap Formation. *Plos One* 7, 7, (2012).
- 426 **Metzler, K. D., Fuchs, T. A., Nauseef, W. M., Reumaux, D., Roesler, J., Schulze, I., Wahn, V.,  
Papayannopoulos, V. & Zychlinsky, A.** Myeloperoxidase is required for neutrophil extracellular trap  
formation: implications for innate immunity. *Blood* 117, 953-959, (2011).
- 427 **Belorgey, D. & Bieth, J. G.** DNA binds neutrophil elastase and mucus proteinase inhibitor and impairs  
their functional activity. *FEBS Letters* 361, 265-268, (1995).
- 428 **Hirsch, J. G.** Bactericidal action of histone. *J. Exp. Med.* 108, 925-944, (1958).
- 429 **Giannone, G., Ronde, P., Gaire, M., Haiech, J. & Takeda, K.** Calcium oscillations trigger focal  
adhesion disassembly in human U87 astrocytoma cells. *J. Biol. Chem.* 277, 26364-26371, (2002).

- 430 **Godbout, C., Castella, L. F., Smith, E. A., Talele, N., Chow, M. L., Garonna, A. & Hinz, B.** The Mechanical Environment Modulates Intracellular Calcium Oscillation Activities of Myofibroblasts. *Plos One* 8, (2013).
- 431 **Tang, J. X. & Janmey, P. A.** The polyelectrolyte nature of F-actin and the mechanism of actin bundle formation. *J. Biol. Chem.* 271, 8556-8563, (1996).
- 432 **Nusse, O. & Lindau, M.** The dynamics of exocytosis in human neutrophils. *J. Cell Biol.* 107, 2117-2123, (1988).
- 433 **Dewitt, S., Francis, R. J. & Hallett, M. B.** Ca<sup>2+</sup> and calpain control membrane expansion during the rapid cell spreading of neutrophils. *J. Cell Sci.* 126, 4627-4635, (2013).
- 434 **Dewitt, S. & Hallett, M. B.** Cytosolic free Ca<sup>2+</sup> changes and calpain activation are required for beta integrin-accelerated phagocytosis by human neutrophils. *J. Cell Biol.* 159, 181-189, (2002).
- 435 **Miyawaki, A., Griesbeck, O., Heim, R. & Tsien, R. Y.** Dynamic and quantitative Ca<sup>2+</sup> measurements using improved cameleons. *Proc. Natl. Acad. Sci. U. S. A.* 96, 2135-2140, (1999).
- 436 **Simko, M.** Cell type specific redox status is responsible for diverse electromagnetic field effects. *Current Medicinal Chemistry* 14, 1141-1152, (2007).
- 437 **Adair, R. K.** Effects of very weak magnetic fields on radical pair reformation. *Bioelectromagnetics* 20, 255-263, (1999).
- 438 **Vanstrijp, J. A. G., Vankessel, K. P. M., Vandertol, M. E. & Verhoef, J.** Complement-mediated phagocytosis of herpes simplex virus by granulocytes - Binding or ingestion. *J. Clin. Invest.* 84, 107-112, (1989).
- 439 **Mansfield, P. J., Hinkovska-Galcheva, V., Shayman, J. A. & Boxer, L. A.** Granulocyte colony-stimulating factor primes NADPH oxidase in neutrophils through translocation of cytochrome b(558) by gelatinase-granule release. *J. Lab. Clin. Med.* 140, 9-16, (2002).
- 440 **Fu, Y. K., Arkins, S., Wang, B. S. & Kelley, K. W.** A novel role of growth hormone and insulin-like growth factor-I. Priming neutrophils for superoxide anion secretion. *J. Immunol.* 146, 1602-1608, (1991).
- 441 **Guthrie, L. A., McPhail, L. C., Henson, P. M. & Johnston, R. B.** Priming of neutrophils for enhanced release of oxygen metabolites by bacterial lipopolysaccharide. Evidence for increased activity of the superoxide-producing enzyme. *J. Exp. Med.* 160, 1656-1671, (1984).
- 442 **Reumaux, D., Vosseveld, P. J. M., Roos, D. & Verhoeven, A. J.** Effect of tumor necrosis factor-induced integrin activation on Fc gamma receptor II-mediated signal transduction: relevance for activation of neutrophils by anti-proteinase 3 or anti-myeloperoxidase antibodies. *Blood* 86, 3189-3195, (1995).
- 443 **El-Benna, J., Dang, P. M. C. & Gougerot-Pocidallo, M. A.** Priming of the neutrophil NADPH oxidase activation: role of p47phox phosphorylation and NOX2 mobilization to the plasma membrane. *Semin. Immunopathol.* 30, 279-289, (2008).
- 444 **Elbim, C., Guichard, C., Dang, P. M. C., Fay, M., Pedruzzi, E., Demur, H., Pouzet, C., El Benna, J. & Gougerot-Pocidallo, M. A.** Interleukin-18 primes the oxidative burst of neutrophils in response to formyl-peptides: Role of cytochrome b558 translocation and N-formyl peptide receptor endocytosis. *Clin. Diagn. Lab. Immunol.* 12, 436-446, (2005).
- 445 **Brown, G. E., Stewart, M. Q., Bissonnette, S. A., Elia, A. E. H., Wilker, E. & Yaffe, M. B.** Distinct ligand-dependent roles for p38 MAPK in priming and activation of the neutrophil NADPH oxidase. *J. Biol. Chem.* 279, 27059-27068, (2004).
- 446 **Makni-Maalej, K., Boussetta, T., Hurtado-Nedelec, M., Belambri, S. A., Gougerot-Pocidallo, M. A. & El-Benna, J.** The TLR7/8 Agonist CL097 Primes N-Formyl-Methionyl-Leucyl-Phenylalanine-Stimulated NADPH Oxidase Activation in Human Neutrophils: Critical Role of p47phox Phosphorylation and the Proline Isomerase Pin1. *J. Immunol.* 189, 4657-4665, (2012).
- 447 **Cox, J. & Mann, M.** Is proteomics the new genomics? *Cell* 130, 395-398, (2007).
- 448 **Kitchen, E., Rossi, A. G., Condliffe, A. M., Haslett, C. & Chilvers, E. R.** Demonstration of reversible priming of human neutrophils using platelet-activating factor. *Blood* 88, 4330-4337, (1996).
- 449 **Summers, C., Chilvers, E. R. & Peters, A. M.** Mathematical modeling supports the presence of neutrophil depriming in vivo. *Physiological reports* 2, e00241-e00241, (2014).
- 450 **Koethe, S. M., Kuhnmuench, J. R. & Becker, C. G.** Neutrophil priming by cigarette smoke condensate and a tobacco anti-idiotypic antibody. *Am. J. Pathol.* 157, 1735-1743, (2000).
- 451 **Hubner, K., Surovtsova, I., Yserentant, K., Hansch, M. & Kummer, U.** Ca<sup>2+</sup>dynamics correlates with phenotype and function in primary human neutrophils. *Biophys. Chem.* 184, 116-125, (2013).
- 452 **Lachin, J. M.** Introduction to sample size determination and power analysis for clinical trials. *Controlled Clin. Trials* 2, 93-113, (1981).



## References

---

- 453 **Fethney, J.** Statistical and clinical significance, and how to use confidence intervals to help interpret both. *Aust. Crit. Care* 23, 93-97, (2010).
- 454 **Thompson, B.** Critique of p-Values. *Int. Stat. Rev.* 74, 1-14, (2006).
- 455 **Leek, J. T. & Peng, R. D.** P values are just the tip of the iceberg. *Nature* 520, 612-612, (2015).
- 456 **Halsey, L. G., Curran-Everett, D., Vowler, S. L. & Drummond, G. B.** The fickle P value generates irreproducible results. *Nat. Methods* 12, 179-185, (2015).



---

References



## Summary

The aim of this thesis was to investigate possible modulatory roles of low frequency electromagnetic fields (LF EMFs) exposure on the innate immune system. Recent decades have seen a huge increase in the use of electronic devices that nowadays enable us to communicate with distant family, enjoy music everywhere or order food without leaving the house. However besides the benefits, this evolution has also resulted in increased public concern about the potential adverse health effects of non-ionizing radiation. Every power line or electronic device emits a wide range of electromagnetic waves, which can pass through our bodies or damage our skin, depending on the characteristics of the waves. The symptoms attributed to continuous EMF exposure range from non-specific physical symptoms, such as fatigue<sup>1</sup>, headaches<sup>2</sup>, and redness of the skin to increased prevalence of childhood leukaemia<sup>3</sup>. Although many theories regarding a potential mechanism of induction are put forward, to date no clear mechanism of action has been elucidated. Experimental evidence that could support an association between exposure and health status appears to be insufficient and inconsistent<sup>4,5</sup>. In this thesis we investigated the potential effect of LF EMF exposure on neutrophils, one of the key players of the innate immune response. We tried to elucidate a possible mechanism of interaction between intracellular signalling pathways and LF EMF exposure. We aimed to investigate calcium signalling, actin reorganization, cell migration and antimicrobial activity during exposure with different *in vitro* approaches.

In a neutrophil, both orchestrated calcium mobilization and tightly-controlled ROS generation are indispensable for the cell's function. Nevertheless, neutrophils appeared to be an overlooked immune cell type in literature about the effect of EMF. Neutrophils are not only important during inflammation and immune responses, but also play an important role in the pathogenesis of several inflammatory disorders including chronic infection, autoimmunity, and cancer. In **chapter 2** we investigated effects of exposure on the calcium mobilisation in neutrophil-like cells. We applied different frequencies (50 Hz sine and Irregular wave forms), exposure levels (5  $\mu$ T up to 500  $\mu$ T) and used an acute and chronic exposure (30 minutes and five days). We investigated the calcium influx induced with a biological stimulus and did not find any changes induced by exposure to LF EMFs. This conventional approach was combined with analyses of gene expression patterns and while differentiation of the cells revealed altered mRNA expression, five days of LF EMF exposure did not influence the expression profiles of calcium-signalling related genes. Detailed analysis of the number of microvilli substantiated the notion that the applied LF EMF did not significantly affect calcium influx, gene expression or cell morphology.

Though, there are numerous reports present in literature that contradict with our observations. Therefore, we performed a systematic review and subsequent meta-analyses in **chapter 3**. In our systematic review, we investigated if there is already evidence in current literature regarding a modulation of the cellular calcium homeostasis by LF EMF exposure. Unlike most systematic reviews examining *in vivo* studies and clinical trial data, we evaluated studies that used *ex vivo* or *in vitro* cell cultures. For this, we first selected a group of *in vitro* studies based on a strict set of quality criterion on both the biological and physical aspects of the reported data. From our comprehensive approach, we concluded that there is a very weak association between LF EMF exposure and intracellular calcium concentrations as well as the frequency of oscillating calcium waves. Furthermore, we reported that there might be EMF sensitive cell types that could explain the contradictory reports in literature. In addition, fields below 200  $\mu$ T, frequencies other than 50/60 Hz, or exposure periods shorted

than 60 minutes showed to also be associated with increased intracellular calcium. From the papers we also extracted all parameters required to calculate the induced electric fields. The strength of these fields showed to be associated to an increased intracellular calcium concentration. However, this correlation was only detected when the total induced electric field generated by the maximum magnetic field and parasitic fields was plotted. This indicated that uncontrolled induced electric fields could unintentionally influence *in vitro* outcomes and cause discrepancy in literature.

In **chapter 4 and 5** we used different imaging techniques to quantify the influence of exposure during dynamic organelle movement and cell migration. First we described a novel method suited to investigate the effect of exposure on the cell's filopodia, small protrusions on the outside of a cell. A cell uses its filopodia to sense the environment for chemical or topographical signals. A filopodium contains a dense core of bundled actin. By means of stable expression of Lifeact, an actin binding protein, conjugated to a fluorescence probe, we visualised the cell's filopodia. Subsequently, in a time-resolved image analysis, we measured and calculated the movement of filopodia. Our method showed to be sensitive and quantitative, but would require faster image acquisition than currently possible.

Next, cell migration was examined with a different approach. During wound-healing, epithelial cells migrate towards each other to close the gap. This occurs without the need of biological signals, but can be stimulated or inhibited by chemicals or biological proteins. We examined if LF EMF exposure influenced the migration speed. Cells were exposed for 2 and 18 hours to a continuous sine wave of 50 Hz with a magnetic flux density of 500  $\mu$ T. The 18-hour exposure did not significantly influence migration speed, but a two-hour exposure indicated a possible effect. This difference was abolished when cell migration was simultaneously stimulated with epidermal growth factor (EGF). Though, further research is required to confirm this observation.

In **chapter 6 and 7**, we studied a recently discovered cellular mechanism called neutrophil extracellular trap (NET) formation. NET formation has been shown to extracellularly capture and kill bacteria. In a process of two to four hours, reactive oxygen species (ROS) are produced, DNA is decondensated and the nuclear envelope is dissolved. The untangled DNA is mixed with antimicrobial peptides from the granules and eventually the cell membrane ruptures and the NETs, DNA coated with peptides, are released. In **chapter 6** we discovered that LF EMF exposure increases NET release, if the cells are simultaneously stimulated with PMA, a chemical component that mimics receptor stimulation. The molecular mechanism involved was shown to be enhanced ROS production during exposure. The NETs are able to capture more bacteria, but at the same time damage epithelial cells. This delicate balance might be distorted by EMF exposure.

Microbes and chemokines are natural stimuli of NET formation; the intracellular mechanisms can be studied with small molecule inhibitors. We found that EHop-016 was also capable of inducing NET formation, even though it was originally designed to interact with Rac 1 and 3 during tumour metastasis. Our research showed that this small molecular inhibitor is related to PAD4 activity and histone citrullination. An interaction of EHop-016 with the immune system could have harmful consequences for future drug therapies.

In conclusion we found that the influence of LF EMF exposure greatly depends on the molecular pathways that are activated in the cell *in vitro*. While calcium was not influenced, our systematic review indicated a possible weak effect, depending on characteristics of the cell and the exposure system. Moreover, migration might be affected when exposures are short, but longer exposure could lead to adaptation. NET formation required activation of the



ROS pathway, before an effect of exposure was detected. These results emphasize the danger of misinterpretation when generalising potential effects of exposure. Hypothesis driven cellular *in vitro* and *in vivo* research with well-defined and carefully monitored exposures and effects will be essential to elucidate possible impact of environmental fields.



## Samenvatting

In dit proefschrift hebben we mogelijke effecten van laag frequente elektromagnetische velden (LF EMV) op het aangeboren immuun systeem onderzocht. In de afgelopen decennia is het gebruik van elektronische apparaten enorm toegenomen. Apparaten die het mogelijk maken te communiceren met verre familie leden, overal te genieten van muziek of eten te bestellen zonder dat je je huis hoeft te verlaten. Maar naast voordelen heeft deze revolutie ook nadelen, want de angst voor mogelijke schadelijke effecten van niet-ioniserende straling is toegenomen. Elke stroomkabel, of elektronisch apparaat genereert een breed scala aan elektromagnetische golven die, afhankelijk van de eigenschappen van die golven, alleen door ons lichaam heen gaan of onze huid beschadigen. De symptomen die toegeschreven worden aan continue EMV blootstelling variëren. Het zijn enerzijds niet-specifieke symptomen zoals moeheid <sup>1</sup>, hoofdpijn <sup>2</sup> en roodheid van de huid, maar ook een verhoogde incidentie van kinderleukemie <sup>3</sup>. Ondanks het feit dat er meerdere theorieën zijn opgesteld over een mogelijk werkingsmechanisme, is er op dit moment nog geen helderheid. Experimenteel bewijs dat de link tussen blootstelling en gezondheid kan onderbouwen is onvolledig en tegenstrijdig <sup>4,5</sup>. In dit proefschrift hebben we onderzoek gedaan naar de mogelijke effecten van LF EMV blootstelling op het functioneren van neutrofielen, belangrijke witte bloedcellen van de aangeboren afweer. We hebben onderzocht of de activiteit van de intracellulaire signaleringsroutes in een neutrofiel veranderd is tijdens of na LF EMV blootstelling. Ons doel was om de calcium huishouding in de cel, de actine reorganisatie, de migratie van de cellen en hun antimicrobiële activiteit gedurende blootstelling te onderzoeken bij cellen in kweek (*in vitro*).

In een neutrofiel, is bij stimulatie een nauwkeurige mobilisatie van calcium en een strak gecontroleerde productie van reactieve zuurstofverbindingen (reactive oxygen species, ROS) onmisbaar voor een goed functioneren bij de afweer. Desondanks werd de neutrofiel in studies over mogelijke effecten van EMV vaak over het hoofd gezien. Neutrofielen zijn niet alleen belangrijk tijdens een immuun reactie en infectie, maar hun activiteit is ook veelal bepalend bij de ontwikkeling van verschillende infectie ziektes, waaronder chronische infectie, auto-immuunziektes en kanker. In **hoofdstuk 2** hebben we de effecten van EMV blootstelling op calcium mobilisatie onderzocht in neutrofiel-achtige cellen. We hebben verschillende frequenties (50 Hz en onregelmatige golven), verschillende veldsterktes (5  $\mu$ T tot 500  $\mu$ T) en zowel acute als chronische blootstelling gebruikt (30 minuten en vijf dagen). We hebben de instroom van calcium ionen gestimuleerd met biologische stimuli en zagen geen verschil door blootstelling aan EMV. Deze veelgebruikte methode was gecombineerd met gen expressie analyse van genen die voor dit proces belangrijk zijn. Terwijl differentiatie van de cellen leidde tot de verwachte veranderde gen expressie patronen, een blootstelling van vijf dagen aan EMV veranderde de expressie patronen van “calcium-genen” niet. Een gedetailleerde analyse van het aantal microvilli op een cel versterkte het idee dat de door ons geproduceerde LF EMV niet in staat was om de calcium huishouding, de gen expressie of de cel morfologie te veranderen.

Toch zijn er vele meldingen in de literatuur die tegenstrijdig zijn aan onze observaties. Daarom hebben we in **hoofdstuk 3** een systematisch review opgesteld met een bijbehorende meta-analyse. Hierin hebben we onderzocht of er al aanwijzingen aanwezig zijn in de huidige wetenschappelijk literatuur voor een invloed van LF EMV blootstelling op de cellulaire calcium huishouding. In tegenstelling tot de meeste systematische reviews, die gedaan zijn voor *in vivo* studies en klinische proeven, hebben wij artikelen onderzocht



die *in vitro* of *ex vivo* cel systemen gebruikten. Hiervoor hebben we eerst een groep *in vitro* studies geselecteerd die voldeden aan al onze vooropgestelde criteria voor de biologische en natuurkundige aspecten. Uit onze uitgebreide aanpak kunnen we concluderen dat er een zeer zwakke associatie is tussen LF EMV blootstelling en intracellulaire calcium concentraties en LF EMV en het patroon van de calcium oscillaties. Bovendien rapporteerden we dat er mogelijk EMV-gevoelige celtypes kunnen zijn die de tegenstrijdigheid in de literatuur zouden kunnen verklaren. Daarnaast laten we zien dat velden kleiner dan 200  $\mu\text{T}$ , andere frequenties dan 50/60 Hz, of een blootstelling korter dan 60 minuten gerelateerd kan zijn met een verhoogde intracellulaire calcium concentratie. Uit de geselecteerde artikelen hebben we ook alle gegevens genoteerd die nodig zijn voor het berekenen van de geïnduceerde elektrische velden. De berekende sterkte van deze velden hing samen met een verhoging van de intracellulaire calcium concentratie. Maar dit verband werd alleen gezien als het totale geïnduceerde elektrisch veld, het veld gegenereerd door het maximale magnetische veld én de parasitaire velden, uitgezet werd. Deze resultaten geven aan dat de niet gecontroleerde geïnduceerde elektrisch velden onbewust de *in vitro* resultaten zouden kunnen beïnvloeden en hiermee een discrepantie in de literatuur kunnen veroorzaken.

In **hoofdstuk 4 en 5** hebben we verschillende beeldvormingstechnieken gebruikt om de invloed van blootstelling aan EMV te kwantificeren tijdens dynamische beweging van organellen en tijdens migratie van cellen. Allereerst beschrijven we een nieuwe methode die gebruikt kan worden om het effect van EMV op filopodia, kleine uitstulpingen op de buitenkant van een cel, te onderzoeken. Een cel gebruikt filopodia om zijn omgeving af te tasten voor chemische of topografische signalen. Het midden van een filopodium bevat dikke actine bundels. In de cel hebben we een stabiele expressie van Lifeact, een actine-bindend eiwit, gegenereerd. Deze Lifeact is geconjugeerd aan een fluorescent eiwit en zo hebben we de filopodia binnen de cel zichtbaar gemaakt. Hierna hebben we met behulp van beeldanalyse de beweging van de filopodia berekend. Onze methode is gevoelig en kwantitatief, maar heeft een hogere beeldsnelheid nodig dan op dit moment mogelijk is.

Vervolgens is de cel migratie onderzocht met een andere methode. Tijdens wondgenezing migreren epitheel cellen naar elkaar om de wond weer te sluiten. Dit gebeurt zonder de aanwezigheid van biologische signalen, maar kan wel gestimuleerd of geremd worden door chemisch of biologische eiwitten. We hebben onderzocht of blootstelling aan LF EMV invloed heeft op de migratie snelheid. De cellen werden 2 en 18 uur blootgesteld aan een continue sinus golf van 50 Hz met een magnetische flux dichtheid van 500  $\mu\text{T}$ . Blootstelling gedurende 18 uur liet geen significant verschil in de migratie snelheid zien, maar bij een blootstelling van 2 uur zagen we wel een mogelijk effect. Dit verschil werd opgeheven als de cellen gelijktijdig gestimuleerd werden met epidermale groeifactor (EGF). Echter, verder onderzoek is nodig om deze observatie te bevestigen.

In **hoofdstuk 6 en 7** bestudeerden we een recent ontdekt cellulair afweer mechanisme: de vorming van “neutrofiel extracellulaire traps” (NET). Het is aangetoond dat NET formatie in staat is om extracellulaire bacteriën te vangen en te doden. In een proces van 2 tot 4 uur wordt ROS geproduceerd, DNA gedecondenseerd en wordt de nucleaire envelop afgebroken. Het ontwarde DNA wordt gemengd met antimicrobiële eiwitten uit cytoplasmatische granula en uiteindelijk breekt het cel membraan open en worden de DNA netten met de vastgeplakte eiwitten los gelaten. In **hoofdstuk 6** hebben we ontdekt dat blootstelling aan LF EMV de vrijlating van NETs door PMA gestimuleerde cellen bevordert. PMA is een chemische component die receptor stimulatie nabootst. Het mogelijke moleculaire mechanisme achter dit proces is mogelijk een verhoogde ROS productie. De NETs kunnen meer bacteriën

vangen, maar zij beschadigen tegelijkertijd ook epitheelcellen. Deze delicate balans zou verstoord kunnen worden door de blootstelling aan EMV.

Microben en chemokines zijn natuurlijke stimuli voor NET formatie; de intracellulaire mechanismes kunnen bestudeerd worden met kleine chemische remmers (small molecule inhibitors). We vonden dat EHop-016 in staat was om NET formatie te induceren, ook al was dit stofje oorspronkelijk ontworpen om een interactie met Rac 1 en 3 tijdens tumor metastase aan te gaan. Ons onderzoek toonde aan dat deze remmer ook gerelateerd is aan PAD4 activiteit en citrullinatie van histonen. Een mogelijke interactie tussen EHop-016 en het immuun systeem kan nadelige gevolgen hebben voor toekomstige toepassingen in geneesmiddelen.

Samengevat, wij vonden tijdens ons *in vitro* onderzoek dat de invloed van blootstelling aan laag frequente elektromagnetische velden sterk afhankelijk is van het geactiveerde moleculaire mechanisme in de cel. Hoewel in onze experimenten de calcium huishouding niet beïnvloed werd, gaf onze systematische review wel een mogelijk zwak effect aan. Dit effect kan afhankelijk zijn van de kenmerken van de cel en van de EMV blootstelling. Daarnaast zou tijdens een korte blootstelling de cel migratie beïnvloedt kunnen worden, terwijl langere blootstelling kan leiden tot adaptatie. Om een effect van EMV op NET formatie te detecteren was activatie van de ROS route nodig. Al deze resultaten benadrukken generaliseren van effecten van mogelijke blootstelling gevaarlijk is en voor een verkeerde interpretatie kan zorgen. Hypothese-gedreven cellulair *in vitro* en *in vivo* onderzoek, met goed definieerde en zorgvuldig gecontroleerde blootstellingen en effecten, is daarom van essentieel belang.



**Miljoenen** cellen  
**Zestigduizend** kilometer  
**Honderdzeventig** pagina's  
**Tweeëntwintig** donoren  
**Vijf** teambuilding weekenden  
**Vier** mooie artikelen en  
**Eén** ZonMw project,  
met als resultaat dit **Proefschrift!**

**Het was een grote uitdaging, die ik niet alleen had kunnen voltooien....**

Beste **Lidy**, als dagelijks begeleider heb je me vanaf het begin vrij gelaten in dit project. Dit was erg fijn, want juist hierdoor heb ik me het project echt eigen kunnen maken. De vrijheid die je mij gaf, in combinatie met mijn interesse voor microscopie en cellen en de motivatie om lastige projecten niet uit de weg te gaan, heeft gezorgd voor een ander proefschrift dan vier jaar geleden op papier stond. Maar het resultaat mag er wezen, een proefschrift waar ik trots op ben! Bedankt voor al je rust en geduld, op mijn té drukke dagen vol experimenten, studenten en schrijfwerk. Bedankt ook voor je vertrouwen en begrip voor mijn situatie, met één been in Wageningen en één in Hengelo. Mede hierdoor was ik in staat om mijn twee levens in balans te houden.

Geen enkel project kan zonder professor, en **Huub** jij bent er eentje uit duizenden. Je passie voor wetenschap en je enthousiasme voor lesgeven breng je met veel plezier over op iedereen. Je openheid maakt het gemakkelijk om lastige discussies aan te gaan, of gewoon voor kleine dingen even binnen te lopen. We zijn aardig wat hobbels tegen gekomen in dit project met begeleidingscommissies en mislukkende experimenten, maar jij bleef altijd optimistisch. Bedankt voor je begeleiding, je vertrouwen in mij en je daverende enthousiasme voor mijn project.

De samenstelling van mijn kantoorgenootjes (**Carmen, Christine, Inge, Nathalie**) wisselden met de jaren, maar altijd was er wel iemand om even tegen te klagen over mislukte experimenten of de vreugde van een geaccepteerd artikel mee te delen. Deze gebeurtenissen gingen vaak samen met dropjes, chocolade en liters thee. **Carmen**, 2,5 jaar geleden kwam jij "ons" kantoor versterken, wat leidde tot nog meer thee en goddelijke taarten. Ik waardeer je onuitputtelijke creativiteit, je kleurrijke verjaardags-creaties, innovatieve oplossingen of bijdehante vrijdagmiddag grapjes. Je bent een inspiratie voor velen!

Als je aan een project werkt dat zowel celbiologisch als natuurkundige is, dan heb je veel expertise nodig van collega's en samenwerkingen. **Gosia**, bedankt voor je hulp met de Western Blot en de bloed donoren. **Marleen**, of ik nou lastige plasmides wilde transfacteren of 200 agar platen moest uitstrijken, jij was altijd bereid om mij te helpen. Met een beetje humor en doorzettingsvermogen kwamen we onze lange dagen achter de confocal door kijkend naar CXCXCXC.. eh. Je nauwkeurigheid is iets waar ik nog veel van kan leren. Dan een grote dank aan alle andere collega's van CBI: **Marloes, Ruth, Hilda, Esther, Sophie, Trudi, Ben, Eva, Sylvia, Jules, Edwin, Hans, Joost, Martin, Lieke vd A, Inge, Olaf, Maria, Adriaan, Geert, Alberto, Carla, Anders, Danilo** en de mensen van **HMI** en **EZO**. Bedankt voor al jullie hulp met experimenten, administratie, studenten en schrijven.

Ik heb mijn natuurkunde aardig moeten bijspijkeren, en daarvoor had ik hulp van experts, **John, Jan** en **Lucas**. Jullie voorzagen mij van advies en mooie real-time exposie-systemen. Dear **Lucas**, thank you so much for all of your help. You always took the time to explain difficult physics problems, even when you needed to explain them a second or even a third time. I am proud of our collaborative article, together we raised our systematic review to a higher level. **Rob de Vries** en collega's, heel erg bedankt voor de geweldige samenwerking voor onze review. We hebben misschien onderschat hoeveel werk er in zou gaan zitten, maar na twee jaar hard ploeteren, kunnen we trots zijn op het resultaat. Beste **Mark**, bedankt voor je hulp in mijn eerste jaar met alle calcium experimenten. Het was erg fijn om samen te werken met een ervaren postdoc binnen CBI die ook de effecten van EMV onderzocht. Binnen CBI was ik de enige, maar binnen Nederland waren er meer mensen die de uitdaging van EMV onderzoek aangingen. **Martje**, bedankt voor je hulp met de calcium analyses en de gezellige gesprekken. Het was fijn om zo nu en dan bij ZonMw meetings onze ervaringen en frustraties te delen. Broertjes, **Siebe** en **Rense**, jullie hebben mij elk op jullie eigen manier gesteund tijdens deze vier jaar. Syb, de geweldige cover van mijn proefschrift is tot stand gekomen met jouw hulp. Bedankt voor je hulp, je creatieve design en de gezelligheid tijdens het carpoolen naar Veenendaal/Wageningen.

De resultaten in dit proefschrift zouden er niet zijn zonder de hulp van mijn studenten: **Sabine, Sofie, José Sandra, Bertine, Dennis, Tomas** en **Eline**. Allemaal hebben jullie bijgedragen aan dit proefschrift met lastige calcium experimenten, onvoorspelbare inhibitors, of complexe ImageJ codes. Bedankt voor alle experimenten, inzichten en uitdagingen. Ik hoop dat ik jullie enthousiast heb kunnen maken voor de wetenschap, ondanks de tegenslagen die we soms tegen kwamen.

Om het drukke werken in het lab zo af en toe van mij af te zetten, was rennen met **Remco** en **Ellen** een heerlijke afleiding. Bedankt, voor de vele kilometers en de gezellige gesprekken. Samen rennen zorgde voor ontspanning en een goede training voor mijn eerste halve marathon.

Een promotie traject is intens en de steun van andere PhD-ers is daarbij onmisbaar. De E-wing groep, bestaande uit PhDs, postdocs en technici van HMI, CBI en EZO, is een hechte en gezellige groep geworden. Een groep waarmee we niet alleen werk deelden, maar ook vele gezellige sociale activiteiten. Dear **Marcela, Bruno, Edo, Linda, Nathalie, Marcel, Mike, Remco, Kees, Uros, Elsa, Sebas, Maurijn, Sander, Olaf, Jules, Eva, Marloes, Christine, Carmen** and **Joeri**, thank you for the great PhD-weekends, ski-trips, BBQs, cocktails,



dinners, and Friday-afternoon drinks. I think that our social activities made us stronger as a group, but also improved collaborations between our three labs. **Sebas**, dankjewel voor je onbezonnen creativiteit, met als resultaat een geweldig *Wie is de mol-weekend in België*. In het bijzonder een bedankje voor “**de jongens van EZO**”, want samen met “de meisjes van CBI” hebben we interessante lunchgesprekken gehad. Van “Hoeveel spiegels heb je nodig om rond de aarde te gaan met een laser?”, tot “Is een naakte molrat echt het lelijkste dier op aarde?”. Het was heerlijk om tijdens pauzes te discussiëren over dingen waar je normaal niet zo snel over nadenkt.

In vier jaar is Wageningen als mijn tweede thuis geworden, mede door de aanwezigheid van drie geweldige huisgenoten. **Hanneke, Max en Femke**. Met jullie kon ik mijn passie voor koken delen en na lange dagen werken stond er altijd een heerlijk bordje eten klaar, ook nadat jullie allemaal verhuisden. Altijd kon ik aanschuiven voor heerlijke Franse quiches, geweldig vers brood of creatieve witlofschotels met nasi kruiden. Bedankt voor jullie kookkunsten en dat jullie zo goed voor mij gezorgd hebben. Zowel in Wageningen als in Hengelo wonen is niet eenvoudig geweest, gelukkig heb ik twee geweldige vriendinnen in Hengelo die altijd voor me klaar stonden. Lieve **Es** en **Lijne**, de afgelopen vier jaar is er veel gebeurd; twee fantastische bruiloften, één lieve Fenna en één bijna-baby. Ik ben blij dat jullie zo flexibel waren, zodat er altijd wel tijd gemaakt werd voor thee of wijntjes. Ik had dit project niet kunnen doen zonder jullie steun. Met jullie kan ik kletsen, lachen, relativeren en genieten van het leven.

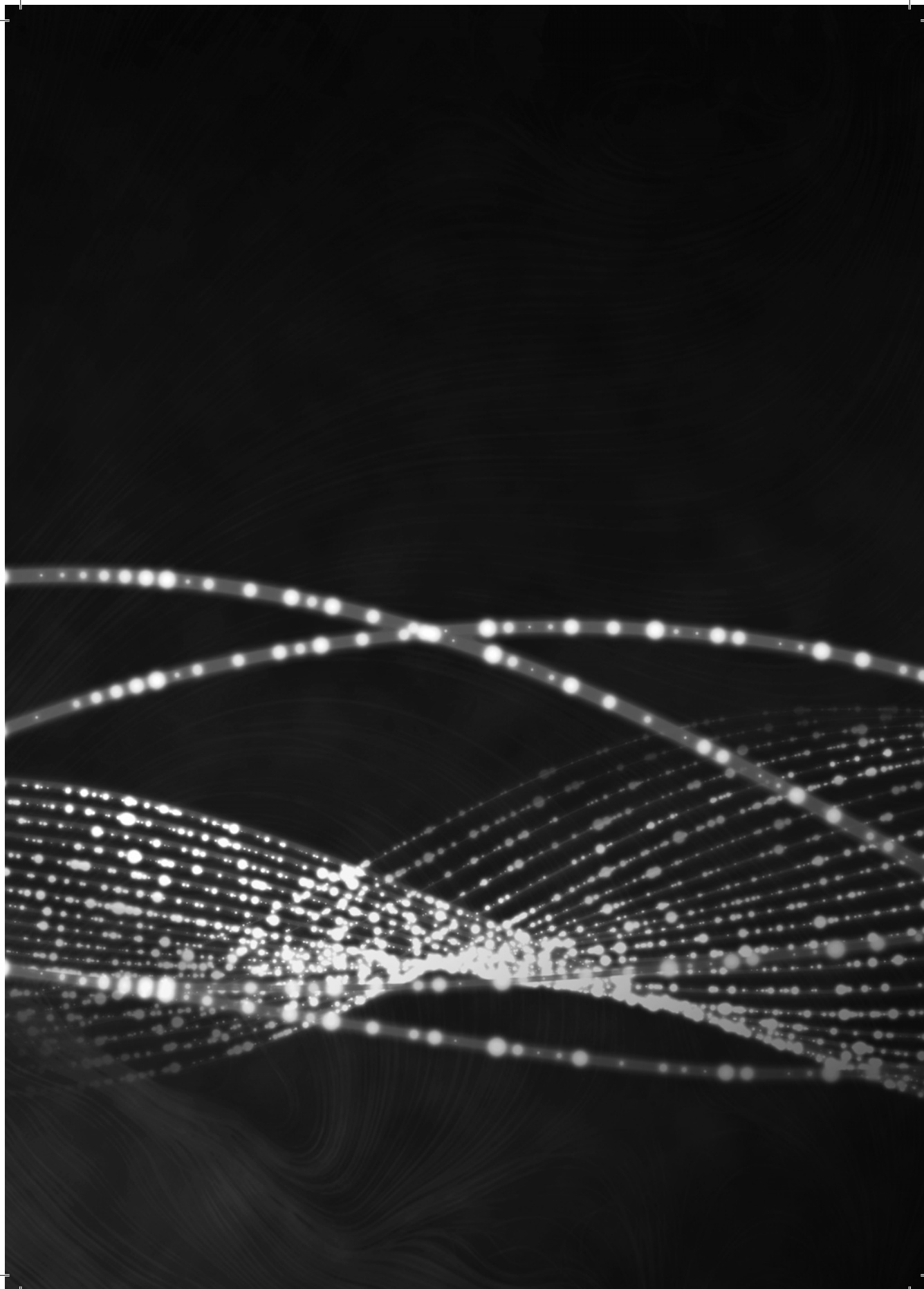
Lieve **Pap** en **Mam**, ik heb mijn proefschrift aan jullie opgedragen, omdat jullie ervoor gezorgd hebben dat ik hier nu sta. Jullie hebben mij opgevoed tot een creatieve, zelfstandige en ondernemende vrouw. Mam, je staat altijd voor mij klaar, zoals alleen een liefdevolle, zorgzame moeder dat kan. Mijn creativiteit heb ik zeker niet van een vreemde, want ik sta hier vandaag in een schitterende jurk die jij speciaal voor mij gemaakt hebt. Pap, je motto was altijd, probeer het beter te krijgen dan dat ik het heb en daar ga ik ook voor. Mijn doctoraat behalen is misschien niet hetzelfde als je eigen succesvolle onderneming starten, maar ik weet zeker dat je trots op me bent voor deze geweldige prestatie. Ik had het niet kunnen doen zonder jullie liefde, adviezen en fantastische vakanties, bedankt!

Mijn paranimfen waren mij steun en toeverlaat de afgelopen vier jaar. Lieve **Christine**, vanaf dag één hebben wij een kantoor gedeeld. Op veel punten zijn we elkaars tegenpolen; ik met mijn chaotische stapel artikelen en altijd verdwijnende pennen, en jij met geordende bakjes en op kleur gesorteerde stiften. Sorry voor alle rotzooi die ik in het kantoor heb gemaakt, vaak samen met mijn medeplichtige (Carmen). Stiene, jouw rust en bescheiden houding was wat ik soms nodig had als de dagen té snel gingen. We praatten over experimenten, begeleiders, studenten en ons leven en ook al zijn we tegenpolen, onze normen en waarden zijn gelijk. Bedankt voor je advies en gezelligheid. Ik ben heel blij en trots dat je tijdens mijn verdediging naast mij staat. Lieve **Joeri**, bij de eerste zin van mijn dankwoord had ik ook nog “vijftig flessen goede wijn” kunnen zetten, maar dat zou misschien een verkeerd signaal geven. De afgelopen vier jaar hebben we niet alleen veel tijd samen in het lab door gebracht tot in de late uurtjes, maar ook aan de keukentafel. Werk, onze twee “eiland projecten”, studenten, muziek, koken of de liefde, elk onderwerp kwam aan bod. Je bent loyaal, eerlijk, lief en “een tikkeltje” chaotisch. Ik heb enorm veel van je geleerd over leidinggeven en efficiënte lab technieken, maar ook over muziek. Jouw passie voor muziek heeft mijn oren geopend

voor de muzikale klanken van Bonobo, Disclosure en Alt-J. Bedankt voor je vriendschap, je klankbord en de heerlijke dinertjes, ik had dit project niet zonder jou willen doen.

Dan kom ik bij het einde van mijn dankwoord en blijft er nog maar één iemand over om te bedanken, **Niek**, mijn lief. Vanaf dag één heb jij mij gesteund in de keuze om naar Wageningen te gaan, ook al betekende dit dat we minder samen zouden zijn. Jouw onvoorwaardelijke steun en liefde is wat mij door dit project heeft gesleept. Jij geeft mij rust als mijn hoofd vol zit en jij relateert mijn frustratie als mijn experimenten in de gootsteen zijn verdwenen. Bedankt voor ALLES! Ik houd van je en kijk uit naar de volgende uitdagingen die we samen aangaan, want het leven met jou is geweldig. Je grapte er altijd over, maar vanaf vandaag ben je toch eindelijk met een doctor getrouwd.

*Liefs Lieke*





# About the author

---

List of publications

Training activities

Curriculum Vitae



About the author \_\_\_\_\_



## Training activities

### *(Inter)national conferences*

BEMS, 2011, Halifax Canada  
BioEM2013, 2013, Thessaloniki Greece  
Invadosomes, 2013, Nijmegen The Netherlands  
NVVI Conference, 2014, Kaatsheuvel The Netherlands

### *Seminars and workshops*

Seminar Yvonne Visser. Allergenicity in food allergy  
Seminar Marjolein Meijerink. Interactions of lactobacilli with the host immune system  
Seminar Lieke vd Aa. TRIM proteins and CXC chemokines  
Seminar Gerco den Hartog. Relevance of IgA in allergy regulation by mucosal factors  
Seminar Danilo Pietretti. Stimulation of the innate immune system of carp  
Seminar Ansa Fiaz. Regulatory mechanisms in developmental biology  
How to write a world class paper, Wageningen  
WIAS science day

### *Presentations*

Cytokine expression profiles in carp phagocytes after in vitro exposure ELF-EMF, BEMS Halifax  
ZonMW Dosimetry workshop, Den Haag  
Real-time quantification of actin dynamics during LF-EMF exposure, BEMS Thessaloniki  
Ex vivo neutrophil extracellular trap (NET) formation during LF-EMF exposure, BEMS Thessaloniki  
Real-time quantification of actin dynamics during LF-EMF exposure, Heidelberg  
Neutrophil extracellular trap (NET) formation during LF-EMF exposure, WIAS

### *Disciplinary and interdisciplinary courses*

Fish workshop, Wageningen  
Advanced Immunology, Utrecht  
For Hands-on training in Synthesis of evidence in animal experimentation, Nijmegen  
Seeing is Believing – Imaging the Processes of Life, Heidelberg  
Statistics for the Life Sciences, Wageningen  
Scientific Writing, Wageningen  
Writing Grant Proposals, Wageningen

### *Didactic Skills Training*

Cell biology Practical  
Cell biology work/discussion groups

### *Supervising Theses*

Supervision of 9 theses (2 BSc, 3 minor MSc, 3 major MSc)

**Total: 52 ECTS (1456 hours)**



## List of publications

*Low-frequency electromagnetic field exposure enhances neutrophil extracellular trap formation via the NADPH-pathway*

**Golbach, L.A.**, Scheer, M.H., Cuppen, J.J.M., Savelkoul, H.F.J., Verburg-van Kemenade, B.M. L (2015). *Journal of Innate Immunity*, DOI:10.1159/000380764

*Calcium signalling in human neutrophil cell lines is not affected by low-frequency electromagnetic fields*

**Golbach, L.A.**, Philippi, J.G., Cuppen, J.J.M., Savelkoul, H.F.J., Verburg-van Kemenade, B.M. L (2015). *Journal of Bioelectromagnetics*, 36 (430-443).

*Characterization and expression analysis of an interferon- $\gamma$ 2 induced chemokine receptor CXCR3 in common carp (*Cyprinus carpio* L.)*

Chadzinska, M., **Golbach, L.**, Pijanowski, L., Scheer, M., Verburg-van Kemenade, B.M.L. (2014). *Developmental and comparative Immunology*, 47 (68-76).

*Carp neutrophilic granulocytes form extracellular traps via ROS-dependent and independent pathways.*

Pijanowski, L., **Golbach, L.**, Kolaczowska, E., Scheer, M., Verburg-van Kemenade, B.M.L., Chadzinska, M. (2013). *Fish & Shellfish Immunology*, 34, (1244-1252).

*Pro-inflammatory functions of carp CXCL8-like and CXCL12 chemokines.*

Van der Aa, L. M., Chadzinska, M., **Golbach, L. A.**, Ribeiro, C. M. S., & Verburg-van Kemenade, B. M. L. (2012). *Developmental and Comparative Immunology*, 36, (741-750).

*Enhanced Collagen Type IV Based Differentiation of Embryonic Stem Cells Towards Flk-1 Expressing Vascular Progenitors by the Wnt/beta-Catenin Synergist QSII.*

Poels, M.W.J., **Golbach, L.A.**, Poot, A.A., Feijen, J., Grijpma, D.W., Kruijer, W. (2011). *Macromolecular Symposia 1* (236-243)



### ***Curriculum vitae***

Lieke Annelies Golbach was born on October 8<sup>th</sup>, 1986 in Deurningen, the Netherlands. After completing secondary school at the Carmel College in Oldenzaal, she started the bachelor program Biology at the Radboud University in Nijmegen. Her interest and knowledge of cell biology expanded and three years later, she enrolled in the Master program medical biology, with a specialization for cell biology, immunology and health. During her Masters, she investigated the cartilage formation by human stem cells and tissue engineering of small blood vessels from induced pluripotent stem cells. In February 2011, Lieke was appointed as a PhD candidate to the department of Cell Biology and Immunology of Huub Savelkoul. Her project was part of a large ZonMw project with the aim to increase the knowledge



regarding electromagnetic field (EMF) exposure. In her project, she looked at the effects of low frequency EMF exposure in immune cells. She focussed on different intracellular cellular pathways and cell behaviour of mainly neutrophils. Furthermore, in collaboration with SYRCLE in Nijmegen, she conducted the first systematic review and meta-analysis of *in vitro* studies to investigate the effect of EMF exposure on calcium. Lieke presented her research at several international conferences and was involved in teaching. Since June 2015, she has been working as a Postdoc on neutrophil adhesion and integrin regulation in the clinic for Anaesthesiology, Intensive care and Pain medicine in Münster Germany.

The work described in this thesis was largely financed by

**ZonMw** Elektromagnetische Velden en Gezondheid project nr 85300006

Cover Siebe Golbach

Layout Fenke Fros

Printing Gildeprint Enschede